The University Of Sheffield.

Influence of Additives on Agglomeration Behaviours / Formation in a Laboratory - Scale Fixed Bed Combustion of Biomass Fuels

By:

Akindele Ojo David

A thesis submitted in partial fulfilment of the requirements for the degree of Doctor of Philosophy

The University of Sheffield

Faculty of Engineering

Department of Mechanical Engineering

February 2018.

Dedication

''Considering every factor influencing successes and other various limitations, I humbly and unostentatiously dedicate this research thesis to the almighty God, who through his words, inspired and encouraged me to forge ahead and complete this research despite all the idiosyncratic experiences. Glory is to God''.

Abstract

This research has focussed on the impact of kaolin as additive on the agglomeration behaviours of willow, white wood, and miscanthus during their combustion processes in a laboratory-scale fixed bed whereby, Gooch ceramic crucible was used as the combustion chamber. It aimed at reducing agglomeration during the combustion of these selected problematic biomass fuels.

Biomass fuels are CO_2 neutral and very rich in alkali metals especially potassium, K and sodium, Na with potassium displaying the predominant roles in the agglomeration formation of these selected biomass fuels. During the combustion processes, agglomerates were formed in the combustion chamber at 750 ^{0} C and 802 ^{0} C under the atmospheric pressure. This was attributed to the formation of eutectic compounds in the form of alkali-silicates (K-silicates or Na- silicates). The eutectic compound has a lower melting temperature than the melting temperature of either the alkali metals or the silica from sand, which is the bed material. It therefore melts abruptly in the bed and formed lumps in form of agglomerates. Energy Dispersive X-ray spectroscopy (EDX) carried out on the agglomerates indicated that, the interior of the agglomerates was dominated with silicon, Si from the sand while the exterior or the peripheries were preponderated with alkali metals potassium K, and sodium Na from the biomass fuels ash. Other trace elements present in the agglomerates as confirmed by EDX analyses are; Aluminium Al, Calcium Ca, Chlorine Cl, Iron Fe, Phosphorus P, and Magnesium Mg. Meanwhile, with the addition of additive (kaolin) $Al_2 Si_2 O_5 (OH)_4$ to the bed materials and the combustion processes repeated under the same operating conditions, no agglomerate was formed at 750 ^{0} C and 802 ^{0} C. However, eutectic compound in the form of alumina-alkali-silicate was formed at a higher melting temperature than the alkali from the biomass fuels and the silica from bed materials, therefore no agglomerate was formed at these temperatures (750 ^{0} C and 802 ^{0} C).

Factsage software was extensively utilized to predict the eutectic points (eutectic temperatures) on both the binary and the ternary phase diagrams. With the inclusion of additive (kaolin) in the bed materials, on the binary phase diagrams, agglomeration was predicted to occur in the combustion bed at 1200 ^{0}C if the biomass fuel is dominated by

potassium, K. Consequently, if the biomass fuel is dominated by sodium, Na, agglomeration was predicted to occur at 1700 ^{0} C in the combustion bed. However, on the ternary phase diagrams, with the addition of kaolin to the bed materials, initial agglomeration was predicted to occur at 1550 ^{0} C if the biomass fuel is dominated by potassium, K but rose to 1700 ^{0} C if the biomass fuel is dominated by sodium, Na. This justifies the affirmation that, Sodium, Na has a higher melting temperature than potassium, K.

Elongation in the biomass particle size from <1mm diameter before combustion to 7mm diameter in the agglomerates formed from the combustion of willow, and 10mm diameter in the agglomerates produced from the combustion of both the miscanthus and white wood is a clear manifestation that, agglomeration actually occurred in the bed. Post combustion analyses; Scanning Electron Microscopy and Energy Dispersive X-ray Spectroscopy (SEM and EDX) carried out on the agglomerate samples also confirmed that, agglomeration took place in the bed. Huge agglomerates were formed at a lower melting temperature of 350 ^{0}C when potassium hydroxide, KOH and silica sand were heated directly (reality test). Harder and tougher agglomerates were produced at 502 ^{0}C. This confirmed that, agglomerates were produced from the formation of a low temperature alkali-silicate in the form of K-silicate.

The results of this research have indicated that, Gooch ceramic crucible is a reliable combustion chamber for the combustion of biomass fuels experiments/tests in a laboratory – scale fixed bed. It accommodated more heat distribution into the combustion chamber than the conventional ceramic crucible. Moreover, kaolin was also confirmed as an additive capable of reducing agglomeration during the combustion of biomass fuels in a laboratory - scale fixed bed and other combustion beds.

Acknowledgement

I wholeheartedly acknowledge and appreciate the fantastic contributions of my pioneer supervisor, Professor Chris Wilson, who because of his protracted illness and subsequent death could not complete the good work he initiated. He was only able to manage the project for nine months. His soul shall continue to find rest in the bosom of our Lord Jesus Christ, amen.

My appreciation also goes to my second pioneer supervisor, Dr Wilson Chung who barely co-ordinated and oversaw the supervision of the project for three months before he resigned from the University of Sheffield in pursuit of his career development elsewhere. His thorough and constructive criticisms at this brief period inspired me to work tirelessly, and defend the project proposal in the presence of the official sponsor, *Biomass and Fossil Fuels Research Alliance (BF2RA)*. The sponsor (BF2RA), withdrew the funding because of the demise of the principal and pioneer supervisor for the project, Professor Chris Wilson. This development led to the modification of my research title and appointment of another set of supervisors.

I have unreserved recognition and admiration for my make-up supervisor, Professor Yang Zhang whose supervisory style is worthy of emulation in academic arena. The ever-interactive weekly meetings schedule to meet with all his research students provided enabling opportunity and avenue for deeper understanding of individual research area. This also gave room for genuine interactions among all the students with a view to assisting each other without fear or favour irrespective of ethnical background.

My profound gratitude goes to my second make-up supervisor, Dr Simon Blakey who doubles as the Doctoral Development Programme (DDP) supervisor. His contribution to the successful completion of my PhD programme is hereby admired. His catalytic roles and diplomatic approach to issues in the overall interest of the success of the project, motivated me to move forward even at the critical period. In fact, his advisory role, as related to the selection of appropriate support programs to attend in terms of the doctoral development program was indeed helpful and relevant throughout the programme.

I remain grateful to the entire staff (research and technical) of the Low Carbon Combustion Centre of the University of Sheffield (located at Beighton) for their immense contributions and

support throughout the period, I was running my experiments at the laboratories. The massive and the overwhelming support, which I enjoyed from them, are hereby, applauded. The technical crew at the Mechanical Engineering Centre Workshop of the University of Sheffield are too fantastic to ignore. Their friendly and patriotic ways of handling workshop related issues without bias, cannot be consigned to oblivion in a hurry. I appreciate you all.

My unflinching gratitude goes to the outgoing vice chancellor of Ekiti State University, Ado-Ekiti, Nigeria, Professor Oladipo Aina who graciously approved the study leaves for my PhD programme. He is a role model whose administrative style is worthy of emulation. I remain indebted to the present vice chancellor of Ekiti State University, Ado-Ekiti, Nigeria, Professor Samuel Oye Bandele for his huge interest in the welfare of all EKSU staff. The Dean Faculty of Engineering EKSU, Professor Okunade, E.A and the entire relentless and uncompromising staff of the Faculty are hereby cherished for their support through prayers at ensuring that, this programme is completed without any itch.

My sagacious gratitude goes to my indefatigable and erudite scholar, Professor Sunday Babatunde Adeyemo, who without mentioning him, this acknowledgement would not be complete. He contributed colossally, remarkably, and absolutely to my entire academic career development. His words of encouragement and concern through series of texts messages, e-mails and prayers inspired me to continue to make head way in my research work. He is hugely admired. I also recognize Professor Oluwaleye, I.O for his immense contributions to the overall success of this research. Professor Ajaja is greatly appreciated for his words of wisdom always. I am grateful to the present Head of the Department of Mechanical Engineering EKSU, Dr Adebayo Adeyinka, and the entire enunciated staff of the department for their co-operation and understanding throughout my academic (PhD) programme at the University of Sheffield, United Kingdom.

My noteworthy, unreserved, heartfelt, and wholehearted gratitude goes to my ever caring, loving, loyal, and trustworthy wife, Taiwo Omoyemi Akindele for her unconditional, uncompromised, and absolute support throughout my sojourn at the University of Sheffield, United Kingdom for my PhD programme. You are truly a woman of virtue. The relative peace of

mind that I enjoyed throughout the entire programme was because of your total co-operation, unprecedented sacrifice, and complete loyalty to our family. God, bless you.

I applaud the endurance and the encouragement by my God given, adorable and destiny children; Tayo, Tope, Tosin, and Tomiwa. Even though, I left home at the time they needed my support most in their career development too, they never relented to give me their maximum co-operation. The absolute support rendered by my children served as their major donation to the successful completion of my PhD programme. I appreciate you with all my heart.

My outstanding appreciation exclusively goes to my delightful parents, Mr Akindele Matthew and Mrs Akindele Alice for their fervent prayers and advice always. They both laboured so hard to see that, I succeed in my chosen career. My step mum is also appreciated for her support. I recognize the support and the co-operation of all my siblings. I have exceptional respect and appreciation for my mother - in- law, Mrs Aduloju Juliana for her continuous and passionate prayers day and night to see that, the dream was not truncated, nor consumed by the uproar and the disturbance of the unforeseen, Mummy, you are wonderful. My father- in – law, Late Pa Aduloju Simeon is remembered for his positive contributions always during his days.

Finally, I want to utilize this opportunity, to appreciate my intimate friend, Dr Stephen J.T who recently bagged his PhD degree at the University of Sheffield. We lived together throughout our abode in the United Kingdom. Our continued mutual relationship since childhood has been attributed to the deep understanding between us, coupled with the mature manner with which we relate together. I also acknowledge the support and contributions of my colleagues who are also TETFUND scholars from Ekiti State University, Ado-Ekiti, Nigeria; Abere Julius, Adeyemi Gbenga, Ayotunde Ojo and Oluwadare Benjamin who is on the PTDF scholarship. Other research mates are; Oku Nyong Ekpeyong and Ubogu Emmamode. Thank you all for making my four and half years' sojourn at the United Kingdom, in quest for additional knowledge, highly and grossly memorable. God bless you all.

Nomenclature

A_2	Cross sectional area of orifice, m^2
A/F	Air – Fuel ratio
C	Orifice flow coefficient, dimensionless
C_d	Coefficient of discharge, dimensionless
C_p	Specific heat at constant pressure
C_v	Specific heat at constant volume
d_p	Diameter of particles, mm
dT	Change in temperature, ^0C
dT/dX	Temperature gradient
EJ/yr	Exajoule per Year
F/A	Fuel – Air ratio
g	Acceleration due to gravity, $9.8m/s^2$
H	Bed height, m
HHV_D	High heating value, kJ/kg
k	Thermal conductivity, $W.m^{-1}k^{-1}$.
K	Specific heat ratio (C_p/C_V), dimensionless
L	Length, m
M_f	Minimum fluidization
m_{air}	Mass of air, kg
m_{fuel}	Mass of fuel, kg
P_1	Fluid upstream pressure, Pa or kg/m^2
P_2	Fluid downstream pressure, Pa or kg/m^2
q	Heat transfer rate, MW
q/A	Heat transfer per unit area, MW/m^2
ΔP	Pressure drop
Q	Volumetric flow rate at any cross – section, m^3/s
R_{ep}	Reynolds number, dimensionless

R	Pressure ratio (P_2/P_1)
SD	Standard deviation
Stoic	Stoichiometric
U_{mb}	Minimum bubbling velocity, m/s
U_{mf}	Minimum fluidization velocity, m/s
V	Volume, m^3
X_i	Weight fraction of solids of size i
dX	Body thickness, m
Y	Expansion factor, dimensionless
ρ_g	Fluid density, g/cm^3
ρ_s	Sand density, g/cm^3
ε_{mf}	Voidage at minimum fluidization velocity,
φ_s	Sphericity of particles, dimensionless
ε	Void fraction, dimensionless
μ_g	Viscosity of gas, g/cm.s or kg/m.s
φ	Equivalence ratio, dimensionless

Table of Contents

List of Tables

List of Figures

1 Introduction

The world's continued reliance on fossil fuels that are fast depleting from the reserve coupled with increasing rate of CO_2 emissions from fossil fuels, calls for serious concern among scientific researchers. Biomass has been adjudged as CO_2 neutral, the amount of CO_2 intake by plants while growing is also released to the atmosphere during its combustion [1]. Biomass is a reliable, sustainable, and dependable alternative energy source that does not contribute to the earth's surface heating but reduces greenhouse CO_2 emissions.

Available fossil fuels (coal, crude oil, and natural gas) in the reserve are sprightly depleting therefore, cannot sustain the world's energy demand and supply through it. Moreover, the world's population growth that is escalating at an alarming rate coupled with increase in energy demand, have prompted researchers to deduce ways to damper the consequences (perennial fuel scarcity, reduced quality assurance, and decrease in production competitiveness) of the sole dependency on these conventional energy resources. Researchers' attention has been shifted to providing energy via a more dependable, reliable and renewable energy resources such as biomass, solar, wind power, geo-thermal, and hydropower.

Energy derived from biomass fuels has been recognized as one of the earliest and ancient sources of energy which ranked fourth as energy resource, accounting for about 14% of the global energy in terms of domestic and industrial applications [2, 3].

Biomass fuels can be sourced from energy crops (short rotation), agricultural wastes / products, municipal wastes, sewage and industrial wastes. Biomass fuels for energy production are environmental friendly and offer other benefits as far as utilization of biomass fuels are concerned [1-3].

In spite of the fact that, thermal (proximate and ultimate), structural and the physical properties of biomass fuels differ greatly, other properties such as the sulphur content, the hydrogen content, and the ignition temperatures are very similar [3, 4]. However, because of the heterogeneous nature of biomass fuels, which accounted for the differences in their characteristics, different types of problems are usually experienced during the combustion of

single biomass fuel or blends of biomass fuels. However, many complications that tends to truncate the whole combustion processes are encountered during the combustion of the selected problematic biomass fuels for this research (miscanthus, willow, and white wood). Some of such problems are agglomeration, erosion, fouling, and slagging [5]. The scope of this research has been limited to the reduction of agglomeration in laboratory-scale fixed bed combustion of biomass fuels using a Gooch crucible as the combustion chamber and silica sand as the bed materials while adding kaolin as additive.

This chapter of the thesis addresses, background of the study, sources and varieties of biomass fuels, relevance of biomass fuels to global development among others.

1.1 Background of the study

Biomass contains alkali metals, potassium K, sodium Na, and mostly elements of group 1 in the periodic table, which through reactions and interactions with silica sand (bed materials) during combustion, cause some problems such as agglomeration, erosion, slagging, and fouling in the bed [5, 6]. Moreover, low melting points of the alkali metals present in biomass may have contributed largely to the low melting temperature possessed by biomass fuels. In addition, biomass fuels have low calorific value and high moisture content therefore, cannot burn easily on its own [6, 7]. In order to improve on the combustion characteristics of biomass fuels, it is usually co - fired with coal, which has higher calorific value. In this research, biomass will be co – fired with coal.

Agglomeration is the formation of sticky coagulates in combustion beds during the combustion of biomass or biomass blend with coal. This occurs because of the reactions between the alkali metals (mostly K and Na) present in biomass and silica in the sand particles (bed materials) leading to the formation of eutectic compound which has a melting point lower than the melting point of either the alkali or the silica from sand particles [8, 9]. Alkali metals possesses low melting points, Figure 1.1 It can be deduced from the figure that, Lithium Li, possessed the highest melting point followed by Sodium Na, and Potassium K.

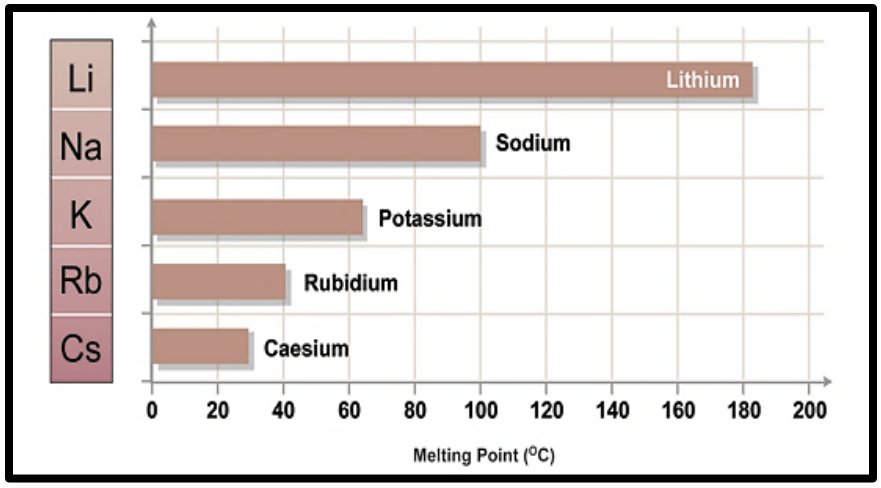

Figure 1-1: Melting points of alkali metals [8, 9]

Eutectic temperatures are largely dependent on the melting points of alkali metals. The oxides of these alkali metals particularly Potassium (K_2O) react with sand particles (SiO_2) to form sticky substances called agglomerates [1, 5, 7]. Moreover, there are other deposits formed during the combustion of biomass fuels and these includes; NaCl, KCl, K_2SO_4, and CaO. Alkali getter (additive) mostly kaolin when added to biomass has been identified to form a eutectic compound which has a higher melting point than either the silica from sand particles or the alkali metals particularly Potassium, K from biomass [5, 7, 10]. This will be mixed with the selected biomass fuel separately and with their blends at different ratios. Chemistry of behaviour of these materials would be studied and the agglomeration tendencies in them be established. Co-firing ratio (weight) of 20% biomass to 80% coal, or 30% biomass to 70% coal has been recommended [10, 11]. Applying these ratios, other problems like slagging and fouling may be avoided. With this, agglomeration problems may be reduced in a combustor bed.

1.2 Specific Statements

Shortage, scarcity, or reduction in the supply of energy is inimical to the technological growth and development globally. Every activity in a system or society would automatically results to a standstill whenever the supply of energy to the system is interrupted intentionally or otherwise

[1, 3, 12-14]. Therefore, it clearly implies that, energy plays a vital and magnificent role in our day-to-day activities for human comfort, production assurance in the industries and research effectiveness in the research institutions globally [15].

Consistent increasing growth rate of the world's population and the regular high demand for energy consumption in terms of conventional energy sources, coupled with the fast depletion rate of the fossil fuels from the reserves, calls for insight into generation of energy through alternative means. [15]. The alternative energy sources include; biomass, solar, wind, nuclear, geothermal, hydrothermal, tidal, etc. Biomass possesses high potentials to contribute to the energy requirement of the global world. It is a renewable energy source mostly from organic matters and agricultural crops otherwise known as energy crops. The highest volume of this is obtainable from wood and wood wastes [2, 4, 13, 16]. Moreover, domestic solid wastes in terms of percentage total, Table 1.1 are available on a large scale and can easily be accessed for heat and power generation. The moderate sulphur S content possessed by biomass has led to the generation of low sulphur dioxide SO_2 emissions. Biomass also possesses the characteristics to replace the fossil fuel energy that is fast depleting from the reserves, because it is renewable and has the potentials for ash management and utilisation. Biomass energy utilization is about 27% out of 6 EJ/yr in the European Union countries [15, 17].

Table 1-1: World's availability of domestic solid waste (percentage total) [18]

Components	Lower limit	Upper limit
Paper waste	33.2	50.7
Food waste	18.3	21.2
Plastics	7.8	11.2
Metal	7.3	10.5
Glass	8.6	10.2
Textiles	2.0	2.8
Wood	1.8	2.9
Leather and rubber	0.6	1.0
Miscellaneous	1.2	1.8

Principle of energy states that, energy cannot be created nor destroyed but can be transformed from one form to the other. There are various forms of energy conversion technologies [19]. Direct combustion, gasification, and pyrolysis are the different forms of thermochemical conversion technologies for heat and power generation from biomass fuels. The other form of biomass conversion technology is the biological conversion processes. These thermochemical conversion technologies are the most widely used because of its simplified method of operations and high reliability [20].

The type of application required determines the method to be adopted for the biomass energy generation, most especially in the production of electricity. Coal utilization and applications in the process of biomass fuels for energy generation is highly commendable. Moreover, biomass high moisture content and low calorific value contribute significantly to the reason why biomass is usually co-fired with coal [2, 4, 13, 16]. On the other hand, coal has low moisture content and high calorific value, which make it burn easily than biomass fuels. Biomass fuels burning flame

is considerably higher than that of coal therefore, it burns with flaming glow which can be likened to oil and gas, while coal on the other hand, burns with char glow and last longer [21, 22].

Combustion of biomass fuels to generate alternative energy has been widely and globally acknowledged through various researches at research Institutes and at the Universities of higher learning [6, 12, 16, 17]. Although, some combustion beds have been used as Combine heat and power, sufficient efforts are still required to maintain stable and regular supply of energy.

1.3 PhD Project Goals

The main purpose of this research encompasses the reduction of agglomeration formation in a Laboratory - scale fixed bed combustion of biomass fuels, using a high thermal resistant Gooch ceramic crucible as the combustion chamber while studying the various forms of mechanisms of agglomeration in the bed.

1.4 Objectives of the Project

- Characterization of the selected biomass for its suitability for combustion processes.
- Study the chemistry of blending biomass fuels and coal with silica sand.
- Factsage software application to predict eutectic points (fusion temperatures) on both the binary and the ternary phase diagrams.
- Evaluation and analysis of the performance of single biomass fuel with coal in a laboratory - scale fixed bed using Gooch ceramic crucible as the combustion chamber.
- Evaluation and analysis of the performance of blends of biomass fuels with coal in a laboratory - scale fixed bed using Gooch ceramic crucible as the combustion chamber.

- Post combustion analyses on bed materials (agglomerates) using Scanning Electron microscopy (SEM) to examine and evaluate the shape and morphological structure of the bed materials with a view to establishing agglomeration tendencies in the bed.
- Post combustion analyses on bed materials (agglomerates) using Energy Dispersive Spectroscope (EDX) to examine and evaluate the inorganic compositions of the bed materials with a view to knowing the elements making up the agglomerates and establish agglomeration tendencies in it.
- Measurement of size and shapes of bed materials before and after the agglomeration tests to study variation in the bed particle size.
- Reality tests (KOH + Silica sand) to establish agglomeration tendencies in the selected biomass fuels.

1.5 Potential Benefits of the Project

- The outcome of this project may offer solutions to reduction of agglomeration in a laboratory - scale fixed bed and other combustion beds (FBC) during the combustion of biomass fuels.
- Blending different proportions of biomass together with a view to solving agglomeration problems may further provide better understanding in the use of biomass and biomass blends for combustion purposes.
- It may also improve the performance of fixed bed combustors.
- Unscheduled boiler / combustion equipment shutdown because of formation of large aggregates and slags within the combustor bed may be avoided.
- Maintenance cost of combustion beds may be reduced to the barest minimum.
- Production effectiveness and quality assurance are guaranteed because; interruption to the combustion process may be largely avoided.

1.6 Contribution of this Research to Knowledge

- An appraisal of the use of a Gooch ceramic crucible as a reliable and dependable combustion chamber for the combustion of single biomass fuel / blends of biomass fuels in a laboratory scale- fixed bed.
- Application of Factsage software as the appropriate tool for the accurate prediction and modeling of eutectic points (temperatures) in both binary and ternary phase diagrams.
- Clear demonstration of the influence of Kaolin $Al_2Si_2O_5(OH)_4$ as a suitable additive to combat or reduce agglomeration formation during the combustion of some problematic biomass fuels in a laboratory-scale combustion of biomass fuels using a Gooch ceramic crucible as the combustion chamber.

1.7 Importance of Biomass to Global Development

Relevance of biomass fuels to the development of global economy through reliable energy supply cannot be over emphasized. Biomass can significantly bring about 60% to 70% of the world energy if adequately harnessed [12, 23-25]. The continuous world population increase also commensurate with high-energy demand for various applications such as heating homes in the extremely cold regions of the world, sustaining quality research at higher institutions of learning and research institutes, various hospital services, and industrial applications. Therefore, regular and uninterrupted supply of energy is required for the technological advancement and stability of global economy [26-28].

The world over dependence on the supply of energy through the conventional means (The fossil fuels; the coal, crude oil and natural gas) is posing economic-instability especially in the developing countries of the world [29, 30]. Many commercial activities in these countries had been crippled because of the shortage in the supply of the fossil fuels. The continuous use of these fuels poses varieties of danger to the society such as air pollution and increased greenhouse effect. These fuels are reducing at a faster rate from the reserve therefore; more

dependable, highly economical and environmentally friendly energy resources should be harnessed to salvage the energy sector from total dependant on fossil fuels that are no longer reliable. Moreover, biomass fuels possess some qualities that make it stand out; less ash content, reduced carbon monoxide CO, and less unburnt carbon [2, 28, 31].

Respiration in biomass (plants) demands that, carbon dioxide CO_2 is taking in while oxygen O_2 is released to the atmosphere. During photosynthesis, Equation 1.1, the absorbed CO_2 in conjunction with water is used to manufacture biomass food in the presence of sunlight and chlorophyll while O_2 is released to the atmosphere for the respiration in man [32, 33].

$$6CO_2 + 6H_2O \xrightarrow{\text{sunlight}} C_6H_{12}O_6 + 6O_2 \qquad 1.1$$

$$\text{Carbon dioxide + water} \xrightarrow{\text{sunlight}} \text{Carbohydrates + Oxygen} \qquad 1.2$$

When biomass dies, decay or burnt, the overall CO_2 it had stored in its entire lifetime is released to the atmosphere thereby, making the whole combustion process of biomass fuels, CO_2 neutral. Figure 1.2 was used to expatiate further.

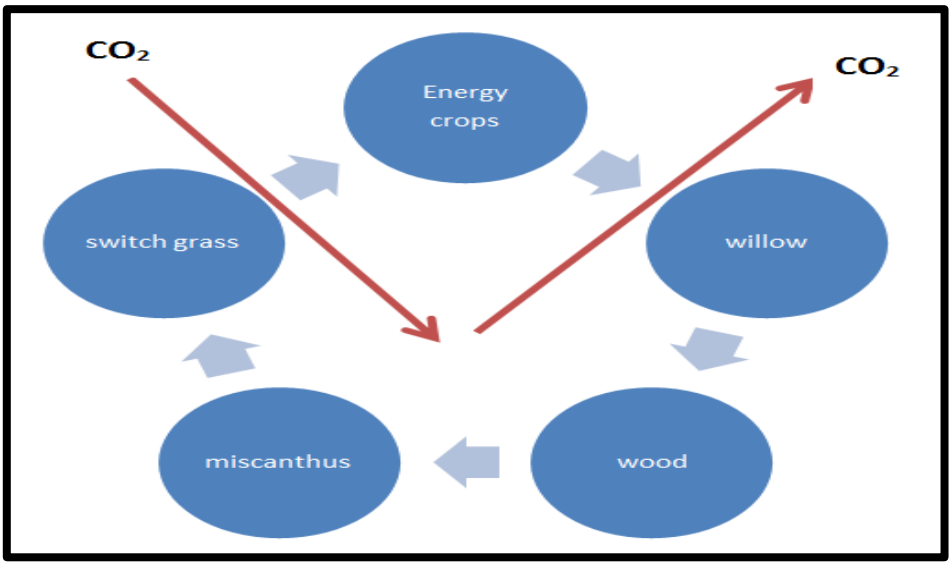

Figure 1-2: Illustration of the overall CO_2 circulation (CO_2 in = CO_2 out) in biomass life.

The leaves that drop off from the biomass tree is also a very rich source of manure and nutrients to the soil for un - interrupted growth of micro - organisms [34, 35].

In tropical regions of the world where rainfall is very predominant, growth of biomass is faster and easier without the application of inorganic manure (fertilizer) or irrigation system. Therefore, 60% of the entire universe land mass is occupied by biomass thereby, making its dependence as alternative energy source to replace fossil fuels very reliable and sustainable.

Biomass fuels as a source of energy can be employed to meet the expectations of man in terms of domestic, kitchen, commercial and industrial water heating purposes because, the heating can be supplied from only one heating source. Wood can be regarded as the most common type of biomass because it can be obtained locally and packaged to support rural economy [23, 36].

Benefits of biomass energy are numerous in terms of applications such as domestic use (heating and cooking), industrial (tobacco curing, beer brewing, coffee and tea drying), and Scientific laboratories [2, 12, 26, 28]. It is an energy source obtained from plants and animal waste, industrial wastes, agricultural wastes, sewage and municipal wastes with the highest percentage of this coming from wood and wood wastes. Biomass fuels processes for energy generation has contributed immensely to the creation of employment. Virtually all the stages involved in the processes such as planting, production, processing and transportation require huge labour. In total comparison with fossil fuels, biomass can accommodate more labour or require more labour than fossil fuels. Biomass was responsible for about eighteen thousand (18,000) work force in German state of Bavaria [3, 15, 16].

1.8 Thesis Arrangement / Layout

The entire PhD thesis comprises of the research work carried out in the last four years. It has been categorized into seven different chapters, and each chapter thoroughly describe detailed work and analyses in each case as follows:

Chapter 1 encompasses the introduction aspect of the whole research. It contains the purpose for which this research was embarked upon. It presented detailed background of the study to include; varieties of biomass fuels available, their sources, and importance of biomass to global

development. Various problems usually associated with combustion of biomass with more emphasis on agglomeration were adequately discussed.

Chapter 2 discusses the review of series of relevant work that have been carried out regarding agglomeration formation in the combustion chambers. Techniques applied to reduce agglomeration in the bed were also reviewed. Moreover, Mechanisms of agglomeration concerning eutectic compounds and eutectic temperatures in the combustion beds were adequately reviewed. Consequences of agglomeration on the industrial application of biomass combustion were also considered. This chapter also discusses agglomeration detection techniques and the significant of co – firing biomass fuels with coal among others.

Chapter 3 considers the theoretical background relating to the combustion of biomass fuels in a fixed bed. The concept of both the binary and ternary phase diagrams was discussed. Some fundamental principles of biomass combustion were also discussed.

Chapter 4 presents the detailed description of the experimental techniques and the entire materials utilized during the conduct of this research. Selected biomass fuels are white wood, willow, and miscanthus. Silica sand was the bed materials while kaolin was adopted as the additive. Characterization of the selected biomass fuels for their suitability for the agglomeration experiments were adequately considered. Post combustion analyses viz-a-viz scanning electron microscopy and the energy dispersive x-ray spectroscopy (SEM & EDX) were adequately analyzed to further confirm agglomeration formation in the biomass fuels. It also contains all the laboratory analyses carried out on the selected biomass fuels during this research

Chapter 5 discusses applications of software to predict the eutectic temperatures on phase diagrams. Significance of both binary and the ternary phase diagrams as related to agglomeration formation during the combustion of the selected biomass fuels in the combustor chamber was properly considered. Simulation using Factsage software to predict/determine the eutectic temperatures on phase diagram was thoroughly carried out.

Chapter 6 considers discussion of all the results obtained from the laboratory combustion experiments carried out during this research. Critical analyses and comparison of the acquired temperature data with simulation results were deeply considered. Simulation results emanated from the use of Factsage software to determine eutectic points on both binary and ternary phase diagrams were appropriately discussed. The experimental aspect focuses on heating the

biomass fuels beyond the sintering temperature (760 ^{0}C) with a view to determining the fusion temperature of the biomass fuels. Charts, tables, graphs and schematics were sufficiently used for the analyses.

Chapter 7 contains the overall conclusions deduced from this research work and relevant recommendations about the proposed future works to commence afterwards.

2 Literature Review

2.1 Introduction

Actualization of regular and uninterrupted supply of energy, particularly electricity in our systems (homes, schools, hospitals, airports, industries and research institutes), have prompted the design of some combustion beds for the production of alternative energy through the combustion of biomass fuels [23, 37]. Dependence on the conventional energy supply (fossil fuels) is no longer reliable and sustainable globally. Apart from the fact that, the resources are fast depleting from the reserve, the flue gases emanating from the combustion of these fuels are not environmentally friendly and tend towards polluting the surroundings [23, 37]. These flue gases also constitutes greatly to greenhouse effects (CO_2 and CH_4) through surface heating [38, 39]. Biomass on the other hand, when compared with fossil fuels, is renewable [40, 41].

In a global context, a reliable, renewable, and environmentally friendly energy source that will contribute immensely to the economic growth of the society is required hence, adoption of biomass as alternative energy source to substitute the almost exhausted fossil fuels. Various problems (agglomeration, fouling, erosion, and slagging) have been identified to associate with the process of generation of alternative energy from biomass, hence, this research. The scope of this research encapsulates reduction of agglomeration in a laboratory - scale fixed bed combustion of biomass fuels using a Gooch crucible as the combustion chamber and kaolin as the additive.

2.2 Biomass energy

Biomass energy is the energy derived from biomass fuel. It is an alternative source of energy which can be used for purposes such as domestic (heating and cooking), industrial (tobacco curing, beer brewing, coffee and tea drying), and laboratory. It is also a renewable energy source obtained from plants and animal waste. Other categories of materials includes energy crops which are crops grown specifically for energy production, virgin wood from forestry or

wood processing, agriculture which are residues from agriculture harvesting, industrial wastes from manufacturing and industrial processing, sewage and municipal wastes (post-consumer wastes), with the highest percentage of these coming from wood and wood wastes [4, 42, 43].

2.3 Heat Transfer by Conduction

Heat transfer is the study of the science of energy transfer that takes place in a body, when there exists a temperature variation between the source and the sink. Thermodynamics refer to this type of energy as heat [44-46]. Temperature on the other hand, is the determination of the coldness or hotness of a body in degree Celsius ^{0}C, degree Fahrenheit ^{0}F, or Kelvin, K. Apart from the way and manner of the transfer, the rate at which the transfer occurs is taking into account [47, 48]. Thermodynamics consider mostly systems in equilibrium state and may be applied to forecast the actual amount of energy that would be required to change a system from one equilibrium state to the other. In order to fully establish heat transfer rates in a system, first and second laws of thermodynamics are applied.

There are three basic modes of heat transfer; heat transfer by conduction, convection, and radiation. The heat transfer by conduction is the most applicable as far as this research is concerned. Heat transfer by conduction occurs in a solid body whenever there is a difference in the temperatures of the sink and the source [49]. Ideally, in a solid body, heat energy flows from a higher temperature region to a lower temperature region.

Heat transfer rate per unit area denoted by q/A is directly proportional to the normal temperature gradient, Equation 2.1

$$q = -kA\frac{dT}{dX} \tag{2.1}$$

Where q represents heat transfer rate, k (positive) is the thermal conductivity of the material under consideration, dT/dX is the temperature gradient in the direction of the flow of the heat,

and A connotes the area of concentration on the body. The dT is a change in the temperature of the body while dX is the body thickness. The minus sign (-) indicates that, heat flows from source, T_1 to sink T_2 in which, the temperature at the source is higher than at the sink. A change in the temperature dT is equivalent to $T_2 - T_1$ which is negative (-ve). Moreover, the minus sign (-) was introduced to equation 2.1 so that second law of thermodynamics would be fulfilled and that, heat must flow downhill on the temperature scale. Equation 2.1 is referred to as the Fourier law of heat conduction. It was named after a French mathematical physicist, Joseph Fourier [50-52].

2.4 Review of Biomass Fuels Conversion Technologies

2.4.1 Fluidized Bed Combustion

This is a combustion technology mostly used in power plants. The technology of fluidized bed combustion is quite different from that of fixed bed in several ways. It has various advantages over the fixed bed combustion system. It can be operated at a low temperature (800 ^{0}C to 900 ^{0}C) [2, 53], therefore generation of NO_X during combustion of biomass is reduced. Reagents such as limestone can be used as bed materials to absorb SO_2.

Some biomass fuels that are difficult to burn by conventional boilers can be fired in fluidized bed. It operates with the principle of fluidization. The major purpose of this research work is the reduction of agglomeration in a laboratory - scale fixed bed using a Gooch crucible as the combustion chamber, but for the purpose of wide comparison, agglomeration in a fluidized bed was briefly reviewed.

There are different types of fluidized bed among which are; Circulating fluidized bed (CFB) and the bubbling fluidized bed (BFB), Figures 2.1 and 2.2 respectively. Principle of fluidization is applied in fluidized bed combustion technology [54].

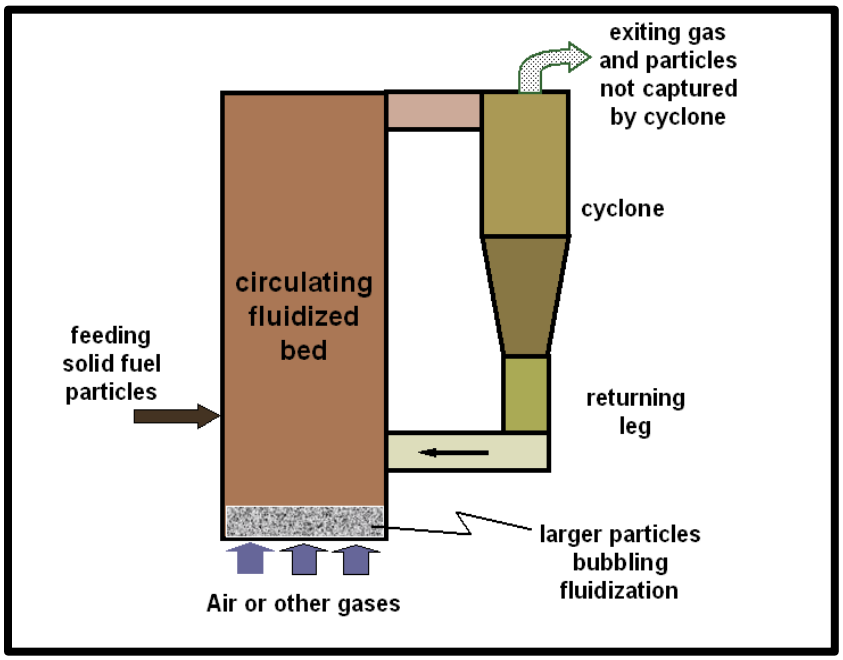

Figure 2-1: A Typical Circulating Fluidized Bed Combustor, CFBC [55]

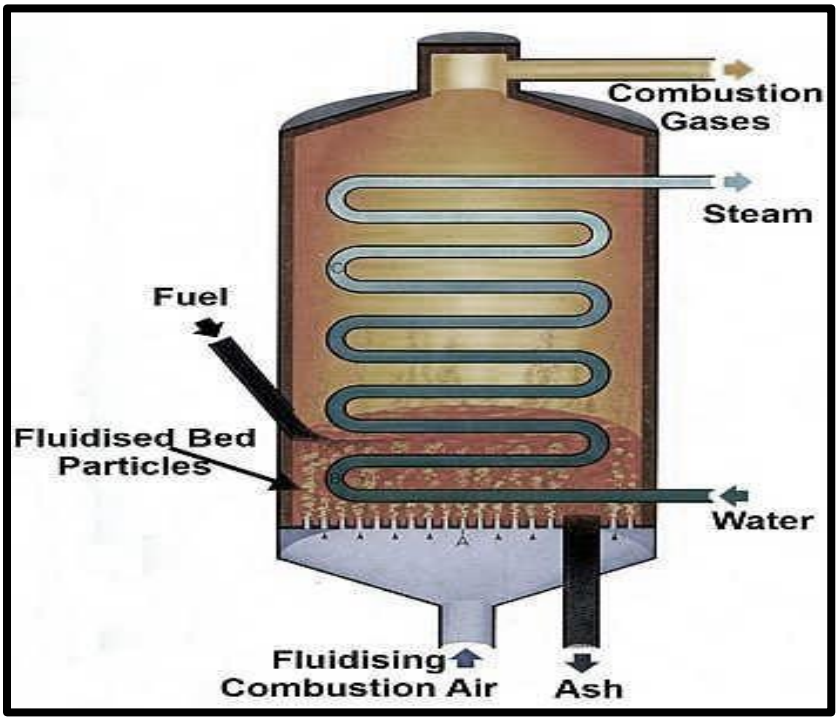

Figure 2-2 : A Typical Bubbling Fluidized Bed Combustor, BFBC [55]

They both operate under the atmospheric conditions. Relative to the installed capacity in MW of each of these fluidized beds, Circulating Fluidized Bed (CFB) is more often used which is the reason why large fluidized bed combustion boilers for power generation are always large CFB and its operating fluid velocity is between 5 -10m/s. On the other hand, bubbling fluidized bed (BFB) boilers are always used for small combined heat and power (CHP) boilers in district heating systems or when applied industrially. Its operating velocity is 1 - 2.5m/s [2]. A third system is the pressurized fluidized bed combustor (PFBC). The technology behind this began in the early 80's but because of several operational problems associated with it such as pressurized coal feed; its patronage has not progressed. When PFBC is installed to its maximum pressure, coal feed and ash removal is always very difficult.

2.4.2 Advantages of Fluidized Bed Combustion (FBC)

- Combustion of difficult to burn low-grade fuels of varying qualities can be accommodated in fluidized bed combustion technology.
- Combustion of single fuel or blend of fuels can take place in the same unit.
- During combustion in fluidized bed combustor, there is very low tendency for thermal NO_X emissions because of its relatively low temperature of operation. Therefore, magnificent environmental benefits are obtained with this type of technology.
- Bubbling fluidized beds are designed with high degree of flexibility. This enhances gas recirculation volumes and air movement in the bed. It also allows adjustment of fuel delivery to the bed to be carried out easily [56].
- Fluidized bed combustion is also used as power boilers mostly circulating fluidized bed boilers with pulverized coal fired boilers as the major competing technology.
- Fluidized Bed Combustion is well equipped for co – firing in large power plant boilers.
- If limestone ($CaCO_3$) is added to the bed materials in fluidized bed combustor, SO_2 emissions can be reduced because, the probability of removing sulphur deposits from the bed would be very high. However, there are some peculiar problems associated

with fluidized bed combustion in which, its effect on the efficiency and general performance of fluidized bed combustors are numerous.

2.4.3 Disadvantages of Fluidized Bed Combustion (FBC)

Listed underneath are the disadvantages of Fluidized Bed Combustion.

- Corrosion
- Clogging
- Starting time of the bed in some cases is tolerably too long
- Emissions from the bed
- Fouling
- Slagging

2.4.4 Fluidization

This phenomenon occurs in a fluidized bed combustor when a fluid is passed upward through a bed of solid particles, which may be sand or other solids. At a low fluid flow rate, the bed remains a fixed bed because the fluid just penetrates through the void spaces between the stationary particles Figure 2.3

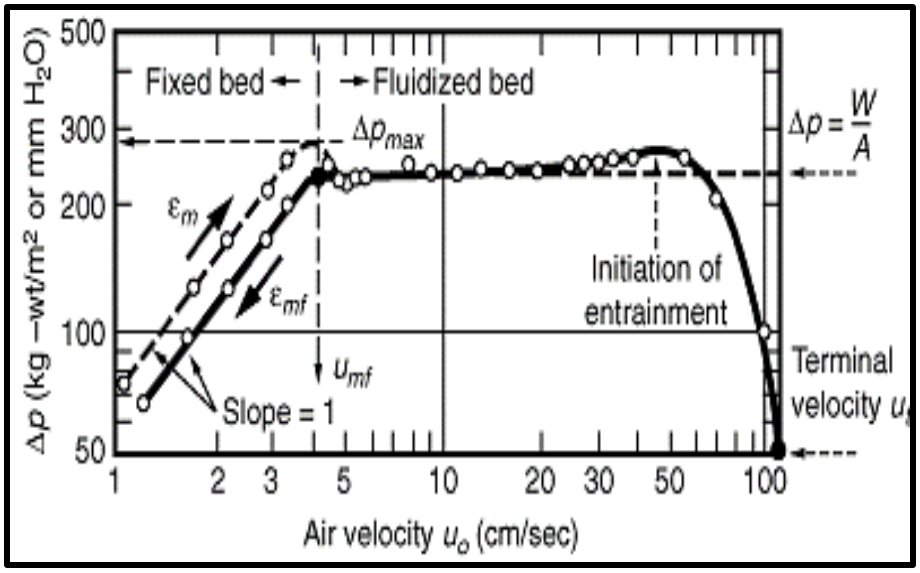

Figure 2-3 Illustration of fluidization particles [54]

A further increase in the fluid flow rate, the force applied is just enough to shake the bed and the bed becomes expanded. At a higher fluid flow rate, a stage is attained when the bed particles become suspended [57, 58].

At this point, the drag force on the particles created because of upward moving fluid counter balances the weight of the bed particles. The bed particles thus become suspended completely and then fluidized. Any further increase in the fluid flow rate will not have any significant impact on the bed pressure drop. This happens because; the bed is already well aerated therefore, may not require any further influence to deform it. The pressure drop across any section of the fluid is almost equal to the weight of fluid and particles in the bed. The Velocity at which fluidization takes place in the bed is the minimum fluidization velocity U_{mf}. Beyond the minimum fluidization velocity, bubbling fluidization occurs in the bed at a minimum bubbling velocity, U_{mb}, Figure 2.4. At this stage, the particles begin to exhibit many of the properties of fluids. [54, 59-61].

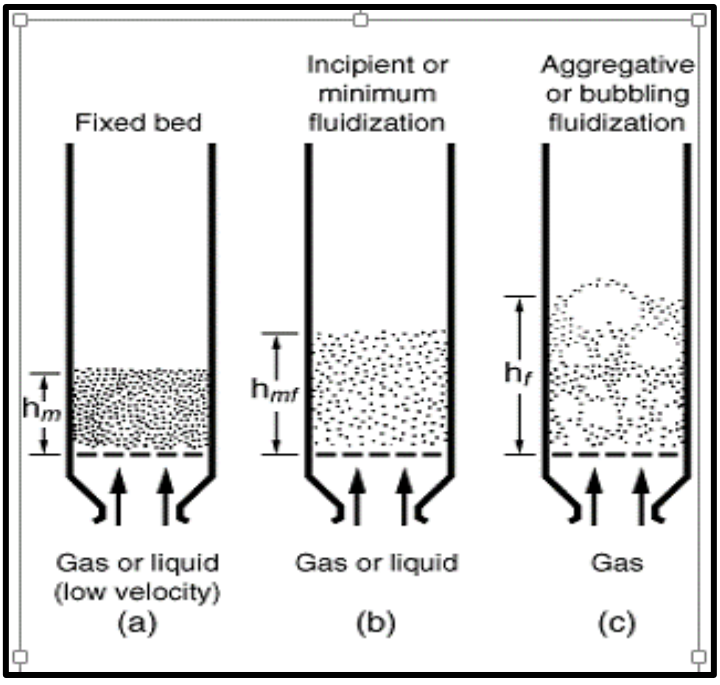

Figure 2-4 Gradual transformation in fluidization of particles [54]

Minimum fluidization velocity is the least amount of velocity required to significantly influence and actualize fluidization of the bed particles in a fluidized bed. Minimum fluidization velocity is not applicable to a fixed bed, since the bed and its contents are static throughout the combustion of biomass fuels process. The minimum fluidization velocity in a fluidized bed can be determined mathematically and analytically using the following Ergun's equations [61]

$$\boldsymbol{U_{mf} = \frac{d_p^2(\rho_s - \rho_g)\cdot \varepsilon_{mf}\varphi_s^2}{150\mu \qquad 1-\varepsilon_{mf}}} \ , \quad \boldsymbol{R_{ep,mf} < 20} \tag{2.2}$$

$$\boldsymbol{R_{ep,mf} = \frac{d_p u_{mf}\rho_g}{\mu}} \tag{2.3}$$

If the values for φ and ε, (sphericity and voidage respectively) for the material are not known, then Equation 2.4 can be used to calculate minimum fluidization velocity. From the equation, it implies that increasing the bed temperature will lead to increase in the minimum fluidization velocity of the bed particles.

$$\boldsymbol{u_{mf} = \frac{\mu}{d_p\rho_g}\left[(28.7)^2 + 0.0494 \ \frac{(d_p^3\,\rho_g\,(\rho_s - \rho_g)g)}{0.00018^2}\right] - 2.87} \tag{2.4}$$

Increasing the bed operating temperature increases the minimum fluidization velocity U_{mf} of the bed particles. Equation 2.4 (Ergun's equation) can be used to predict minimum fluidization velocity in FBC. In a sodium oxide dominated biomass fuels, the eutectic temperature at which agglomeration occur in the bed is higher than when a potassium oxide dominated biomass fuels are combusted even at the same pressure.

Bed height has significant influence on the pressure drop on bed particles during the combustion of biomass fuels in fluidized bed. Bed pressure drop increases as the bed height increases [14, 16, 51]. The following modified Carman-Kozney equation is very relevant in the prediction of pressure drop at various bed heights for mixture of irregular particles [10, 62].

$$\Delta P = 180 \frac{U_g \mu_g (1-\varepsilon)^2}{\varphi_s^2 d_{p,sm}^2 \varepsilon^3} H \quad 2.5$$

Increasing the gas velocity to adequately high value, the drag force on the particles will overcome and surpass the gravitational force on the particles. At this stage, the particles will be entrained in a gas and carried out of the bed. The point at which the drag force is about to exceed the exerted gravitational force is the maximum fluidization velocity. The terminal velocity is the velocity of the particles when the gas velocity is equal to zero. It is the same as the slip velocity between the particles and the fluid in a pneumatic transport [54, 59-61].

Aside from agglomeration, other problems associated with combustion of biomass fuels in beds are corrosion, fouling, erosion, and slagging. Some researchers have carried out some research work in this area but their work has concentrated on combustion of single or blend of biomass fuels in fluidized bed combustors. This research work will look at combustion of some selected single and blend of biomass fuels in a laboratory-scale fixed bed using a Gooch crucible as the combustion chamber.

2.5 Fixed Bed Technology

The two most prominent energy conversion technologies are the fixed bed and the fluidized bed. Fixed bed technology is gaining popularity in the conversion of biomass fuels to energy. In a fixed bed, the solid fuel is introduced into the bed through the opening at the top and allowed to flow downward the reactor or the combustor where reaction of the materials take place [63, 64]. The combustion gas (heat source) may be applied from the bottom (counter current) or from the top (co-current). The downdraft fixed bed is the best cost effective for small and medium scale energy conversion technologies and operations [65]. The biomass fuel particles are fed to the combustion chamber through the top and allowed to react with the pre-heated bed materials (silica sand) while heat was supplied to the combustion chamber through the grates. In this present research, the perforated bottom of the Gooch crucible represents the grates, Figure 2.5

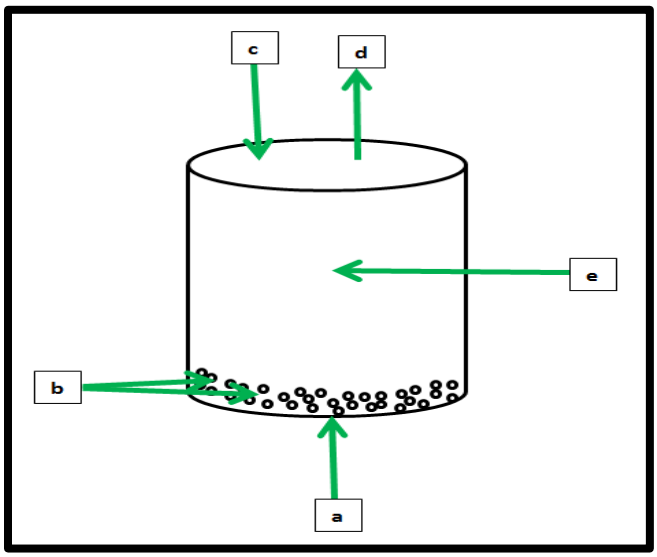

Figure 2-5 Schematic of a typical downdraft Fixed bed

a) Oxidant (heat source)
b) Grates
c) Biomass fuels
d) Gas emitted
e) Fixed bed of biomass fuels.

In fixed beds, combustion of fuels takes place in a stationary bed. There are two major types and they are “underfeed stocker and the grating firing”. Generally, with these methods, primary air is supplied through the grate from below and initial combustion of fuel takes place on the grate through gasification process[65].

The underfeed stocker is a relatively cheap option for biomass combustion but only palatable for small – scale systems. It is very easy to control compared to other technologies. This also has some shortcomings such as ash removal problems, limited in terms of fuel types because ash rich fuels may not be successfully burn with this system and this may cause instability of combustion conditions. The grate firing has some advantages over the under feed stocker such as accommodation of high fuels with high ash and moisture contents. In addition, fuels with

different particle sizes can be accommodated. Other types of grate firing systems are travelling grates, moving grates, fixed grates, and rotating grates.

However, there are some advantages and disadvantages associated with this type of technology as listed below:

Advantages of fixed bed technology are;

- Very easy to develop
- High conversion rate per weight of catalyst
- Affordable and low cost of construction, operation and maintenance
- The technology is very effective at high temperatures and pressures

Disadvantages of fixed bed technology are;

- Heat transfer from or to the reactor may be difficult
- Occasional side reactions may occur
- Temperature control may be difficult
- There is possibility of temperature gradient occurrence.
- Replacement of catalyst may be difficult during operation.

2.6 Energy Sources

There are three major forms of energy sources; the renewable, non-renewable, and nuclear energy [28, 66]. Non-renewable energy is also referred to as the conventional form of energy, which includes the fossil fuels (coal, crude oil, and natural gas). Renewable energy resources are also termed alternative energy resources that may be inexhaustible and these includes; biomass, solar, wind, hydropower, marine and geothermal energies. Good percentage of renewable energy comes from biomass [67]. Selection of an energy to be used at a specific time must be based on the economic value, social, environmental and safety. There is a positive

correlation between availability of energy and economic activities of a given society either large or small [28, 68].

Biomass energy is the energy derived from the combustion of biomass fuels using the energy conversion technology. Different categories of conversion technologies include the fixed bed and the fluidized beds. Fixed bed was the traditional method of biomass / coal conversion in the past [58, 69]. Fluidized bed on the other hand may be atmospheric (circulating or bubbling), or pressurized type. Biomass energy is an alternative source of energy that is very useful in some applications such as; domestic (heating and cooking), industrial (tobacco curing, beer brewing, coffee and tea drying) and in the laboratories [17, 59, 70]. It is obtained from plants and animal waste, industrial wastes, agricultural wastes, sewage and municipal wastes with the highest percentage of this coming from wood and wood wastes [2, 23, 29]. Conversion of organic wastes to useful fuels (synthetic) can be achieved through gasification, pyrolysis, bioconversion, and hydrogenation processes.

Demirbas [2, 28] in his research showed that the presence of metals in ash, in association with other elements (sulphur and silica) in fuel and coupled with the availability of chlorine, are the major cause of unwarranted problems and reactions within the fluidized bed. Chemistry of the ash formed in the bed indicated that, some elements such as K, Na, Mg, S, Cl, P, Ca, Fe and Si, are actively involved in reactions leading to the development of problems such as fouling, slagging and agglomeration in the bed during biomass combustion [2, 12, 71, 72].

In biomass fuel containing high alkali content especially potassium, direct coalescence of potassium with quartz sand particles in gas phase usually contribute to the formation of a eutectic compound, potassium silicate, K_2SiO_3 that has a lower melting point than the alkali or the silica in the sand particles [3, 4, 10, 21, 73]. It thus melts and form coatings on the sand particles which results to agglomeration in the bed.

2.6.1 The organic wastes

Organic residues or wastes are those that contain some carbon compounds, which are derived from plants or animal materials. Numerous biomass fuels fall under this category [26, 27].

2.6.2 Municipal solid wastes

These include mostly the organic solid proportion of waste products emanated from urban settlements especially the cities. It is a combination of domestic, demolition, and light industrial wastes [26].

2.6.3 Commercial and Industrial solid waste

These consist of wastes having organic origin (organic part of the waste) emanated from commercial and industrial processes or manufacturing operations. About 36 mega tons of these wastes are generated in the United Kingdom each year. About one third of this is combustible. The furniture industry has been estimated to burn about 35,000 tons as off-cuts and this represented about one third of its total production [58].

2.6.4 Wastes from the industries

These may either be woody or non – woody wastes. Woody wastes are sawdust, chips, pellets, logs and, off – cuts. Examples of non – woody waste are paper pulp/ waste [74], textile wastes, and sewage sludge [19, 26]. Sewage sludge is the liquid waste from the industries and the cities. The moisture content is very high therefore, it would require drying for it to be suitable for combustion processes in the combustion beds [75].

2.6.5 Agricultural wastes

This refers to the waste products from agricultural activities and systems, which may be either dry or wet [17, 26, 34]. The dry stuff includes those agricultural products that are not primarily for immediate consumption. Examples are straw, poultry litter and corn Stover (leaf and stalk from harvested maize). The wet wastes include wastes from dairy cattle, beef cattle, pigs, and sheep [76].

2.6.6 Food wastes

These are wastes from all food supply, processing or any food chain. In most cases, the moisture content is always high, therefore proper drying of biomass is necessary for it to be suitable for the anticipated combustion purposes.

2.7 Energy Crops

This refers to plants or crops that are cultivated or planted and grown specifically for energy production. They are further classified into herbaceous crops (miscanthus), short rotation woody crops (willow), and grass (switch grass) [77, 78].

2.8 Forms of Biomass Fuels

Biomass fuels appear in various forms; pellets, chips and pulverized. Wood pellets are very good form of biomass for combustion processes. These are type of wood fuel generally produced from compacted sawdust or other wastes from sawmilling processes. It can also be obtained from other sources such as branches of trees leftover after logging. Pellets are produced in different types and grades as fuel for electric power plants, homes, and other applications [79-82].

One of the qualities that make it suitable for combustion purposes is its regular geometry and small sizes which make it easy to load into the burner through the hopper. In an industrial zone, loading of pellets into the burner can be done pneumatically via conveyor or manually depending on the capacity of the burner [83]. Pellets high density also allows compact storage and rational transport through a long distance.

To have a perfect and complete combustion, pulverized coal can be co–fired with biomass. This is widely used in large power stations. Coal is finely shredded to about 70% - 80% of it by weight. The combustion reaction is always faster using this method because finely grounded coal has large surface area per unit weight than larger particles, thereby reducing complete combustion time by 1 to 2 seconds [84].

In most cases, particularly for industrial applications, the pellet size is about 6mm to 8mm diameter and about 20mm to 25mm long. It can be produced with low moisture content below 10% that allows it to be able to burn with high combustion efficiency [4]. However, the pellets

are grinded to smaller particles before the commencement of the combustion processes on them.

2.9 Coal Utilization in a Fixed Bed Combustion of Biomass Fuels

Coal is a non-uniform organic fuel, formed from partly or largely decomposed plant materials. It is widely co-fired with biomass fuels to enhance the biomass combustion characteristics. Coal formations usually occur through a process under very high pressures and temperatures. Coal took its source from different types of plants. This singular fact about coal makes it to have different types of characteristics and properties [85, 86].

2.9.1 Coal Processes (Thermo Chemical Combustion Processes of Coal)

There are different types of coal combustion processes available with the most commonly used being the direct combustion while others are gasification, carbonization, coking, and liquefaction. Direct combustion was the dominant coal process in the past [87-89]. The combustion also depends largely on the particle size of the coal as itemized below:

Pulverized coal combustion - (smallest particles are required).

Fluidized bed combustion - (medium - sized particles are required).

Fixed bed combustion - (larger sized particles are required).

2.9.2 Coal Slurry

Coal slurry can be produced appropriately when mixed with either water or oil. When mixed with water, it is referred to as coal- water mixture, (CWM). This could serve as a replacement fuel for oil fired boilers. It is also very useful in the ignition of pulverized coal in existing furnace systems and as a substitute fuel in gas turbine [90-92]. When mixed with oil, it is termed coal-oil mixture, (COM). Research has indicated that, this cannot be used as oil replacement fuel because there is always the problem of ash fouling associated with it when used [93, 94].

2.9.3 Coal Classification and Characteristics

There are various types of coal in existence. The best way to classify coal is through the use of the standard set by the American Society of Testing Materials, ASTM [95]. This is based on the heating value and the fixed carbon content of the coal under consideration. Coal is classified into four categories; lignite, sub-bituminous, bituminous, and anthracite.

(i) Lignite: This coal has the lowest value in terms of ranking. It has very high moisture content and a low heating value [96] .

(ii) Sub Bituminous: This is dull and black in colour. It actually lost some moisture content but still has low heating value and splits parallel to the bedding [37, 96].

(iii) Bituminous: This type of coal is dense, brittle, compacted, banded and display columnar cleavage and a dark black colour. It also shows more resistant to disintegration in air than the lignite and the sub bituminous coals [96, 97]. It also has low moisture content and a high heating value.

(iv) Anthracite: This is a highly metamorphosed coal with jet-black colouration. It is very hard, lustrous, and brittle. It breaks with a conchoidal fracture (smooth rounded surface). It has a very low moisture content and very high heating value and carbon content [98].

Coal possesses some properties upon which its characterization could be developed. Among these are; specific gravity, thermal conductivity, specific heat, density, swelling index, temperature, moisture content, and the heating value [97, 98].

Precisely, to use coal appropriately, its composition as characterized by proximate and the ultimate analyses must be known [98, 99]. The proximate analysis determines the moisture content by drying, percentage of volatile matter, ash content, heating value and the fixed carbon content. While the ultimate analysis gives the composition by weight of carbon C, hydrogen H, oxygen O, Nitrogen N, and Sulphur, S.

2.9.4 Specific Gravity of Various Species of Coal

Specific gravity is the ratio of the density of a substance to the density of a known reference substance at the same volume. The reference substance is always water. Specific gravity of some coals are shown in Table 2.1

Table 2-1: Specific Gravity of Different Species of Coals [100]

TYPES OF COALS	SPECIFIC GRAVITY
Anthracites	1.7
Bituminous	1.4
Sub bituminous	1.3
Lignite	1.2

It clearly shows that, anthracite coal has the highest specific gravity while lignite coal has the least. This makes anthracite coal the best for co-firing purposes because it exhibits more char glow during combustion and last longer [69, 100].

2.9.5 Ignition Characteristics of Coals

Coal ignition is a phenomenon whereby a visible flame is produced at high temperature or a no visible flame at low temperature when there is a reaction between the fuels (coal) and an oxidizer (usually oxygen) [101, 102]. It is often characterized by the time required to achieve a temperature for a specific combustion task. It is worthwhile to note that, there is no specific ignition time recommended or exist but it all depends on a particular combustion task [102, 103]. This is a very important factor in the use of coal as fuel during the combustion of biomass fuels.

A typical biomass fuel on dry basis possesses moisture content of between 4% and 8% and low calorific value of 17MJ/Kg to 18MJ/Kg. Coal on the other hand, has very high calorific value of

23.02MJ/Kg which contributes largely to its ability to burn effectively with char glow [104]. Burning flame of biomass fuel is higher than that of the coal, but burning time of coal is much longer than that of biomass fuel. Biomass fuels burn with flaming glow while coal burns with char glow.

To improve on the combustion characteristics of biomass fuels in the combustor chamber, biomass fuels are usually co-fired with coal. The ignition time of coal depends largely upon the coal particle arrangements [101, 104]. There are three of such arrangements;

(i) Single coal particles: There is no interaction among the particles in this category.

(ii) Coal piles: This occurs in moving bed, fixed beds and coal storage layers.

(iii) Coal clouds: This exists in pulverized – coal combustors, furnaces, and in gasifiers. It is more pronounce in fluidized bed combustors.

2.9.6 Variables Influencing Coal Ignition and Propagation Processes.

Literature survey revealed that, dry coal would ignite faster than the wet coals because self-heating criteria are more pronounced in the dry coals. It was also discovered that, the adiabatic self-heating temperature (ASHT) above which ignition will occur for lignite is 291 K (18 ^{0}C) and 378 K (105 ^{O}C) for bituminous coals in an adiabatic calorimeter. Dry and high volatile content coals will self-ignite in 7 hours if exposed to air that is moist [101, 105]. Some of the factors affecting coal ignition are presented in Table 2.2

Table 2-2: Variables Influencing Coal Ignition

Coal type	Oxygen percentage	Rate of energy addition
Coal size	Initial temperature	Initial pressure
Coal size distribution	Dust concentration	Auxiliary gaseous fuels

It takes several hours at low temperature for a coal pile to ignite meanwhile a coal dust can be ignited in milliseconds at high temperatures. Generally, in coal processes, heating rate of 10^{6} k/s had been established. Some researchers concentrated their research on the mechanisms of bed

agglomerations coupled with the prediction time and temperatures at which it would occur [106]. Others depended on the use of standard ash test but this was criticized because agglomeration could occur below the deformation temperature of the ash.

Addition of very good forest biomass to energy crops could reduce the formation of SO_X, NO_X, and HCl emissions. It can also lead to reduction in agglomeration formation by diluting the presence of alkali metals like Na and K and minimize every other problem associated with low ash fusibility temperatures such as slagging and fouling [107]. The use of additives like dolomite CaMg $(CO_3)_2$ would result in a reliable bed management and may also control SO_2, HCl and agglomeration.

Biomass briquettes can be applied to reduce CO_2 emissions in fixed bed combustion. It is a substitute to coal and charcoal [108, 109]. They are used in the industries to heat up boilers in order to generate electricity from steam. It is also useful in the developed Countries as co-firing. This can be achieved when coal is pre-mixed with briquettes to generate enough heat to the combustor. This will reduce CO_2 emissions by partially replacing coal with materials already contained in the carbon cycle. Briquettes contain majorly organic materials [110-112].

2.10 Effects of Moisture Content on Heating Values of Biomass Fuel

Moisture content of biomass fuel is the reduction in weight recorded when the fuel is combusted to a temperature of about 108 ± 2 ^{0}C in an oven and allowed to cool down [79]. Heating value of any substance or fuel is the amount of energy released per unit mass or per unit volume of the fuel when the fuel is completely burnt. Percentage of moisture content in each biomass fuel has a magnificent influence on the heating value of such fuel [113].

The higher the moisture content, the higher the latent heat of vapourization which also plays prominent role in the determination of both the higher heating values and the lower heating values of biomass fuels. Net calorific values of biomass fuels decreases as the moisture contents increases while the density increases as the moisture contents increases, Figures 2.6 and 2.7

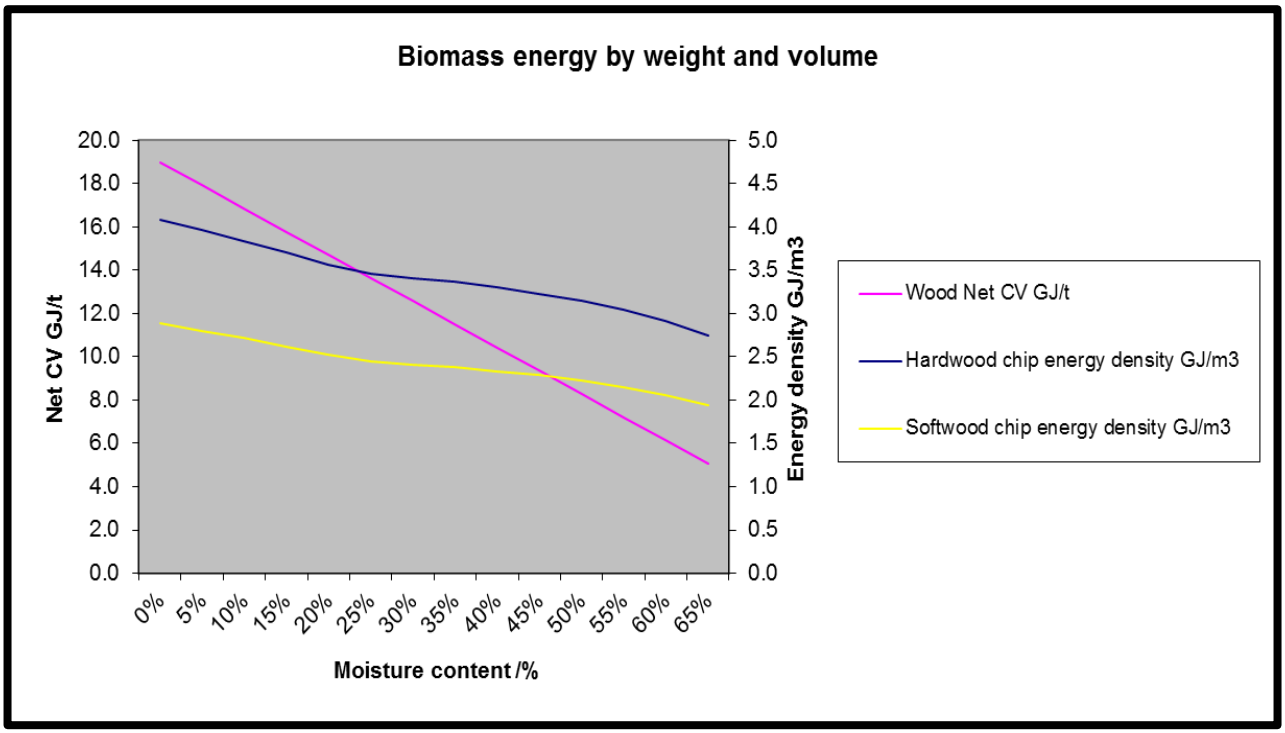

Figure 2-6: Influence of moisture content on Biomass Energy and volume [79].

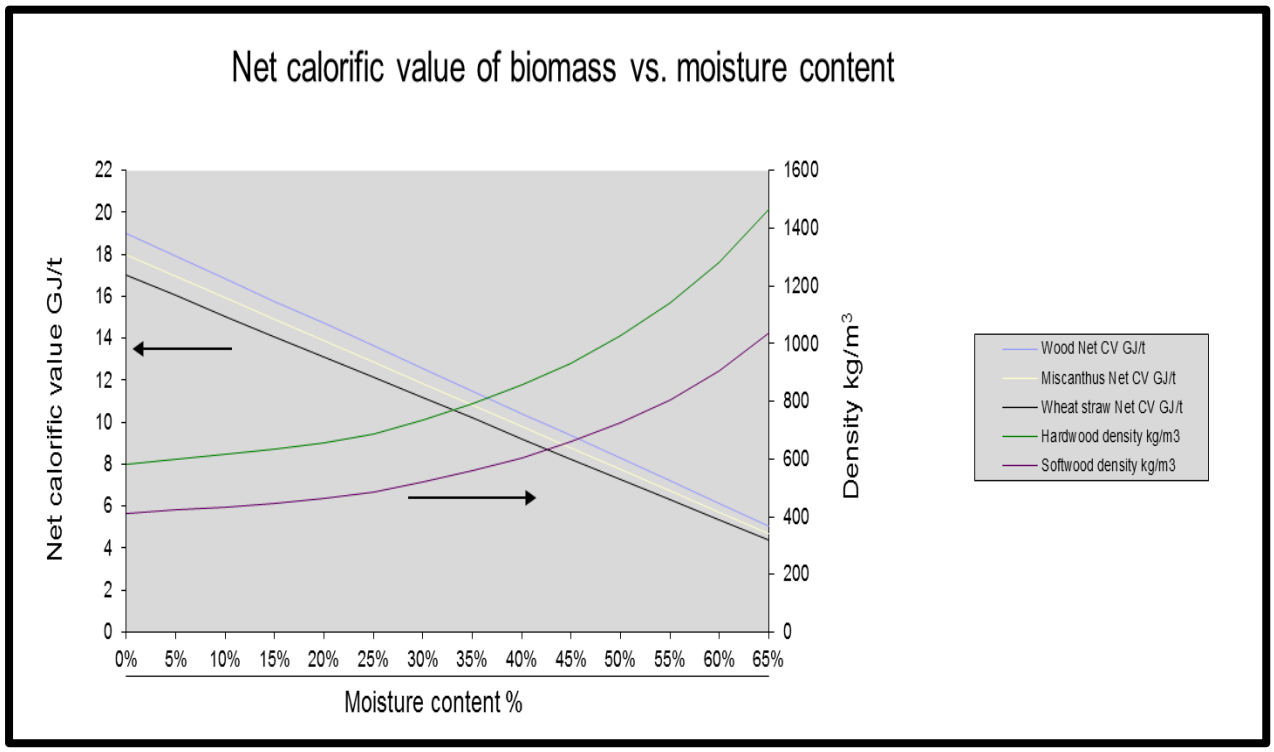

Figure 2-7: Influence of moisture content on the calorific values of Biomass Fuels [79].

2.10.1 The proximate analyses

It is also referred to as thermo gravimetric analyses (TGA). It shows the contents of biomass fuels in terms of the moisture content, volatile matters, fixed carbon and the ash. However, the fixed carbon content in each biomass fuel is also very significant in the determination of the heating value of biomass fuels [114].

2.10.2 Fixed carbon

Fixed carbon refers to the solid left in the furnace after volatile matters has been distilled off. This mostly comprised of carbon but contain traces of hydrogen, oxygen, Sulphur and nitrogen that did not completely escape with the flue gases. The quantity or the percentage of fixed carbon available in biomass fuels has much influence on the heating values. In fact, it has been used to estimate the heating value of coal in the past [115]. This is different from the ultimate carbon of the fuels because some of the carbon is usually lost in hydrocarbons alongside the volatiles.

Analytically, fixed carbon can be determined thus;

Fixed carbon = 100 – (moisture content + volatile matter + ash) 2.6

Therefore;

Fixed carbon + moisture content + volatile matter + ash = 100 2.7

2.10.3 Lower heating value, LHV

This implies that, water completely remain as vapour therefore, the latent heat is not released with the combustion products. Lower heating value is the net heating value, NHV. It can also be described as the overall amount of heat given out when a unit mass (1 Kg) or a unit volume of fuel is completely combusted in the presence of excess oxygen O_2 while the bye products of the combustion is permitted to disappear to the atmosphere without the latent heat [115].

Analytically; [6, 113]

LHV = HHV - Latent heat of vapourization, KJ/kg 2.8

2.10.4 Higher heating value, HHV

Higher heating value indicates that, water is in liquid state; hence, the heat released includes the latent heat. This is the same as gross heating value, GHV. It is described as the total amount of heat generated during the complete combustion of a unit mass (1 kg) of fuel in the presence of excess oxygen while water vapour (product of combustion) cool down to liquid at a room temperature. The SI unit is MJ/kg. Latent heat of vapourization is added to the total heat evolved [116].

Mathematically stated;

HHV = LHV + Latent heat of vapourization, KJ/kg 2.9

These values are very significant in analysing the combustion characteristics of biomass fuels and could be determined experimentally or by calculation using some empirical equations. Experimentally, the bomb calorimeter or adiabatic calorimeter could be used to determine the heating values of biomass fuels [116]. Biomass fuel with higher heating value is a very good material for combustion purposes. The heating values of a biomass fuel can be estimated from its compositional analysis using the empirical equation 2.10 based on the ultimate analysis of the fuels:

$HHV_D = 0.35X_C + 1.18X_H + 0.01X_S - 0.02X_N - 0.10X_O - 0.02X_{ASH}$ [3, 114, 116]. 2.10

Where, X_C, X_H, X_S, X_N, X_O, and X_{ASH} are the mass fraction of the compositions of the biomass fuel on percentage dry basis of Carbon C, Hydrogen H, Sulphur S, Nitrogen N, Oxygen O, and Ash contents respectively. Unit is in KJ/kg dry mass.

The HHV is also a function of the fixed carbon (FC) and can be computed using Equation 2.11

$HHV = 0.196(FC) + 14.119$ 2.11

Where HHV_D = Higher heating value on dry basis. This equation is suitable for the determination of the HHV for both biomass fuels and coal [3, 114, 116].

2.11 Significance of Heating Value of Biomass Fuels and Coal

Heating value of a substance (biomass fuels and coal) is a measure of the ability or tendency of that substance to undergo self-heating reactions while supported by cellulosic or other fibrous materials in air. In addition, it represents the auto ignition ability of the substance under such condition [12, 114]. Proximate and ultimate analyses data are significant in the analytical determination of the higher heating values of some selected biomass samples. Specifically, in the research conducted by [6, 116], 12 samples obtained from Turkish sources were analysed and the correlation of the obtained values was checked with the calculated values using equations 2.10 and 2.11. The results are presented in Table 2.3

Experimentally**,** the higher heating values were measured with the use of the bomb calorimeter per the ASTM D2015 standard method. Proximate analyses were carried out according to the ASTM E870-82 standard test methods [114].

Structural and chemical analyses of biomass samples were carried out per ASTM D1103-80 and ASTM D1104-56 standard test methods. Blend of some of the biomass samples could produce good and suitable materials for fluidized bed combustion [117]. Moreover, the blends could also generate valuable materials for combustion in a fixed bed.

Table 2-3: Comparison between the calculated and experimental calorific values (HHV, MJ/kg) of some selected biomass fuels [114]

Sample	C	H	O	N	Ash	Experimental HHV, MJ/Kg	Calculated HHV, MJ/Kg (eqn 2.10)	Calculated HHV, MJ/Kg (eqn 2.11)
Olive husk	50.0	6.2	42.2	1.6	3.6	19.0	18.8	19.2
Hazelnut shell	52.9	5.6	42.7	1.4	1.4	19.3	19.2	19.7
Hazel seed coat	51.0	5.4	42.3	1.3	1.8	19.3	19.2	19.4
Soft wood	52.1	6.1	41.0	0.2	1.7	20.0	19.8	19.6
Hard wood	48.6	6.2	41.1	0.4	2.7	18.8	19.0	19.0
Wheat straw	45.5	5.1	34.1	1.8	13.5	17.0	17.3	18.7
Wood bark	53.1	6.1	40.6	0.2	1.6	20.5	20.3	20.4
Waste materials	48.3	5.7	45.3	0.7	4.5	17.1	17.2	17.4
Tea waste	48.6	5.5	39.5	0.5	1.4	17.1	17.2	16.8
Spruce wood	51.9	6.1	40.9	0.3	1.5	20.1	19.7	19.7
Beech wood	49.5	6.2	41.2	0.4	1.4	19.2	19.0	18.9
Ailanthus	49.5	6.2	41.0	0.3	1.7	19.0	18.9	19.0

Comparing the calculated higher heating values obtained using the two equations 2.10 and 2.11, there is appreciable correlation in the values. This was observed in hazelnut shell, hazelnut seed coat, soft wood, hard wood, wood bark, waste materials and spruce wood. On a broad outlook, in comparison between the calculated and experimentally obtained higher heating values, there is a good correlation between the obtained values. This was clearly displayed in hazel nutshell, hazel seed coat, wood bark, and waste materials. Generally, there exist close similarity in the high heating values obtained experimentally and the calculated.

2.11.1 Volatile Matters in Biomass Fuels

These combustible gases vaporize easily whenever biomass fuels are being combusted. In most cases, they are hydrocarbons such as carbon monoxide CO, methane CH_4 and hydrogen H [118, 119]. In addition, some incombustibles such as carbon dioxide CO_2 and nitrogen N could be present. Volatile matter is an index of the percentage of gaseous fuels contained in biomass fuels and coal. Typical range of volatile matter in biomass fuels is from 70% to 80% while coal volatiles ranges from 8% to 45% [3, 120].

2.12 Ash Content of Biomass fuels and Coal

The percentage of ash content present in biomass fuels is one of the factors used to determine its suitability for combustion purposes. The leftover of unburnt fuels in the combustion chamber / bed is termed the ash content [121]. Its value is significant in the combustion of biomass fuels experiment especially in the design of the furnace grate and ash handling system of the furnace Biomass fuels with high ash contents are capable or have very high tendency of complicating combustion problems especially agglomeration in the bed during combustion [114, 122]. Composition of main ash forming elements in biomass are K, Na, Ca, Al, Si, Mg, P, Mn, Fe, S, and Cl. Pure sawdust, peat, mixture of 10% peat/sawdust, and 20% peat/sawdust were investigated and analysed. Percentage of potassium K in all the samples appeared to be similar. Silicon content in the pure peat and 20% peat/sawdust are higher than the pure sawdust. Manganese Mn content in all the samples is almost negligible. However, all the elements are present in the samples but in varying quantities, Figure 2.8

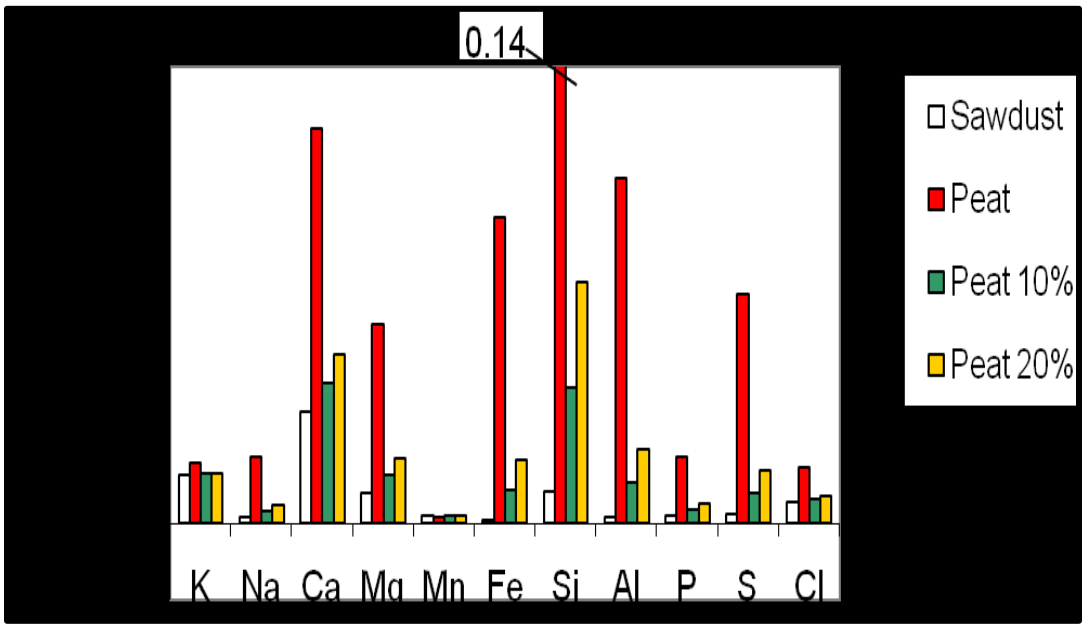

Figure 2-8 Composition of main ash forming elements in biomass [114]

Moisture contents of typical coals from literature fall within the range 4.3 % to 9.43 % by weight on dry basis. In the same trend, the ash contents, volatile matters, and the fixed carbon of these coals appeared relatively moderate, Tables 2.4 and 2.5

Table 2-4: Typical Proximate Analyses of Some Selected Coals [123, 124]

Parameter	**Indian Coal, %**	**Indonesian Coal, %**	**South African Coal, %**
Moisture	5.98	9.43	8.5
Ash	38.63	13.99	17
Volatile matter	20.70	29.79	23.28
Fixed Carbon	34.69	46.79	51.22

Table 2-5: Typical Ultimate Analyses of Some Selected Bituminous Coals Samples [123, 124]

Parameter	Sample 1, %	Sample 2, %	Indonesian coal, %
Moisture	5.98	4.39	9.43
Ash	38.63	47.86	13.99
Carbon	42.11	36.22	58.96
Hydrogen	2.76	2.64	4.16
Nitrogen	1.22	1.09	1.02
Sulphur	0.41	0.55	0.56
Oxygen	9.89	7.25	11.88

2.13 Setback Associated with Combustion of Biomass Fuels

Various complications are usually experienced during the combustion of problematic biomass fuels / blends of biomass fuels in fixed beds and fluidized beds. This menace, if not controlled could disrupt the whole combustion process or even damage the combustion equipment. Some of these unwarranted occurrences are as discussed below:

2.13.1 Bed agglomeration

This is a fundamental problem usually experienced during the combustion processes involving biomass fuels or coal blended with biomass fuels. Severe case of agglomeration can lead to complete defluidization or total loss of the bed contents [10, 125]. Agglomeration is produced in the bed because of the reaction between the alkali metals in the biomass fuels and the silica from the sand, this union usually led to the formation of eutectic compounds [126]. These alkali metals especially potassium, K are always released during the combustion process and react with the silica SiO_2 from the sand to form coagulates or sticky layers on the surface of the bed

materials as a results of the eutectic compound produced (alkali-silicates) [10, 125]. The silica sand conserves heat and act as a heat reservoir [59].

The Eutectic compounds have a lower melting point than either the silica in the sand or the alkali in the biomass fuel. Consequent upon this, it melts sharply below the melting point of either the silica or the alkali and form coagulates on the surface of the sand particles [10, 125, 127]. Ash fusion temperature for biomass fuel is between 1000 ^{0}C to 1600 ^{0}C [36, 128].

2.13.2 Corrosion

This is the Corrosion of the interior walls of the combustion chamber or the tubes within the boiler but, the extent of the damage is largely dependent on the feedstock introduced during combustion process [129].

2.13.3 Clogging

This is a phenomenon whereby, some thick and sticky substances emanating from the combustion process are formed within the bed or on the internal surface of the combustion chamber thereby interrupting the efficient operation of the bed. It can lead to uneven bed temperature distribution.

2.13.4 Emissions

These are the specific emissions emanating from the bed during the combustion processes of biomass fuels. It includes CO_2, SO_2, CO, and NO, although biomass is CO_2 neutral. Thermal NO_x formation is experienced at elevated temperatures.

2.13.5 Slagging and Fouling

Formation of deposits especially on the boilers wall in areas directly opened to flame radiation is called slagging. Meanwhile, fouling on the other side refers to deposits formed on the areas not directly exposed to flame radiation such as closely spaced tubes in the convention areas of

boilers. This has devastating effects on the combustion equipment in that; it can complicate the deposition rates within the equipment.

Accumulation of irrelevant substances on the surface of the bed combustor is termed fouling. It is a serious problem in design and operation. It poses a major threat in the operations of the bed for quality assurance and production reliability [3, 130]. Where this occurs, the thermal conductivity on the affected surface is reduced or interrupted. This can lead to decrease in the effectiveness of the processing device (heat exchanger). If this persists, there is every tendency for the surface area to be reduced and this may cause pressure drop across the entire device. Additional or extra cost would be required to normalize the bed surfaces if production targets are to be met. Moreover, fouling is believed to have been produced because of vapourization of the volatile inorganic elements during the process of combustion.

Although reduction or total elimination of agglomeration in a laboratory - scale fixed bed combustion of biomass fuels is the major/specific task of this research, an attempt will be made to control any emissions that may arise from the combustion processes.

2.14 Consequences of Agglomeration in Combustion Beds

Loss of bed content and intent are the major consequences of bed agglomeration. Agglomeration causes steady rise in bed temperature particularly when the combustion of biomass fuels takes place in a fluidized bed. When agglomerates are produced in the bed, melt layers increase and this causes formation of lots of lumps with wide voidage. The drag force created by the upward fluid flow no longer counter balances the weight of the particles (weight of suspended particles > drag force) therefore, the bed becomes depressed or defluidized.

Defluidization time decreases with increasing bed temperature (The higher the temperature the quicker agglomeration occurs in the bed), Figure 2.9

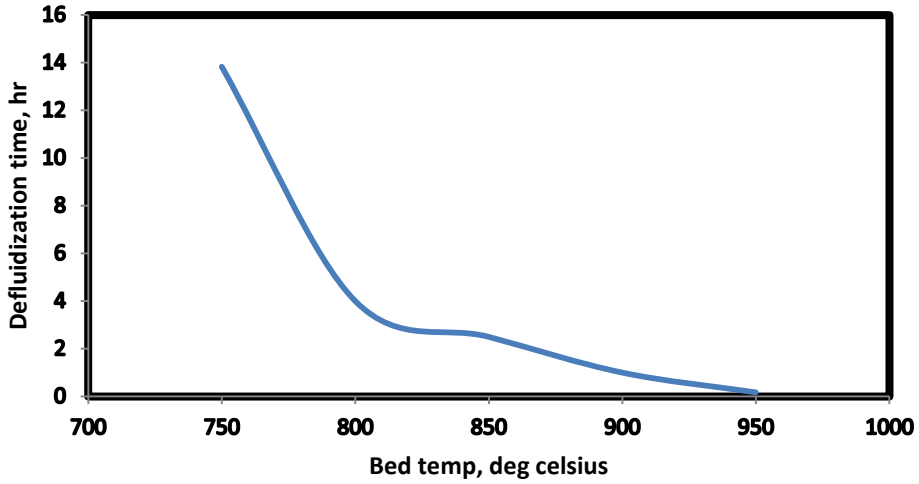

Figure 2-9: Graph of bed temperature versus defluidization time [131]

However, in fixed bed combustion of biomass fuels, there is no suspension of bed particles or bed materials before the formation of agglomerates in the bed. Temperature plays a major role in agglomerates formation in the bed. Addition of biomass fuels to the bed materials (silica sand) that has been pre-heated to the ignition temperature of between 250 ^{0}C to 260 ^{0}C causes an increase in the combustion chamber temperature [17, 22]. Biomass fuels burns with fuming flame while coal burns with char flame. As interaction among the bed particles continue, alkali metals (mostly Potassium K) from biomass fuel react with the silica from sand and produced a low melting temperature eutectic mixture in the form of alkali – silicate. The eutectic mixture has a lower melting point than the parent materials (alkali and silica sand). It melts quickly and produce lumps of agglomerates in the combustion chamber.

2.15 Effects of Pressure, Gas Velocity, Bed Height and Temperature on Bed Particles during Combustion

Pressure has significant effects on the agglomeration formation in fixed bed reactors. The higher the pressure in the combustion chamber, the lower is the risk of agglomeration formation

within the bed reactor. With addition of additive (kaolin) and increasing the pressure in the combustion chamber, agglomeration has been established to occur only at elevated temperatures [2, 4, 10, 132]. Consequently, pressure, temperature, fluidization velocity, and air mass flow rate are operating conditions that can have significant effects on agglomeration in combustion beds. Increase in the gas velocity in the combustion bed will lead to a better interaction and proper mixing of the particles thereby elevating the force acting on the agglomerates. Consequently, fuel ash in the gas will also increase and defluidization in the bed will be decelerated. Increase in the gas velocity leads to extension of the defluidization time, Figure 2.10 Pressure fluctuations are also very conversant with fluidized beds combustion of biomass fuel experiments. Variance of high frequency pressure fluctuations was considered as agglomeration warning in fluidized bed combustion of pine seed shell [59, 133].

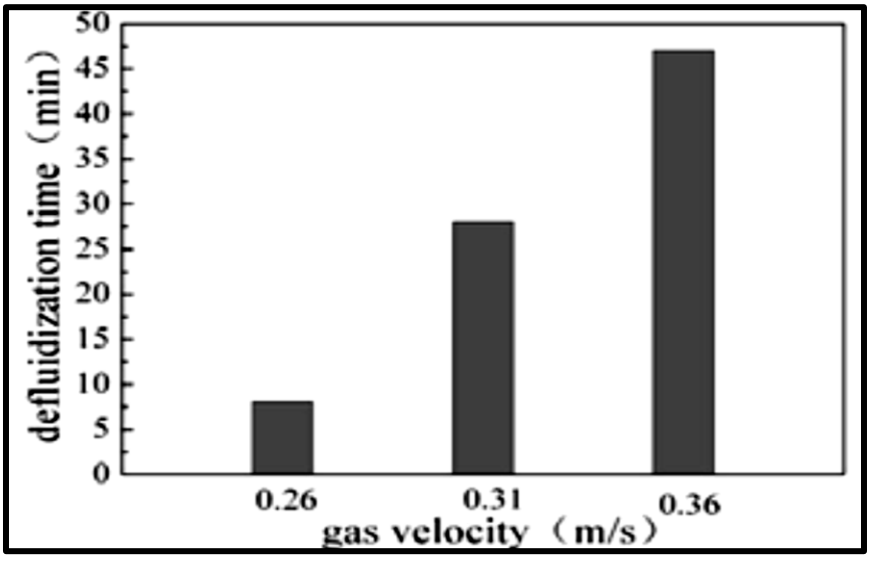

Figure 2-10 Influence of gas velocity on defluidization time in beds [59]

Many experiments on bench-scale and pilot-scale indicated a continuous decrease of the variance based on high frequency (100 Hz) pressure fluctuation measurement during the experiment involving pine seed shell. As agglomeration proceeds in the bed, variance in the pressure changes significantly, Figure 2.11

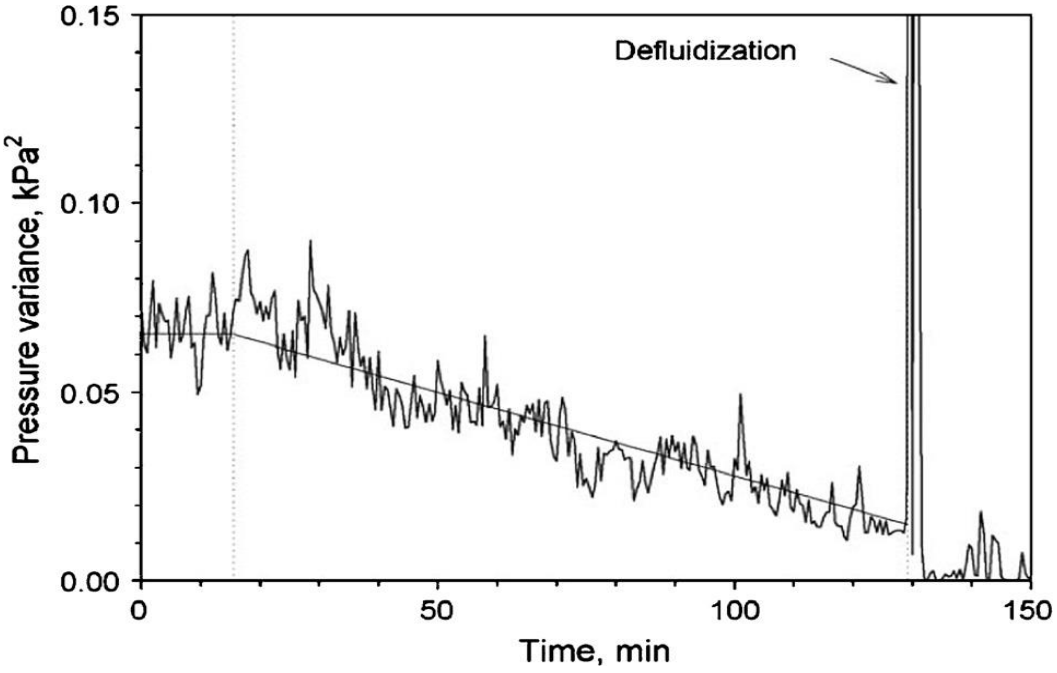

Figure 2-11 Pressure fluctuation variance in FBC during the combustion of pine seed shell [59]

Fluidization velocity and air mass flow rate have more influence on agglomeration in fluidized bed compared to a fixed bed where temperature and pressure are the predominant factors that influences agglomeration in the combustion beds [59, 133]. Temperature has appreciable effect on defluidization time that decreases as temperature increases. Cost incurred in the processing of the combustion of biomass fuels is considerably increased. Moreover, combustion efficiency of the equipment (boiler) is reliable.

2.16 Preceding Approach to Solve Agglomeration Problem

Some researchers have attempted to tackle the agglomeration problem with different approaches. The ash composition for coal is quite different from that of biomass. A research conducted showed that, the presence of metals in ash, in association with other elements (Sulphur and Silica) in fuel and coupled with the availability of chlorine, are the major cause of unwarranted problems and reactions within the bed [2, 134].

The chemistry of the ash formed indicated that, some elements such as; K, Na, Mg, S, Cl, P, Ca, Fe and Si are actively involved in reactions resulting in the formation of fouling, agglomeration

and slagging in the bed during biomass combustion. It was made clear that, Chlorine reactions could also lead to the formation of corrosion within the bed thereby complicating agglomeration and that, at high temperatures, ash formation could also contribute to severe corrosion formation in the bed [135].

Some bed materials and the agglomerates formed during the combustion of selected biomass; straw, olive residues, peat, bark, and reed canary grass were subjected to electronic analysis using the scanning electron microscopy (SEM) and energy - dispersive X-ray spectroscopy (EDX) to determine the structure and the elements making-up the samples respectively.

In addition, the reaction of calcium with the quartz sand (bed materials) by diffusion was identified as an aid and mechanism of agglomeration in the bed. Diffusion of potassium in a very small available space where other ash compounds could not reach resulted in the formation of potassium silicate. At an operational temperature, these materials were, melted and hence allowed other higher diffusion rate of potassium leading to the formation of silicates. Calcium silicate was discovered to be more stable than any of the silicate compound formed [125, 134, 136].

Moreover, it was discovered that, the coating or the outer layer formed was relatively inhomogeneous and consisted of small particles in form of fuel-ash compositions. Apart from the fact that, the small particles formed sticks to the quartz sand, there may be gas-phase reactions, condensations and collision with melted ash particles to form agglomerates. These actually displayed the mechanisms for the formation of agglomeration, particularly in fluidized beds.

A research on bed agglomeration was carried out which led to the prediction of time and mechanisms of bed agglomeration in the bed [5, 137]. During the research, agglomeration problems were observed. Fluidized bed combustion of some biomass residues (Pine seed shells) was conducted and it was discovered that, agglomeration was the major problem observed during this process [125]. This was again due to the high alkali contents present in the biomass. The combustion was carried out in both the bench-scale and a pilot- scale reactor. It was also observed that, some factors had magnificent influence on the agglomeration problems among which are the sand particle size, the combustor size, and the type of biomass used. Further

analysis conducted on the particles after the bed had been defluidized indicated that, potassium and sodium formed a eutectic compound with the sand, which melted at a temperature below the melting point of either the sand or the alkali [138].

The analysis was done with the use of SEM and EDX. All the experiments conducted using the two facilities eventually ended up in bed defluidization. Samples of agglomerates generated is shown in Figure 2.12

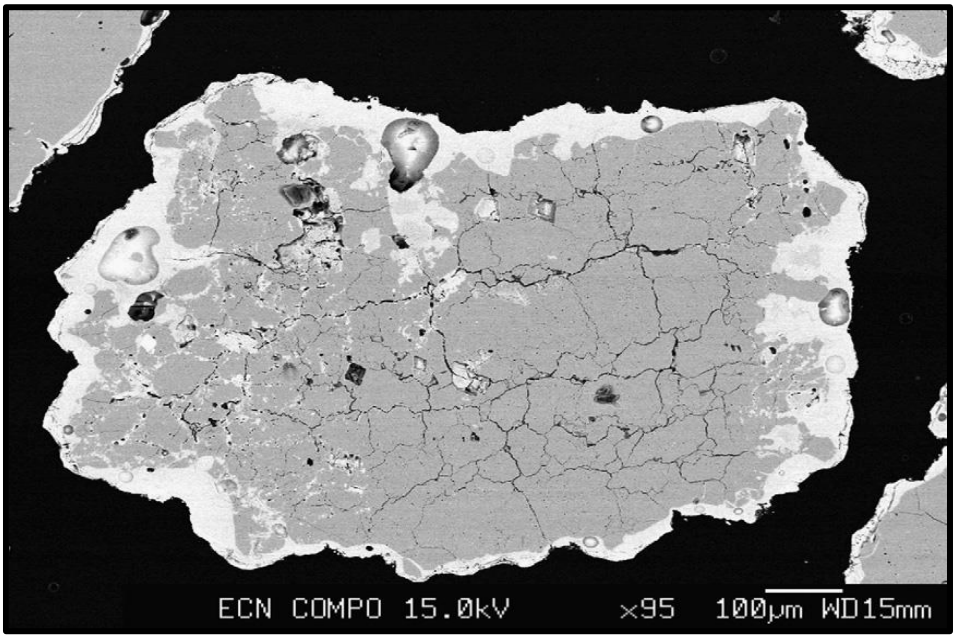

Figure 2-12 SEM image of agglomerate produced from pine seed shell [138]

Formation of agglomeration in the combustion bed began because of two major reactions [139]. The first was the reactions between the sand particles and the alkali present in the fuel which led to the formation eutectic compound that has a lower melting point than the sand, or the alkali thereby forming agglomerates [7, 10, 125]. The other one is the continuous usage of inertial force to break the formed agglomerates against the internal surfaces of the bed. If the first reaction prevails, defluidization of the bed is certain even though the agglomerates are brittle.

Agglomeration behaviours of wheat stalk was investigated. Results indicated that, defluidization time decreases with increasing the combustion temperature. Samples were retrieved at 750 ^{0}C

and 800 ^{0}C. Post combustion analyses carried out on the bed samples was analysed with SEM and EDX at 750 ^{0}C and 800 ^{0}C Figures 2.13 and 2.14 respectively.

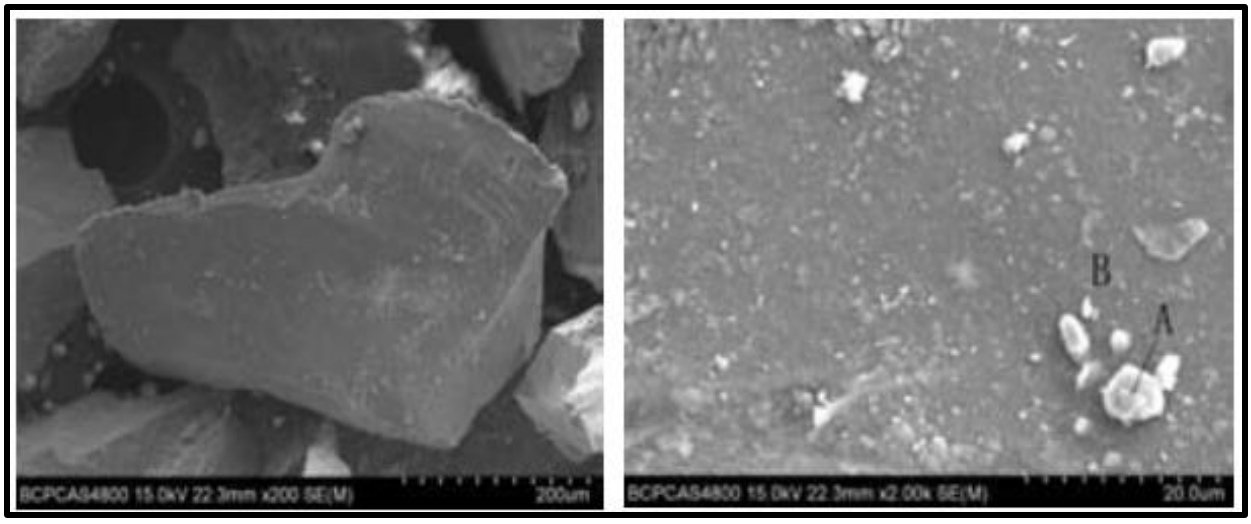

Figure 2-13 SEM image of particles and EDX analyses at 750 ^{0}C [10]

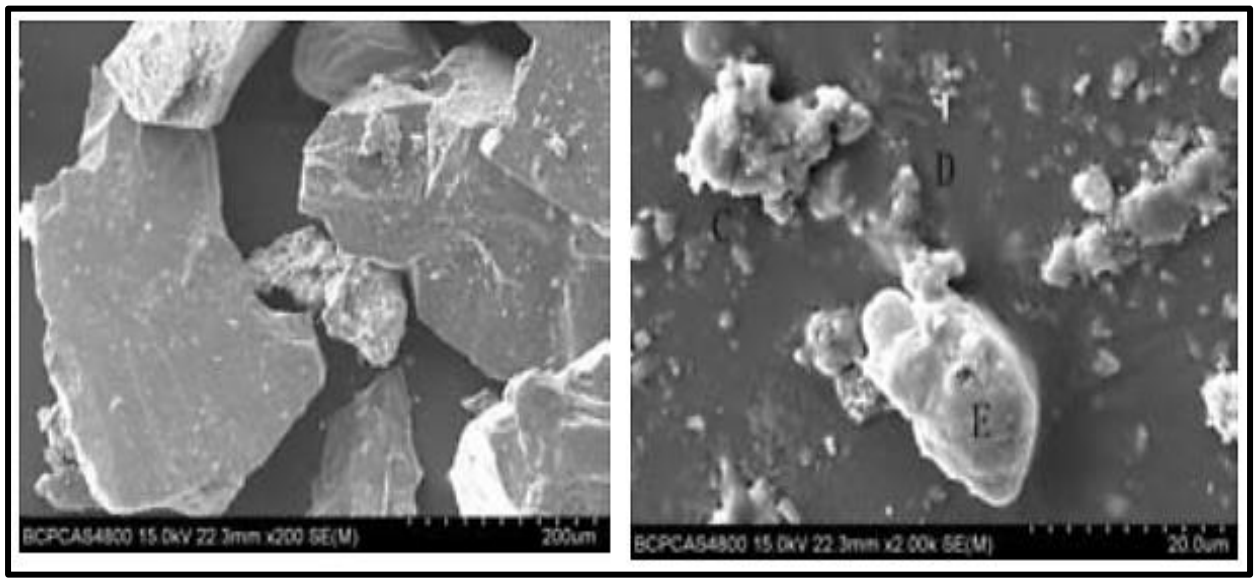

Figure 2-14 SEM image of particles and EDX analyses at 800 ^{0}C [10]

SEM results showed that, elongation in the particle size was an indication that, agglomeration had occurred in the bed. EDX results also confirmed that, Potassium K, calcium Ca, and silicon Si played prominent roles in agglomerates formation in the bed. Some of the elements present at the spots considered could not be determined hence; they were represented on the EDX Table 2.6 as nd.

Table 2-6 EDX of wheat particles on the surface (wt. %) [7, 10, 125]

spot	O	Si	K	Ca	Cl	Mg	P
A	52.23	17.20	10.96	8.54	4.52	2.52	4.04
B	53.52	46. 48	nd	nd	nd	nd	nd
C	49.88	27.09	15.41	7.62	nd	nd	nd
D	47.83	43.54	8.63	nd	nd	nd	nd
E	48.80	35.99	15.21	nd	nd	nd	nd

Two South Australian low rank coals (Kingston and Lochiel) were known to be very rich in sodium and sulphur (Na & S). Fluidized bed combustion of these fuels was carried out under a tightly controlled operating condition. At a certain time, operational problems were noticed within the bed [140, 141]. It was observed that, the particles of the bed became sticky, agglomerates formed and the bed defluidized. This was caused by melting of alkali because of the reaction between the alkali (sodium) and sand particles, which formed sodium sulphates, a eutectic compound that has a lower melting point than either the sand or the alkali thereby forming agglomerates. This research was carried out to compare the behaviour of these two coals [140-142]. The experiment was performed using both the bench – scale and the pilot – plant operation. Additive, kaolin (clay rich) was added to the Kingston coal during the combustion. An examination of the ashes formed from the two coals indicated that, ash formed from the Kingston coal was found to be less sticky than that from the lochiel coal. This led to the Kingston having a longer time before agglomeration was noticed compared to the Lochiel coal in which agglomeration of its particles was experienced too early and very predominant. Upon analysis of the ashes, it was revealed that the kaolin had reacted with sodium to form a compound, nepheline. This has a very high melting point that reduced the formation of sodium sulphates (agglomerates) within the bed [143]. This actually displayed the effectiveness of kaolin at combating agglomeration.

Combustion behaviours of phosphates rich fuel are grossly different from that of woody fuels. It was established that, phosphate rich fuels exhibit very high stability during combustion.

Moreover, phosphorus has very high affinity for cations such as potassium more than silicon and this is the major element responsible for ash transformation reactions.

Agglomeration and defluidization could occur when resources are co- combusted or combusted separately. This was investigated when high-sodium, high - Sulphur South Australian lignite (coal) was allowed to undergo combustion through spouted-bed gasification process [138, 144]. It was noticed that, agglomeration could be avoided in the bed if the operations are conducted under a low bed temperature below 850^{o}C, maintaining consistent increase in the fluid velocity, and maintaining ash content of the bed below 80 in terms of percentage by volume. An average South Australian coal contained high sodium and sulphur. During fluidized bed combustion of these coals, these elements form a eutectic compound in form of sodium - calcium - sulphates that has a very low melting point. This created a very sticky paste within the bed. The lumps continued interaction with the inert bed materials (silica sand) causing the particles to further stick together and forming larger sized agglomerates.

Investigations revealed that some elements such as potassium K, sulphur S, and chlorine Cl are, released during the co-combustion of coal and biomass (straw) [145-147]. It was discovered that, the amount of KCl released during the co-combustion was far more than available during the combustion of biomass fuel alone. This was carried out under a controlled temperature of between 800^{o}C and 1100^{o}C and the amount of gaseous potassium released was merely lower than what the value should be. Meanwhile, the amount of sulphur released during this process depends largely on the temperatures and the proportion of the mixtures. At elevated temperatures and lower straw (biomass), percentage of sulphur S, released in the mixture was high because of the reactions between the K_2SO_4 obtained from straw and coal-clay minerals [144]. With high straw percentage and under a low temperature, sulphur from coal would not be predominant because, it would have been captured by the calcium and potassium present in the straw.

This therefore, is one of the best methods to control emissions emanated from co-firing in fluidized bed combustion. It was discovered that, firing of pure straw resulted at a great disadvantage because the bed was characterized by various degrees of bed operational problems such as fouling, high emissions such as HCl and SO_2. With the co - combustion of coal

with low sulphur biofuels, emissions such as CO_2 and SO_2 would be greatly reduced. A good proportion mixture of 20% straw was suggested [144, 148].

Analysis of the variations in measured bed temperatures and pressures were initially used to determine bed agglomeration tendencies. Experiments were conducted on about eight different process variables. The results indicated that, for a fuel, the amount of bed material and air to fuel ratio during heating and ashing, could not adversely affect or influence bed agglomeration temperatures. It was clarified further that, bed particle size, the ashing temperature and the ash to bed materials ratio could have a significant impact on bed agglomeration temperatures [3, 140]. The agglomeration temperature was determined to be 899^{o}C with a reproducibility of ± 5^{o}C (Standard Deviation). With this method, agglomeration temperature of various blends of biomass fuels could be determined [2, 149].

2.17 Emissions from Combustion of Biomass Fuels

Emissions are products of combustion, it may be gaseous, solid and other particles usually released to the atmosphere during combustion processes [150]. Emissions emanated from automobiles and industrial zones are very common in the society. When emissions are released to the atmosphere, there would be uncomfortable and contaminated air available. Heavy pollution increased global warming, and gross threat to the global eco system [151].

The emissions from the bed combustion of solid fuels especially biomass fuels includes; CO_2, CO, N, NO, NO_2, SO_2, NO_X, SO_X, S [152] . These emissions depend largely on the type of materials being combusted. Biomass is a very good material for combustion purposes because it is CO_2 neutral [4, 153]. Addition of calcium carbonate, $CaCO_3$ (lime stone) to the bed will remove Sulphur, S emissions from the system. The operating condition of fluidized bed combustion in terms of temperature (600 ^{O}C to 1000 ^{0}C) does not permit formation of thermal NO_X. High thermal NO_X would be produced at elevated temperatures 1450 ^{O}C and above [154-156].

2.18 Fuel NOx and the Thermal NOx

Fuel NO_X refers to the oxides of nitrogen that are produced during biomass fuel combustion resulting from the reaction between the organically bounded nitrogen and the oxygen in the fuels [157, 158]. This is also called oxidation reaction. Meanwhile, thermal NO_X are the oxides of nitrogen that are generated because of the reaction between the nitrogen in the combustion air with excess air at elevated temperatures above 1000 ^{0}C although, it can be controlled by adhering strictly to the normal operating conditions of the bed. NO_X is highly hazardous in that, it can react with water in the atmosphere and produce acid rain or corrosive acid, nitric acid (HNO_3) which is dangerous to the body [159, 160].

2.19 Sintering Temperature for Biomass Samples during Combustion

Sintering is heating and pressing a material close to its melting point to form a solid shape. Sintering temperature is therefore the temperature at which biomass fuel begins to form porous powdered mass by heating it close to its melting point [11, 125, 161, 162].

A little, above this temperature, melting and fusion of biomass fuels occur and this usually aggravates agglomeration formation in the bed. Generally, biomass fuels have similar properties. The sintering temperature of these biomass fuels is very significant in that; it can be used to study their ash fusion characteristics and agglomeration behaviour in the bed. Sintering temperature of some selected typical biomass fuels are as shown in Table 2.7.

Table 2-7: Typical Sintering temperature of some selected biomass fuels [163]

Samples	Sintering Temperature, °C
Reed canary grass	800 – 900
Wheat straw	700 – 750
Bagasse	800 – 850
Bagasse leaves	850 – 950
Wheat straw B	650 – 700
Olive stone	950 – 1050
Forest residue	>1000
Lucerne	625 – 650
Eucalyptus	700 – 750

2.20 Agglomeration in a Fixed Bed Combustion of Biomass fuels

Agglomeration is the major operational problem usually experienced during the combustion of biomass or biomass co-fired with coal in combustion beds. If agglomerates formation in the bed during combustion processes is not controlled, the consequence is that, it may lead to complications in the combustion process [5, 125, 140]. Agglomeration is the formation of agglomerates in combustion beds. It occurs because of melting and fusion of alkali metals (Sodium Na, Potassium, and K) present in biomass fuels with silica present in sand particles forming a eutectic compound [134, 138]. This eutectic compound has a lower melting temperature than either the alkali or the silica. It melts abruptly below the melting point of either the silica or the alkali with potassium K playing the prominent roles [10, 22].

Outcome of a research carried out [164, 165] showcased the mechanisms by which agglomeration takes place in a fluidized bed combustor during the combustion of biomass fuels or biomass fuels

blends. It was discovered that, the main mechanism of agglomeration and defluidization in fluidized beds is the reaction between biomass fuels and silica from sand which changes the fluidization behaviour of sand particles at high temperature. The research was conducted on pine seed, agglomeration occurred during the combustion process. The combustion was carried out in both the bench-scale and a pilot- scale reactor. SEM and EDX analyses were conducted on the bed samples (agglomerates). It was established that, agglomeration actually occurred in the combustor bed. Alkali metals, Potassium K and sodium Na formed eutectic compounds with the silica in sand particles and this melted at a temperature below the melting point of either the sand or the alkali [166]. This was a confirmation that, agglomeration was caused by the high presence of alkali metals in biomass particularly potassium K and sodium Na. Similarly, a research conducted [166] clearly indicated that, agglomeration usually occur in the combustor beds during the combustion processes. Samples of the agglomerates formed during this process are shown in Figures 2.15 and 2.16. Scanning electron microscopy image of the agglomerate produced is shown in Figure 2.16 d.

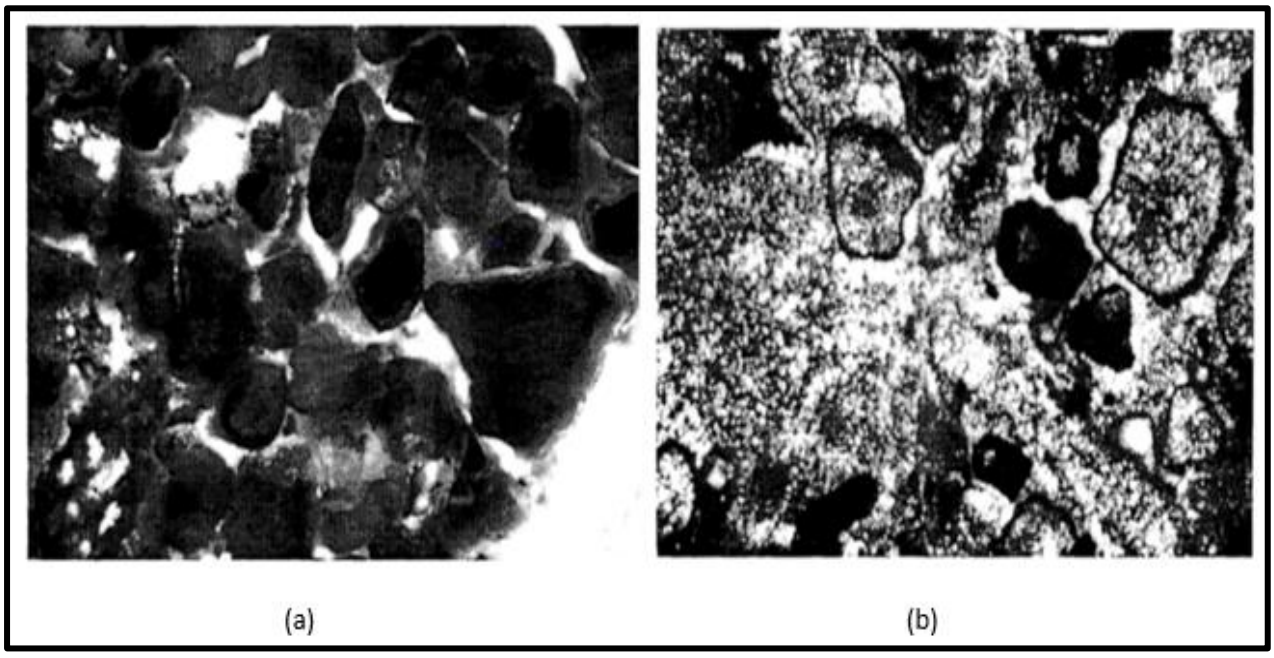

Figure 2-15 (a) Photomicrograph of a particle from an agglomerate found on the wall in a circulating fluidized bed combustor, (b) Photomicrograph of agglomerate in the loop seal area of a circulating fluidized bed combustor [166].

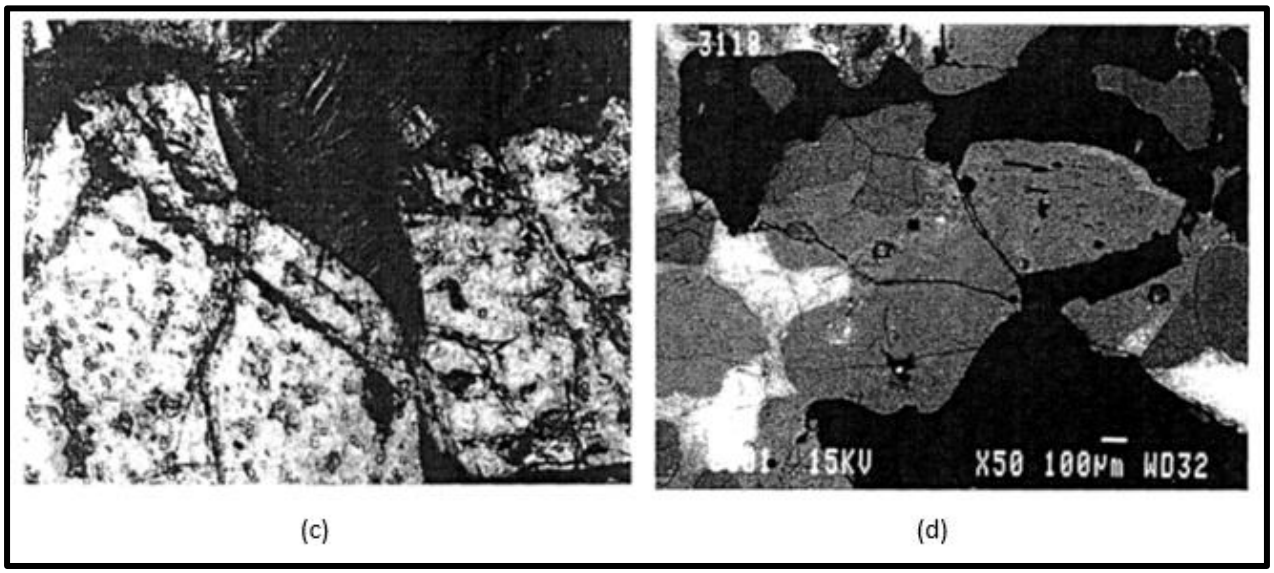

Figure 2-16 (c) Photomicrograph showing mineral reactions around quartz grains in the agglomerated bed material, (d) Scanning electron photograph of agglomerated bed particles. [166]

Combustion of some fuels such as willow, logging residues, wheat straw, and wheat distiller's dried grain with soluble (wheat DDGS) was carried out in a 5Kw bench-scale bubbling fluidized-bed reactor using olivine and quartz sand as bed material [167]. During the combustion process, agglomeration was observed to have occurred in the bed. Post combustion analysis was carried out on the bed materials, bed ash particles, and the agglomerates using scanning electron microscopy SEM and energy dispersive X - Ray spectroscopy EDX for morphology and elemental composition respectively. Powder X - Ray Diffraction (XRD) for the determination of crystalline phases was also conducted on the bed samples.

Results indicated that, agglomerates were produced with the inner layer consisting majorly bed material composition and outer layer containing composition like fuel ash characteristic. The inner layer elemental composition comprised of Si, K and Ca. Agglomeration was also formed because of adhesion of bed particles by molten silicate in form of K-Silicate. This conforms to findings from other researchers[3, 22]. Analysis of the variations in the measured bed

temperatures and pressures were initially used to determine bed agglomeration tendencies. It was clarified further that, bed particle size, the ashing temperature and the ash to bed materials ratio could have a significant impact on bed agglomeration temperatures [127, 138, 168]. With this method, agglomeration temperature of various biomass fuel blends could be predicted.

2.21 Mechanisms of Agglomeration in combustion beds

Mechanism of agglomeration formation refers to the process by which agglomeration occur in the combustor bed. The basic mechanism of agglomeration is the formation of a low melting compound that lead to increased particle stickiness and subsequent formation of agglomerates [14,7]. Biomass fuels are very rich in alkali metals. These alkali metals mostly potassium K (metals in group 1 of the periodic table of elements) react with the silica in sand forming a eutectic compound (alkali – silicate) which has a melting point lower than that of the alkali or the silica. This compound melts abruptly and form lumps called agglomerates in the bed. Viscous flow sintering was identified as the major mechanism of agglomeration, in a fluidized bed. Diffusion/migration of potassium compounds through a very small available space where other ash compounds could not penetrate amounted to the formation of potassium silicate [3, 10]. At an operational temperature, these materials melted and hence allowed other higher diffusion rate of potassium leading to the formation of silicates. Calcium silicate was found to be more stable than any of the silicates compound formed especially potassium silicates.

This revelation actually conforms to the outcome the research conducted [169-171] that, alkali metals or its oxides, particularly Potassium K, are the main determinants of agglomeration formation in the beds during the combustion of biomass fuels for energy generation purposes. Other alkali metal that could adequately contribute to agglomeration formation in the combustion chambers is the Sodium Na or its oxides. Alkaline earth metals (elements in the group two of the periodic tables), Magnesium Mg, Calcium Ca, also display a significant degree of coalescence during agglomeration in the combustion beds.

Biomass is the percentage of living organisms by weight in a locality. There are two major classes of biomass resources; organic residues / wastes, and the energy crops [2, 172, 173].

Various mechanisms that have been identified to be responsible for the formation of agglomerates in combustor beds are discussed below:

2.21.1 Sintering of coatings mechanism

This is the formation of agglomerates in the combustor bed because of the sintering of coatings mechanism undergone by the biomass fuels particles, Figure 2.17. Sintering is the formation of shapes mostly from solid (powdered form) by heating the substance close to its melting point. During combustion, most of the ash formed appeared as fly ash while the remaining proportion remains in the bed. The inner layer is mostly comprised of the bed materials (silica sand) while the outer layer is made up of the composition very alike the fuel ashes resulting from the combustion processes.

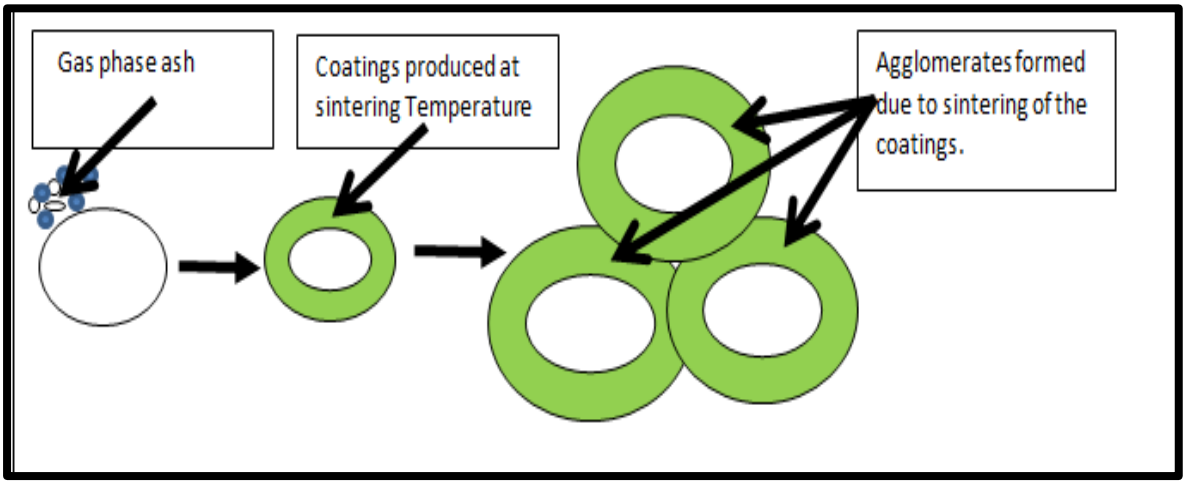

Figure 2-17 : Mechanisms of agglomeration formation by sintering of coatings

2.21.2 Particle interaction mechanism

The other type is the particle interaction mechanism leading to the formation of agglomerates by ash melts. Depending on materials and operating conditions, molten ash particles are,

formed between bed materials [174]. As this persist, the formed molten ash become concentrated between different bed materials resulting in formation of agglomerates, Figure 2.18

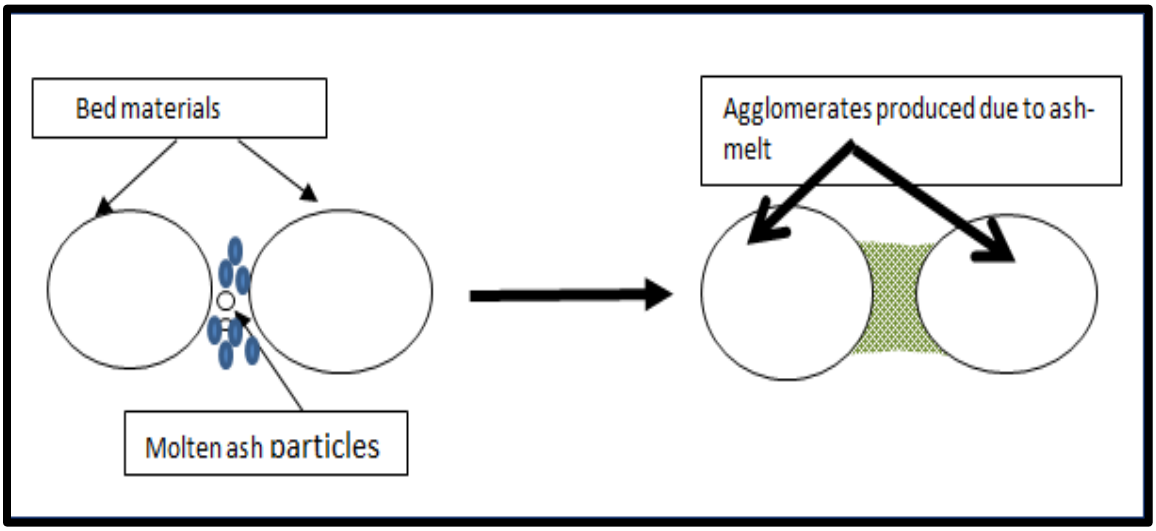

Figure 2-18: Mechanisms of agglomeration by particles interaction

2.21.3 Coating - induced agglomeration mechanism

Reaction and diffusion of calcium into the silica have been identified as the dominating mechanism for typical wood fuels. Low melting calcium based silicate with little traces of potassium K were formed with subsequent viscous – flow sintering and agglomeration [10, 145, 175]. In other biomass containing high alkali, direct attack of the bed particles (silica) by potassium compound in a gas phase formed a low melting potassium silicate, K_2SiO_3. This compound melts quickly and subsequently form agglomerates in the bed [16]. This low melting point is below a typical operating temperature of fluidized beds of 850 ^{o}C.

2.21.4 Mechanisms of chemical reactions

Most agglomeration occurrences in beds at high temperature are induced by chemical reactions through which cohesive particles are formed. It is caused by generation of ash, which has a low melting temperature and reacts with bed materials. Formation of ash from fuels with a high content of alkali especially Na and K has a low melting temperature [176]. Biomass ashes are usually dominated by potassium K, calcium Ca, silicon Si, and traces of aluminium Al. If chlorine is present in the fuels, potassium may likely be released as potassium chloride KCl. Without chlorine in the fuels, carbonates, oxides, hydroxides, or sulphates may be formed.

Under normal fluidized bed combustion, fuels ash interaction occurs resulting in the formation of molten silicates from potassium, sodium, calcium and sulphate-components and possibly solid-solid reactions [177, 178]. Alkali has high mobility therefore; its ability to come into physical contact with other materials is also high with potassium always playing the significant role. Agglomerates produced in fluidized beds are always composed of potassium and silicon sometimes with a little amount of calcium implying that compounds consisting of K_2O-SiO_2 or/and K_2O-CaO-SiO_2 are formed [179, 180]. Eutectic temperature of K_2O-SiO_2 is as low as 770^oC while that of K_2O-CaO-SiO_2 in even lower. Gas-gas reactions may alter the gas-phase composition and route of formation of smaller particles. This is illustrated with chemical Equation 2.12

$$KCl_{(g)} + SO_{2(g)} + H_2O_{(g)} \rightarrow K_2SO_{4(s)} + HCl_{(g)} \qquad 2.12$$

Fuel ashes dominated by calcium can produce crystals that form sintering in bed even at a temperature as low as 500^oC. A little temperature above this, the crystal will melt, Equation 2.13 [133].

$$CaO + SO_2 \rightarrow CaSO_4 \text{ (crystal)} \qquad 2.13$$

Low temperature melting ash constituents can induce formation and accumulation of agglomerate in fluidized bed combustor. These agglomerates are usually composed of sand and

ash particles, bound by fused glassy materials, can result to defluidization (loss of fluidization) or unscheduled shutdown of the bed [59, 181].

A research was carried out [182] scanning electron microscopy (SEM) examination on agglomerates produced in an experiment on some biomass fuels, olive husk and pine seed. The inner region of the agglomerates where extensive melting occurs was enriched with potassium K and sodium Na. The external region was composed of sand particles. Principally, agglomeration mechanism or process is because of the reaction between the alkali in biomass fuels and silica in sand particles.

2.21.5 Continuous impaction of ash particles

This is usually experienced because of accumulation of ash particles at high temperatures thereby leading to the formation of slags inform of agglomerates. The rate of the agglomerates formation is hugely dependent on the particle flux. If not controlled, it can occupy the whole combustion chamber and complicate ash removal processes. [183, 184]

2.21.6 Condensation of volatile matters

Biomass fuels possesses high volatile matters. During the combustion processes of these fuels, biomass exhibits fuming glow ignition with the volatile matters circulating in form of flue gases within the combustion chamber. Upon making contacts with cooled surface, condensation of the hot gases takes place and agglomerates resulted if the process is prolonged [183-185].

2.21.7 Long-term effects of Thermophoresis

This refers to the movement and accumulation of ash particles because of gas temperature gradients in the combustion chamber. It is very common in minute particles especially during initial process [186].

2.22 Chemistry of Agglomeration Formation in Combustion Beds

Formation of agglomerates usually takes place in combustion beds (fluidized and fixed beds) because of continuous interaction between the biomass fuels and the sand (bed materials) during combustion. Alkali metals present in biomass fuels are mostly the elements of the first group of the periodic table, Potassium K, Sodium Na, and Lithium Li. Most Predominant alkali in biomass fuels is the Potassium, K. Sodium Na is often found and could dominate biomass fuels. Agglomerates are produced in the combustion beds upon reaction with the bed materials, sand. [10, 145]

The alkali metal, K possessed the affinity to form eutectic compounds or mixtures with the silica SiO_2 in the sand. The produced eutectic compound has a melting point lower than either of the parent materials; alkali metals and the silica, therefore it melts sharply below the temperature of the parent material. Prolonged interaction of biomass fuels and the bed materials at the same operating condition, usually leads to these materials gluing together and forming agglomerates in the combustion bed. The reaction between the alkali and the silica produces Potassium Silicate K_2SiO_3 that is water soluble, and glass forming silicate or Sodium Silicate $NaSiO_3$ which is also a water glass that can be used as coagulant agent in the wastewater treatment plant.

$$2K + SiO_2 \rightarrow K_2SiO_3 \qquad 2.14$$

$$2Na + SiO_2 \rightarrow Na_2SiO_3 \qquad 2.15$$

Potassium sulphate K_2SO_4 and Potassium chloride KCl usually condensed at the upper furnace walls where it mixed with fly ash. Boiler design, fuel properties and boiler operations contributes significantly to deposits formation during biomass fuels combustion. Most compounds containing potassium K, sulphur S, and chlorine Cl constitutes the principal agents in formation of deposits.

Some sulphur S reacts with alkali metals to produce sulphates, which oxidises to SO_2 during combustion, Equation 2.16

$$4K + 2SO_2 \rightarrow 2K_2SO_4 \qquad 2.16$$

Alkali sulphates are very unstable at typical temperatures such as 900 ^{0}C. At this stage, they are found clinched or condensed on fly ash. Mixtures of fly ash with alkali sulphate always encourage formation of agglomeration in the combustion beds.

Chlorine Cl is an important facilitator of agglomeration in the beds. A reaction between chlorine and alkali metals produces salt on the surface in the form of chlorides, Equation 2.17

$$K + Cl \rightarrow KCl \qquad 2.17$$

When potassium chloride KCl reacts with potassium sulphate K_2SO_4, sticky substance or coating that induces particle attachment because of inertial impaction are formed. Alkaline earth metal like calcium and potassium sometimes react with silicates deposited as fly ash to produce molten and glassy phase leading to the formation of tightly bonded structure, Equation 2.18

$$Ca + SiO_4 \rightarrow CaSiO_4 \qquad 2.18$$

In wood, potassium K is more reduced while calcium Ca and other alkaline earth metals predominate. Alkaline earth metals are elements of group 2 on the periodic table.

2.23 Prediction of Agglomeration in Combustion Beds

Some researchers [4, 5] conducted a research on prediction time at which agglomeration would occur in a fluidized bed and this is also applicable to a fixed bed. Their research was conducted on fluidized bed combustion of biomass residue (Pine seed shells). Agglomeration was the major problem observed during the combustion process. High alkali content particularly potassium present in the biomass fuel accounted for the formation of agglomeration in the bed. The experiment was carried out in both the bench-scale and in a pilot- scale reactor. Further analysis conducted on the particles after the bed had been defluidized indicated that, potassium and sodium formed a compound with the sand, which melted at a temperature below the melting point of either the silica or the alkali. The analysis was done with the use of scanning electron

microscopy SEM and the energy dispersive X-ray spectroscopy, EDX. A study of variations in the bed pressure was conducted. Approximately 60% decrease of the variance from the steady average value was measured indicating the beginning of defluidization. This occurred at exactly 130 minutes in the bench – scale, and occurred at 113 minutes on the pilot – scale FBC. This occurrence largely depends on the operating conditions of the bed.

In another research conducted on fresh rice straw in a bubbling fluidized bed under different operating conditions. Agglomerates were produced in the bed during the combustion experiment. Upon examination through scanning electron microscopy SEM and energy dispersive x-ray spectroscopy EDX, potassium K was the dominating alkali in the fuel just like a typical biomass fuel while there was tremendous increase in the size of the particles after combustion [4, 5]. SEM and optical images of the agglomerates are as shown in Figure 2.19

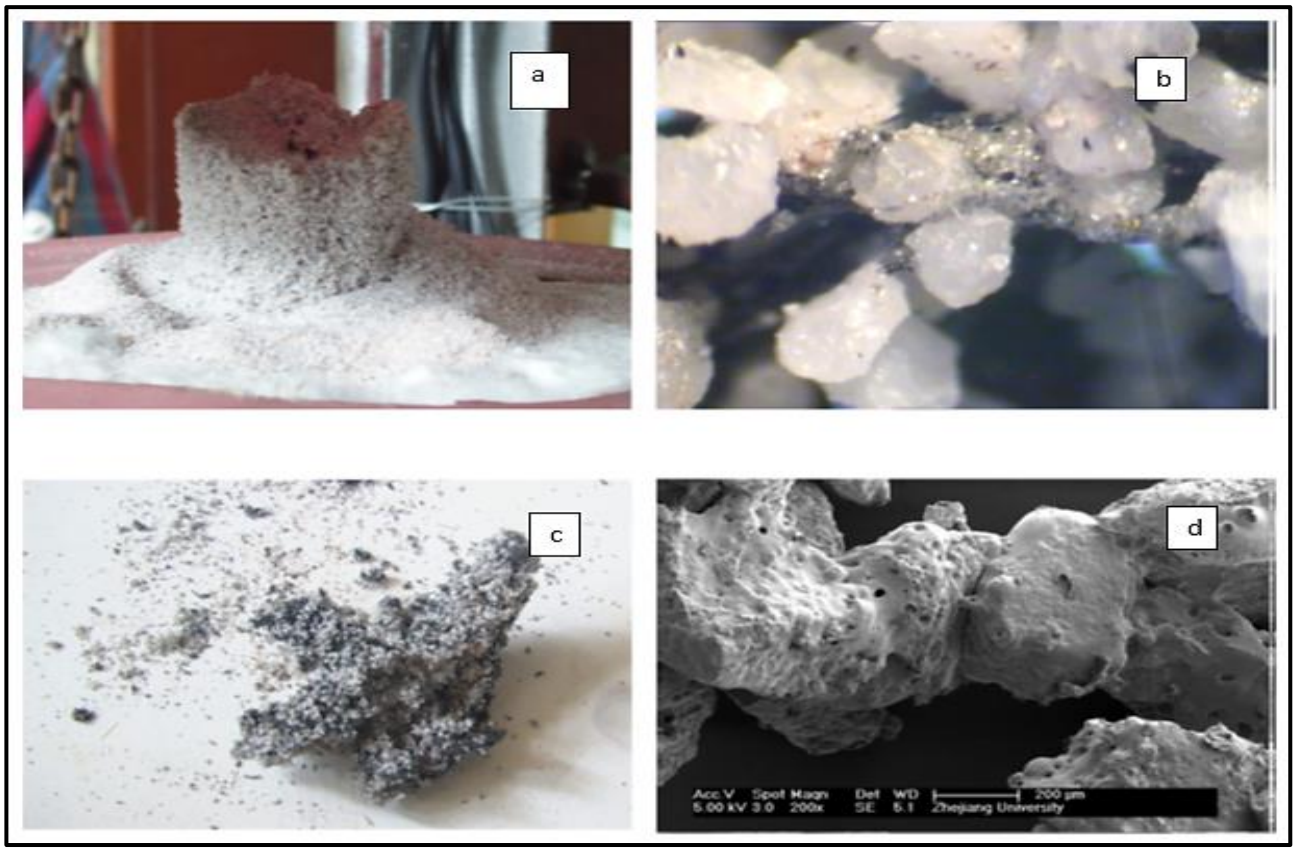

Figure 2-19 (a) Agglomerates produced in the combustion bed (b) Small slag block produced in the bed (c) Detail of bed materials agglomerates under optical microscope (d) Bed material agglomerates under SEM [5]

A research that involved the combustion of some mixtures of biomass (rapeseed cake and spruce bark) in a bench – scale bubbling fluidized bed reactor was carried out [187]. Quartz sand was used as the bed particles. After the combustion of these fuels, the agglomerates and the ash formed were examined with scanning electronic microscopy (SEM). Each fuel has different agglomeration tendencies. Total defluidization occurs in the pure bark at a temperature of 1045^0C while defluidization occurred in the rapeseed at a temperature of 800^0C. The low defluidization temperature of rapeseed was because of the sticky ash dominated by phosphates (Calcium - potassium/sodium phosphates). This shows that biomass fuels containing high percentage of alkali are prone to produce agglomerates in fixed beds and fluidized beds during combustion of biomass fuels [125, 134, 175].

Agglomeration may be experienced when fuels are co - fired or combusted separately. This was investigated when high-sodium, high-sulphur South Australian lignite (coal) was allowed to undergo combustion through spouted-bed gasification process. It was noticed that, agglomeration could be avoided in the bed if the operations are conducted under a low bed temperature below 850^oC, maintaining consistent increase in the fluid velocity, and ash content of the bed below 80 % [145-147]. An average South Australian coal contained high sodium, Na and sulphur, S. During fluidized bed combustion of the coals, these elements form a eutectic compound sodium - calcium - sulphates which has very low melting point compared to individual element melting point and created a very sticky paste within the bed (agglomerates).

At elevated temperatures and lower straw (biomass), the release was high because of the reactions between K_2SO_4 obtained from straw and coal-clay minerals. With high straw percentage and under a low temperature, sulphur from coal would not be predominant because it would have been arrested by the calcium and potassium present in the straw. This therefore, is one of the best methods to control emissions emanated from co-firing in fluidized bed combustion [188].

2.24 Evaluating agglomeration potential in biomass fuels

In fact, the fuel type and bed materials usually determines the control of the overall bed chemistry and introduction of additives to the bed materials is a universal way of reducing formation of agglomerates in combustion beds. Interaction between the fuel ash components and bed materials is very important factor to be considered [2, 11]. This agglomeration indicator technique is particularly applicable to a bed where silica sand, SiO_2 is the bed materials. The technique is further illustrated with equation 2.19

$$(Na + K) / (2S + Cl) > 1 \qquad 2.19$$

Considering the agglomeration indicator technique Equation 2.19, it may be assumed that, high alkali in biomass fuels induced agglomeration tendency [11, 125]. At a temperature greater than 700^{o}C, if the ratio (Na + K) / (2S + Cl) is greater than 1, there is every tendency that agglomeration may occur during the combustion of the biomass fuels. The implication is that, the biomass fuel is hugely dominated by alkali. The assumption for the indicator technique is that, all the Sulphur S and Chlorine Cl in the fuel react with the fuel alkali species.

Consequent upon findings from related literature, it can be deduced that, the major process of agglomeration formation in the fluidized bed is the formation of a eutectic compound between alkali metals present in biomass fuels and silica in the sand particles as earlier discussed [125, 138]. The eutectic compound usually melts sharply below the melting point of the parent materials and subsequently causes agglomeration in the bed. Eutectic point at which fusion of the selected biomass fuels occurred in the bed would be determined on both the binary and the ternary phase diagrams.

2.24.1 Phase Diagram

A phase diagram is a chart used to depict conditions at which thermodynamically distinct phases can occur at equilibrium while a phase is a region in space at which substances remain homogenous throughout its state [189-191]. Phase diagram is also a broad module that allows the

determination of different combinations of pressure, temperature, volume, compositions, chemical potential, and phase fraction. Phase diagram could be in form of unary, binary, ternary, and multicomponent phase diagrams [132, 192-194]. In the case of the present research, analyses have been strictly focussed on binary and the ternary phase diagrams.

Status of substances at a phase indicates that, their physical properties particularly pressure, temperature and density usually remain constant. Phase transitions occur along lines of equilibrium.

Generally, phase diagrams indicate physical states of substances at equilibrium. Temperature and pressure are always considered as the key actors[147, 191].

Temperature is plotted against concentration of two components at different compositions in a binary mixture. Meanwhile in the ternary phase diagram, three components at different compositions were considered simultaneously. This type of solution could be either a solid solution or eutectic. A eutectic point is a point on the phase diagram where a eutectic mixture/compound is formed. A eutectic mixture is that which melts at a temperature below the melting point of the individual components making up the mixture [195, 196]. The mixture is always a solid. A typical example of a phase diagram illustrating the onset of formation of eutectic compound is as shown in Figure 2.20

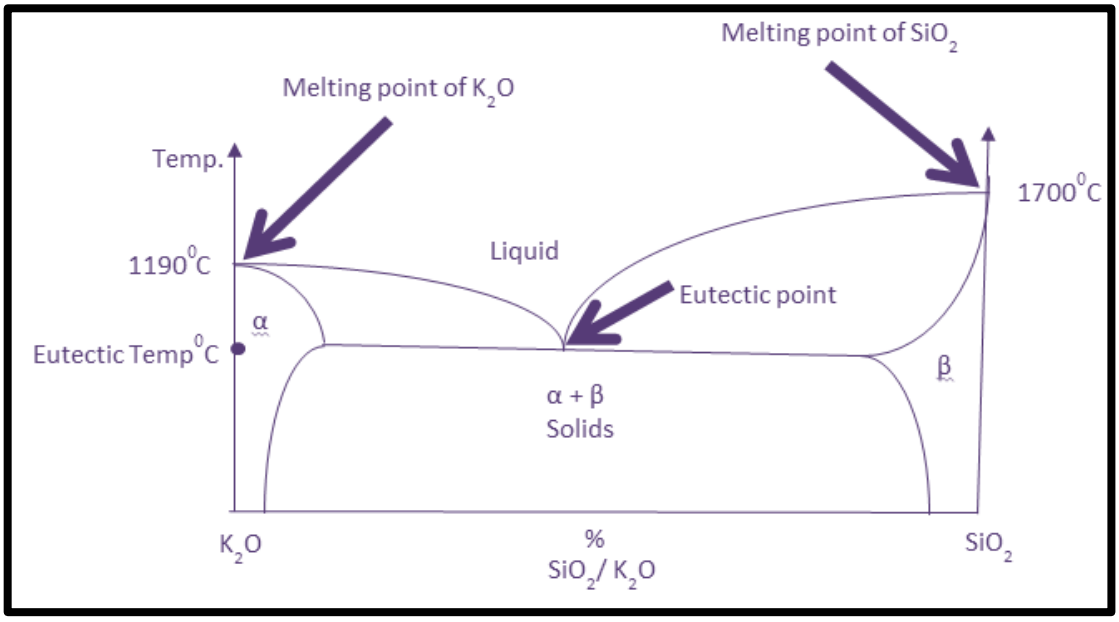

Figure 2-20: Schematic of a typical binary Phase diagram

The binary phase diagram consists of the temperature as the ordinate and the compositions of the $SiO_2$and K_2O components in the mixture as the abscissa. Potassium oxide from biomass fuels and silicon oxide from the bed materials are plotted on the phase diagram. The melting point of SiO_2 is 1700 ^{0}C while the melting point of K_2O is 1190 ^{0}C.

These two compounds react together to form potassium silicate K_2SiO_3 which is a eutectic compound having a lower melting point temperature than either the K_2O or the SiO_2. The temperature at which the formed compound melts is the eutectic temperature, which occurs at the eutectic point.

Agglomerates formation in the bed is also likened to the adhesion of the fuel particles because of the produced molten fuel ash in the form of potassium-silicate, K-Silicate. The produced eutectic mixture melts abruptly on the surface of the bed materials and form lumps in form of agglomerates [4, 5, 10, 188, 197]. The inner core of the agglomerates is predominantly comprised of the bed materials (silica) while the outer layer is make-up of the ashes from the burnt biomass fuels. Figure 2.21 below was used to illustrate further.

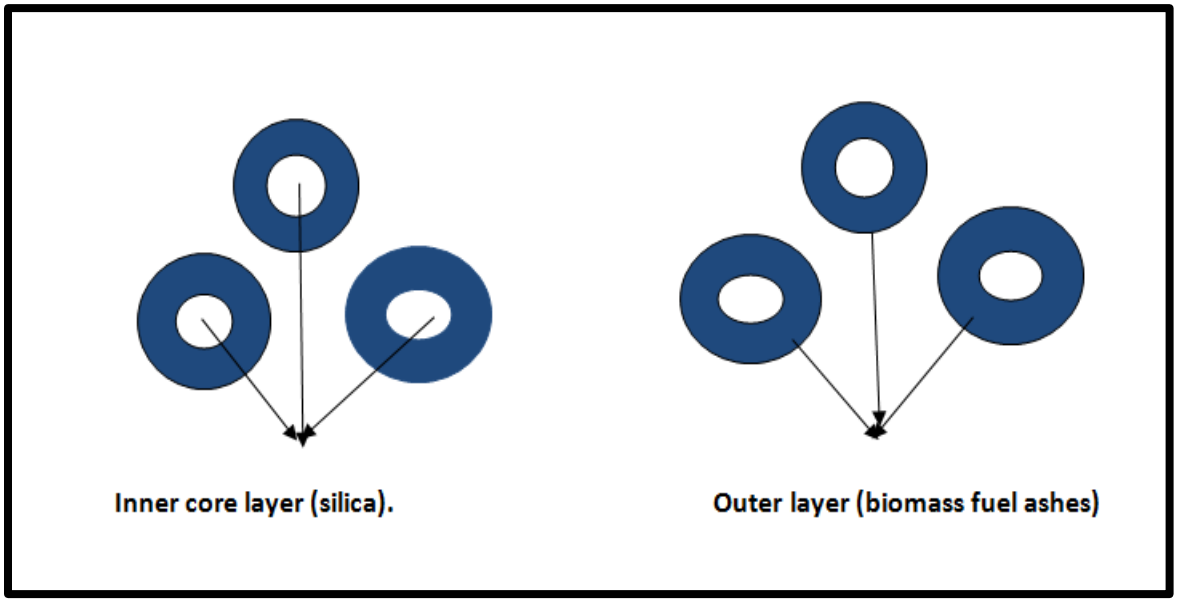

Figure 2-21: Composition of Agglomerates in bed

2.25 Distinction between Simulation and Modelling

Modelling refers to the act of representing part of a system or the entire system as a whole in a more simplified approach with the intention to promote better understanding of the system[198, 199]. A good model contains all the necessary facts needed to exist about the system under consideration otherwise, it will not be genuine and valuable details would have been lost during the modelling. Moreover, models, which are not too complex, would facilitate easy understanding of the message it is disseminating and the simulation process. Models are simplifications of reality and are therefore, less complicated than reality [200]. Models are subject to change but must maintain its correspondence with reality. Models could be static or dynamic. A static model indicates a set of element and any relationship that exists between them. While a dynamic model is that which describes the behaviour of one or more elements of the system. However, on the other hand, Simulation is the use of a well-written computer program (software) to intensify interactions among parts of the system of the model with a view to establishing the expected facts. It is always made interactive for easy understanding. It can simply be referred to as computerized version of the model which is run over time to study the implications of the defined interactions[201].

2.26 Reduction of Agglomeration Techniques in Combustion Beds

Addition of additives to biomass or biomass blends co-fired with coal can reduce agglomeration tendencies of biomass fuel in combustion beds (a fixed bed and fluidized beds) by removing alkalis from alkali chlorides or alkali oxides. This can prevent the release of gaseous potassium chloride, $KCl_{(g)}$ or react with the potassium chlorides to produce a component, which is a less destructive component [202, 203]. Example of these is alumina-silicates $Al_2Si_2O_5(OH)_4$ called kaolin or China clay. This compound (aluminosilicates) is made up of oxides of aluminium and silicon (Al_2O_3 & SiO_2). The common form of the compound is kaolinites whose chemical formula is $Al_2Si_2O_5(OH)_4$ which is the main source of kaolin.

Reaction of the additives with Potassium K, produces K – alumina - silicates which has great affinity for reducing the formation of Potassium Chlorides, $KCl_{(g)}$ in the combustion chamber.

This method had been applied by some researchers [4, 204]. In most of the researches, kaolin was added to the bed materials while co-firing single biomass with coal. In this research work, blends of biomass fuels, coal, and kaolin will be combusted in the bed combustor. Addition of kaolin to biomass fuels or blend of biomass fuels with coal may reduce agglomeration tendencies of these fuels. Kaolin can alter the chemistry of the reaction that causes agglomeration in the bed and thereby reducing the tendency for the formation of agglomerates. Kaolinites can remove the alkalis present in chlorides (NaCl & KCl) in coal ash at an operating temperature of $1200\ ^0C$ [205, 206].

If alumina rich compounds such as kaolin are present in the bed materials, the solid-to-solid reaction may result in the formation of alkali-aluminium-silicates, $K_2O\text{-}Al_2O_3\text{-}SiO_2$ that has a much higher melting temperature than alkali-silicates, $K_2O\text{-}SiO_2$ [23]. Operating the bed combustor at this condition may not lead to agglomeration formation in the bed except at elevated temperatures [197, 207].

Other methods to reduce agglomeration include; the use of alternative bed materials, improved reactor design and modified operating conditions.

2.27 Co – Firing Coal in Combustion Beds

Coal is a non-uniform organic fuel, formed from partly or largely decomposed plant materials. Coal formations usually occur through a process under very high pressures and temperatures. Coal took its source from different types of plants [23, 89, 208]. This singular fact about coal contributes significantly to the differences in its characteristics and properties. Comparison between biomass and coal, biomass has very high moisture content and low calorific value therefore, may not burn easily hence, it is usually co – fired with coal in combustion beds (fluidized bed and fixed beds).

Co – firing is the combustion of more than one type of fuel simultaneously in the same furnace at the same time [151, 209]. It is advantageous because both fuels are solids. Biomass has high moisture content, high oxygen and hydrogen fractions than coal. Coal on the other hand is

denser and has more carbon fraction than biomass. Because of this, biomass tends to generate less energy compared to coal. In addition, biomass has high volatile matter than coal and therefore has more flaming combustion than char combustion. In terms of ash content, coal has higher ash content than biomass. However, biomass ash is prone to formation of deposits (slagging and fouling) within the bed [84, 210].

In terms of mixing ratio, if the percentage of biomass in the total mixture is 30% or more, formation of slagging and fouling may be a significant problem within the bed. However, approximately 5% to 10 % biomass of the total mixture appears not to cause any noticeable problem of slagging and fouling in the bed. Less than 30% of biomass in the total mixture is recommended for effective co- firing [3, 211, 212]. Addition of calcium carbonate, $CaCO_3$ (lime stone) to the bed will remove Sulphur, S emissions from the system.

2.28 Summary

With particular reference to the journal papers reviewed, it can be concluded that, agglomeration is a major problem usually observed during the combustion processes of problematic biomass fuels. Agglomeration was experienced in most of the researches conducted on the combustion of biomass fuels in combustor beds. Sections 2.13 and 2.14 discussed consequences of agglomeration during the combustion of biomass fuels. Biomass is CO_2 neutral and very rich in alkali metals potentially potassium and K and sodium Na. Reactions between the alkali metals and the silica from sand leading to the formation of eutectic compounds is the main mechanism for agglomeration in the combustor beds. The eutectic compounds have lower melting temperatures than the alkali and the silica therefore, melts quickly and formed lumps (agglomerates) in the combustor beds. Agglomeration and subsequent defluidization occurred at 800 ^{0}C during the combustion of rapeseed cake in a bench-scale bubbling fluidized bed reactor. Also, agglomeration was experienced at 113 minutes in a pilot-scale combustion of pine seed shells and at 130 minutes in a bench - scale fluidized bed reactors [4, 5]. Addition of additives such as kaolin, $Al_2Si_2O_4(OH)_5$ to bed materials during biomass fuels combustion may reduce the formation of agglomerates in the combustor beds. Most of the researches conducted on the combustion of biomass fuels were carried out using the conventional combustion chambers; fixed bed and fluidized bed (pilot - scale and

laboratory - scale) but in this present research, Gooch crucible was introduced as the combustion chamber. This was to enhance temperature distribution within the combustion chamber.

3 Theoretical Background

3.1 Introduction

Theoretical background of this research work comprises of the theoretical concept, fundamentals and the basics of agglomeration problems in combustion beds. This is particularly applicable to fluidized bed and fixed bed. Appropriate biomass fuels for this research were jointly selected with the industry-based supervisor who was initially co-supervising this project. The selected biomass fuels are; willow, white wood, and miscanthus. Biomass fuels could appear in various forms such as pellets, pulverized, and chips. However, white wood and the miscanthus were prepared in pellets form while willow was prepared in chips form (as received from the supplier). These fuels were crushed to the same particle size in readiness for the combustion process anticipated to be carried out on them. During the combustion of biomass fuels, agglomeration is experienced at a temperature a little beyond the sintering temperature which indicates the beginning of the formation of porous powder like substances [11, 125, 161, 162]. The ignition temperature of biomass fuels is between 240 ^{0}C to 260 ^{0}C [4, 5, 84, 106, 213].

3.2 Concepts of Agglomeration

Agglomeration is the formation of solid lumps in the combustion chamber during the combustion of biomass fuels. Silica sand, which is the bed material, contains silica oxides (SiO_2) while biomass fuels contain alkali metals; Na, K of group one on the periodic table of elements. At a temperature just above the sintering temperature of biomass fuels, interactions begin to take place among the bed materials and the biomass fuels in both fluidized and fixed beds. This leads to the formation of a eutectic compound in the form of alkali-silicate (K_2SiO_3) [5, 10, 145, 197]. Addition of additive to the bed materials would prevent occurrence of agglomeration in the bed. Kaolin was selected as the additive to be used in this research. Addition of kaolin, $Al_2Si_2O_4(OH)_5$ to the bed contents (premixed or added in the process), will form an alkali-alumina - silicate compound (K - alumina - Silicates or Na - alumina - Silicates) that has a much higher

melting temperature than either the silica from the sand or the alkali from the biomass fuels [125, 202, 214]. This melting temperature is also higher than the recommended operating temperature (750^0 C to 900^0 C) in combustion beds (fixed beds and fluidized beds). This simply implies that, with the addition of kaolin as additive to the bed contents during combustion of biomass fuels, agglomeration was predicted to occur at elevated temperatures of 1200 ^{0} C to 1700 ^{0} C depending on the dominating alkali metal (K or Na).

3.3 Pyrolysis of Solid Fuels (Biomass Fuels)

Pyrolysis can be described as the thermochemical conversion of solid fuels (biomass fuels) at elevated temperatures in the absence of oxygen to produce gases and liquid as by-products leaving char as the residue. The char is highly rich in carbon. In a situation whereby the char produced is mostly dominated by carbon, the process is termed carbonization. The word pyrolysis is derived or borrowed from a Greek word as ''pyro means fire'' while ''lysis implies separating''. The starting temperature of pyrolysis is between 200^0 C - 300^0 C [124, 215-217].
In this research, the combustion of biomass fuels experiments that was targeted at reducing agglomeration by the addition of additive can be likened to pyrolysis because the process and the operating conditions appears similar. However, their differences and similarities would be considered in detail at the appropriate chapter in this thesis write up.

3.4 Stoichiometric Combustion

In an air/fuel mixture, stoichiometric combustion is the ideal combustion process when the theoretical air supplied is exactly enough to completely burn the required fuel. This is not always practicable therefore; additional air is required to completely burn the fuel. The additional air is termed excess air [13, 16, 21]. To protect the life expectancy of the combustion equipment, it is advisable to run such equipment (boiler) at 10% to 20% more than the required air to burn the fuel completely.

In a situation whereby inadequate air is supplied during the combustion process, an incomplete combustion ensued. Combustion products at this stage include; soot, carbon monoxide CO, and unpalatable smoke. This development can cause environmental pollution, surface fouling, instability in the combustion flame, and gross reduction in the efficiency (performance) of the combustion device [12].

3.5 Air/Fuel Ratio (AFR)

This rationale is very important in the determination of the appropriate proportion of air and fuel in the mixture during combustion processes particularly in fluidized beds. Air-Fuel mixture is termed lean mixture when the proportion of air in the mixture is more than the stoichiometric while a rich mixture ensued when the proportion of air in the mixture is less than the stoichiometric [1, 14, 21]. The air is the oxidizer. The general chemical equation for the stoichiometric combustion of a hydrocarbon (methane, CH4) is as given below:

$$CH_4 + 2(O_2 + 3.76N_2) \rightarrow CO_2 + 2H_2O + 7.52N_2 \qquad 3.1$$

CO_2 compositions in the flue gases decreases as the excess air increases while O_2 compositions in the flue gases increases as the excess air increases. Figure 3.1 was used to illustrate the combustion processes during the combustion of biomass fuels in combustion beds while Table 3.1 shows the combustion variables. Meanwhile, ''nd'' on the Table 3.1 implies not determined.

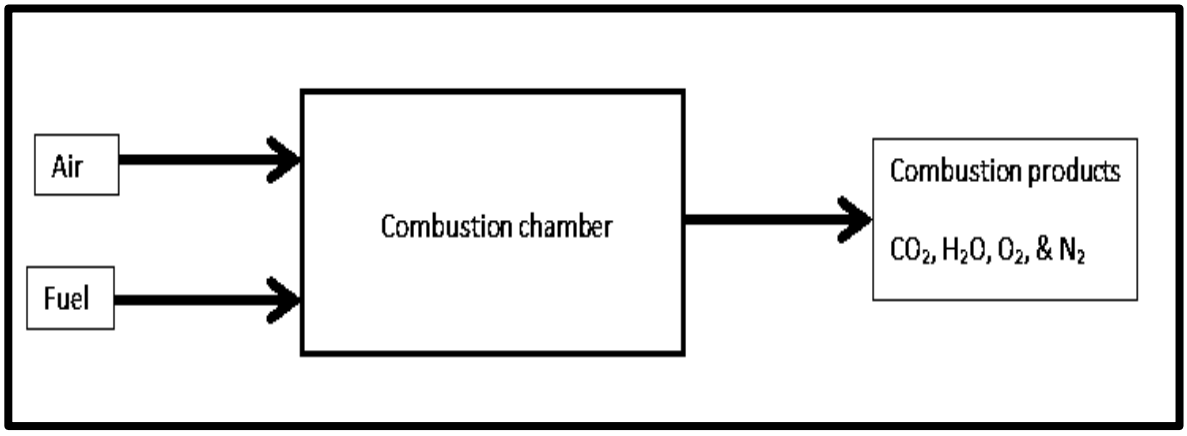

Figure 3-1: Schematic of the combustion processes

Table 3-1: Combustion variables

Element symbols	Atomic mass	Molecular mass	Combustion Products
C	12	nd	CO_2
H	1	2	H_2O
N	14	28	nd
S	32	nd	SO_2
O	16	32	nd

3.6 Thermal Conductivity

Fourier's law is the governing equation for thermal conductivity in solids. In this research, Fourier's law was applied to determine the amount of heat transfer from the burner flame to the Gooch ceramic crucible as follows believing that, the system is in a steady state (no change of temperature with time). The unit of thermal conductivity is in watt per meter per degree Celsius when the heat flow is expressed in watts.

Heat transfer through the high alumina Gooch ceramic into the combustion chamber was calculated thus;

Thermal conductivity for alumina ceramic, K = 32 $W.m^{-1}k^{-1}$

Flame temperature of burner T_1 = 1059 ^0C

Temperature within the chamber T_2 = 802 ^0C

Crucible thickness dX = 3mm

Change in temperature, dT = T_2 - T_1 = 802 - 1059 = 257 ^0C = - 530 K

$$\frac{q}{A} = -k\frac{dT}{dX} \qquad 3.2$$

Therefore, amount of heat transferred through the ceramic crucible is determined using the Fourier's equation of heat conduction below;

$\frac{q}{A}$ = - 32 $W.m^{-1}k^{-1}$ * - 530 K / 0.003 m

= 5.7 MW/m^2

3.7 Energy Dispersive X- Ray Spectroscopy (EDX)

Energy Dispersive X- Ray Spectroscopy (EDX) analysis conducted on the retrieved agglomerates after combustion was meant to determine the elemental compositions of both the outer and the inner layers of the agglomerates, with more emphasis on the dominating alkali in the particles using the electron microscope.

Apart from the elemental composition determination, it also takes into consideration; electron distribution in the K, L, and the M shells of the elements making-up the samples [218, 219].

During this process, electron e- from the SEM space dropped on one of the electrons on the K-shell of the sample's atom thereby creating an electron vacancy. The vacancy is quickly occupied with another electron from a higher energy level. This was illustrated with Figure 3.2

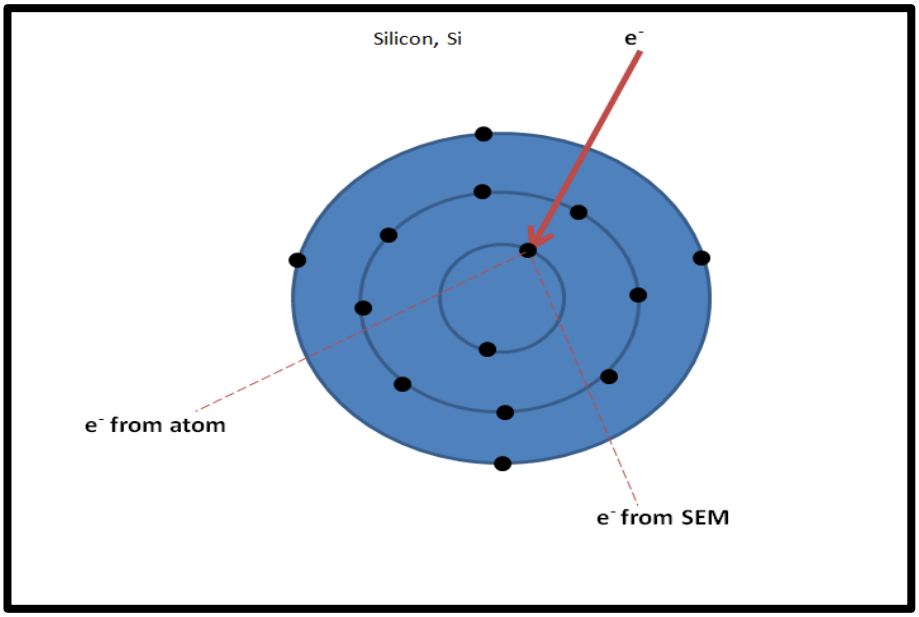

Figure 3-2: Electron's behaviour during SEM analysis

Transition of the elements and the energy of the X-ray machine are completely dependent on the characteristics of the elements. The X-ray machine can easily detect majority of the elements on the periodic table except the noble gases (Helium, Neon, and Argon) [220].

3.7.1 EDX Spot Analysis

This is the identification of a particular point on the sample and then determine the elemental composition at that spot [220].

3.7.2 Spectrum Analysis

This is the division of samples into array of spectra. Each spectrum is analyzed with a view to determining the elemental composition in it [221]. The elements making-up the samples are confirmed via this methods and mapping.

3.7.3 Element Mapping

Mapping is the separation or breaking of the sample (post combustion specimen) into various segments to critically distinguished the elements making-up each of the segments. This is to ensure that, the elements in the samples under consideration are equally distributed. The maps are compared with the SEM image to verify if they are in conformity in terms of shapes, colour, and structure [222]. The elements are classified into K-α, K-β, and K-γ.

Element mappings emanated from the SEM and the EDX analyses of the biomass fuels for this project are presented in chapter 7 of this thesis. Generally, in terms of appearance, there are many similarities in them as displayed. In the mappings, the dominating elements in each case are clearly shown.

3.7.4 Scanning electron microscopy

Scanning Electron Microscopy (SEM) analysis of bed samples after combustion and agglomeration tests on the biomass fuels is to examine microscopically, details of the particle's surface in terms of growth or increase in morphological structure, shape and texture of the particles. These are displayed conspicuously on the SEM micrographs. Increase in the size and

shape of bed particles is an indication that, the bed particles have lumped or fused together to form agglomerates.

3.7.5 Particle size measurement

This is the determination of the size of the biomass fuels particles, before and after the agglomeration experiment. An elongation in the size of the particles after the combustion processes is a manifestation of the fact that, fusion of the particles had occurred. It was performed differently on the bed samples collected at various bed temperatures (700 ^{O}C, 750 ^{O}C, and 802 ^{O}C) and compare with the initial (before experiment) bed particle size of < 1mm. Increase in the bed particle size is an indication that bed particles have fused together and thus produced agglomerates in the bed. Large Stuck of ash particles in the bed is the main reason for bed agglomeration [223].

4 Experimental Techniques and Procedures

4.1 Introduction

This chapter contains the experimental set up for the conduct of the combustion experiment in the Laboratory. It comprises of all the equipment and the procedures guiding the experiment. The experiment was conducted at the combustion laboratory, Department of Mechanical Engineering, University of Sheffield. The equipment used are; High alumina Gooch crucible, Roxio Burner, butane/propane mix cartridges, wire gauze, platinum thermocouple, stainless steel tripod stand, temperature data acquisition or data lodger (Pico instrument), smoke tunnel, and a lighter. Materials used for the experiment are; biomass fuels (willow chips, miscanthus pellets, and white wood pellets), silica sand (bed materials), coal (Cerrejon coal), and kaolin (additive).

Other aspect of the experiment is the thermal analyses which encompasses of the thermo gravimetric analyses (proximate analyses) and the ultimate analyses (C, H, N, S & O) using the Perkin Elmer instruments. The thermo gravimetric analyses (proximate analyses) and the C, H, N, S, & O (ultimate analyses) were conducted at the combustion laboratory located at the Low Carbon Combustion Centre of the University of Sheffield (Beighton site) while post combustion analyses (SEM and EDX) of the produced agglomerates were carried out at the SORBY Centre, North Campus, University of Sheffield.

4.2 Materials Adoption

Identification and selection of suitable raw materials that are required for the overall conduct of this research work are discussed in this sub section. The materials were carefully selected in conjunction with the Industrial based Supervisor of the ''Biomass and Fossil Fuels Research Alliance'' BF2RA. During the combustion of biomass fuels at the industry, there used to be eruption of some combustion problems particularly agglomeration. The interest of the BF2RA is to investigate the mechanisms of agglomeration in the bed with a view to finding a lasting solution to its reduction hence, the selection of these biomass fuels. The selected biomass fuels are willow, miscanthus and white wood. Other materials are coal, silica sand, and additive. The

coal is El-Cerrejon (Columbian coal) while the alkali absorber (additive) used is kaolin, $Al_2Si_2O_5(OH)_4$.

4.3 Materials Selection

Apart from the fact that, biomass possessed similar characteristics and properties, there are other factors that needs to be considered while selecting biomass fuels for experimental purposes. One of such factors is availability of the materials. Biomass fuels considered for this research includes; switch grass, white wood, willow, tobacco leaf, miscanthus, hard wood and wheat straw. Ash contents by weight percentage of these fuels from literature survey are; switch grass 7.1%, sorghum 14.15%, tobacco leaf 17.2%, hard wood 2.7%, wheat straw 13.5%, willow 4.5%, white wood 0.9%, and miscanthus 4.5%. Switch grass was not readily available as at the time of the conduct of the experiments. Every effort to procure switch grass proved abortive because the harvest season had passed.

Moreover, tobacco leaf, sorghum, switch grass, and wheat straw contained high ash contents as indicated above. High ash contents biomass fuels have the tendency of aggravating combustion problems such as agglomeration, slagging, and fouling in the combustion beds. Despite the fact that willow, miscanthus, and white wood Biomass fuels were readily available, they also contained moderate ash contents hence, they were selected as the appropriate biomass fuels for this research. These selected biomass fuels are alkali rich [4, 141], predominantly Potassium K. This is one of the qualities that make the fuels suitable for the agglomeration tests to be carried out on them. Potassium K plays significant roles in agglomeration formation during the combustion of biomass fuels in the combustion chambers. These selected biomass fuels and coal (willow, miscanthus, wood, silica sand and Columbian coal) are all suitable for agglomeration tests/experiments anticipated on them. Additives considered in this research work include dolomites, calcium carbonate $CaCO_3$, sewage sludge, and Kaolin. After much consideration, kaolin was adopted as the additive in this research because it is readily available. Columbian coal was selected because it possessed the following qualities; it contains moderate ash content therefore, formation of ash related problems in the bed will be reduced, low

sulphur content which will reduce formation of SO_X, good resistant to cracking and has long burning time performance. These materials were crushed to less than 1mm particle size Figure 4.1, in readiness for the combustion / agglomeration test on them.

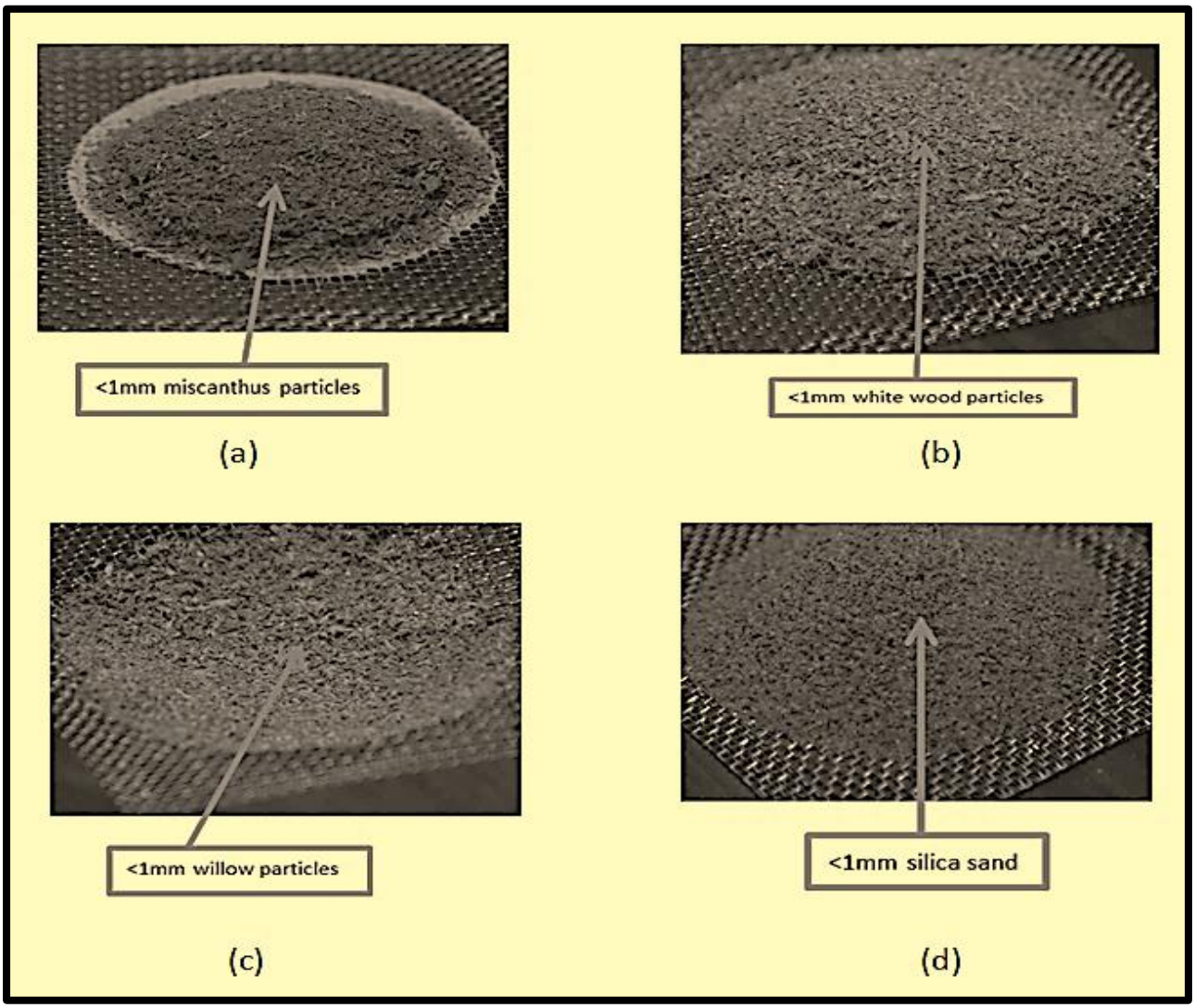

Figure 4-1: (a) <1mm miscanthus particles (b) <1mm white wood particle (c) <1mm willow particles (d) <1mm quartz sand as the bed materials.

To improve on the combustion characteristics of biomass fuels and make it burn effectively, they are usually co-fired with coal. The percentage of ash presents in these biomass fuels; willow, miscanthus, and white wood also appeared moderate; 1.16, 0.74 and 4.10 respectively.

This make them suitable for agglomeration tests because fuels containing high ash content can complicate combustion processes and cause the formation of incombustible residue that forms lumps after the combustion of coal (clinkering) and formation of molten deposits on the wall of combustion beds (slagging). Effect of moisture content in biomass fuel is indirectly proportional to the corresponding calorific values. Referring to the selected biomass fuels for this research, calorific values increases as the moisture contents decreases, Figure 4.2

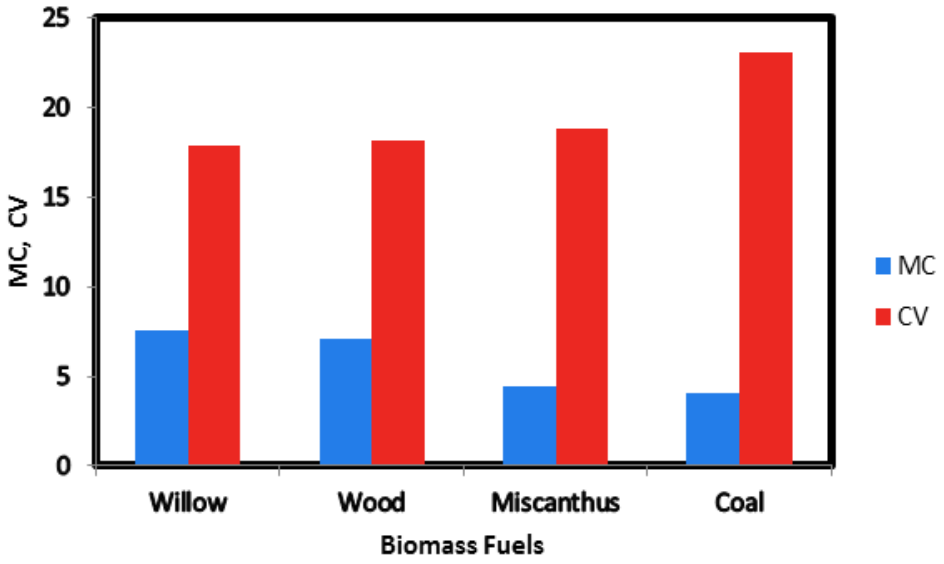

Figure 4-2: Relationship between moisture contents and the calorific values of the biomass fuels for this research.

4.4 Suitability of the Selected Biomass Fuels for Agglomeration Tests

Three biomass fuels were selected for agglomeration investigation in this research work. The biomass fuels are; willow, miscanthus, and white wood. Among these fuels, only willow was in chip forms while miscanthus and white wood pellets were prepared in pellet forms, Figure 4.3

Figure 4-3: Biomass fuel samples for this research

Apparently, for the combustion experiments, these fuels would be crushed to the same particle size (less than 1mm). PerkinElmer instruments, TGA analyser and CHNS/O were used to conduct the proximate and the ultimate analyses respectively on the selected biomass fuels on dry basis.

4.4.1 The Proximate Analyses

Proximate analyses reveals the moisture content, volatile matter, the fixed carbon, and the ash content contained in the biomass fuels or coal under consideration. Results of the proximate analysis (TGA) carried out on the selected biomass fuels; Table 4.1 shows that, the percentage of volatile matters in the selected biomass fuels for this project is relatively moderate when compared with typical volatile matters in literature.

Table 4-1: Proximate analysis of the selected fuels on dry basis, Wt. %

Biomass	Moisture Content	Volatile Matter	Fixed Carbon	Ash Content
Willow	7.54	68.71	19.25	4.50
White Wood	7.11	71.48	20.51	0.90
Miscanthus	4.41	67.02	24.02	4.55
Coal	4.10	22.91	48.42	24.57

White wood contained the highest volatile matter, 71.48% closely followed by willow, 68.71%, and miscanthus 67.02%. The percentage of fixed carbon in coal was the highest, 48.42%. This was followed by miscanthus, 24.02% while wood and willow has 20.51% and 19.25% respectively. High volatile matters in some biomass fuels is responsible for the flaming ignition usually experience during the combustion processes [79]. Meanwhile, coal on the other side has a low volatile matter (22.91%) and high fixed carbon (48.42%), therefore burns with char glow. These conform to literature findings. Temperature profiles showing the results of the TGA analyses are contained in Figures 4.4 and 4.5

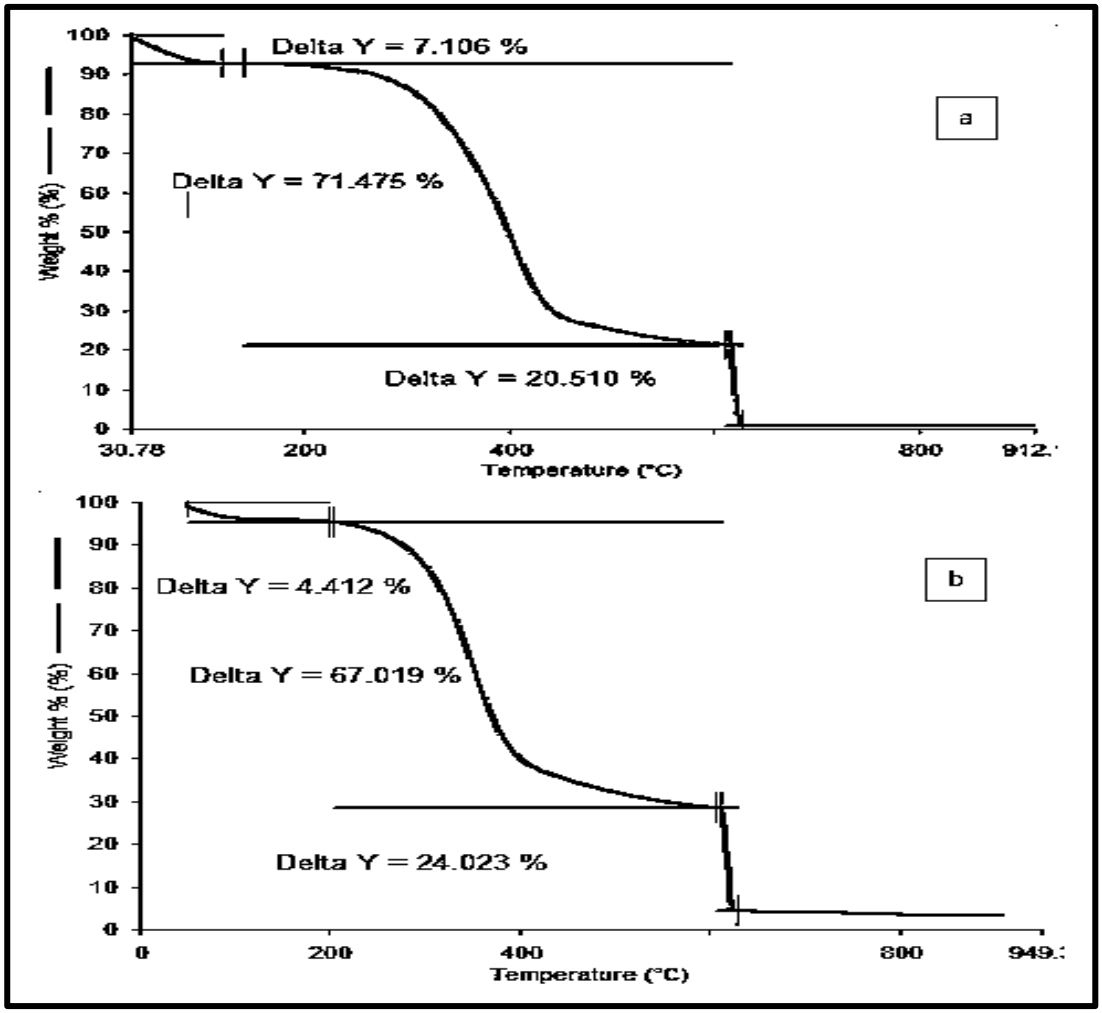

Figure 4-4: (a) Temperature profile for the proximate analyses (TGA) on <1mm white wood particles, (b) Temperature profile for the proximate analyses (TGA) on <1mm miscanthus particles.

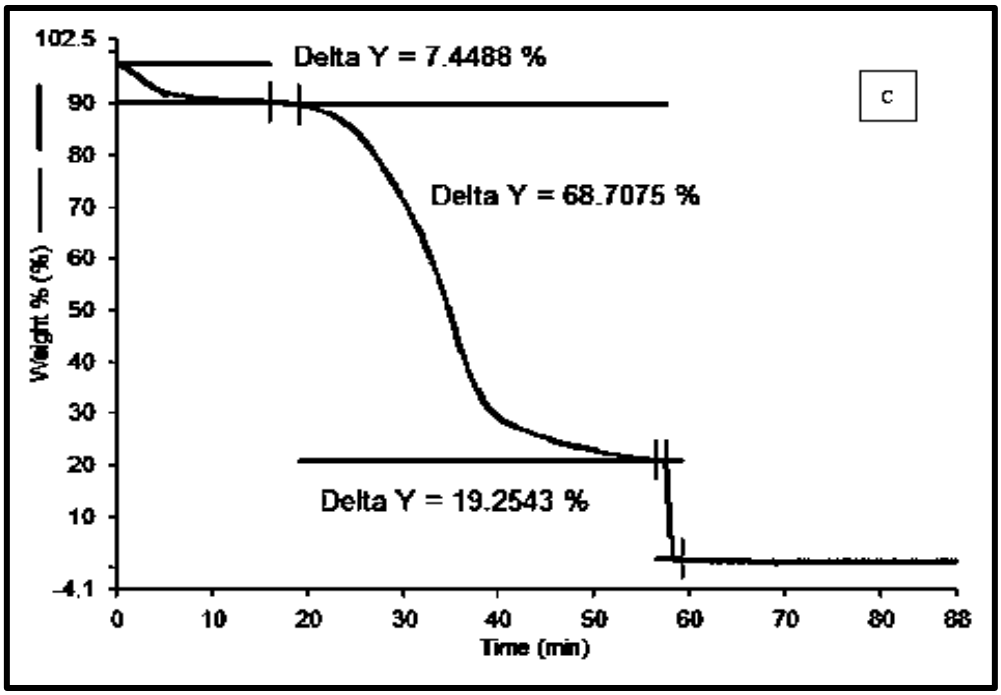

Figure 4-5 Temperature profile for the proximate analyses (TGA) on <1mm willow particles

4.4.2 The Ultimate Analyses

The ultimate analysis determines the organic carbon C, hydrogen H, nitrogen N, sulphur S, and oxygen O that are present in biomass fuels [122]. The CHNS/O (ultimate analysis) results for the selected biomass fuels, Table 4.2, which revealed the organic elemental compositions of the biomass fuels, indicated that, wood possessed the highest percentage of carbon, 48.24% followed by willow, which has 47.47% of carbon and then, miscanthus with 43.91%. These values are moderate and are similar to results obtained from literature. Moreover, the sulphur contents of these biomass fuels appear relatively high. Adequate precautions would be taken to control emissions (SO_2) likely to emanate because of this high sulphur content. These are very significant in the determination of the calorific values and the heating values of biomass fuels. These values are also indication that the selected fuels are suitable for combustion purposes.

In comparison with values available from literature, both the sulphur and the ash contents of the selected biomass fuels (willow, wood and miscanthus) are moderate and therefore, make them suitable for agglomeration tests anticipated to be carried out on them.

Table 4-2: Ultimate analysis CHNS/O and calculated calorific values of the selected biomass fuels for this project on dry basis, %

Biomass	C	H	N	S	O	Ash	Calorific value, MJ/Kg
Willow	47.47	6.54	1.07	0.6	39.82	4.50	18.92
Wood	48.24	6.44	0.38	0.72	43.32	0.90	18.65
Miscanthus	43.91	6.14	0.04	0.73	44.63	4.55	16.56
Coal	49.89	4.48	1.26	0.82	9.88	24.57	23.02

The significant of the calculated calorific values is that, it conforms to the calorific values of some typical biomass fuels. The results of the TGA and the CHNS/O coupled with the physical properties; particle density, bulk density, particle size, colour, moisture content, and the ash content of the biomass fuels, clearly show that, the biomass fuels are suitable for the agglomeration tests/experiments anticipated on them.

4.5 Characterization of the Selected Biomass Fuels

Characterization of biomass fuels is the classification or categorization of the fuels for their suitability for combustion processes in combustor beds [4, 12, 43]. Critical analyses of the selected biomass fuels in terms of thermo - chemical analyses, physical property, and physical analyses clearly indicated that these fuels are suitable for combustion purposes intended on them. Relatively, Physical properties of these fuels vary [125, 224]. These are bulk density, particle density, particle size, porosity and shape distribution. All these depend on fuel sample

preparation and fuel species. Thermo - chemical analysis of biomass fuels include; Thermo gravimetric analysis TGA (proximate analysis), CHNS/O (Ultimate analysis), and calorific values [125, 133, 225].

(i) The TGA is the proximate analysis, which reveals the percentage of moisture content, volatile matter, fixed carbon and the ash content in biomass fuels. Results of the thermo gravimetric analyses carried out on the selected biomass fuels indicated that, they are all suitable for combustion processes anticipated on them.

(ii) The ash content is relatively moderate therefore; the tendency of ash problems formation such as slagging and fouling in the combustion chamber would be minimal. The percentage of moisture content in the fuels is generally similar to the values obtained from literature [4, 130, 226].

(iii) The fixed carbon is the solid left in the furnace after volatile matter has been distilled off completely. It comprises mostly of carbon. Fixed carbon gives rough estimate of the heating values of the combusted solid fuels. It is very important in the determination of the heating values of these fuels. Percentage of fixed carbon in the selected fuels for this project is also moderate when compared to other biomass fuels from literature. Generally, biomass fuels possess similar characteristics therefore, the selected biomass fuels for this research also possessed akin properties and characteristics.

(iv) Calorific value is the energy released in KJ/Kg when 1Kg of a substance is completely combusted. It has a direct link with the heating values of these fuels. The higher the heating values of the fuel, the better the combustion products and the process. The standard unit of heating value and calorific value is KJ/Kg in SI units or Btu/Ib in English units. It represents the theoretical overall energy in the substance or fuel. There are two types of calorific values; the gross calorific values and the net calorific values [79]. The gross calorific values usually include latent heat of vapourization (heat energy required to transform the substance from water to

vapour) in the water vapour while in the net calorific value, heat of vapourization is not included. Therefore,

Net Calorific value, NCV = Gross calorific value – Heat of vapourization KJ/Kg 4.1

Proximate and ultimate analyses are very important in the determination of heating values of biomass fuels.

(v) The ultimate analysis indicates the percentage of the organic content by mass of carbon, hydrogen, nitrogen, sulphur and oxygen (CHNS&O) in the fuels [4, 116, 122]. The results of the ultimate analyses conducted on these fuels clearly indicated that, the fuels are eligible for the combustion processes intended to be carried out on them.

Inductively coupled plasma – Mass Spectrometry (ICP-MS) and Energy Dispersive X-ray Spectroscopy (EDS) are usually used to determine the trace elements and the elemental compositions of biomass fuels respectively before and after combustion processes on the biomass fuels [133, 227]. With respect to the present research, an instrument that has combined facilities for both EDX and SEM was used to determine the elemental compositions of the samples after combustion. The results obtained from the physical and the thermo - chemical analyses of the biomass fuels for this project, clearly indicated that, the fuels are suitable for combustion processes anticipated on them.

(vi) Density: Density of biomass is the mass of the fuels content per unit volume in Kg/m^3. There are two distinguished types of density as related to biomass; the particle and the bulk density. The two are highly significant in the characterization of biomass fuels [228].

(vii) Biomass particle density: This is the density of individual particle making up the entire biomass fuels. It is the mass of individual biomass fuel divided by its volume measured differently in Kg/m^3 [229, 230]. The shape of individual biomass fuel particularly in pellets form

can be geometrically, likened to that of the cylinder; therefore, the expression for the determination of the volume of a cylinder is applicable to biomass fuels too as follows;

Volume, $\boldsymbol{V = \frac{\pi}{4} D^2 L}$ 4.2

Where V is the volume of the biomass single particle in m^3, D and L are the diameter and length of the biomass particles respectively. The unit is metre, m.

(viii) Biomass bulk density: Considering space acquisition, biomass bulk density has a significant influence on the total economic value of production of alternative energy from biomass fuels. The cost of biomass fuels supplied to a storage area depends on the bulk density of the fuels. Apparently, because of the non-uniformity in shapes and sizes of biomass particles, high cost is usually incurred to transport and store biomass fuels of various forms (pellets, chips, leaves, bark and pulverized) [228, 231-233]. Compaction technique could be adopted to increase biomass bulk density. This involved close-packing two or more biomass fuels together. Switch grass and wheat straw were close - packed and compacted to increase the bulk density of these fuels, Figure 4.6. It consists of grey-like and whitish biomass fuels mixed. This demonstration displayed the importance of bulk density as a very important factor in the characterization of biomass fuels for their eligibility for combustion purposes.

Figure 4-6: Bulk density of mixed particles of switch grass and wheat straw (wet and dry) [228, 231-233]

A Group of researchers [125, 133, 225] conducted a research on characterization of some Canadian biomass. In their research, they considered wheat straw, barley straw, flax straw, timothy grass, and pinewood. Wheat straw and pinewood have the highest calorific value therefore indicated that they have good heating capability which make them suitable biomass materials for combustion processes[133, 216]. Moreover, barley has the highest ash percentage (9.8%). This makes it less suitable for combustion process because too much ash will lead to other problems such as ash sintering and slagging in the bed.

This method has been applied to characterize the selected fuels (willow, miscanthus, white wood, and coal) for this research. The ash contents of the selected fuels for this research are relatively moderate hence; make them suitable for the combustion process and agglomeration test in the bed. The relatively low sulphur contents of the fuels indicate that production of SO_2 emissions from these fuels will be very low. This also makes them suitable for combustion process in FBC. The moisture content in these fuels is relatively high when compared to a typical coal, which is one of the reasons why biomass is being co – fired with coal. Generally, fuels selected for this research are suitable for combustion and agglomeration tests in a Fluidized bed combustor.

The selected sand is silica sand (Garside Leighton Buzzard 16/30).

Sand diameter = 1mm approx.

Sand density = 1201 Kg/m^3

Volume of the Gooch Crucible (combustion chamber) = 500 mL = 0.0005m^3

Mass of sand = 0.6005 Kg

A sketch of the Gooch ceramic crucible is as shown, Figure 4.7

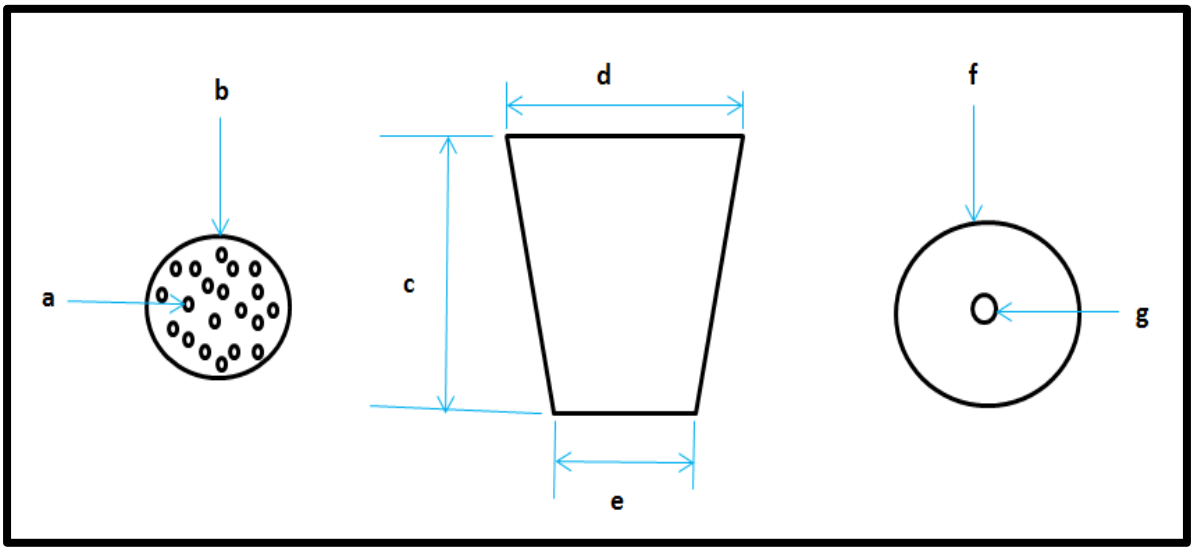

Figure 4-7: A sketch of the Engineering drawings of the Gooch ceramic crucible

Part list of the Gooch ceramic crucible:

(a) 1mm perforated holes on crucible base

(b) 80 mm diameter crucible base

(c) 120 mm crucible height

(d) 100 mm diameter crucible top

(e) 80 mm diameter crucible base

(f) 100 mm diameter crucible lid

(g) 7.5 mm thermocouple hole

Literature survey on this research, coupled with the various post combustion analyses carried out on the biomass fuels samples indicated that, the selected biomass fuels are rich in alkali

content. Post combustion analyses carried out on the fuels include; Scanning Electron Microscopy (SEM) and Energy Dispersive X-Ray Spectroscopy (EDX) analyses. Scanning Electron Microscopy analysis verified the changes (growth) in the morphological structure, form, shape and pattern of the bed materials after combustion. Energy Dispersive X-Ray Spectroscopy revealed the elements contained in the bed materials [125, 164, 202].

Major elemental compositions of the bed particles are Potassium K, Calcium Ca, Silicon Si, Magnesium Mg, Aluminum Al, Sodium Na, and Phosphorus P while minor elements include; Barium Ba, Molybdenum Mo, Nickel Ni, Lead Pb, Copper Cu, and Zinc Zn. Major elements as components of their oxides are very significant in the process of agglomeration formation in combustion beds. They include; Potassium oxide K_2O, Calcium oxide CaO, Silicon oxide SiO_2, Magnesium oxide MgO, Sodium oxide Na_2O, Aluminum oxide Al_2O_3. The most important of these elements and their oxides as related to agglomeration in combustion beds are K, Na, Ca, Si, K_2O, Na_2O, CaO, and SiO_2 [7, 150, 234].

4.6 Experimental Algorithm

- The experiment was set up as shown in the diagram. The platinum thermocouple was inserted to the combustion chamber through a 7.5 mm diameter hole on the Gooch crucible lid. The thermocouple was connected to a temperature data lodger (Pico instrument) linked to a computer system to capture the temperature within the combustion chamber as phase transformation progresses.
- Bed material; 200 grams of silica sand was heated to the ignition peak temperature of biomass fuels (225 ^{0}C to 302) [4, 235].
- Single biomass fuel; 25 grams each of willow, wood and miscanthus particles were added to the heated bed materials each at a time.
- Samples were collected at temperature intervals of; 700 ^{0}C, 750 ^{0}C, & 802^{0}C.
- The experiment was repeated for the blends/mixtures of the biomass fuels.
- The experiment was strictly carried out as itemized above. The experimental set-up is as shown in Figure 4.8

4.7 Experimental Set Up

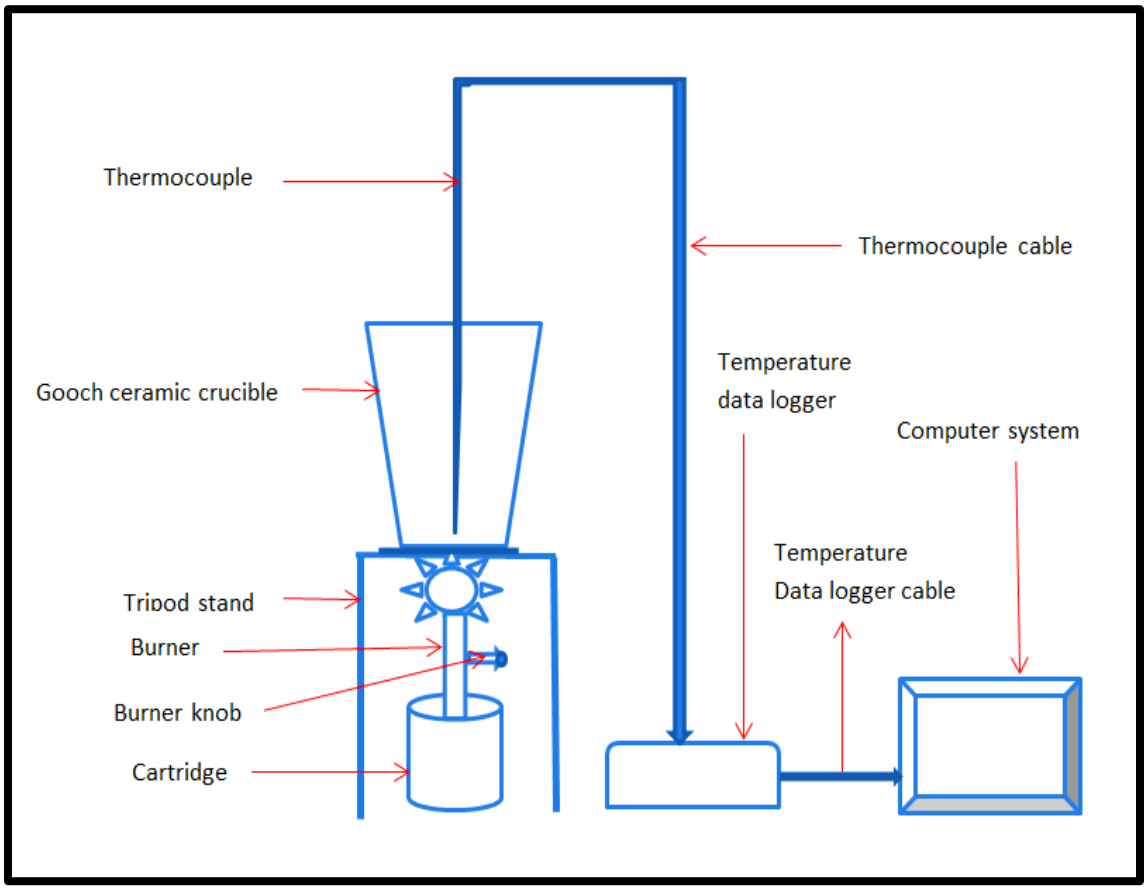

Figure 4-8 Schematic of Rig set-up

A close monitoring of the thermodynamic property (temperature of the surrounding fluids) indicated that, the chamber has the highest temperature compared with the temperature of the surrounding most especially that, the combustion chamber was fully lagged with thermal insulation sheets [49, 51]. Heat is transferred into the combustion chamber through the perforated area located at the bottom of the chamber (Gooch alumina crucible) by conduction. The Gooch crucible, Figure 4.9 can be used to filter substances (filtrates and substrates) into another container but in this case, it has been used as a combustion chamber. This is similar to a distributor plate made of metal sheets used in Fluidized bed combustor.

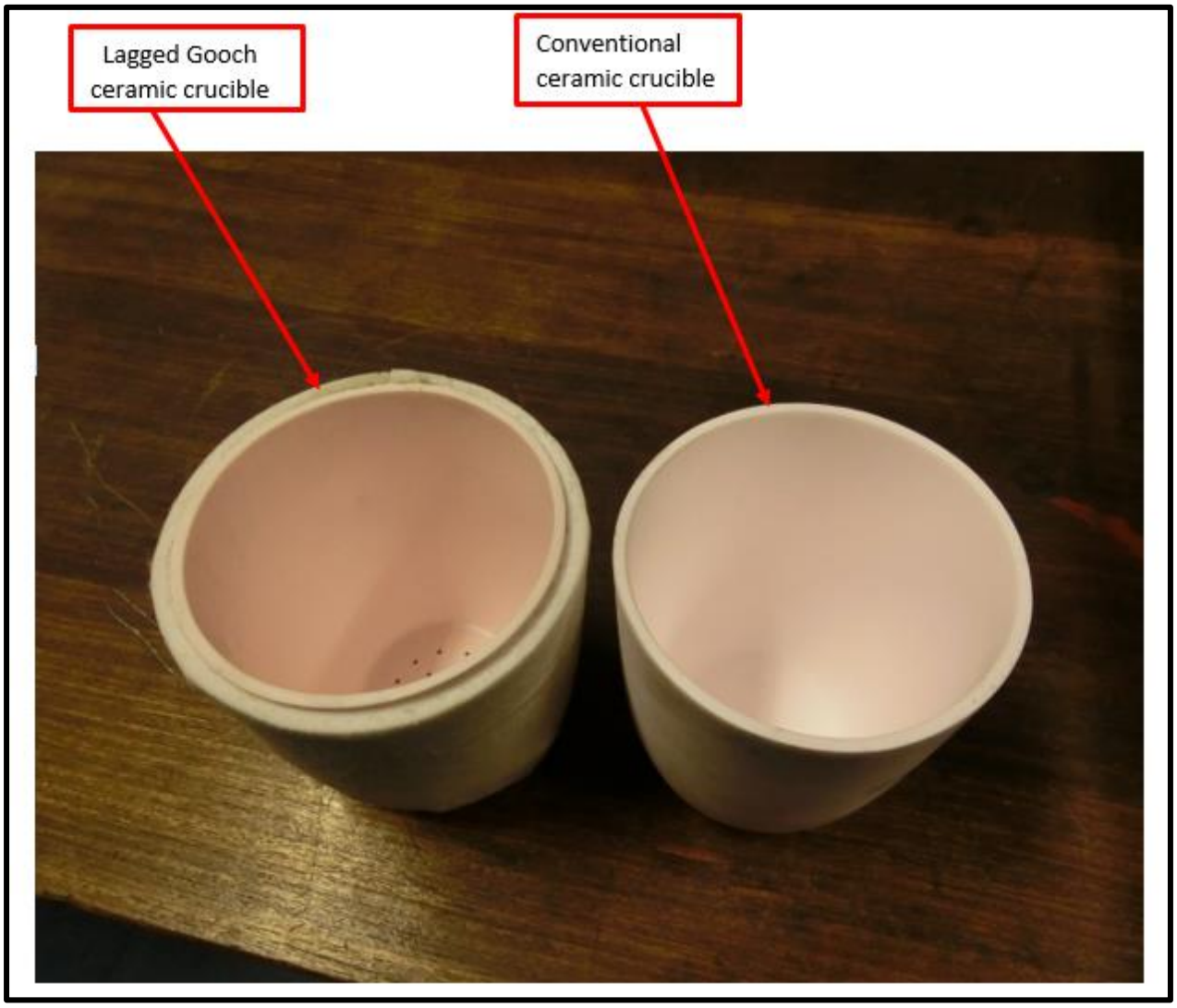

Figure 4-9: Lagged 500ml Gooch ceramic crucible and 500ml conventional ceramic crucible.

Interaction of fluids in the bed has significant effect on the formation of agglomerates in the bed [5, 10, 236]. Biomass fuels are very rich in moisture content but have low calorific value hence, mixing / blending biomass with coal which has a low moisture content and high calorific value would improve the combustion characteristics of biomass fuels [3, 17, 21].

The Columbian coal has been selected for this research because of its relatively low ash content. Biomass fuels has high volatile matters which is responsible for its glow burning while coal has low volatile matter which enhances its char burning nature [3, 22]. In most cases, biomass fuels with high ash content are not very suitable for combustion purposes because of the tendencies to form ash fusion at a lower temperature is always very high [7, 15, 22, 133, 236]. The ash

content for the selected biomass fuels for this project is considerably moderate and therefore suitable for combustion experiments anticipated on them. This was confirmed by the proximate analyses carried out on the biomass fuels as shown earlier in this report.

4.8 List of Experimental Equipment and Descriptions

(i) Ceramic Gooch Crucible: This is a ceramic crucible named after Frank Austen Gooch, hence the name. It has a thermal resistant of about 1750 ^{0}C. It was perforated at the bottom to further enhance and improve heat transfer/distribution within the crucible in other to be able to attain the anticipated agglomeration temperature of 750 ^{0}C and above.

(ii) Burner with a Cartridge: The burner, which is made of brass, has been, designed, for use with Butane/Propane mix gas cartridges. It can attain temperatures of well above 1000 ^{0}C. The burner can be, attached and detached from the cartridges as desired. This makes its transport and storage easier. It also has a replaceable perforated head. The standard burning time for the burner is 2.75 hours when used with the 220g cartridge.

(iii) Wire Gauze: The wire gauze has ceramic-coated plate at its center. It provides a comfortable seat for the crucible when placed on the triangular tripod stand.

(iv) Thermal Insulation Sheet: This very flexible super wool 607 thermal insulating sheet was used to insulate the Gooch crucible to prevent heat lost to the surroundings during the combustion of the biomass fuels. It is a high temperature gasket recommended for excellent thermal insulation purposes. It has a continuous temperature resistance of about 1200 ^{0}C and highly resistance to solvents and chemicals.

(v) Tripod stand: This is a Zinc plated steel triangular tripod stand. It is 210mm high and 6mm diameter support legs. It is the platform on which, the ceramic crucible was, placed while ignited from beyond by the burner.

(vi) Furnace Tong: This is a stainless steel made tong with flat hinge, specially designed for holding and handling hot crucibles during the combustion of biomass fuels. The serrated tapered tips close firmly when grapping objects.

(vii) Platinum Thermocouple: Temperature resistant of the platinum thermocouple is about 1650 ^{0}C. It is very relevant for the agglomeration experiments. It contains ceramic protection tube and connector which can withstand a temperature up to 650 ^{0}C. To increase its temperature resistance, the elements are insulated by a double - bore high purity hard-fired alumina insulator.

Progress of the experimental conduct are depicted, Figures 4.10, 4.11, and 4.12

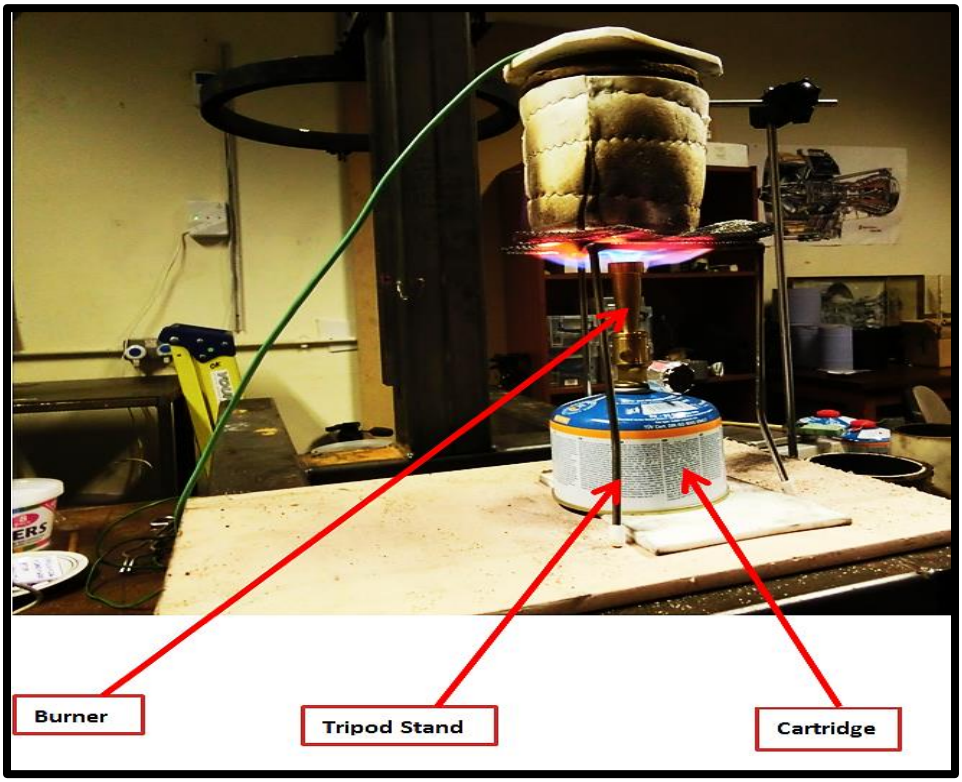

Figure 4-10: Experiment highlighting the burner and the cartridge

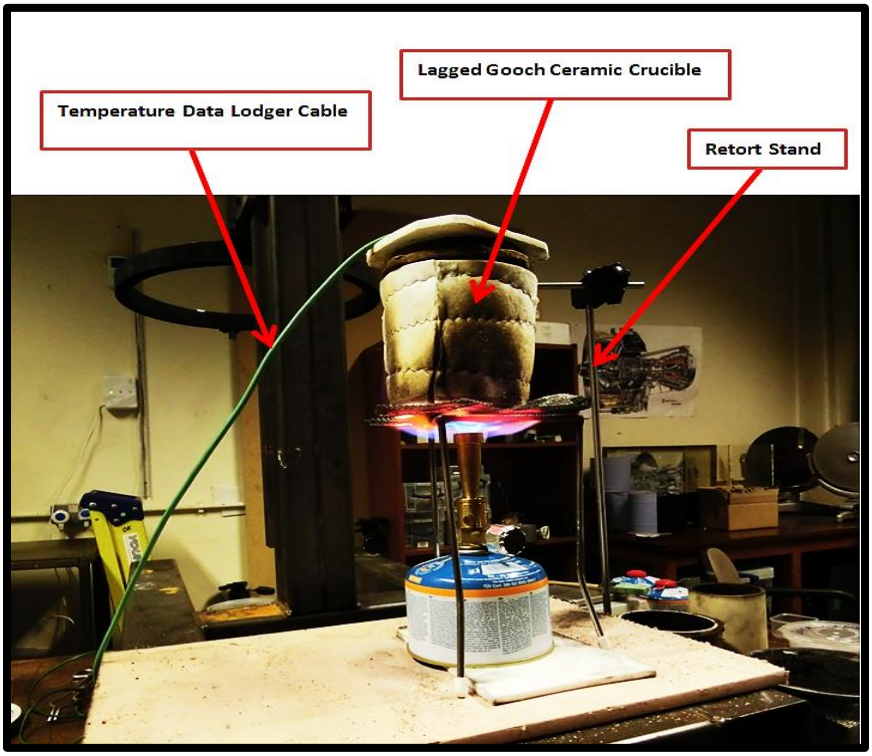

Figure 4-11: Experimental Set-Up highlighting the Gooch ceramic crucible

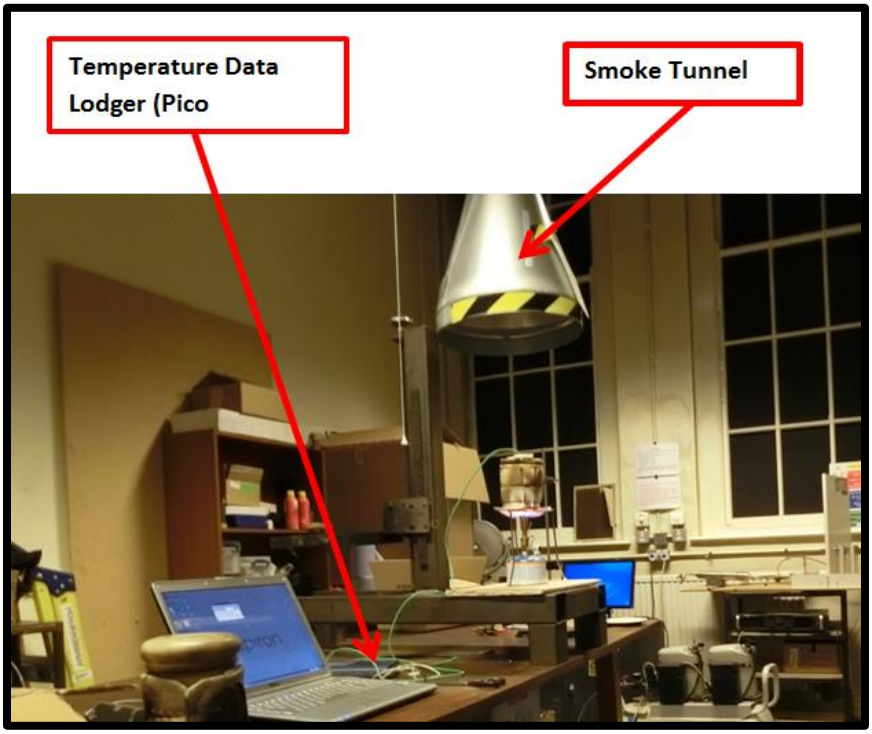

Figure 4-12: Experimental Set-Up highlighting the smoke tunnel

4.9 Thermal Analyses

4.9.1 Thermo Gravimetric Analyses (TGA) and C, H, N, S & O (Ultimate analyses)

Proximate and ultimate analyses (Thermo gravimetric and C H N S & O analyses respectively) are very essential in the characterization of biomass fuels for its suitability for combustion purposes. Pyris 1, Perkin Elmer instruments, Figure 4.13 were used to carry out both thermo gravimetric (Proximate analysis) and C H N S & O (Ultimate analysis) analyses on the selected biomass fuels for this project (willow, miscanthus, and white wood). The white wood and the miscanthus were prepared in pellets forms of 6mm diameter and 20mm long while willow was in the chips form. They were all grinded to particle size of less than 1mm for the combustion experiments. Proximate analyses results revealed the percentage of moisture contents, volatile matter, fixed carbon content and ash content in the biomass fuels while ultimate analysis showed the percentage of organic elemental compositions of the fuels i.e.; the carbon, hydrogen, nitrogen, sulphur and oxygen on dry basis. Detail analyses of these results are contained in results / discussion section of this thesis.

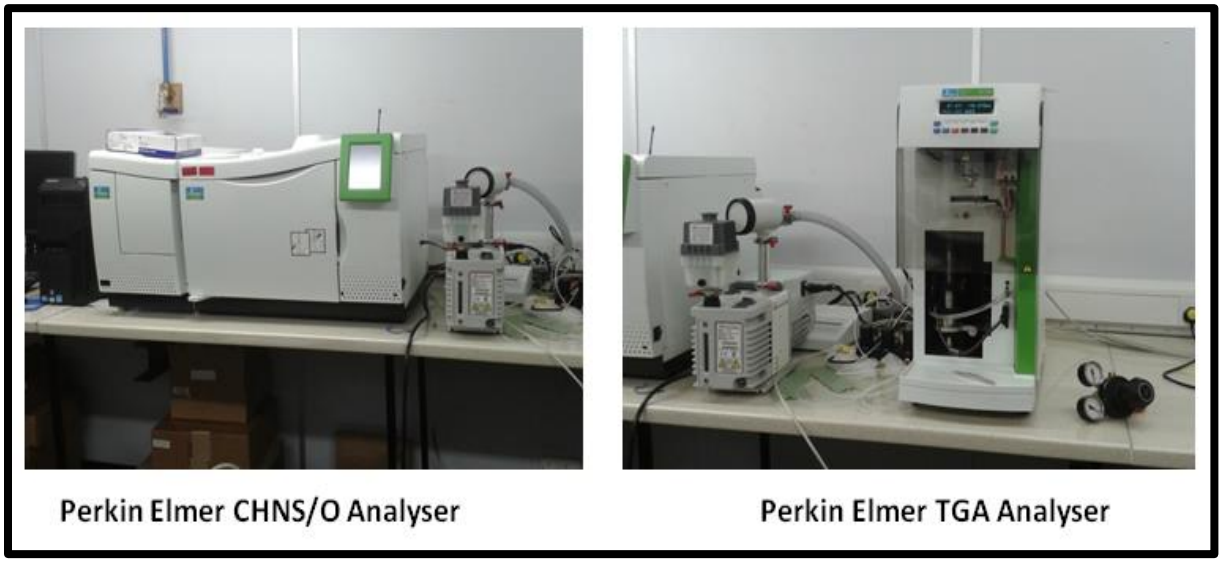

Figure 4-13: PerkinElmer instruments

4.9.2 Operational Principles of the Pyris 1, Perkin Elmer Instruments

(i) Sample Nomenclature: The operation begins by putting identification tags on the samples and aligning it with operator's notes for easy identification of the specimen. Operation sequence can be created in form of playlist [237, 238]. This is to enable series of iterations to be carried out without the incessant interference of the operator in charge of the experiment. The playlist is viewed occasionally or at will to reveal the, macro-view of the sequences [73]. Sample list page is viewed to show the spread sheet containing information like; the method adopted for the experiment, the sample identification (ID), and the sample weight. The historical page and the sample history page were created to show the historical views of the completed experimental steps and the historical views of all the samples run respectively [238].

(ii) Cleaning the TGA furnace: For this purpose, the furnace is opened to allow air into it. The temperature can build up to 900 ^{0}C to bake off all the organic condensate and residues from the furnace. Mild soap or appropriate solvent with bottlebrush was recommended for the cleaning up of the furnace tube. It is also advisable to have at least two furnace tubes so that, the other one can serve as a spare.

(iii) Sample preparation: Approximately, the same sample weight was used throughout the experiment. This was done to protect the integrity of the results by ensuring that, uniform data were captured under the same operating conditions. 1 mg of the sample was loaded onto the weighing balance and then transferred to the furnace in each case.

(iv) Temperature range for samples: This depends largely on the sample type, the nature of the experiment, the analyst decision. A survey scan was run at 20 ^{0}C /min through to 100 ^{0}C. It could also be carried out at 10 ^{0}C / min through to 100 ^{0}C /min or better still, at 50 ^{0}C /min if a faster rate is preferred to safe more time. The recommended rate is 20 ^{0}C / min while recommended gas cylinder pressure for the Pyris 1 TGA is 300 Psi. The purge gas is always Nitrogen, N_2 even though there might be a need to switch the gas later. It is advisable never to purge the balance with a reactive gas. This is to forestall a situation, whereby there will be back

streaming into the balance area. Oxidative gas can be introduced at the beginning, or at half way into the experiment through a mass flow controller built into the analyser and controlled by Pyris software. The balance purge was carried out at 10 mL / minute higher than the sample purge, which was 20 mL / minute.

(v) Calibration of the TGA Instrument: It is advisable; to usually restore the instrument to a default setting. This was done at regular intervals more especially, if the instrument calibration in terms of temperature exceeds the acceptable temperature range. The typical calibration accuracy limits are within $1\ ^{0}C$ and $5\ ^{0}C$ of the anticipated value. It is always advisable to refer to the calibration routine to serve as a guide.

4.10 Calorific values of the selected biomass fuels (Heating values)

Calorific value of any substance or fuel is the amount of energy released per unit mass or per unit volume of the fuel when the fuel is completely burned [114, 117, 122]. The standard unit of calorific value and the heating value is KJ/kg. Proximate and ultimate analyses are very important in the determination of the heating values of substances. Biomass fuels with high moisture content are bound to have a low calorific value.

Lower heating value LHV or lower calorific LCV implies that, water in form of vapour is not allowed to escape from the combustion products therefore, latent heat of vapourization is not added to the heat released while higher calorific value, HCV or higher heating value, HHV indicates that, water in the final combustion products remain as vapour or steam. Therefore, latent heat of vapourization is added to the heat released. Higher heating value is the same as gross heating value (GHV) while lower heating value is also known as the net heating value (NHV)[79, 82, 113, 226]. These values could be determined experimentally or by calculation using some empirical equations. The device for the conduct of the experiment is called bomb calorimeter or adiabatic calorimeter [163, 239]. Biomass fuel with higher heating values is recommended as the best materials for combustion purposes. The higher calorific value of standard biomass fuel is between 17MJ/Kg and 18MJ/Kg [239]. The heating values of any solid

fuel can be estimated from the results of its proximate analysis and using the empirical Equation 4.3 or any preferred empirical equation.

$HHV_D = 0.3536FC + 0.1559VM + 0.0078ASH$ (MJ/kg) 4.3

Where FC is the fixed carbon, VM is the volatile matters, and ASH is the ash content.

However, heating values of the selected biomass fuels for this project were calculated using Equation 4.4 and presented in Table 4.3. The equation is absolutely a function of the fixed carbon content determined from the proximate analyses carried out on the biomass fuels.

$HHV = 0.196\ (FC) + 14.119$ 4.4

Table 4-3: Heating Values of the selected biomass Fuels for this project

Biomass fuels	Higher heating value, MJ/Kg
Willow	17.89
Wood	18.14
Miscanthus	18.83
Coal	23.02

The average absolute error in this correlation is 2.2843% [114].

Comparing the heating values of the selected biomass fuels for this research, willow, miscanthus, and white wood, there are similarities in their values and combustion characteristics. The heating values actually fall within the range of the heating values of typical biomass fuels. Coal on the other hand, has higher heating values therefore, can burn effectively during combustion processes.

4.11 Samples Retrieval Method and Frequency of Collection

Samples were collected at the end of each experiment when the combustor chamber might have cooled down to the room temperature, 20 ^{0}C. Approximately four hours was allowed for the combustion chamber to properly cool down. The samples were collected after the burner might have been shut down at; 700 ^{O}C, 750 ^{O}C and 802 ^{O}C in each case. Collection of samples at these temperatures was done to allow for wider comparison of temperature data, during analyses. Additive (Kaolin) was added to the bed materials. The experiments were also repeated without the addition of kaolin.

4.12 Online analyses and Data acquisition

Online analyses comprise of the acquisition of temperature data recorded during the combustion experiment in the bed. The data were acquired by the temperature data acquisition unit (Pico instrument) also known as Pico TC-08 Thermocouple Data Logger, Figure 4.14. The instrument displayed the data on the computer system connected to the test rig.

Figure 4-14: temperature Data Logger (Pico TC - 08 Thermocouple/temperature Data Logger)

The instrument is appropriate for a broad range of temperature measurement and other recording applications. It can measure temperature from –270 ^{0}C to +1820 ^{0}C with any common

thermocouple. These data will be analyzed adequately and critically in the appropriate chapter of this thesis. Continuous decrease in the bed temperature during combustion of biomass fuels is an indication that, the fuel and the air intakes (air flow rate) from the cartridge to the burner-required adjustment.

4.13 Post combustion analyses

Post combustion analyses to be conducted on the retrieved bed samples include; Scanning Electron Microscopy (SEM), and Energy Dispersive X - Ray Spectroscopy (EDX). The specimens were carbon - coated and gold - coated. Other post combustion analyses is the Particle size measurement to verify growth in size and shape.

4.14 Samples Preparation for SEM and EDX

The biomass fuels samples collected for post combustion analyses are poor or non-conductors therefore, they were carbon coated to improve on their conductivity and to make them suitable for the SEM and the EDX analyses envisaged on them. The agglomerate samples are as depicted in figure 4.15 while the carbon coating machine used was ''Speedivac Coating Unit'' model 12E6 / 1589 produced by Edward High Vacuum Limited based in the Sussex, England, Figure 4.16.

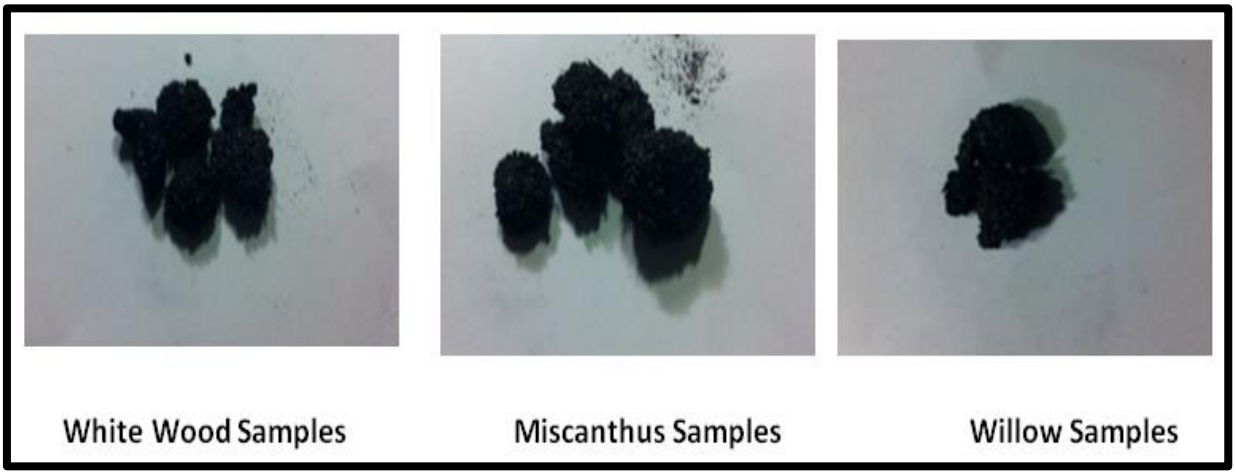

Figure 4-15: Samples of agglomerates produced from the biomass fuel combustion in a Gooch ceramic crucible at 802 ^{0}C

The samples were initially mounted in resin solution, thoroughly washed in an iso - propanol, and then air-dried in preparation for the carbon coating processes.

Figure 4-16: Carbon Coating Instrument, Speedivac Coating Unit.

The Speedivac coating unit was produced by Edward high vacuum limited that based in the Sussex, England. Some of the samples could not be mounted in a resin solution because, they are non-conductors hence; Sputter Coater was used to coat and polished the samples in preparation for the SEM and EDX analyses while using the electron microscopes.

Sputter coating is a recognized method of preparing the non-conducting samples for observation in a scanning electron microscopy. The sample's surface was sputter coated with gold (Au) that is a non-oxidizing metal. The sputter coater used in this research is as shown, Figure 4.17

Figure 4-17: SC7620 Mini Sputter Coater/Glow Discharge System.

5 Software Applications

5.1 Introduction

Chapter 5 discusses various applications of Factsage software for the prediction of eutectic points (eutectic temperatures) on phase diagrams. Fusion of substances occurs in the combustion bed at this eutectic temperature. Fusion takes place at the solid state of the substances under consideration. Significance of both the binary and the ternary phase diagrams as related to agglomeration formation during the combustion of the selected biomass fuels in the combustor chamber was considered properly. Factsage package contains FACT-Win / FACT and CHEMSAGE, SOLGASMIX thermochemical. It comprises of several databases, information, calculation and manipulation modules, which permits access to the control of pure substances and solution database. The Gibbs energy minimization workhorse of Factsage is the equilibrium module and some other common programs [132].

Factsage software is thermochemical software and databases. It runs on PC operating under MS windows [240]. It has been used extensively to predict eutectic point on phase diagrams at which melting and fusion of solid particles in a fixed bed combustor during the combustion process of blends of biomass fuels with coal.

In this research work, Factsage software had been effectively utilized to predict the eutectic points on both the binary and the ternary phase diagrams. Agglomerates were formed in a laboratory-scale fixed bed using high alumina Gooch crucible as the combustion chamber at this temperature. The corresponding temperature to the eutectic point on the temperature axis, which is the eutectic point, is the agglomeration temperature in the combustor bed.

The eutectic point on phase diagram is largely influenced by the percentage of the inorganics (K_2O, KOH, Na_2O or SiO_2) in the mixture [240].

5.2 Simulation Using Factsage Software

Factsage software is a thermochemical software and databases. It runs on PC operating under MS windows. It has been extensively used to predict eutectic points on binary and ternary phase diagrams. The eutectic points refer to the points on phase diagrams where melting and

fusion of biomass fuel particles occur during the combustion of single/blends of biomass fuels with coal.

Factsage software specifically determines the behaviours and characteristics of substances on phase diagram using their thermodynamic properties. Phase diagram is a broad module that allows the determination of different combinations of pressure, temperature, volume, compositions, chemical potential, and phase fraction. Phase diagram could be in the form of unary, binary, ternary or multi components phase diagrams.

The corresponding temperature to the eutectic point on the temperature axis is the eutectic point. It is the equivalent agglomeration temperature in the combustor bed. The eutectic point on phase diagram is largely influenced by the percentage of the inorganics (K_2O, KOH, Na_2O or SiO_2) in the mixture. The eutectic points on binary and the ternary phase diagrams varied considerably, even though, the operating conditions may be the same.

5.3 Validation of FactSage software as an appropriate tool

Combination of two software package F*A*C*T/FACT-Win and ChemSage otherwise referred to as FactSage was introduced in 2001. It is made up of several information, calculations, and modules that enable researchers to access pure substances and databases. Many thermochemical calculations can be performed with the series of modules available in the package. With this, thermochemical calculations can be processed to generate graphs, figures, and tables of high interest to the corrosion and chemical engineers, physical metallurgist, environmentalists, geochemists, electrochemists, ceramists, and other relevant fields of study [240]. This application permit acquisition of new databases, calculation, and manipulation of both phase diagrams and other complex phase.

Initially, the F*A*C*T package was designed to simulate the thermochemistry of pyrometallurgical processing but, with the introduction of the Windows-based FACT-WIN which undergo amazing metamorphosis to FactSage, the applications have been expanded to accommodate combustion, electrometallurgy, glass technology, hydrometallurgy, ceramics, environmental studies, corrosion, and geology. Relative to program usage and assistance of proper documentation, practical understanding of the principles of thermochemistry can easily

be acquired in relation to complex phase equilibria. The relevant modifications that was carried out on both the software and the databases, provided enhancement for calculation and manipulation of phase diagrams and also easy access to the various modules in the package. There are various versions of the software. The version under consideration is 6.1. The modules are grouped into different categories: Info, databases, calculate, and manipulate, Figure 5.1

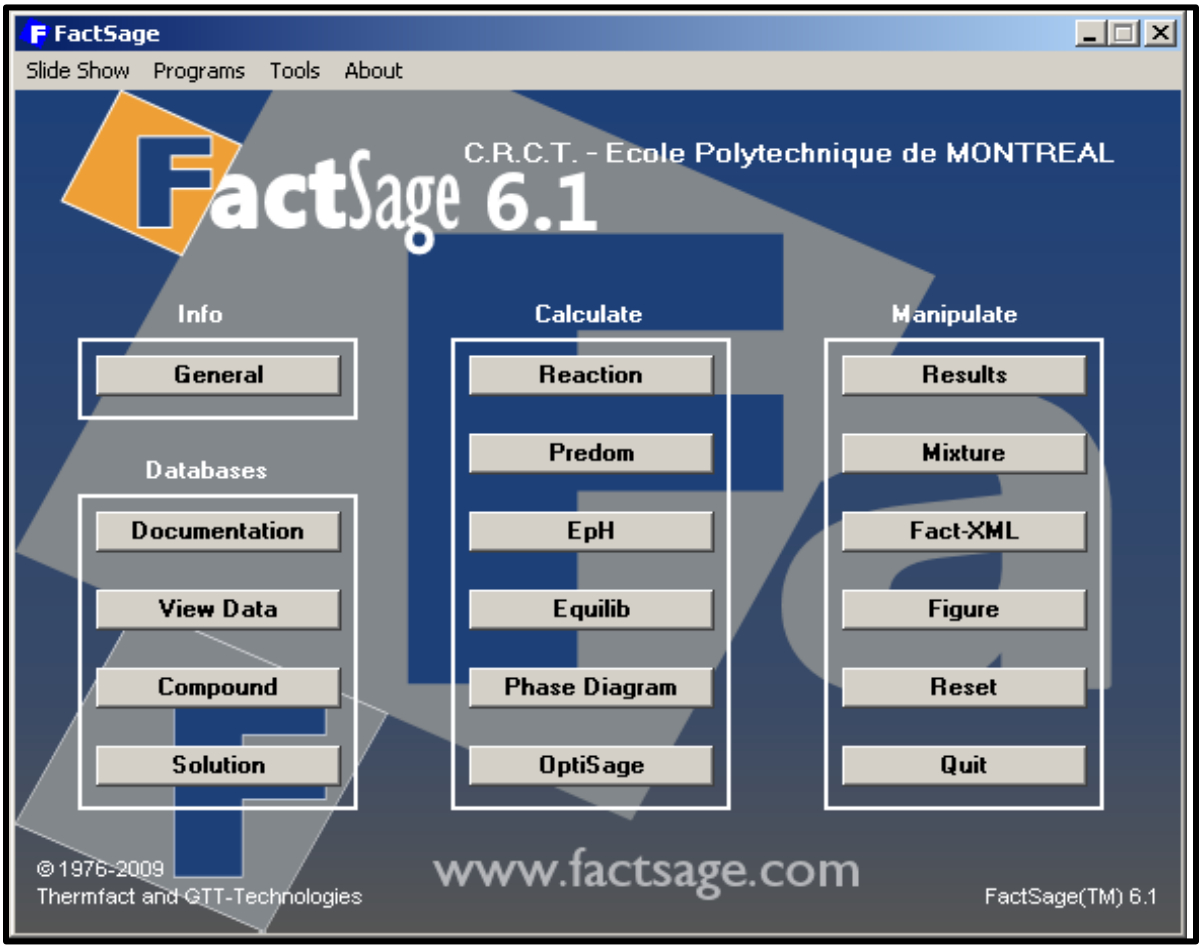

Figure 5-1 Series of modules in Factsage software, version 6.1 [240]

Binary alloy database comprised of 115 of the binary systems retrieved from the SGTE alloy database that contained over 300 much-accessed binary systems and 120 ternary and higher-order systems that include 78 elements. Two composition variables, FeO – TiO_2 were processed at 1600 ^{0}C, 1 atmosphere, and 1 mole each. Image capture of the reaction as produced from the Factsage software is as shown in Figure 5.2

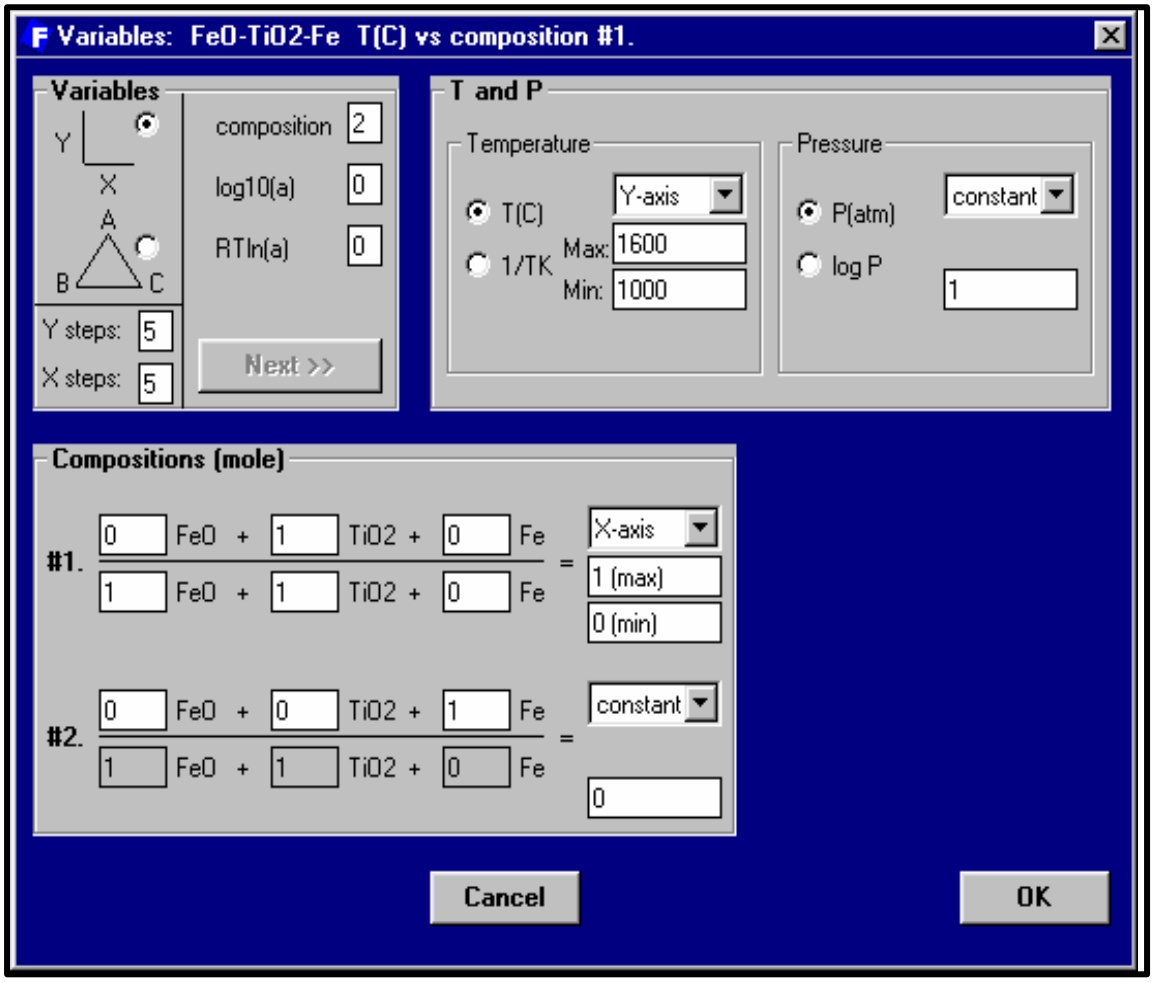

Figure 5-2 Two composition variables FeO – TiO_2 at 1600 ^{0}C and 1 atm [240]

Bale [240] utilized Factsage software to process two composition variables CaO – SiO_2 and the fusion temperature (eutectic point) was determined at the meeting points of the liquidus. Image capture of the output is as depicted in Figure 5.3. Clicking on the calculate module button, the phase diagram is automatically calculated and plotted. The figure module uses the graph as a dynamic interface. The tie lines and stable phases are automatically labelled by pointing to a particular domain. Equilibrium compositions and phase amounts at any point on the diagram can be determined. This is also applicable to three composition variables.

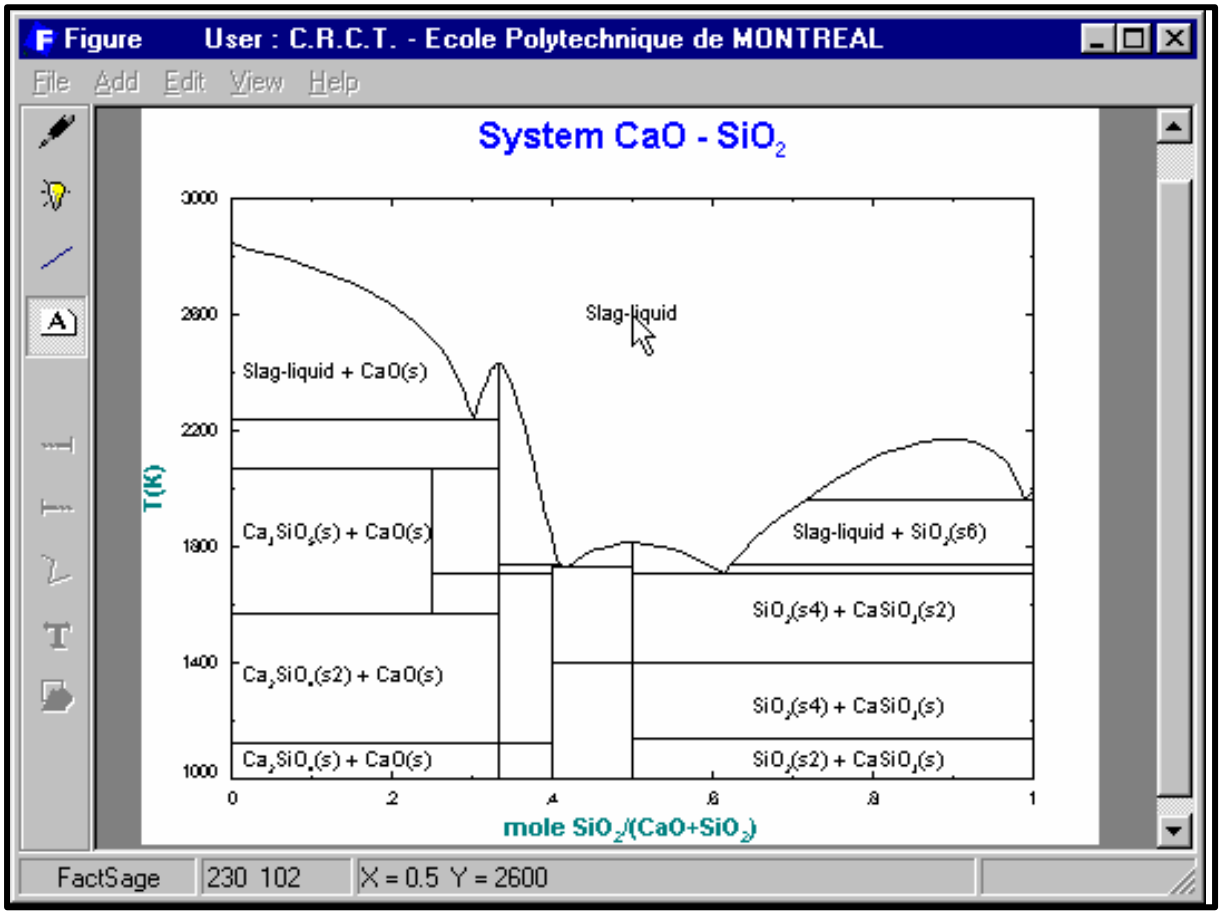

Figure 5-3 Phase Diagram Module –CaO-SiO2 system [240]

Similarly, the software was also applied to process three composition variables SiO_2 - CaO – Al_2O_3 at 1600 ^{0}C, 1 atmosphere, and 1 mole each. The image capture of the reaction is as shown in Figure 5.4. This is a confirmation of the reliability of the software as an appropriate tool for this research.

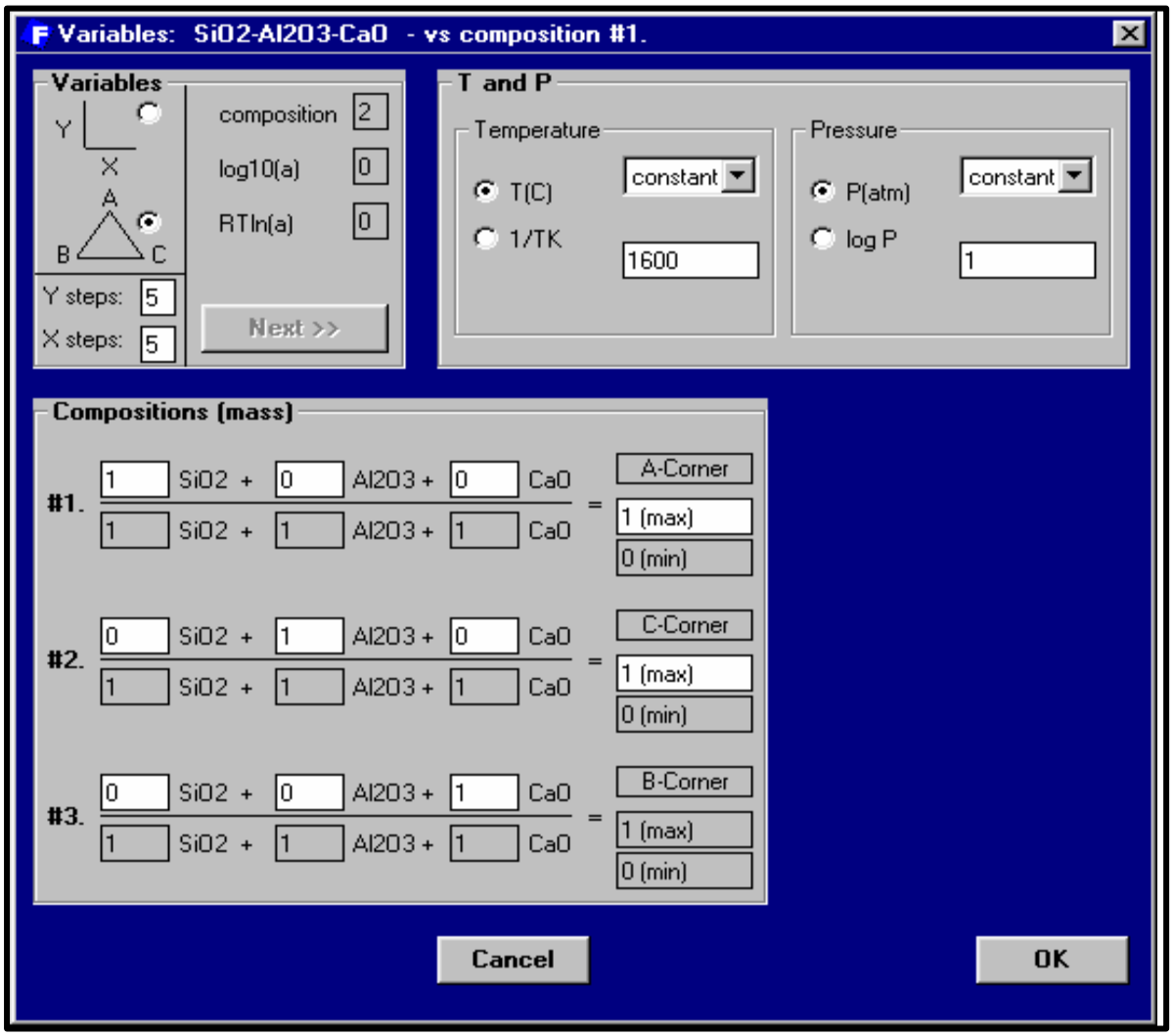

Figure 5-4 Three composition variables SiO_2 - CaO – Al_2O_3 at 1600 ^{0}C and 1 atm [240]

5.4 Locating Eutectic Points on the binary Phase Diagram

Determination of the eutectic points on binary phase diagrams can be accomplish by utilizing a graph of temperature against the compositions of the two substances under study at a constant pressure, P. The system is at a gas phase (γ) or vapour state when the temperature of the system is very high while at a lower temperature, the system is at a liquid phase (α). At the intermediary between the gas and the liquid phase, is the solid phase (β)[241]. Between the two

states (vapour and liquid), the system is at an equilibrium with each other therefore, fusion of the substances take place at this point.

The particular spot at which this occurs, is the eutectic point EP [242]. The eutectic point is very significant in this research work because, the temperature at eutectic point determines the temperature at which agglomeration will occur in the laboratory-scale fixed bed whereby the Gooch ceramic crucible is the combustor. In binary phase diagram, temperature T is plotted against the mole fractions of the two substances under consideration, Figure 5.5

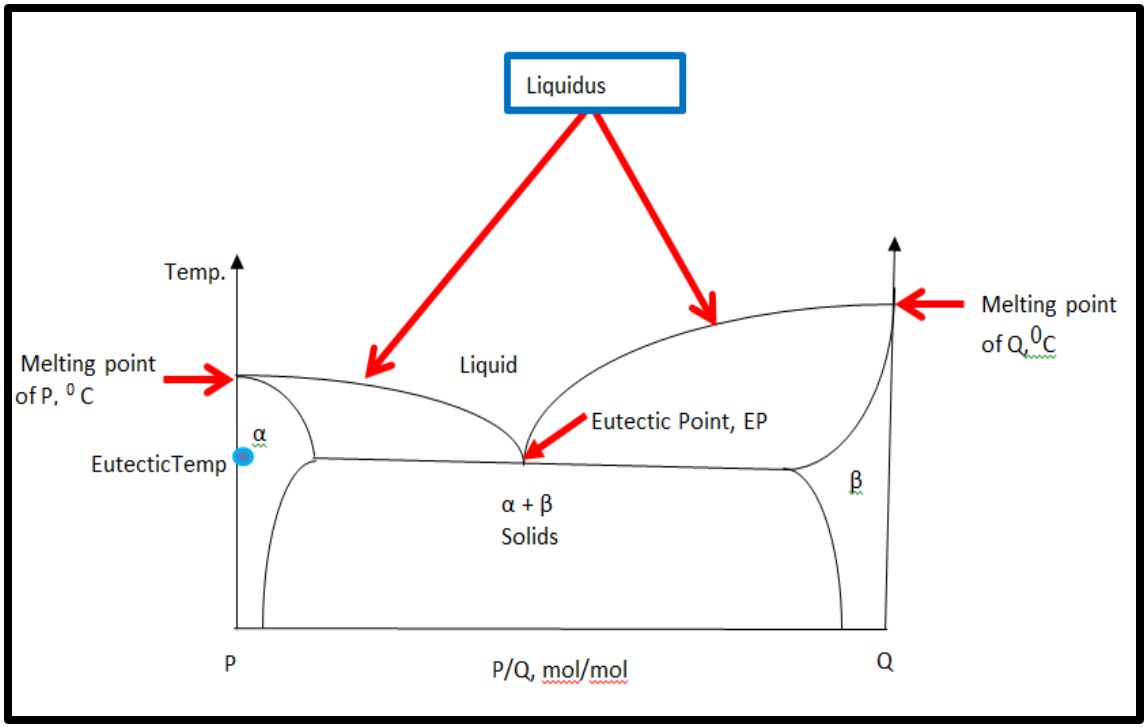

Figure 5-5 Schematic of a eutectic point on a typical binary phase diagram

Freezing point reduces as attention is moved from the pure substances under consideration, for instance P and Q. This implies that, the tendency of solids formation is very high as focus is moved away from one solid to the other.

The liquidus line separates the liquid phase from the two-phase region of pure solid and liquid (α + L and β + L). In the two-phase region on the binary phase diagram, a line parallel to the compositions axis (tie line) is drawn from the meeting point of the liquidus to the temperature axis. The point of intersection of the tie line on the temperature axis, indicates the eutectic temperature of the materials under consideration [242].

As focus is being shifted from one solid region to the other, the former crystallizes out gradually therefore, the liquid proportion of the mixture is richer in the later solid than the former solid. A tie line is also drawn at meeting point of the two liquidus. The point of intersection between the meeting point of the two liquidus and the tie line is the eutectic point. At eutectic, the melting point is always lower than the melting points of the two solids under consideration on the binary phase diagram. The two solids crystallize out isothermally at eutectic and produces common crystals, which appears homogenous to the ordinary eyes [241].

Above the eutectic point is the liquid phase. Scanning electron microscope (SEM) is utilized to determine the real morphological structure of the mixture (structural arrangement) while Energy Dispersive X-ray spectroscopy is used to analyze the elemental compositions of the mixture.

If heat is continually removed from the mixture at eutectic point, the mixture will remain at eutectic until all become solidified. As the temperature reduces below the eutectic point, two-phase region is reached which comprises of pure solids of the two mixtures. Variations in the atomic radii of the various metals making – up the mixtures influence the different phases usually produced. Factsage software was applied to predict eutectic points on binary phase diagrams. With the addition of kaolin to a potassium, K dominated biomass fuel, agglomeration was predicted to occur at 1200 ^{0} C, Figure 5.6

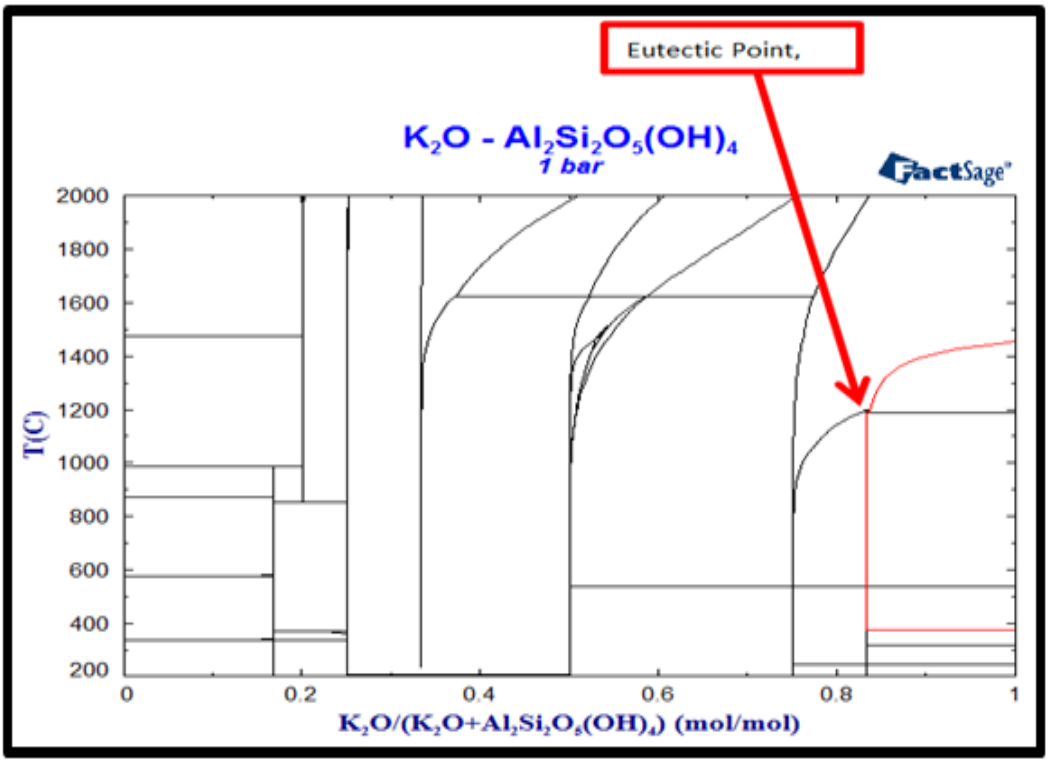

Figure 5-6: Eutectic points on Binary Phase diagram at 1200 ^{0}C with addition of 1 mole of kaolin.

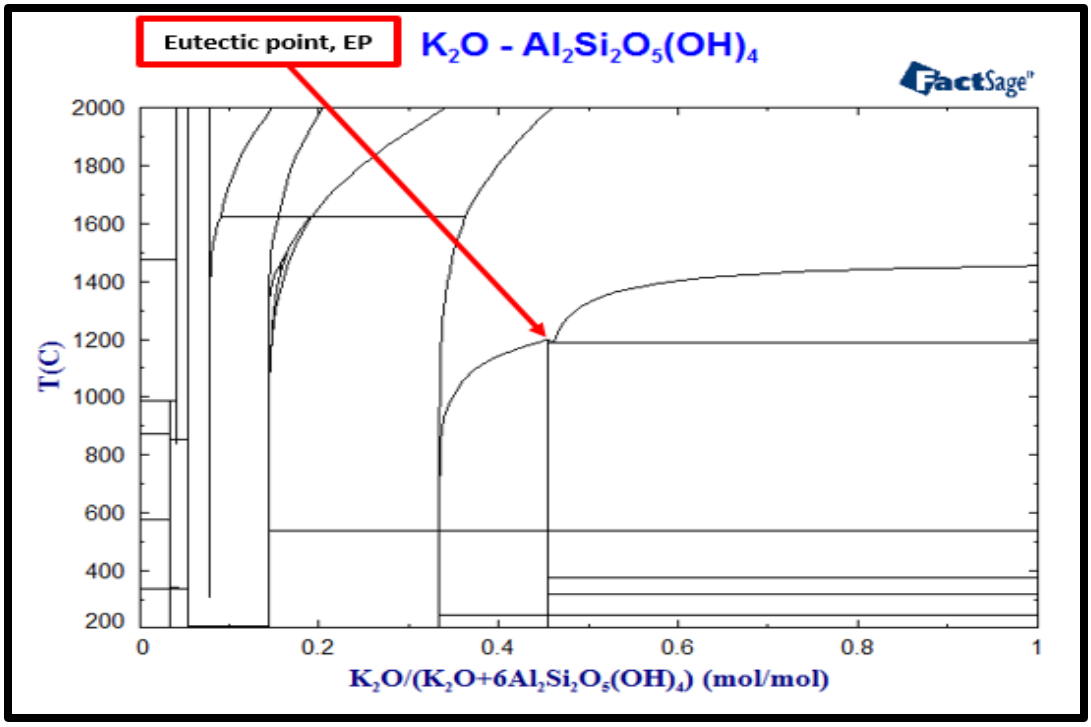

Figure 5-7 Eutectic point on a binary phase diagram at 1200 ^{0}C with addition of 6 moles of kaolin.

5.5 Locating Eutectic Points on the Ternary Phase Diagram

Ternary phase diagram is a phase diagram comprising of three concurrent components with four dimensions. That is the 3-components and the Temperature axis. It can be likened to a quadrilateral triangle. The composition of the component at the vortex is 100%. Moreover, the composition of each component at the two edges is 100% each [243]. Eutectic point is formed within the interior of the triangle and this depends on the compositions of each component in the entire system. The ternary eutectic point is the point at which, three boundary curves appear together at a triple junction in a ternary phase diagram[244]. The corresponding temperature at which eutectic point was formed is the eutectic temperature. It is the temperature at which the three components crystallizes out at isothermal as shown in triangle ABC, Figure 5.8

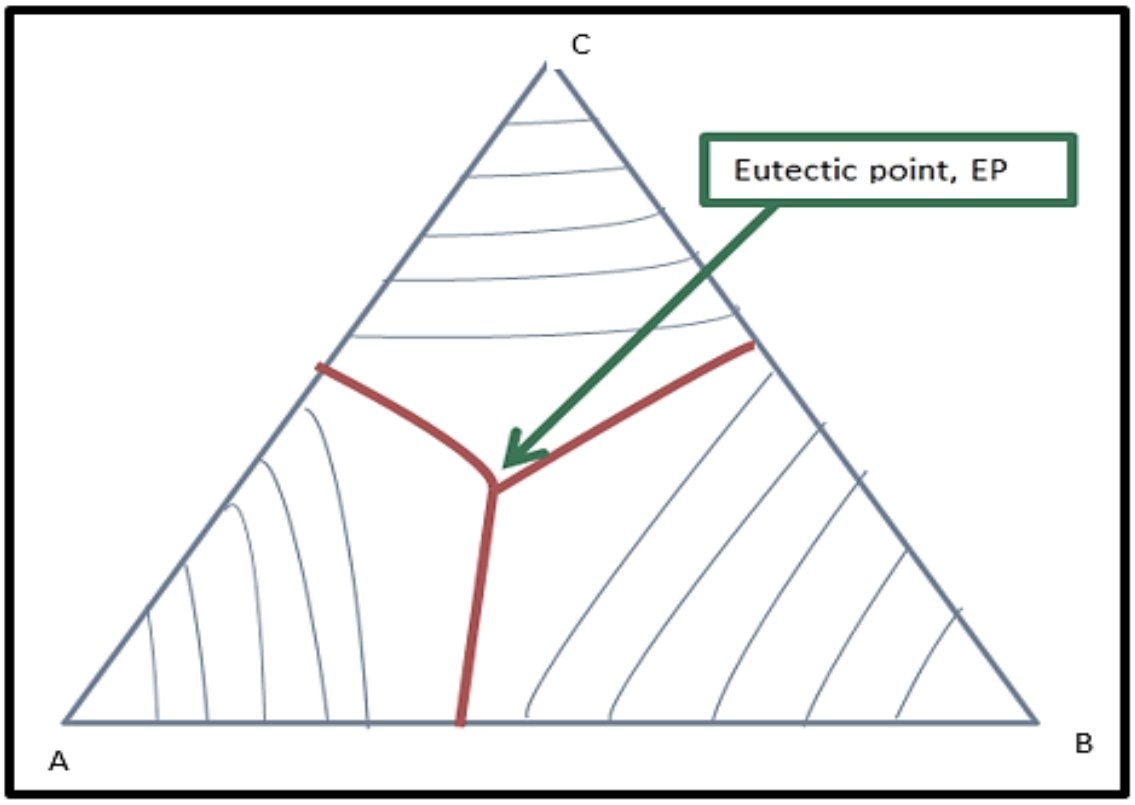

Figure 5-8: Schematic of Eutectic point on a typical ternary phase diagram

Factsage software was applied to predict eutectic points on both the binary and the ternary phase diagrams. Few of the graphs Figures 5.9 and 5.10 are as shown below while detailed analyses are contained in the results and discussions chapter of this thesis.

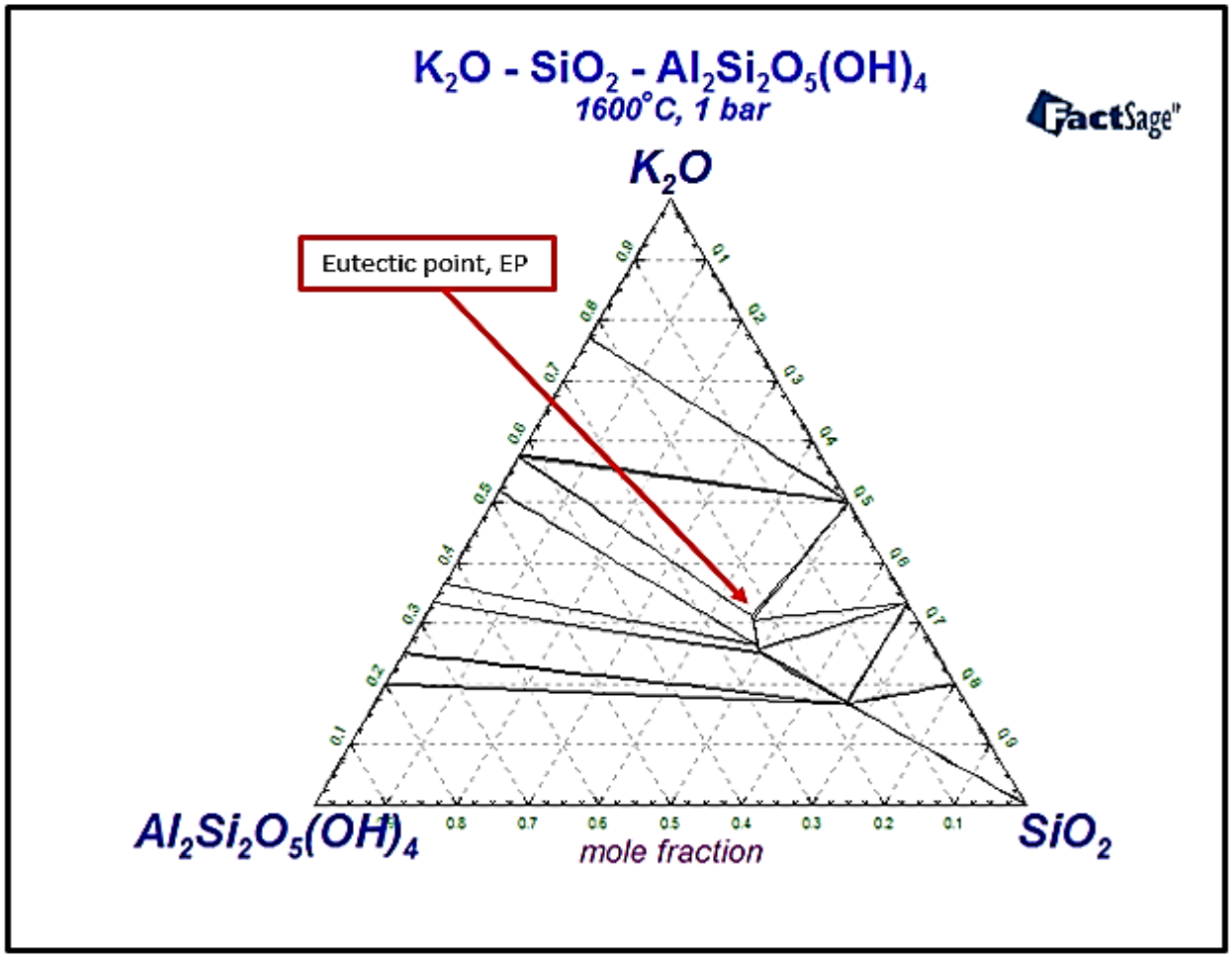

Figure 5-9 Eutectic point on a ternary phase diagram at 1600 ^{0}C and 1 bar

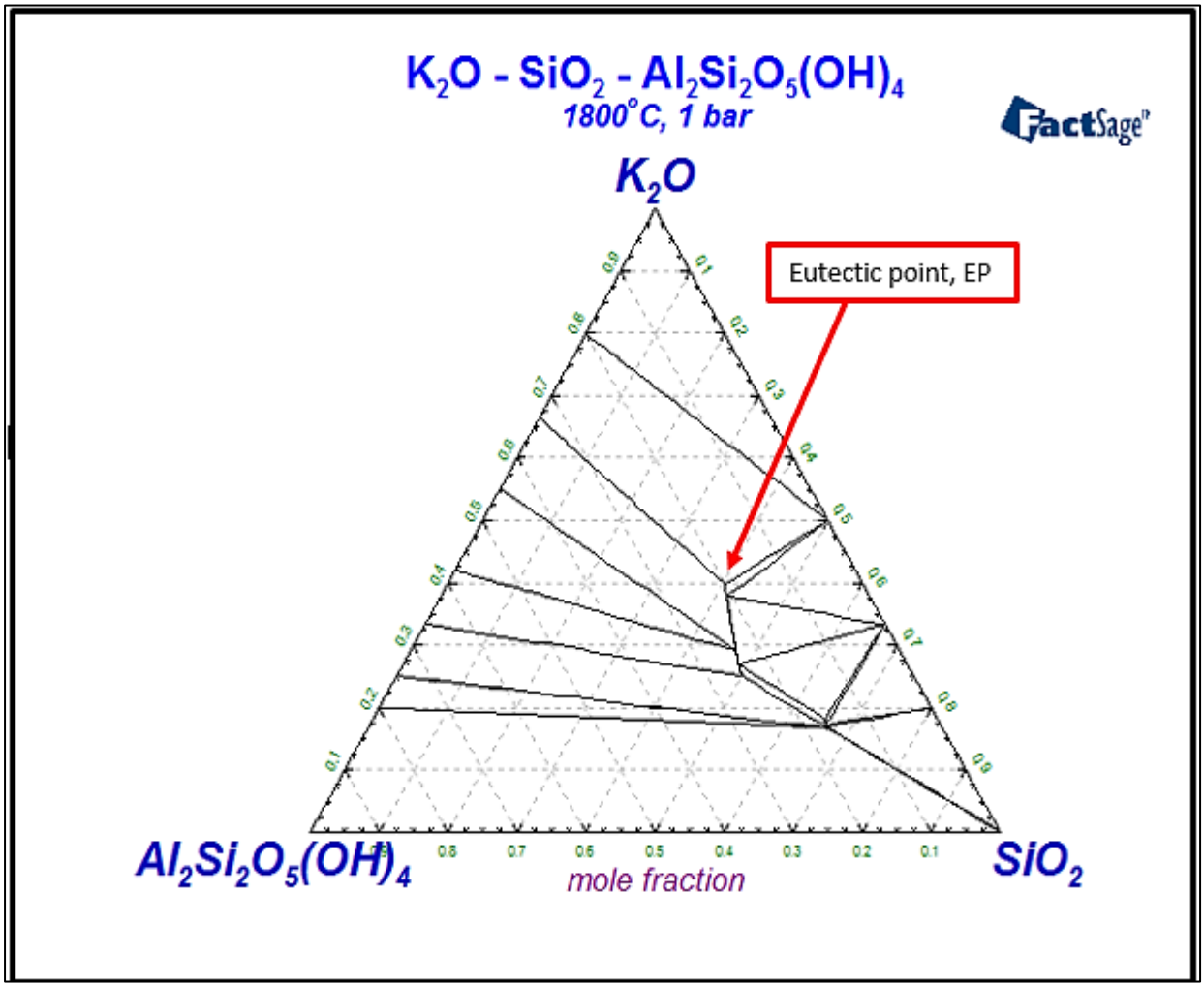

Figure 5-10 Eutectic point on a ternary phase diagram at 1800 ^{0}C and 1 bar

5.6 Comparison of Experimental results with Simulation data

Factsage software predicts the eutectic point which is the temperature at which agglomeration occurs in the combustion bed. These were depicted by series of phase diagram charts at different fuel compositions. Data obtained from these analyses would be compared with the post combustion analyses results with a view to establishing agglomeration tendencies in the combustor bed. Detailed analyses on this are contained in chapter 7 of this thesis.

5.7 Effects of Variations in the composition of components in moles or grams

Composition of individual component in moles or grams in the mixture of kaolin/potassium oxide or in kaolin/sodium oxide during the combustion of biomass fuels, does not seems to have any significant effect or influence on the agglomeration formation in the bed. Eutectic point was formed at the same temperature 1200 ^{0}C when ten moles of kaolin reacted with one mole of potassium oxide, Figures 5.11. Twelve moles of kaolin reacted with one mole of potassium oxide, Figure 5.12. Factsage software simulation results on the binary and ternary phase diagrams further emphasized this fact as discussed in the results analysis of this thesis.

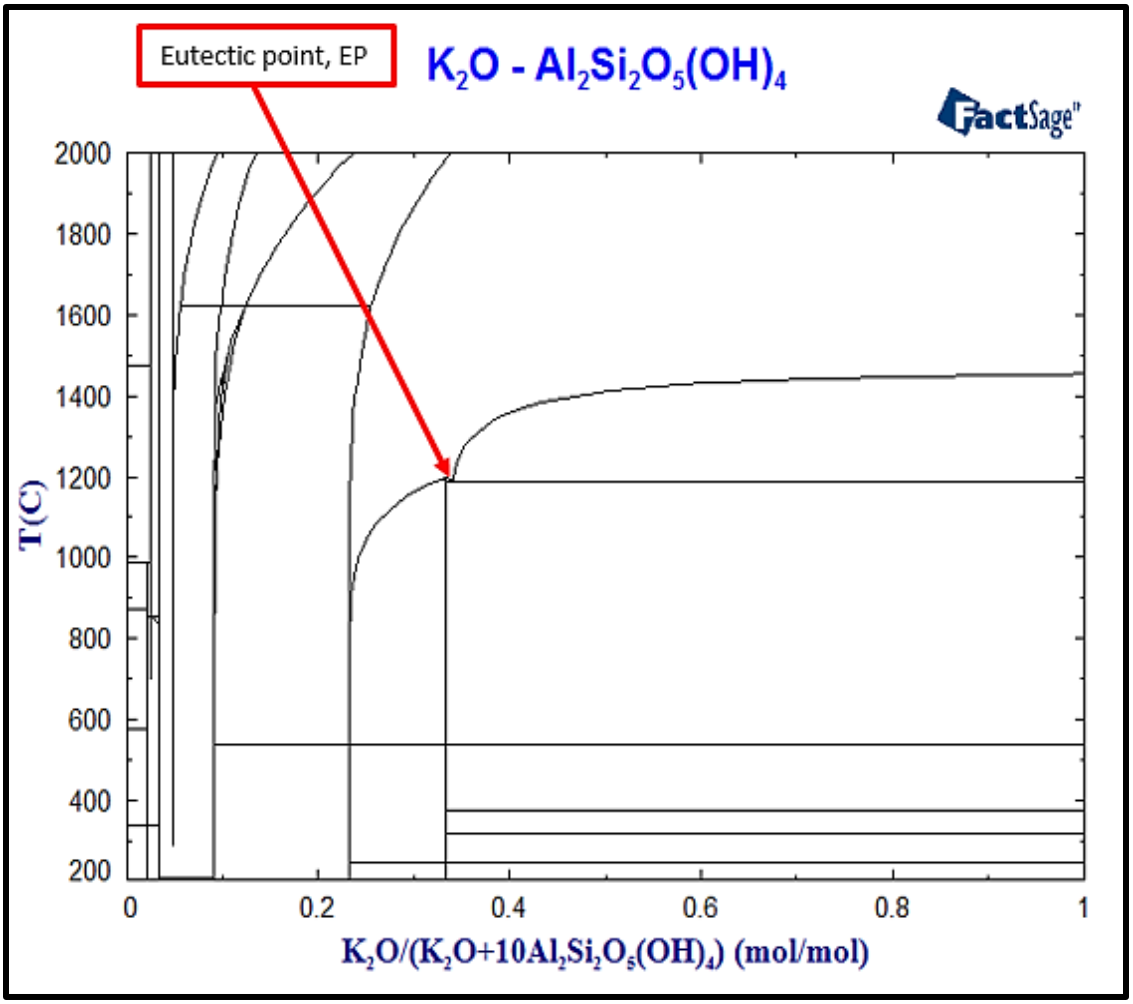

Figure 5-11: Eutectic point on a binary phase diagram at 1200 ^{0}C with addition of 10 moles of kaolin.

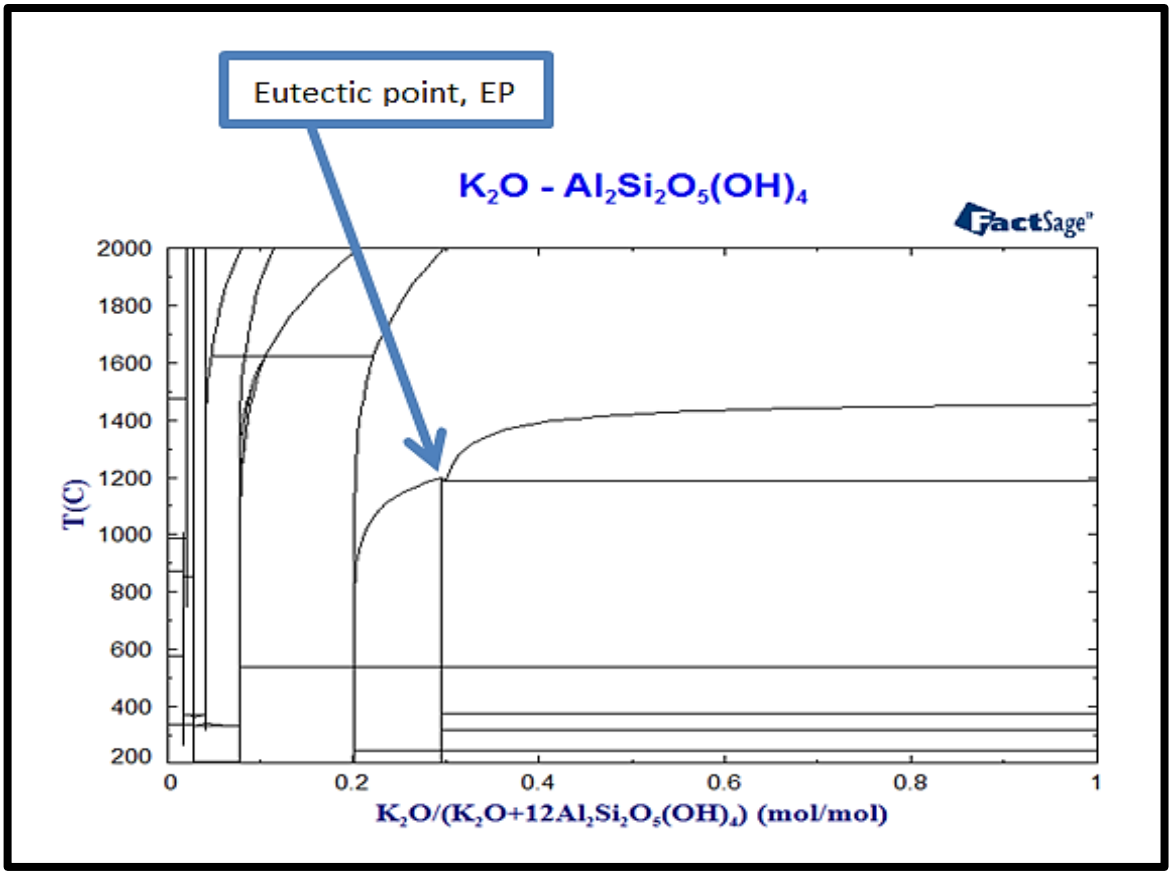

Figure 5-12 Eutectic point on a binary phase diagram at 1200 ^{0}C with addition of 12 moles of kaolin

In this research, Factsage software was utilized to predict the eutectic points (fusion temperatures) of the bed materials when additive (kaolin) was added to the bed materials. With the addition of the additives, a eutectic mixture whose melting point is higher than that of the parent materials (silica sand and K_2O from biomass fuel) was produced [7, 22, 128, 245].

In the simulation results, with the addition of additive, kaolin, $Al_2 Si_2 O_5 (OH)_4$ to the biomass fuels, it was shown that, agglomerates could be produced at elevated temperature of 1200 ^{0}C if the material is hugely dominated by Potassium oxide, K_2O, Figure 5.13. The volume of the additive, kaolin or the biomass fuels does not seem to have any noticeable significant effect or influence on the eutectic temperatures as depicted.

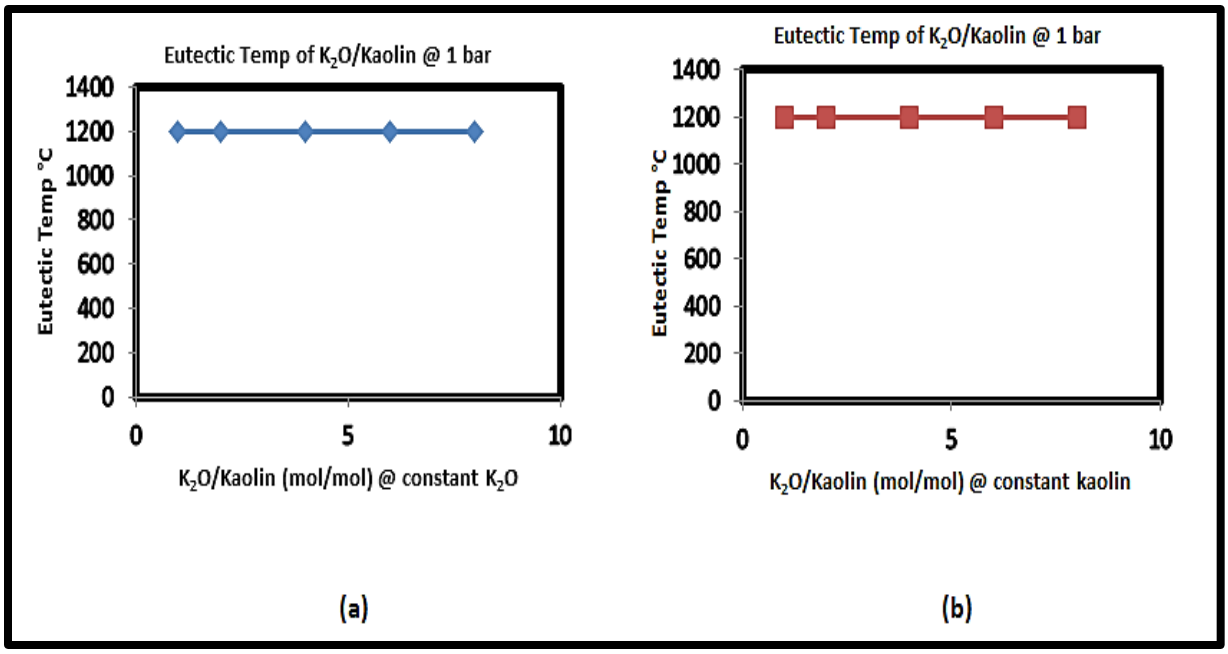

Figure 5-13: (a) Eutectic temperature between kaolin and potassium oxide at constant K_2O, on binary phase diagram at 1200 ^{0}C. (b) Eutectic temperature between kaolin and potassium oxide at constant kaolin, on binary phase diagram at 1200 ^{0}C

Meanwhile, in a Sodium oxide, Na_2O dominated biomass fuels; simulation results indicated that agglomerates would be produce at a temperature of 1700^0 C irrespective of the volume of the additive or the biomass fuels in the composition. Figure 5.14 further expatiate on this fact but detailed analyses on these are contained in the results and discussions section of this thesis.

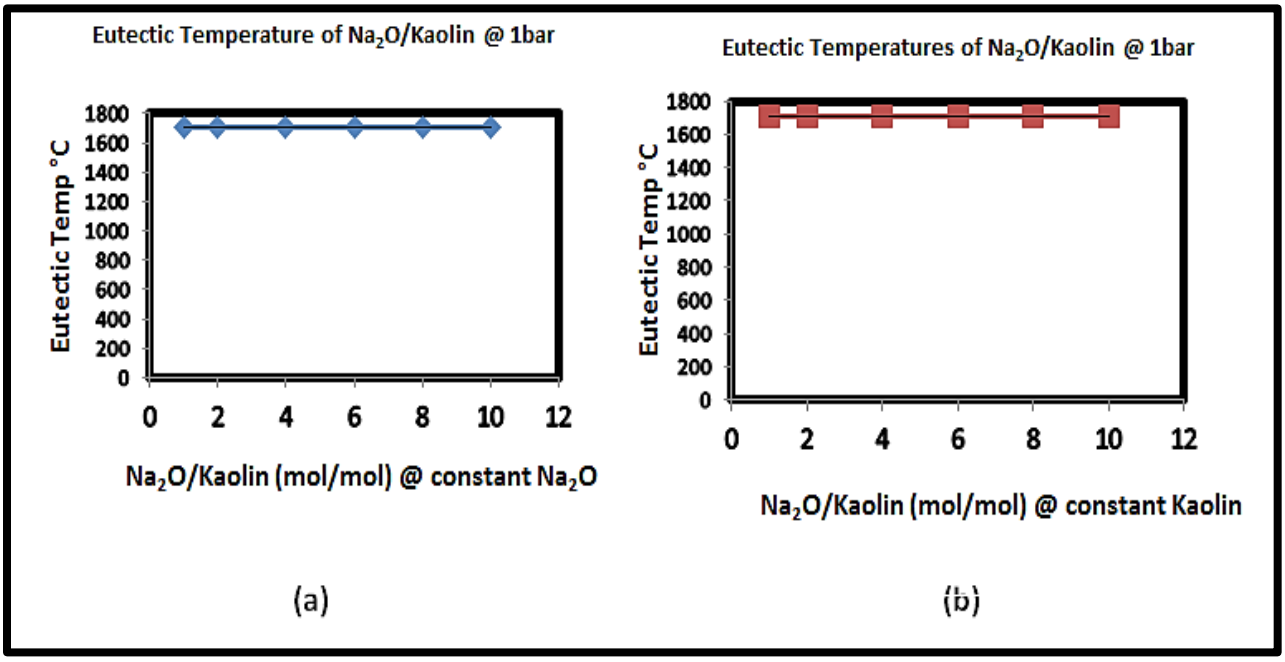

Figure 5-14: (a) Eutectic temperature between kaolin and sodium oxide at constant Na_2O, on binary phase diagram at 1700 ^{0}C. (b) Eutectic temperature between kaolin and sodium oxide at constant kaolin, on binary phase diagram at 1700 ^{0}C

5.8 Influence of pressure on agglomeration

Simulation results obtained from Factsage software clearly indicated that, operating the bed at a higher pressure would extend/prolong the time for agglomeration formation in a fixed bed. At a bed pressure of 1 bar in a Potassium K dominated biomass, the eutectic temperature at which agglomeration would occur in the bed is 1200 ^{O}C.

Meanwhile, in a Sodium Na dominated biomass, the eutectic temperature at which agglomeration would occur in the bed is 1700 ^{O} C at 1bar, Figure 5.15

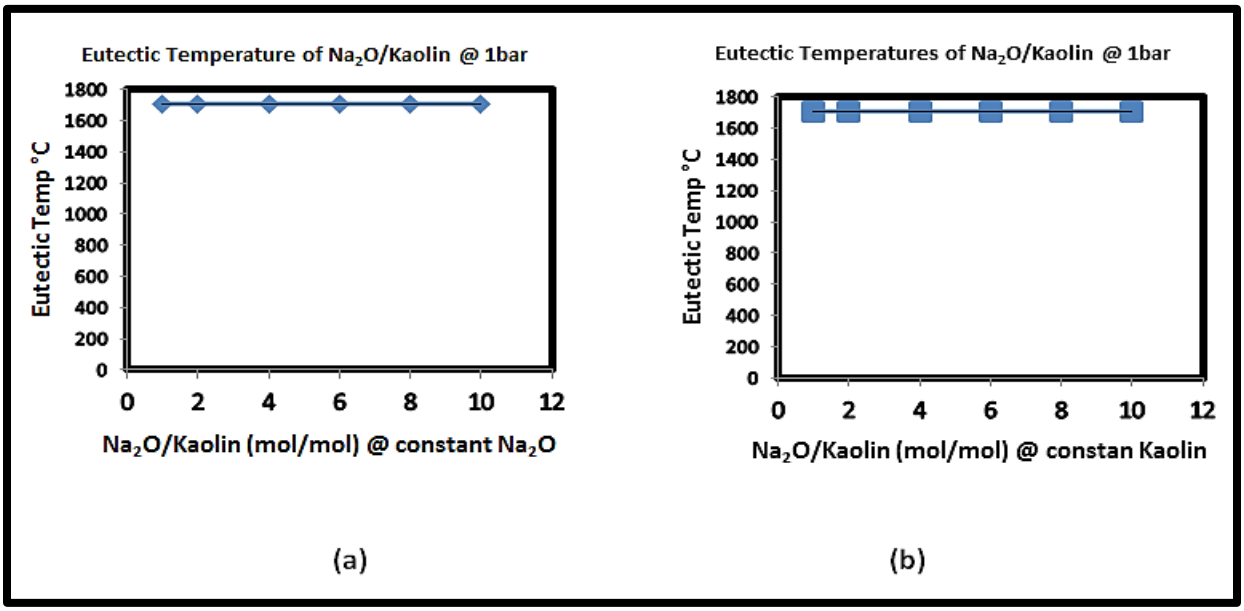

Figure 5-15: (a) Eutectic temperature between kaolin and Sodium oxide at constant Na_2O, on binary phase diagram at 1700 ^{0}C. (b) Eutectic temperature between kaolin and Sodium oxide at constant kaolin, on binary phase diagram at 1700 ^{0}C

However, as the pressure increases, so also the agglomeration time and temperature increases. At a pressure of 5 bar, in a Potassium K dominated biomass, the eutectic temperature at which agglomeration would occur in the bed is 1600 ^{O}C, Figure 5.16a and 5.16b as against 1200 ^{O}C when the pressure in the combustion chamber was 1bar.

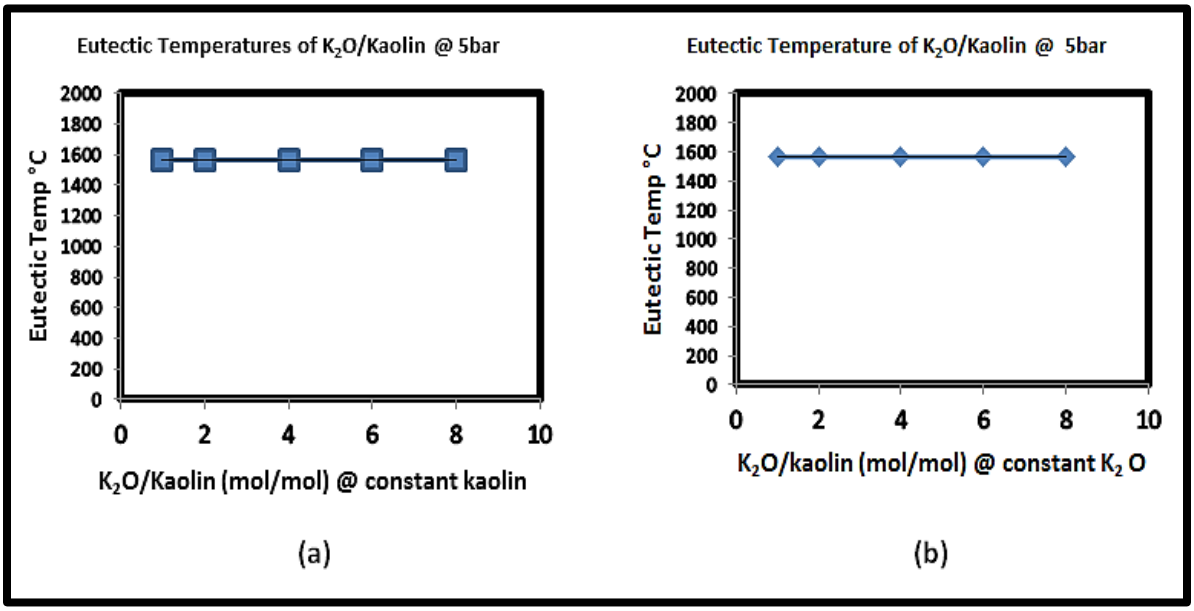

Figure 5-16: (a) Eutectic temperature between kaolin and potassium oxide at constant kaolin, on binary phase diagram at 1600 ^{0}C. (b) Eutectic temperature between kaolin and potassium oxide at constant K_2 O, on binary phase diagram at 1600 ^{0}C

Furthermore, at 5 bar, in a Sodium Na dominated biomass, the eutectic temperature at which agglomeration would occur in the bed is 2038 ^{O} C, Figure 5.17a and 5.17b.

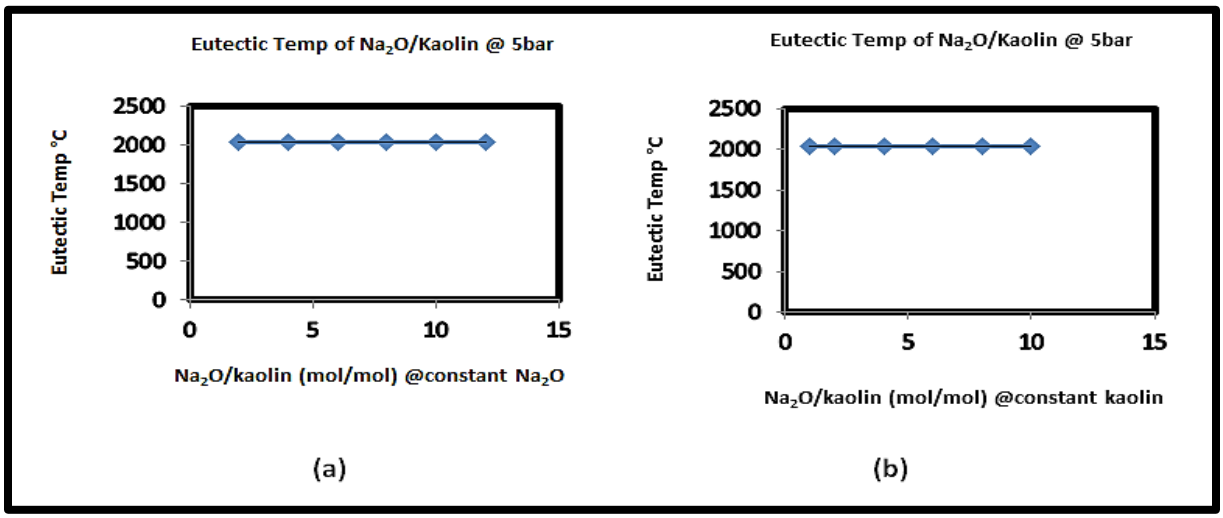

Figure 5-17: (a) Eutectic temperature between kaolin and Sodium oxide at constant Na2O, on binary phase diagram at 2000 0C. (b) Eutectic temperature between kaolin and Sodium oxide at constant kaolin, on binary phase diagram at 2000 ^{0}C

In Comparison with fluidized bed combustor, bed pressure increases as air flow rate increases [4,5]. Voidage at minimum fluidization ϵ_{mf}, increases slightly with increasing bed pressure while minimum fluidization velocity decreases with rise in the operating pressure but it is negligible for beds having fine particles with diameter d_p less than 100µm [59, 246]. Particle voidage at minimum fluidization ϵ_{mf}, increases with rise in the bed operating temperature for fine particles but may not have any effect on coarse particles. Minimum fluidization velocity U_{mf} of sand particles decreases with rise in bed operating temperature [2, 10, 246].

6 Results and Analyses

6.1 Introduction

This chapter hopes to bridge the already identified gaps during the broad outlook of the combustion of biomass fuels (chapter two) in a fixed bed, particularly in a Gooch crucible (combustion chamber). Considering the problems associated with the combustion of biomass fuels; fouling, erosion, slagging with specific interest in reduction of agglomeration during the combustion processes of willow, white wood, and miscanthus (selected fuels for this project). The scope of the present work has limited the research area to encapsulate only agglomeration out of all the problems listed above.

Moreover, as contained in chapters 2, 3, and 4 with emphasis on chapters 2 and 4, agglomeration usually occur in the combustion beds at temperatures that is a little higher than the average sintering temperature (670 ^{0}C) of the respective biomass fuels.

Addition of additive (kaolin) to the bed materials prior to the combustion process or during the combustion process, caused agglomeration to be avoided even when the materials were heated at the same temperature. With kaolin added, agglomeration was predicted (Factsage software) to occur at elevated temperatures of 1200 ^{0}C in a potassium, K dominated biomass fuels and 1700 ^{0}C in a sodium, Na dominated biomass fuels. Variations in the composition of the components do not have appreciable influence on the eutectic temperatures and agglomeration in the combustion beds.

The experimental results emanated from the combustion of single biomass fuel and its blends indicated that, agglomerates are produced in the combustion chamber (Gooch crucible) at a temperature range of between 750 ^{0}C and 802 ^{0}C but when additive (kaolin) was added, agglomerates were not produced at these temperatures.

However, chapter 6 has been separated into sub-sections and cases for ease of discussion in no specific order.

6.2 Analyses of Results (Computational)

Case 1 recaps series of the simulation results emanated from the application of the Factsage software to predict the eutectic points on binary and the ternary phase diagrams. The eutectic temperature is the temperature at which fusion of alkali metals (K, Na) and silica (SiO_2) from the sand (bed material) occurs in the combustion bed during the combustion process of the problematic biomass fuels.

Variations in the composition of the components do not have any noticeable effects on the agglomeration and the eutectic points. Two components (additive and alkali oxides) were compared simultaneously on the binary phase diagrams.

Alkali oxides considered are potassium oxide K_2O and sodium oxide Na_2O while the additive is kaolin, $Al_2 Si_2 O_5 (OH)_4$. With the dominant alkali in the biomass fuels as potassium K, eutectic point was located on the phase diagram at a eutectic temperature of 1200 ^{0}C as indicated by the meeting point of the two liquidus on the tie lines, Figures 6.1, 6.2, 6.3, and 6.4.

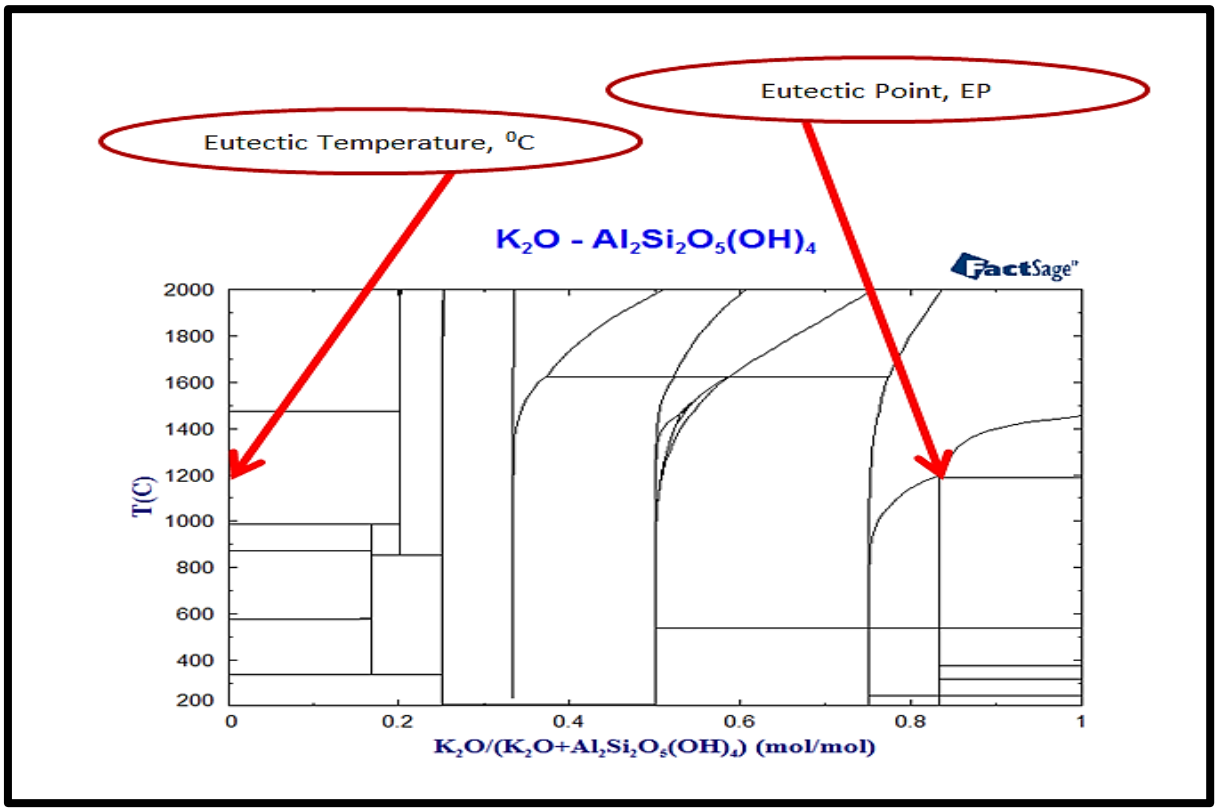

Figure 6-1: Locating eutectic points on binary phase diagrams at 1200 ^{0}C

Irrespective of variations in the composition of the components, the eutectic point remained unaltered at 1200 ^{0}C in a potassium dominated biomass fuels, Figure 6.2

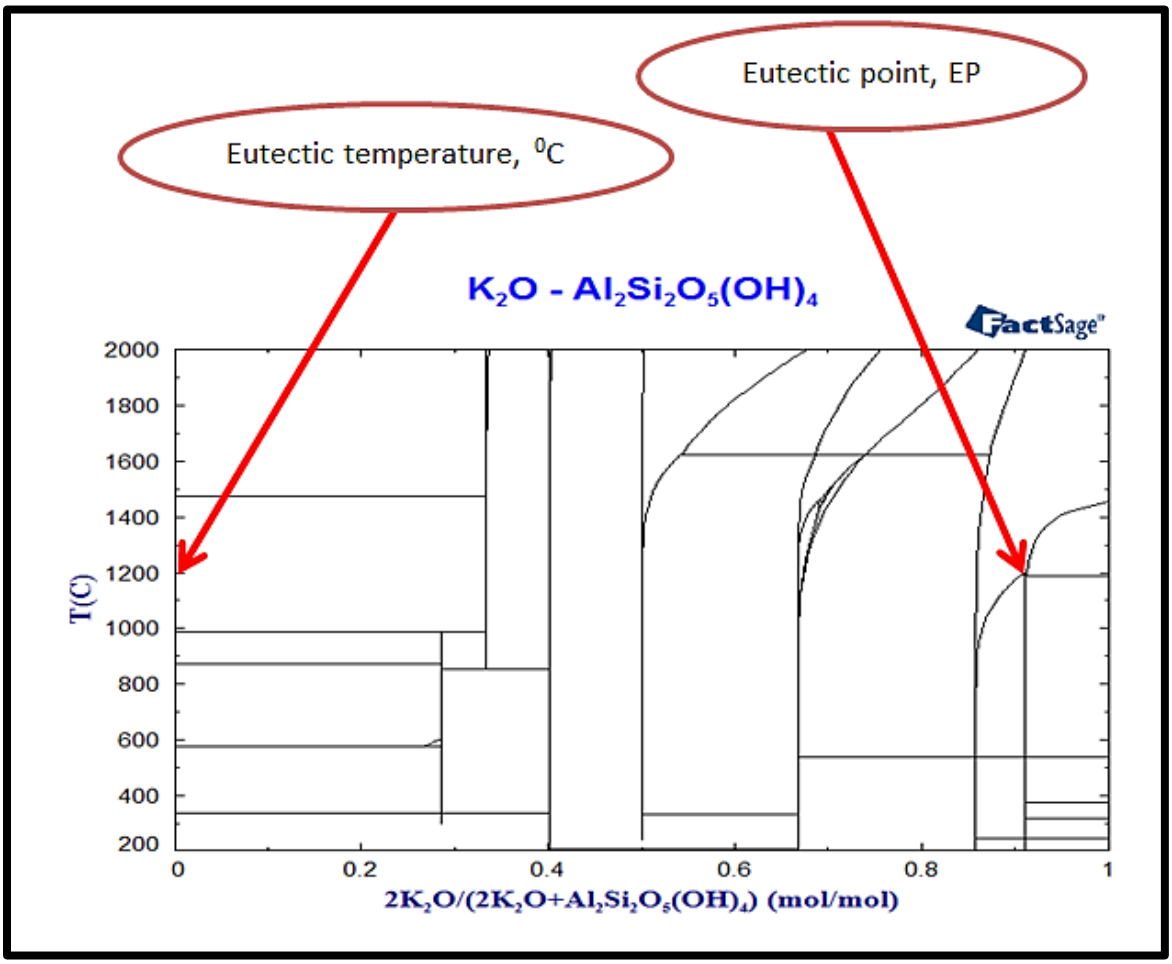

Figure 6-2: Locating eutectic points on binary phase diagrams at 1200 ^{0}C

In figure 6.2, two moles of potassium oxide reacted with one mole of kaolin in the combustion chamber, agglomeration occurred at a temperature of 1200 ^{0}C. This is equivalent to the eutectic temperature recorded when one mole of potassium oxide reacted with1 mole of kaolin under the same operating condition of pressure, 1 bar, Figure 6.3

Alternatively, two moles of kaolin were added to one mole of potassium oxide under the same operating conditions, the same eutectic temperature of 1200 ^{0}C was also recorded as depicted in figure 6.3

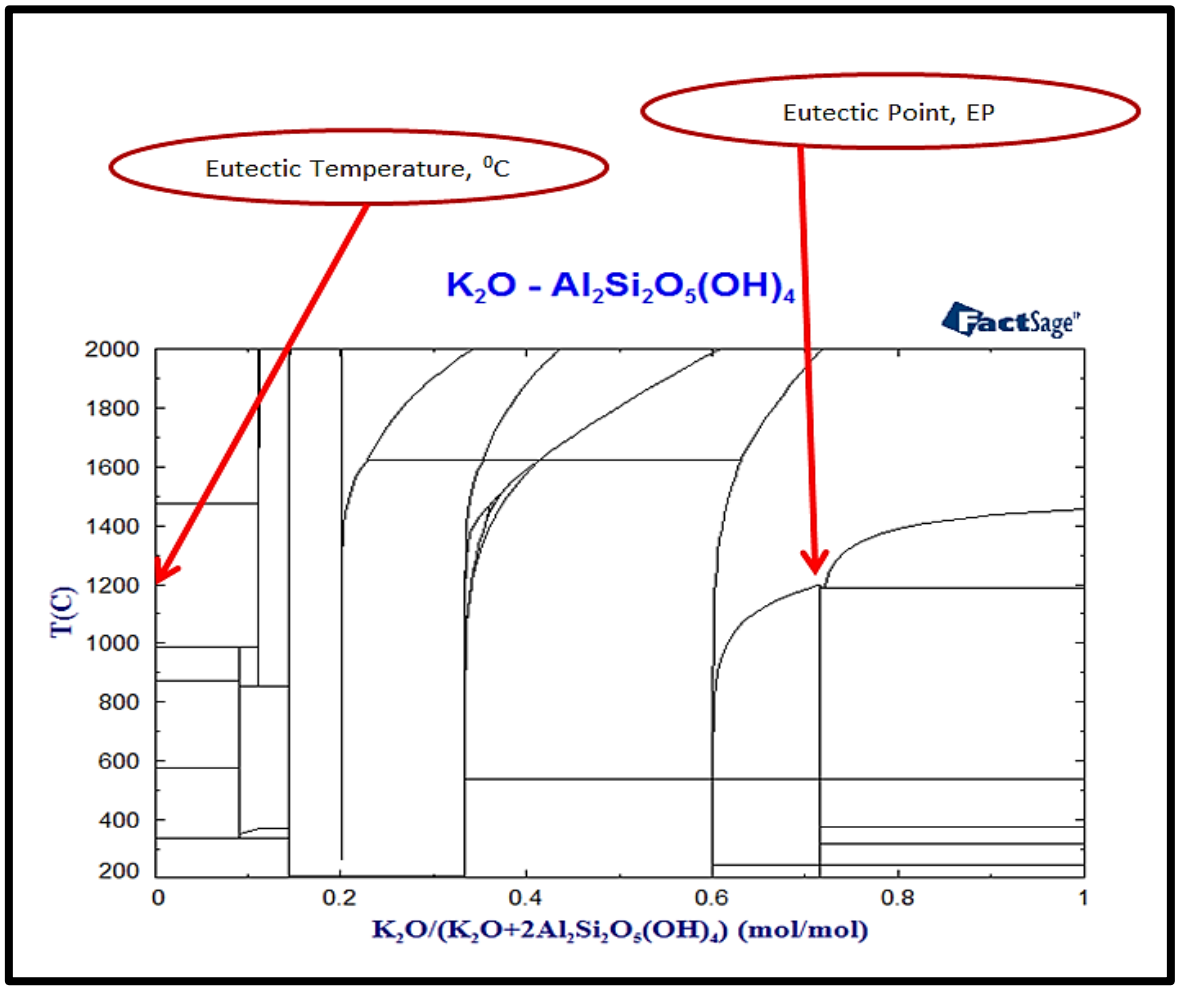

Figure 6-3: Locating eutectic points on binary phase diagrams at 1200 ^{0}C

In the same pattern, four moles of kaolin were added to one mole of potassium oxide under the same operating conditions. A eutectic point was located at an equivalent temperature of 1200 ^{0}C with an increase in the percentage composition of kaolin to four moles, Figure 6.4

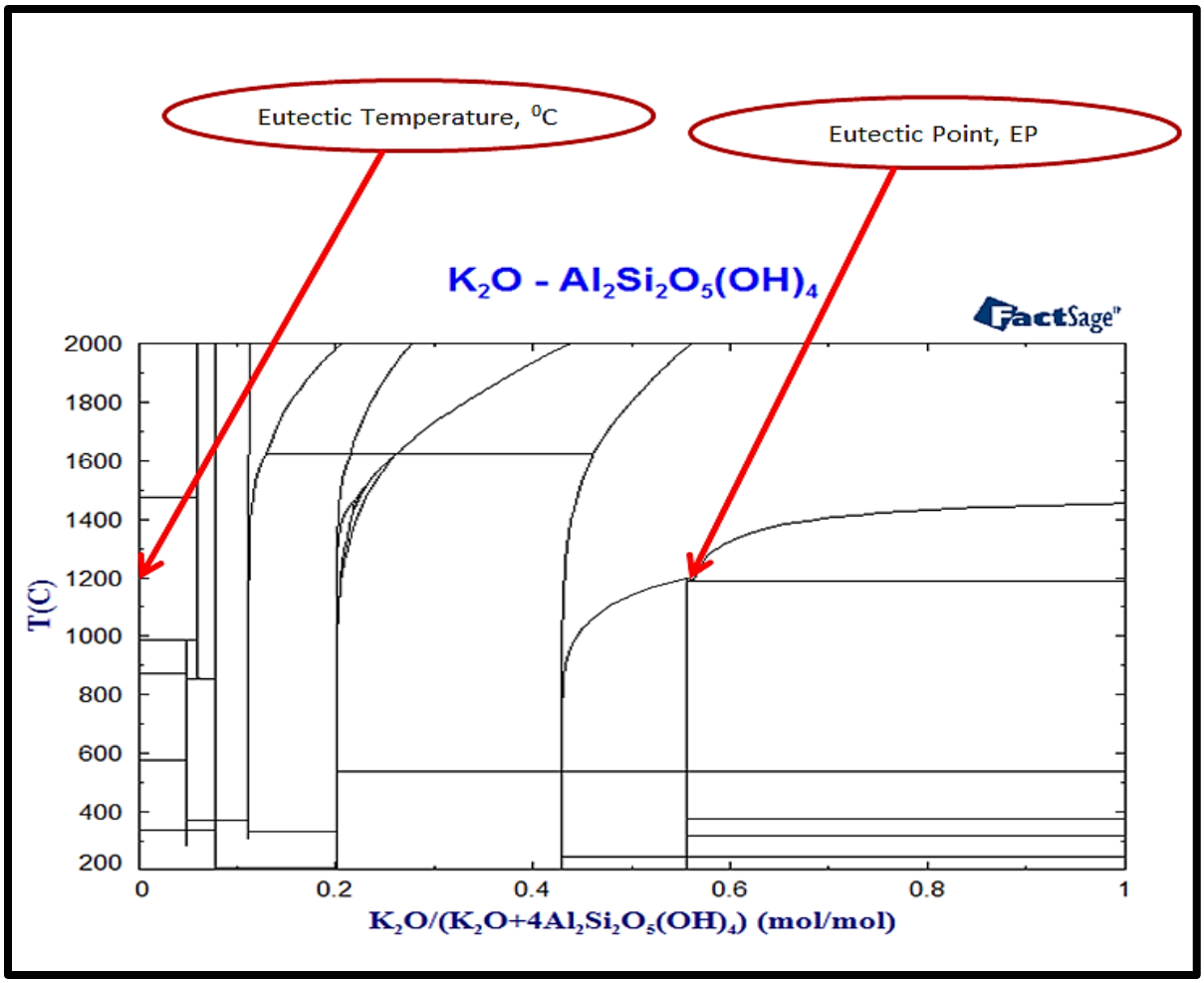

Figure 6-4: Locating eutectic points on binary phase diagrams 1200 ^{0}C

Increase or decrease in the proportion of the components, under the same operating conditions does not have any noticeable influence on the eutectic point viz a viz the equivalent eutectic temperatures. This assertion, is further ascertained while considering the combustion of sodium dominated biomass fuels in a laboratory – scale fixed bed using a Gooch crucible as the combustion chamber.

Utilizing Factsage software to predict the eutectic temperatures in a sodium dominated biomass fuels, a eutectic point was located on the binary phase diagrams at a temperature of 1600 ^{0}C irrespective of the volume of the individual component in the mixture, Figures 6.5, 6.6, 6.7, and

6.8. In a mixture of one mole of sodium oxide and one mole of kaolin, a eutectic point was located at an equivalent temperature on the binary phase diagram, Figure 6.5.

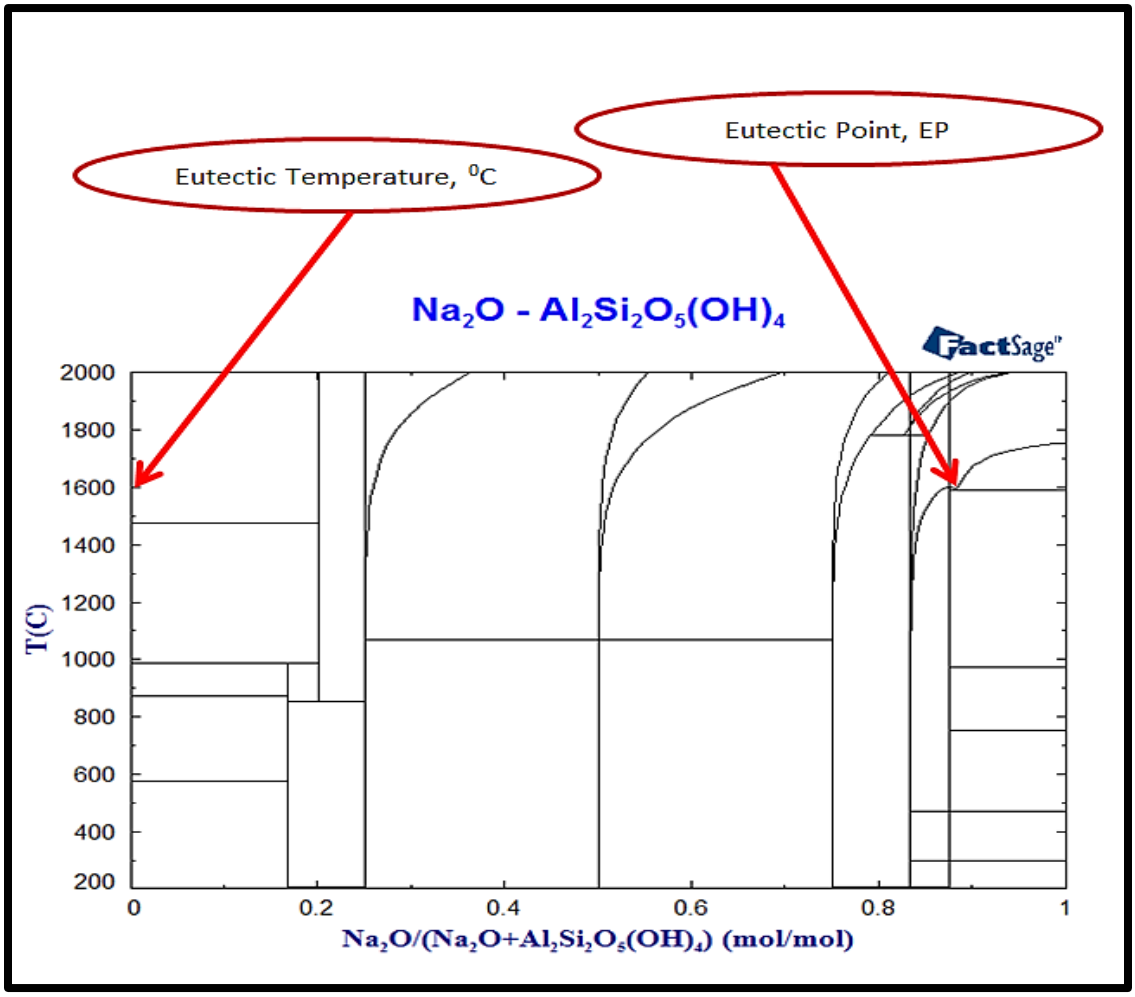

Figure 6-5: Locating eutectic points on binary phase diagrams at 1600 ^{0}C

Increasing the number of moles of sodium oxide in the mixture yielded a eutectic point at the same eutectic temperature of 1600 ^{0}C, Figure 6.6. This is an indication that, variation in the volume of the components does not have any significant control or effect on the eutectic point on the phase diagram and on the eutectic temperature in the combustion chamber during the combustion of the problematic biomass fuels.

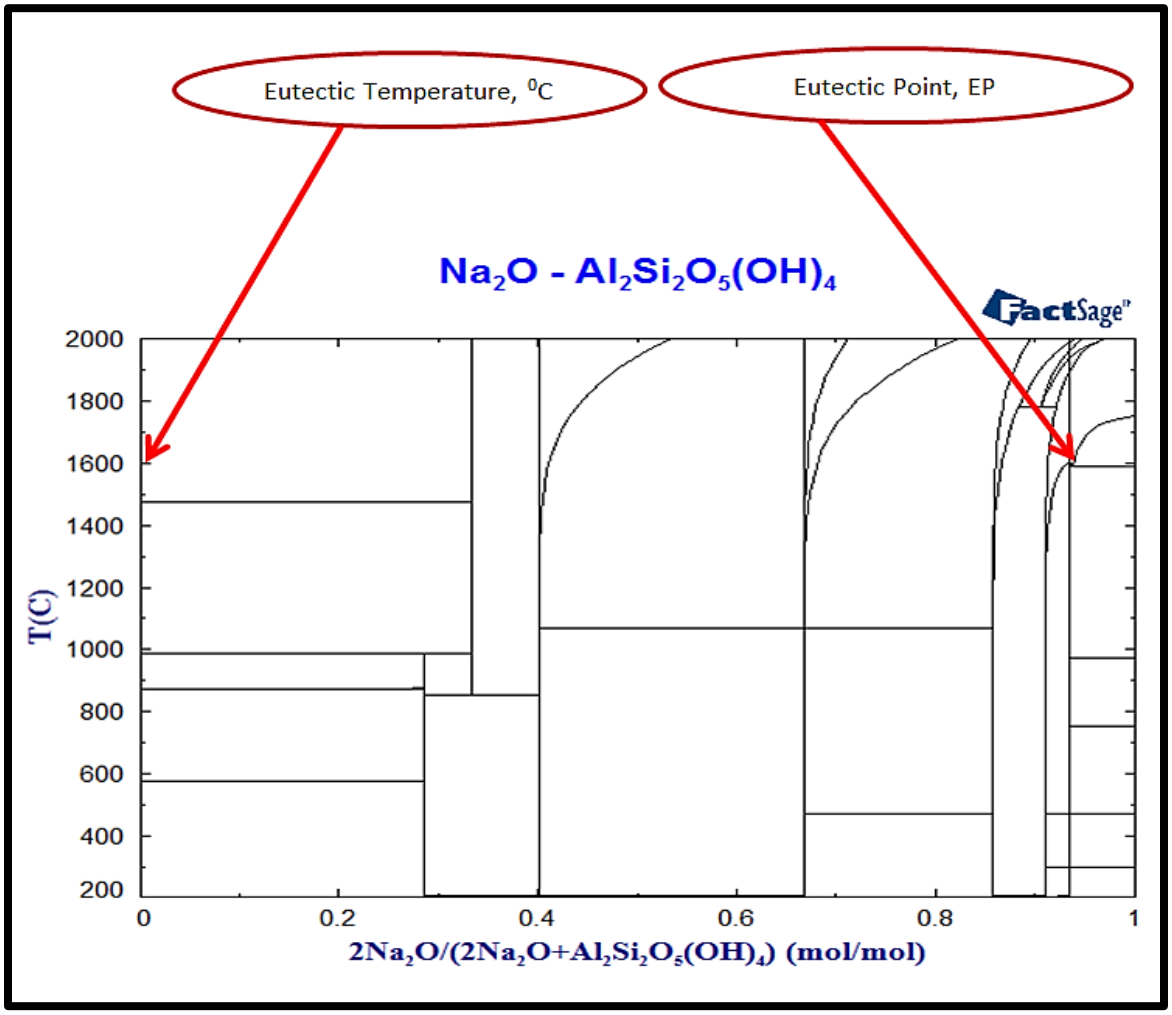

Figure 6-6: Locating eutectic points on binary phase diagrams at 1600 ^{0}C

On the other hand, increase in the number of moles of kaolin to two and then four while keeping the number of moles of the alkali oxide (sodium oxide) constant at one mole, does not have any specific change in both the eutectic point and eutectic temperatures as seen in Figures 6.6 and 6.7. In comparison with the ternary phase diagram, the eutectic temperature remained at 1600 ^{0}C and 1800 ^{0}C. This is the temperature at which agglomerates are expected to be produced during the combustion of the selected problematic biomass fuels; willow, miscanthus, and white wood.

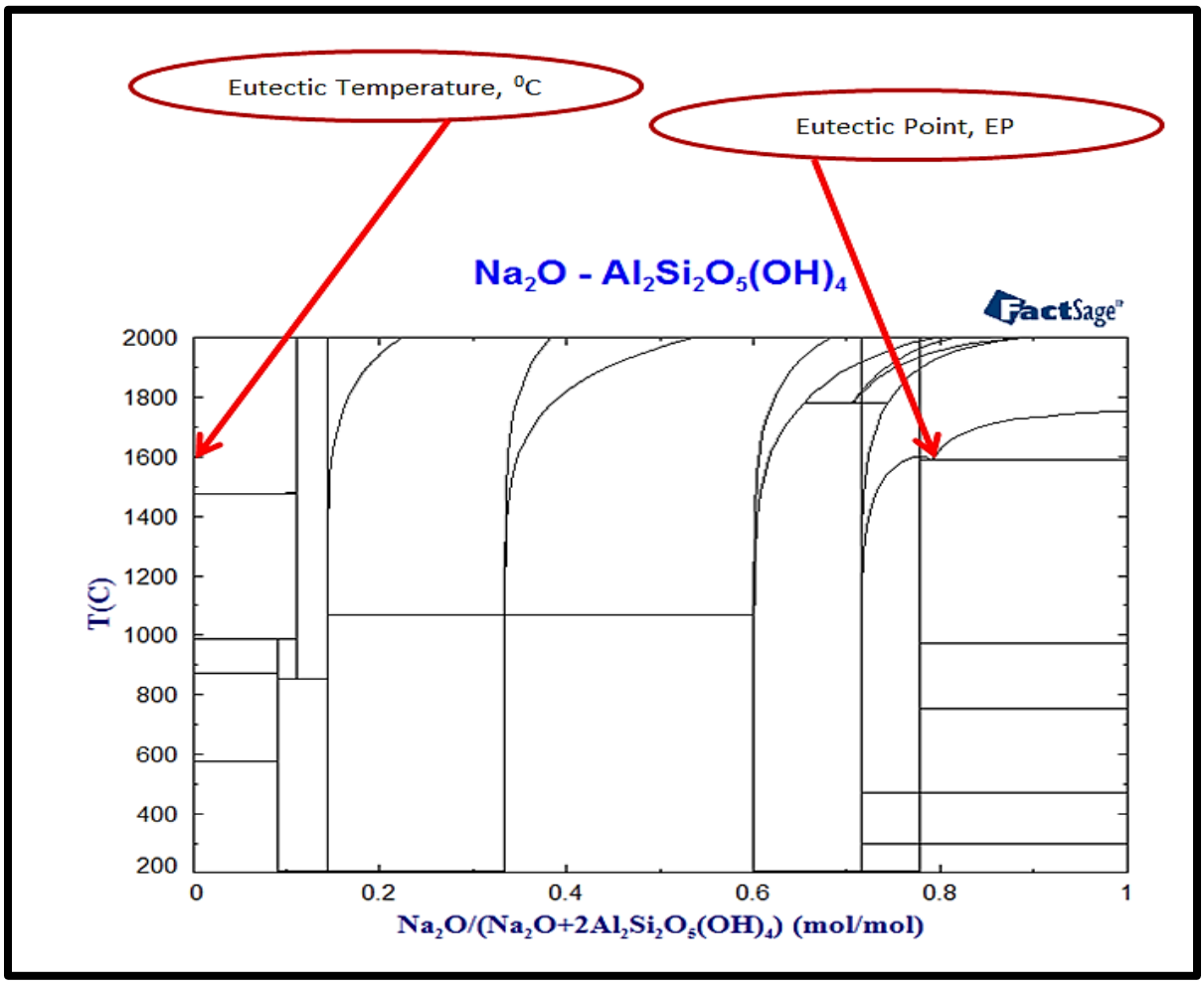

Figure 6-7: Locating eutectic points on binary phase diagrams at 1600 ^{0}C

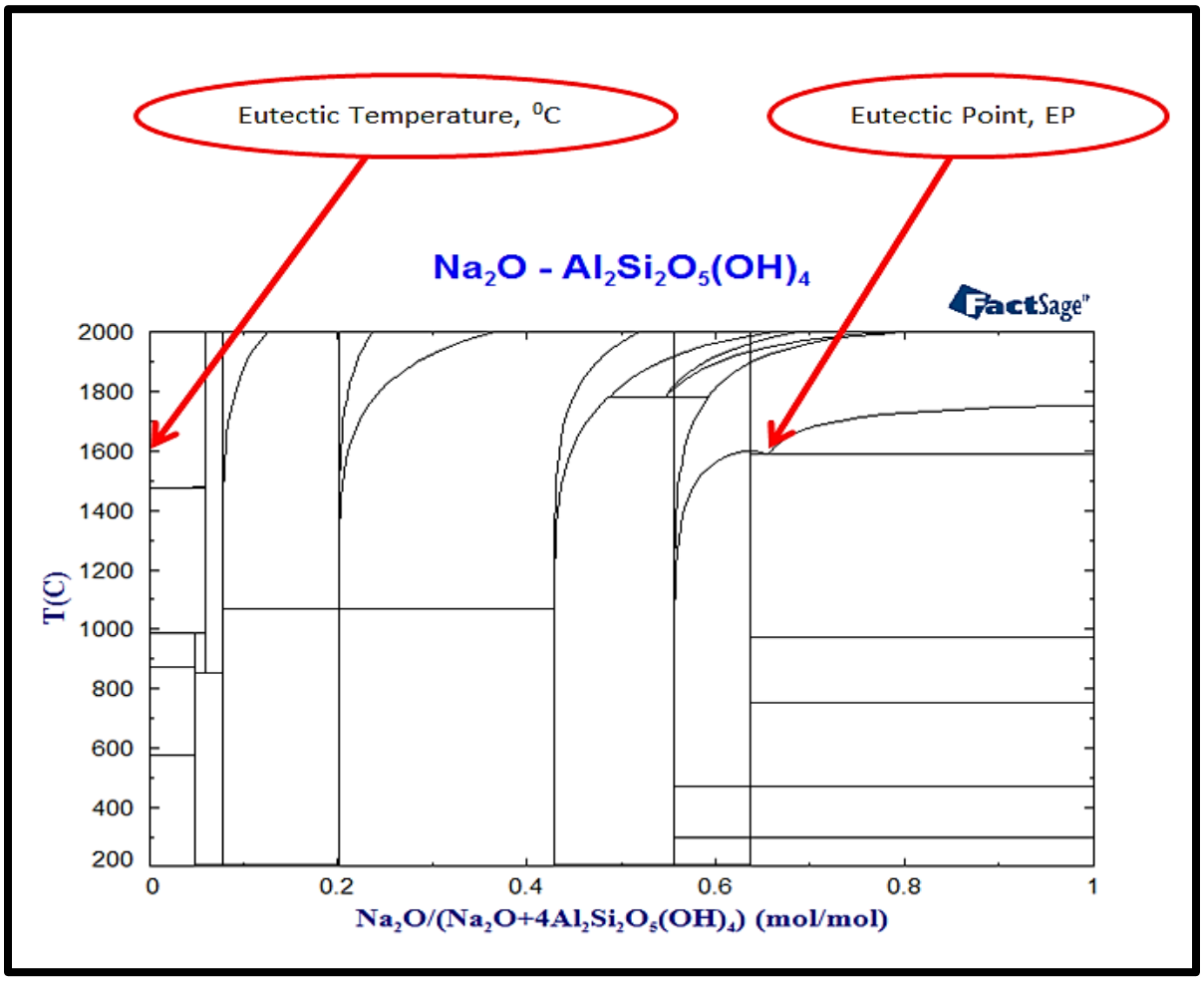

Figure 6-8: Locating eutectic points on binary phase diagrams at 1600 ^{0}C

6.3 Influence of Additive and Pressure on Agglomeration Tendencies

This sub-section considers the influence of additive and pressure on the agglomeration tendencies of the selected biomass fuels. Simulation results indicated that, with the addition of kaolin to the bed contents, pressure has tremendous influence on the formation of agglomerates in the beds during the combustion of the problematic biomass fuels.

The higher the pressure in the bed, the higher the temperature at which agglomeration will occur in the bed. Considering the binary phase diagrams emanated from the combustion of the

selected biomass fuels (willow, miscanthus, and white wood), only two components were compared simultaneously (kaolin and alkali compounds) while in the ternary phase diagrams, three components were compared together simultaneously (alkali compounds, kaolin, and silica). Moreover, simulation results gathered from the series of binary phase diagrams, at a pressure of 1 bar, predicted the occurrence of agglomeration at elevated temperatures of 1200 ^{0}C and 1708 ^{0}C in the combustion if the dominant alkali metals are potassium, K and sodium, Na respectively Figures 6.9 and 6.10 respectively.

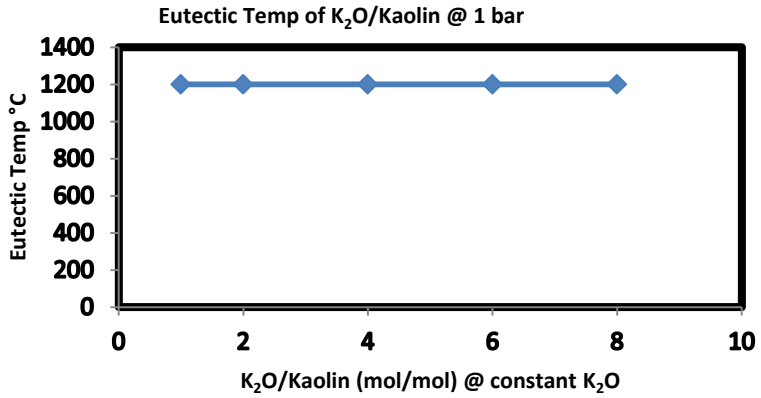

Figure 6-9: Eutectic Temperature with Factsage software application at 1200 ^{0}C

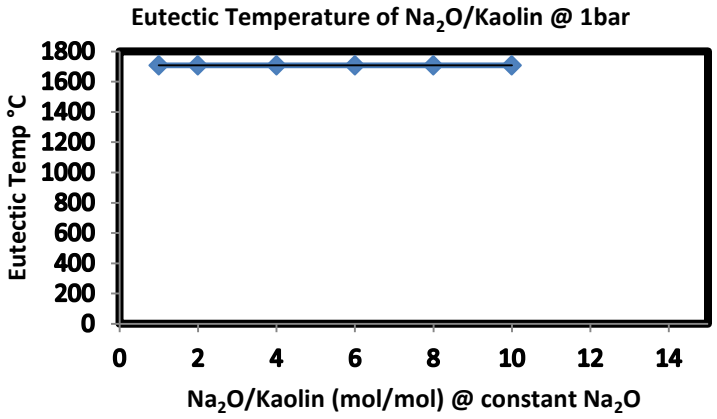

Figure 6-10: Eutectic Temperature with Factsage software application at 1700 ^{0}C

However, temperature at which agglomeration occurs in the bed increases as the pressure increases. At a pressure of 5 bar, and if the dominant alkali metal is potassium K, eutectic temperature was predicted to be 1566 ^{0}C, Figure 6.11

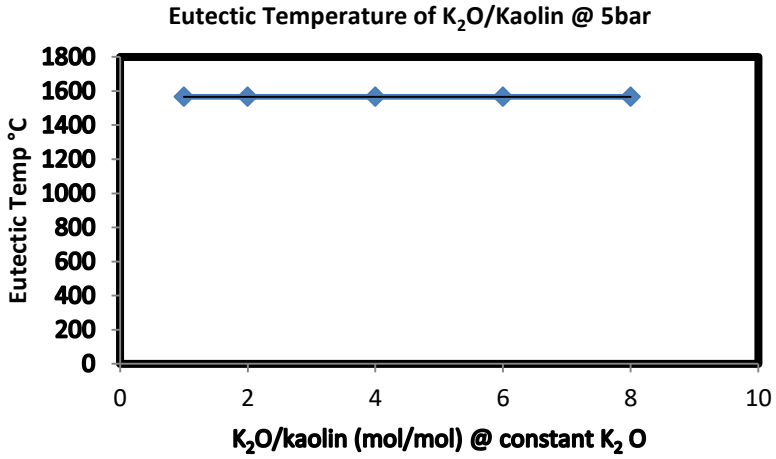

Figure 6-11: Eutectic Temperature with Factsage software application at 1600 ^{0}C

Meanwhile, if the dominant alkali metal is sodium Na, agglomeration was predicted to occur in the bed at a temperature of 2038 ^{0}C, Figure 6.12 (eutectic temperature).

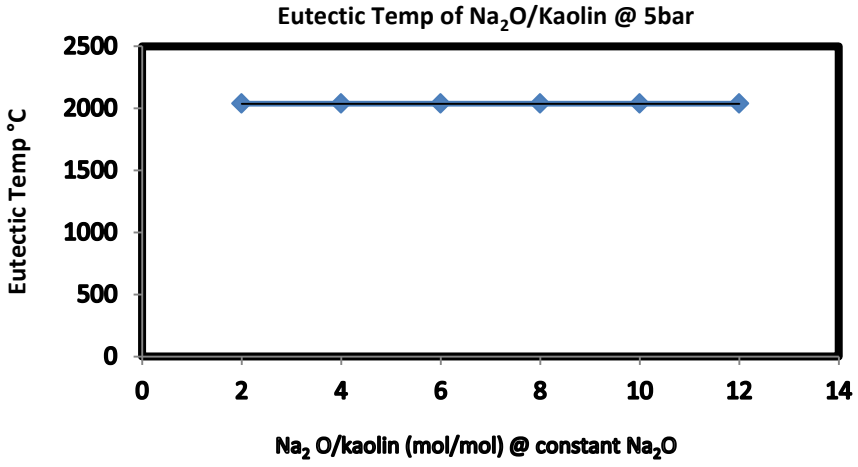

Figure 6-12: Eutectic Temperature with Factsage software application at 2000 ^{0}C

Moreover, with the pressure maintained at 5bar and kaolin is kept constant, it was predicted that, agglomeration will occur in the bed at a temperature of 1600 ^{0}C when the dominating alkali metal is potassium K, Figure 6.13

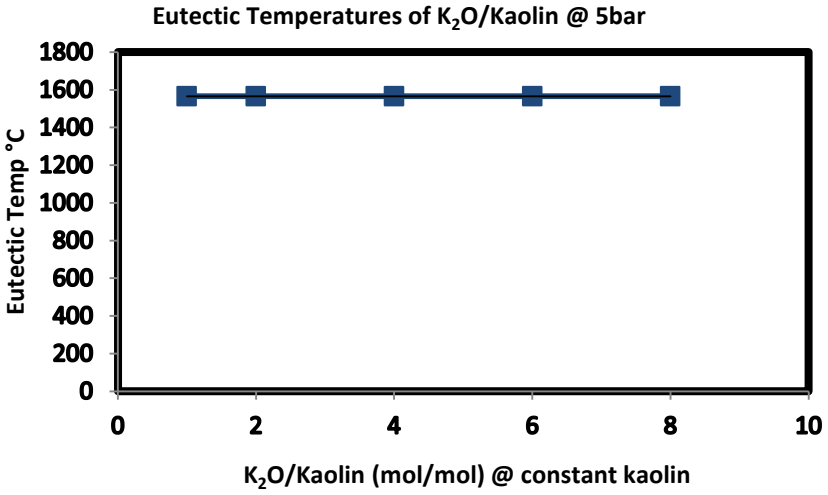

Figure 6-13: Eutectic Temperature (1600 ^{0}C) with Factsage software application at 5bar.

In the ternary phase diagram, no eutectic point was observed at temperatures of 1300 ^{0}C and 1400 ^{0}C, Figures 6.14 and 6.15 respectively.

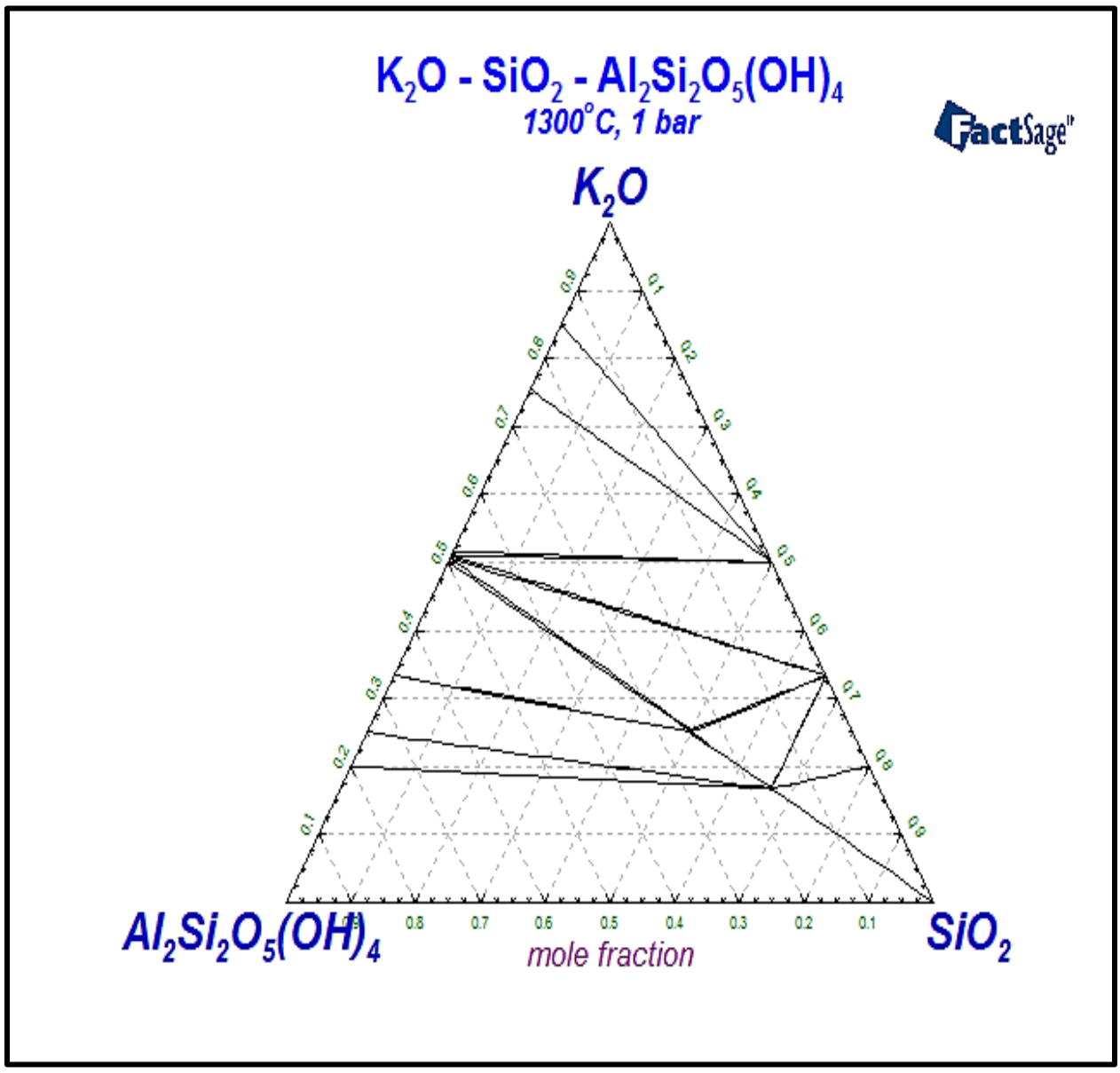

Figure 6-14: No eutectic point formed at 1300 ^{0}C on ternary phase diagram

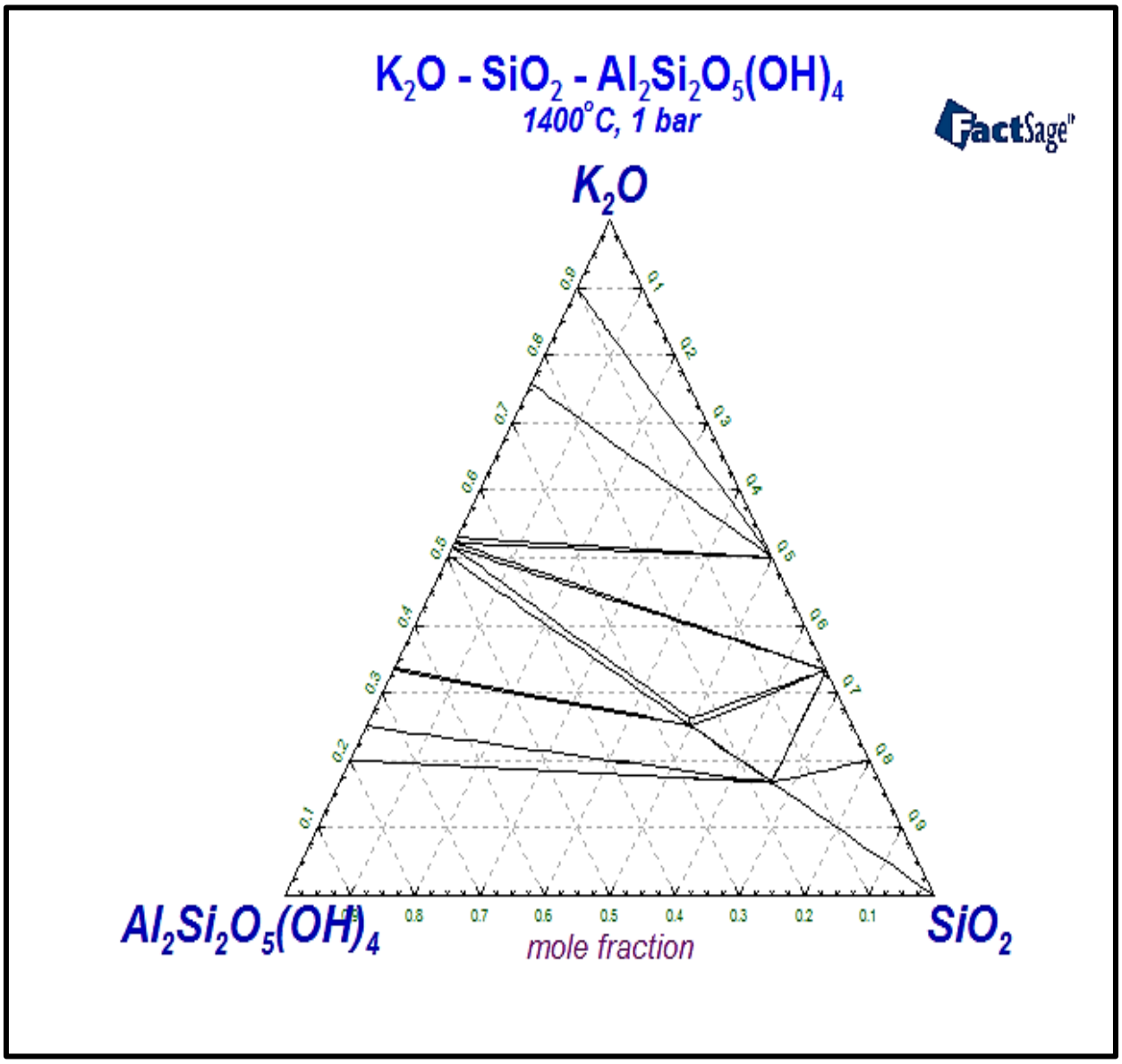

Figure 6-15: No eutectic point formed at 1400 ^{0}C on ternary phase diagram

It is expected that, eutectic points would be formed at higher temperatures than experienced in the binary phase diagrams. This is because, three components interacted simultaneously K_2O - SiO_2 – $Al_2Si_2O_5(OH)_4$. This compound has a higher melting temperature than the K_2O - $Al_2Si_2O_5(OH)_4$ hence, higher eutectic points. Eutectic point was first noticed at 1550 ^{0}C and became obvious at 1650 ^{0}C, Figures 6.16 and 6.17 respectively.

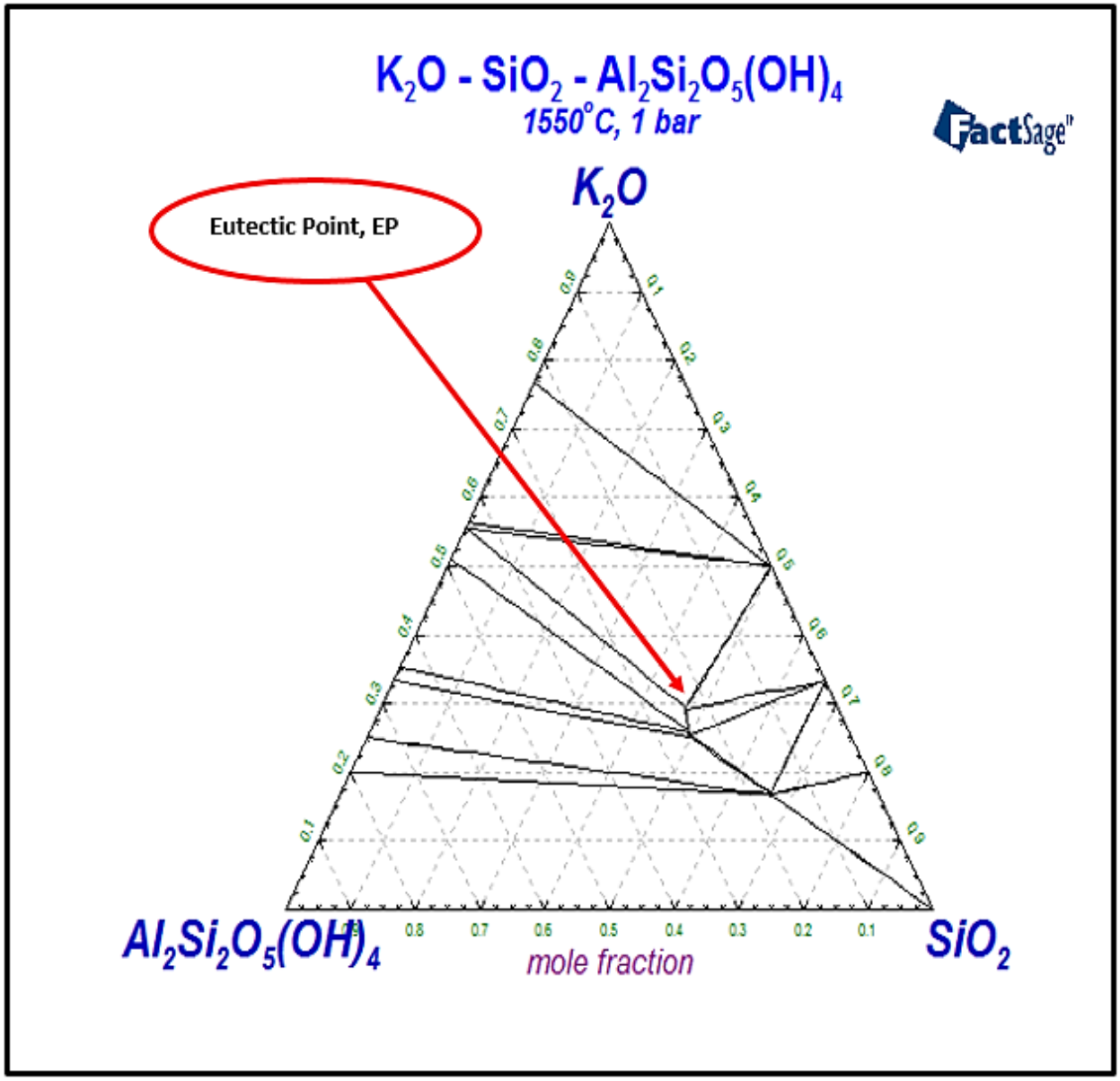

Figure 6-16: Eutectic point noticed at 1550 ^{o}C on ternary phase diagram

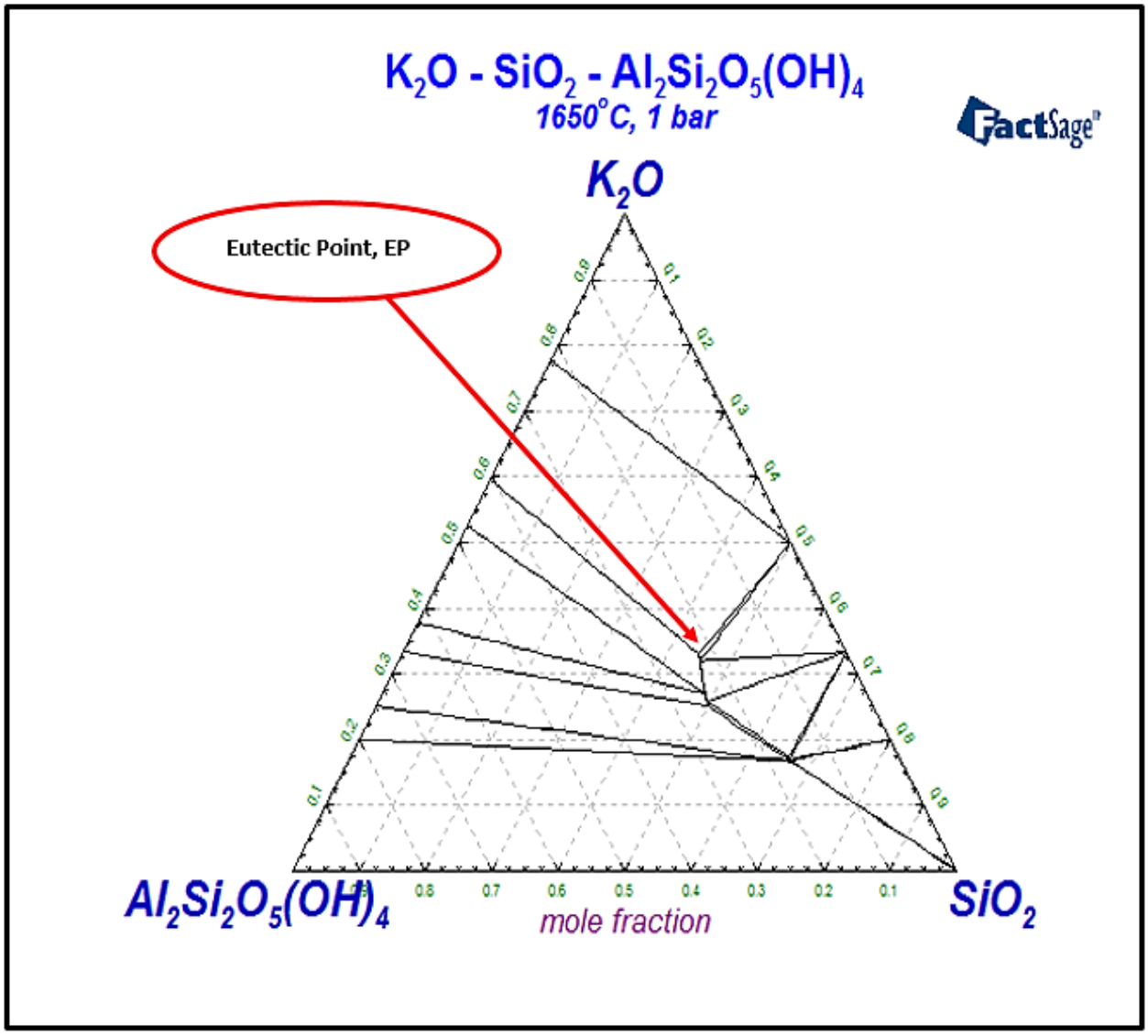

Figure 6-17: Eutectic point confirmed at 1650 ^{o}C on ternary phase diagram

Generally, during the combustion of the selected biomass fuels in a laboratory scale fixed bed, both the time and the temperature increases as the pressure increases in the bed. However, the scope of this research coupled with the limitations of the experimental set-up, does not permit further experimental investigations into the influence or impact of pressure on the combustion characteristics and agglomeration tendencies of the selected biomass fuels (miscanthus, white

wood, and willow). This has been included in the proposed future works to continue this research chapter 7.

6.4 Analyses of Results (Experimental)

This sub section focuses on the results obtained from the series of the combustion experiments conducted on the single and blends of biomass fuels with the intention to establishment of agglomeration tendencies in them. The experimental campaign was in the order of; burning of individual single biomass fuels (willow, white wood, miscanthus, and silica sand) with and without the addition of additive (kaolin), and burning of blends of these biomass fuels with and without the addition of kaolin.

6.5 Burner Flame Temperature, ^{0}C

Flame temperature indicates the temperature of the naked flame of the Roxio burner. During the combustion experiment, the platinum K-type thermocouple was used to record the burner outside flame temperature, 1054 ^{0}C maximum temperature was recorded within a period of 12 seconds, Figure 6.18

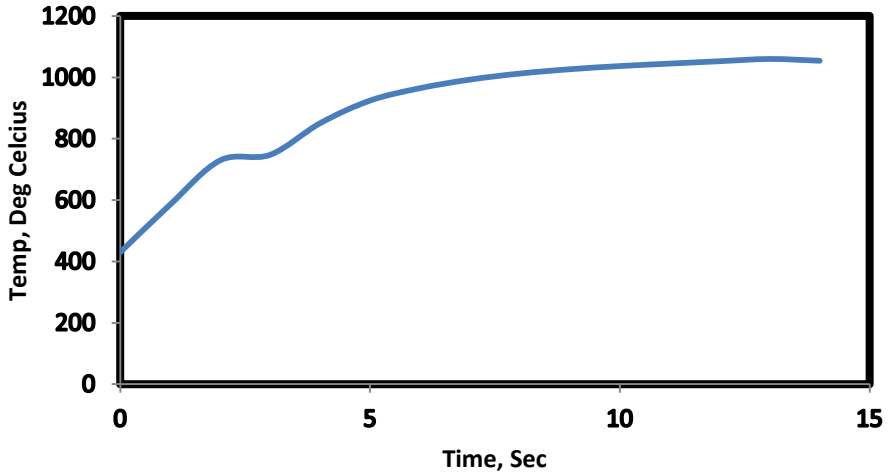

Figure 6-18: Flame Temperature (1054 ^{0}C) of the Roxio burner

However, when the conventional ceramic crucible was used as the combustion chamber, only a temperature of 445 ^{0}C was achieved within the chamber, Figure 6.19. This prompted the search

for a more thermally efficient and reliable crucible (Gooch ceramic crucible) that was used for the whole biomass fuels combustion experiments.

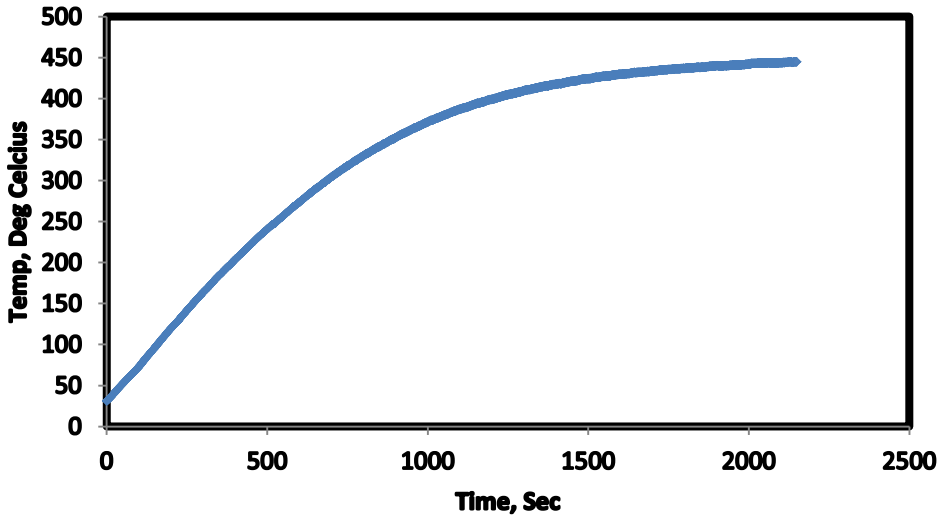

Figure 6-19: Maximum Bed Temperature (445 ^{0}C) during the combustion of <1mm diameter wood particles in a conventional ceramic crucible.

Utilizing the experimental rig as set up in chapter 5, the experiment was conducted as itemized. < 1mm diameter miscanthus particles were pre-mixed with coal particles in ratio 20% to 80% (biomass fuel to coal particles). The mixture was added to the 300g of silica sand (bed materials) that had been pre-heated above the ignition point of biomass fuels (260 ^{0}C) in the combustion chamber (Gooch crucible) in a period of 15 minutes. Graph illustrating this is shown in Figure 6.20

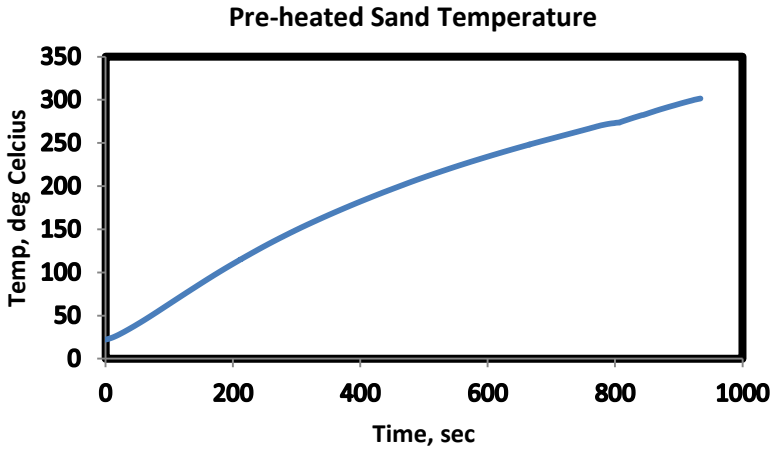

Figure 6-20: Pre-heated Sand Temperature

Acknowledging that, the sintering temperature of biomass fuels is 670 ^{0}C, burning of the biomass fuels was stopped at a little above this temperature at 700 ^{0}C, 750 ^{0}C, and 802 ^{0}C at the equivalent time of 109.2 minutes, 119.6 minutes, and 120 minutes respectively.

6.6 Combustion of <1mm Diameter Miscanthus Particles

The experiment was strictly followed as itemized in section 4.6. Silica sand (200 grams) was heated to the ignition temperature of biomass fuels. 25 grams of biomass fuels was added to the heated silica sand. After cooling to room temperature, the samples were retrieved from the combustion chamber. Upon close examination, at 700 ^{0}C, no agglomerate was spotted in the samples. At 750 ^{0}C, traces of flake like agglomerates were observed in the samples. These signs mark the beginning of agglomeration in the combustion chamber. Meanwhile, at 802 ^{0}C, the samples were observed to have increased in size, formed different shapes, and fused together into huge lumps of agglomerates. The combustion experiment was repeated for three times and the average data compiled. Huge lumps of particles found in the samples confirm that, agglomeration has occurred in the combustion bed while burning the selected problematic

biomass fuel (miscanthus). Temperature distribution in the combustion chamber at 750 ^{0}C and 802 ^{0}C are depicted in Figures 6.21 and 6.22 respectively.

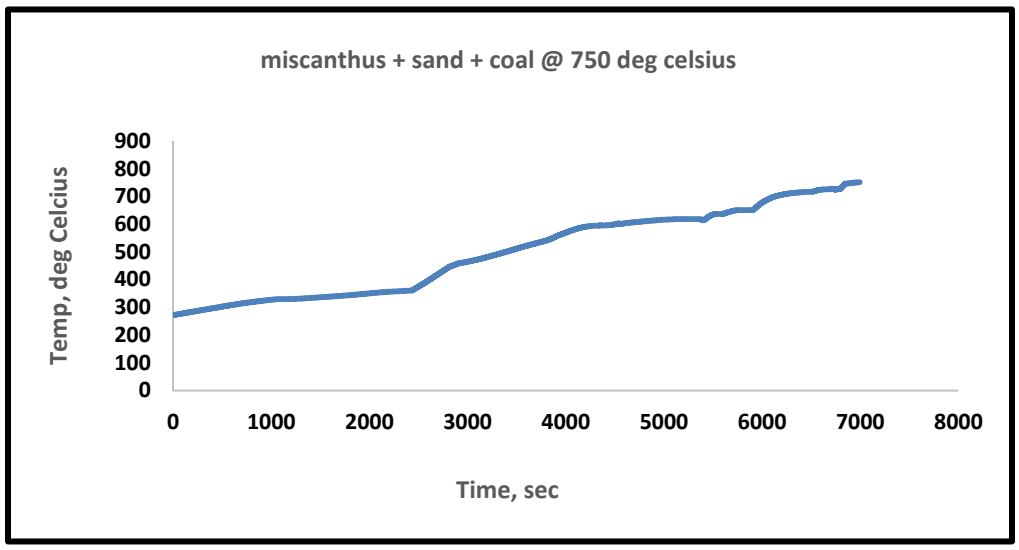

Figure 6-21: Miscanthus + Sand + Coal at 750 ^{0}C

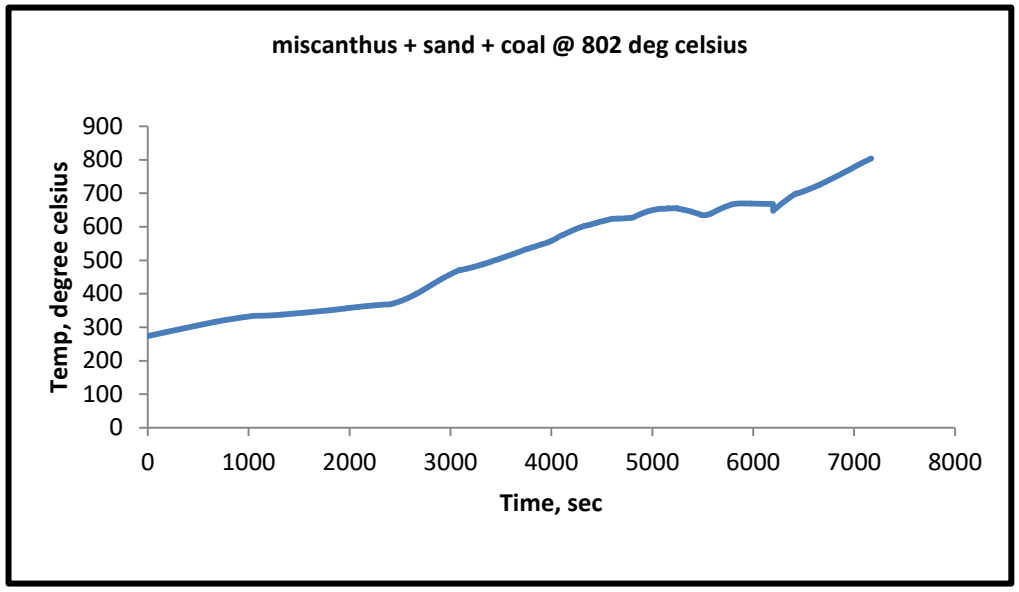

Figure 6-22: Miscanthus + Sand + Coal at 802 ^{0}C

6.7 Combustion of <1mm diameter White Wood Particles

Biomass fuels have similar characteristics. At 700 ^{0}C, no trace of agglomeration was noticed until at a temperature of 750 ^{0}C and 802 ^{0}C. Agglomeration was first observed at 750 ^{0}C but became more conspicuous later. At 802 ^{0}C and atmospheric pressure, agglomeration fully occurred in the combustion bed. This confirms the affirmation that, eutectic mixture in the form of alkali-silicate had been produced between the alkali from biomass fuels and the silica from the quartz sand (bed materials).

The eutectic mixture has a lower melting point than the silica and the alkali, therefore melts promptly in the bed forming lumps of different shapes on the surface of the bed materials. The experiment was conducted three times and the average data collected. Temperature distribution in the combustion chamber is shown in Figures 6.23 and 6.24. SEM and EDX analyses reveal the morphological structures, shapes and the elemental compositions of the agglomerates respectively. Details on these (SEM and EDX) are contained in the appropriate section of chapter 7.

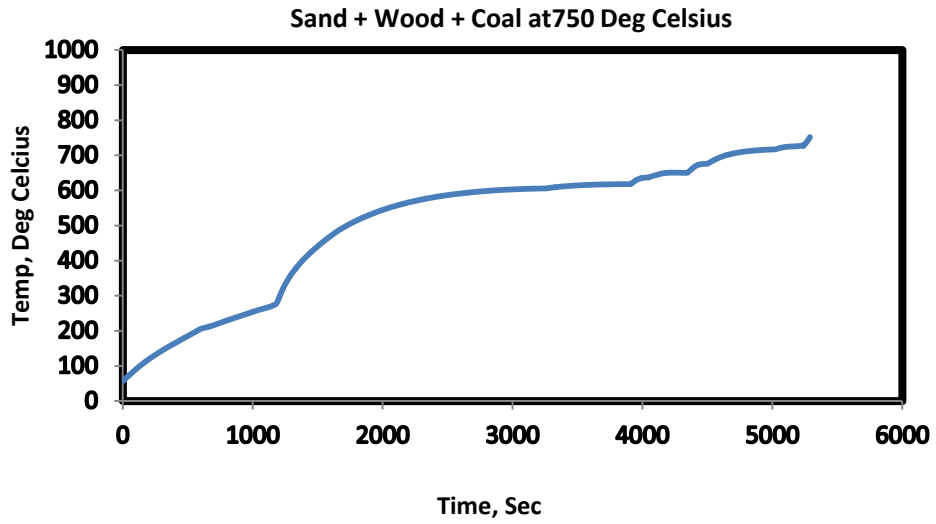

Figure 6-23: Sand + Wood + Coal at 750 ^{0}C

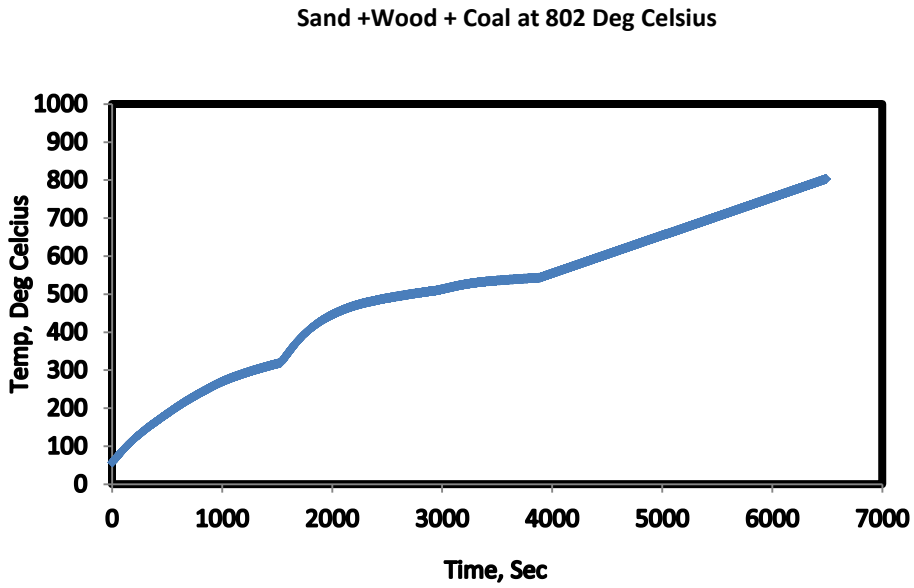

Figure 6-24: Sand +Wood + Coal at 802 ^{0}C

6.8 Combustion of <1mm diameter Willow Particles

Despite the observable similar characteristics exhibited by biomass fuels generally, willow possess peculiar characteristics associated with it. During the combustion of willow particles (< 1mm), no traces of agglomeration was observed at both 700 ^{0}C and 750 ^{0}C unlike other two previous biomass fuels (miscanthus and white wood) where agglomeration was noticed at 750^{0}C. The experiment was replicated three times and the average data collected.

Quantities of agglomerates produced during the combustion of willow particles at 802 ^{0}C were little, compared to miscanthus and white wood.

The implication is that, agglomeration formation during the combustion of willow particles was not as sturdy as found in miscanthus and white wood. Willow may be a very reliable biomass fuels for the industrial production of heat, power or combined heat and power generation because, fewer agglomerates are generated during the combustion of the willow particles, silica sand, and coal.

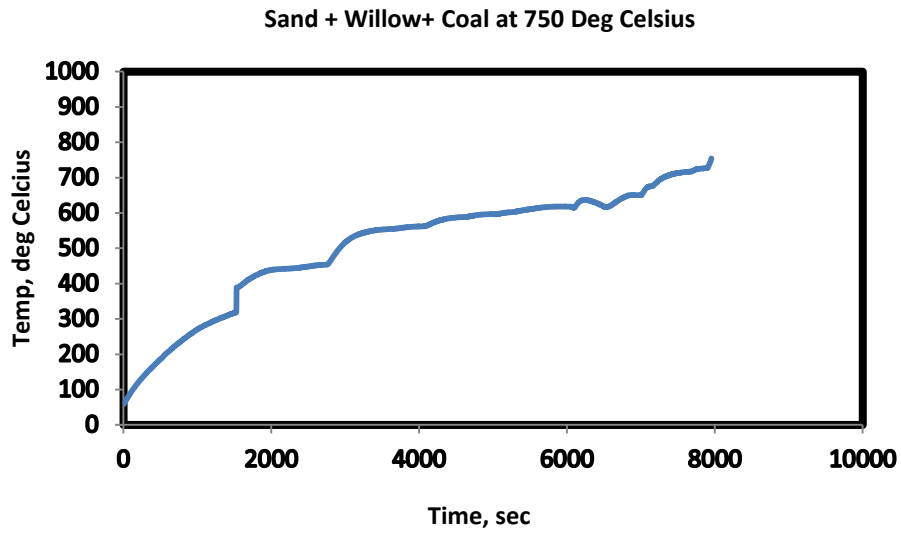

Figure 6-25: Sand + Willow+ Coal at 750 ^{0}C

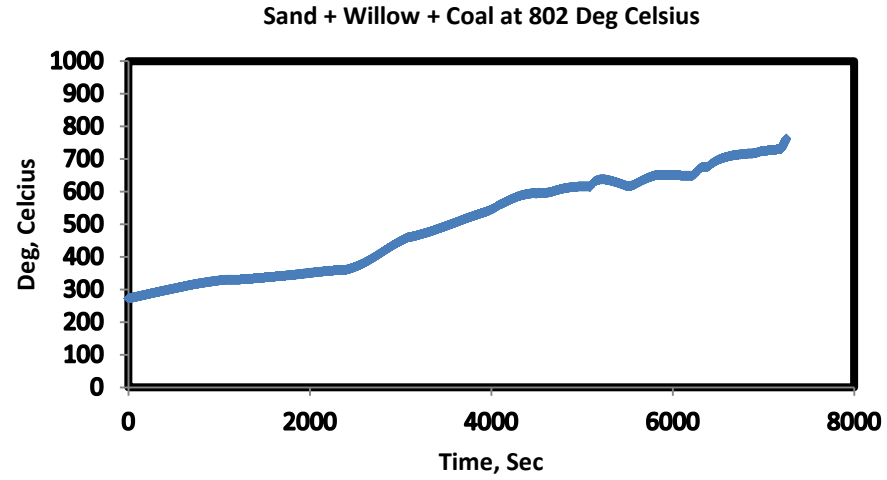

Figure 6-26: Sand + Willow + Coal at 802 ^{0}C.

Combustion experiments conducted on the three selected problematic biomass fuels (white wood, willow, and miscanthus) categorically confirmed that, agglomeration occurred in the bed during the combustion processes of these fuels. Agglomerates were produced at 750 ^{0} C at a temperature a little above the sintering temperature (670 ^{0} C) of biomass fuels.

During the combustion process of the <1mm willow particles, samples were retrieved at 750 ^{0} C and subsequently at 802 ^{0} C with agglomerates appeared conspicuously at those samples collected at 802 ^{0} C. However, in miscanthus and the white wood particles, agglomerates formation was conspicuously noticed in the samples at 750 ^{0} C. The nature and the quantity of the agglomerates produced at 750 ^{0} C were quite different from those generated at 802 ^{0} C with later appearing stronger and harder while the former appeared weaker and brittle. Generally, in the combustion experiments conducted on the three biomass fuels, agglomeration was ascertained and confirmed at 802 ^{0} C.

Massive lumps of solid particles of about 10 mm diameter were produced at 802 ^{0} C during the combustion of miscanthus and wood while the agglomerates produced from the combustion of willow were minor of about 6 mm diameter. In other words, it may be easier to carry out combustion tests or experiments on willow particles because lesser agglomerates are produced during this process. This is being attributed to the percentage of the alkali (potassium, K) present particularly in willow compared to other biomass fuels as revealed by the EDX analyses carried out on the samples.

Case 3 establishes on the reality tests conducted to validate the simulation and the experimental results obtained from the combustion of the selected problematic biomass fuels (white wood, willow, and miscanthus). The reality tests were carried out by heating a mixture of 60g of potassium hydroxide, KOH and 180g silica sand. Most of the expected potassium compounds in biomass possessed high melting temperatures; potassium sulphites K_2SO_2, 1069 ^{0}C, potassium chloride KCl, 770 ^{0}C, potassium oxide K_2O, 740 ^{0}C, potassium carbonate K_2CO_3, 891 ^{0}C. However, potassium hydroxide, KOH possessed relatively low melting point, 360 ^{0}C therefore, it was selected for the reality tests.

The experiments were conducted under the same operating conditions and control as the previous combustion of biomass fuels experiments. The melting point of silica, SiO_2 is 1700 ^{0}C. At 350 ^{0}C, some samples were collected from the combustion chamber and examined. A huge form of agglomerates was formed at a very low temperature of 350 ^{0}C, Figure 6.27A. This temperature is lower than the melting point of any of the parent materials (silica and potassium

hydroxide). Further heating of the mixtures to a higher temperature of 502 ^{0}C produced stronger, tougher, and hard lumps, Figure 6.27 B

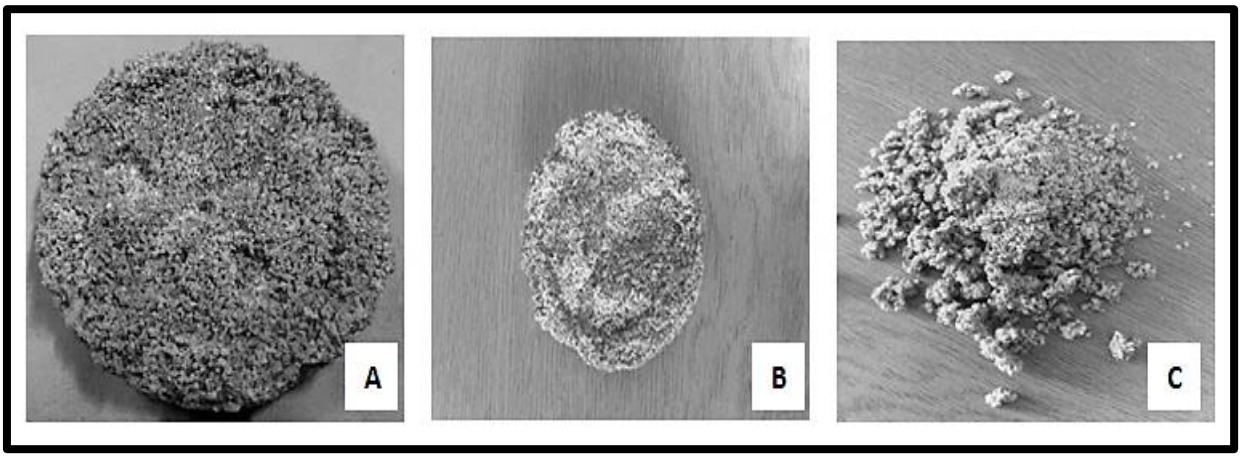

Figure 6-27: (A) Reality test agglomerates at 350 ^{0}C, (B) Reality test agglomerates at 502 ^{0}C (C) Reality test brittle agglomerates produced at 502 ^{0}C with kaolin addition.

The nature of the agglomerates produced has been attributed to the alteration in the chemistry and agglomeration mechanisms, which was introduced by the addition of kaolin to the mixture. The potassium hydroxide melts sharply and the resulting moist particles reacted with silica from the bed materials (sand). A eutectic mixture was formed in the form of alkali silicate, K_2SiO_3 (potassium silicate). Potassium silicate has a lower melting point, 976 ^{0}C than the silica 1700 ^{0}C therefore, it melts quickly on the surface of the bed materials and formed massive lumps. Chemical equation 6.1 has been used to illustrate the reactions.

$$2KOH + SiO_2 = K_2SiO_3 + H_2O \qquad 6.1$$

With this discovery, it clearly connotes that, potassium K plays leading and prominent roles in the formation of agglomerates in the bed during the combustion of biomass fuels. Additive, kaolin was added to the mixture and the experiment was repeated under the same operating conditions. Weaker and brittle agglomerate was produced, Figure 6.27C. This is a confirmation

that, addition of kaolin to the bed contents before combustion will grossly reduce the occurrence of agglomeration during the combustion process of the selected biomass fuels (willow, miscanthus, and white wood). It is also a clarification that, addition of kaolin to the mixture may reduce agglomeration in the beds.

6.9 Error Analysis

Experimental researches are not always completely free of errors, which could be spread across the acquired data. The commonly applied measure of spread is the variance σ^2 and the standard variation σ. The variance is a measure of how well spread a set of data look like. It is calculated as the average squared deviation of each number from the mean of the data set. The standard deviation is calculated as the squared root of the variance and considered as a better measure of dispersion. In this research, combustion experiments were conducted on three biomass fuels (willow, white wood, and miscanthus). These fuels possess similar combustion characteristics. Standard deviation of the data emanated from the combustion of willow at 802 ^{0}C was calculated and presented below while detailed computational analyses are presented in appendix B.

X = Total temperature data acquired = 3582555

N = Total number of times data were acquired = 9015

$X_{Mean} = X/N$ 6.2

= 3582555/9015

= 397.40

Variance $\sigma^2 = \frac{1}{N}\sum_{i=1}^{N} (X - \mathrm{XMean})^2$ 6.3

= 32780.55452

= 32780.55

$$SD = \sqrt{\frac{1}{N}\sum_{i=1}^{N} (X - \mathrm{XMean})^2} \quad 6.4$$

= 181.05

Therefore, standard deviation SD from the mean = 181.05

6.10 Influence of kaolin on the combustion characteristics of the selected biomass fuels

Additive (10 % kaolin) was pre-mixed with the individual biomass fuel (willow, white wood, and miscanthus). Throughout the combustion of the pre-mixed biomass fuels with kaolin, no agglomeration was observed in the bed at 750 ^{0}C and 802 ^{0}C compared to when these biomass fuels were combusted without the addition of kaolin; agglomerates were formed at these temperatures.

Previous research confirmed that, additive from water waste resources could serve as a reliable additive in the handling of agglomeration problems in combustion beds. One of such additives is the sewage sludge used as additive during a research conducted on wheat straw and wood waste ash [247]. It was concluded that, sewage sludge has the affinity to reduce ash related problems during the combustion of problematic biomass fuels by encouraging the production of high melting temperature alkali-silicate (potassium or sodium silicate) and reduced fouling and slag formation in the reactor. The change in the chemistry and mechanisms of agglomerates formation led to reduction in ash deposit formation on the surface of the furnace (combustion chamber)[202, 247].

Kaolin, $Al_2Si_2O_5(OH)_4$ has great affinity to form eutectic mixtures with the alkali present in the biomass fuels in the form of Alkali-Alumina-Silicate [149, 205]. This mixture has higher melting point than the parent materials (alkali, sand, and kaolin). Therefore, kaolin was adopted as the preferred additive for this research.

Prediction with Factsage software clearly indicated that, with the addition of kaolin to the combustion bed contents (biomass fuels and silica), agglomeration will only occur at an elevated temperature of 1300 ^{0}C if the biomass fuel is dominated by potassium, K or potassium oxide, K_2O. Moreover, if the biomass fuel is hugely dominated by Sodium, Na or its oxide, agglomeration will occur at a temperature of 1700 ^{0}C.

Addition of kaolin hindered both the sintering of the wood particles and subsequent melting or fusion that may have followed. Bulk of the samples retrieved from the mixture of wood particles and kaolin at 802 ^{0}C did not show any trace of bonded particles. As identified earlier in chapter

2, aluminium-silicates, Al_2O_3-SiO_2 from kaolin may react with the low melting alkali -silicate from wood particles (biomass fuel) to form alkali-aluminium-silicate. This mixture has a very high melting temperature higher than the melting point of the parent materials. Therefore, the degree of ash sintering was reduced and melting of the biomass fuels at 802 ^{0}C was completely avoided.

With this, it is advisable to always add kaolin to blends of biomass fuels or single biomass fuel as a suitable additive while conducting combustion experiments on them or when they are being processed for industrial heat and power generation.

6.11 Scanning Electron Microscopy (SEM) Analyses of the Samples (Willow, Miscanthus, and White Wood) After Combustion

Post combustion analyses were carried out on the bed specimen (samples) with specific interest and focus on the Scanning Electron Microscopy, SEM and the Energy Dispersive X-ray Spectroscopy, EDX. Series of post combustion analyses were conducted on the bed samples which were collected at 700 ^{0}C, 750 ^{0}C, and 802 ^{0}C. Scanning Electron Microscopy, SEM revealed the morphological structure (structural arrangements), size, and shapes of the samples after combustion, Figure 6.28

Comparing the bed samples before and after combustion, increment in the sizes, changes in the shapes and structure of the samples were observed. In all the three samples examined (willow, white wood, and miscanthus), initiation of agglomerates formation was noticed at 750 ^{0}C with huge lumped structures produced at 802 ^{0}C except in willow where only little agglomerates were produced.

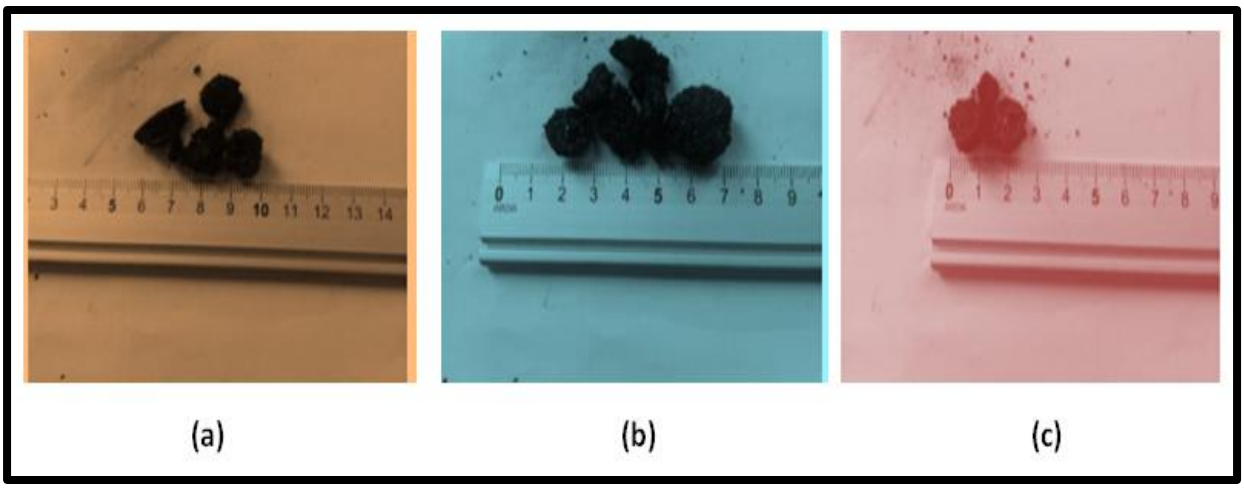

Figure 6-28: (a) Agglomerates from <1mm white wood particles at 802 ^{0}C. (b) Agglomerates from <1mm miscanthus particles at 802 ^{0}C, (c) Agglomerates from <1mm willow particles at 802 ^{0}C

Initial size of the samples was <1mm before the combustion process. After the combustion of the particles, the size of agglomerates formed in white wood and miscanthus particles increased to an average of 10mm diameter while the size of the agglomerates produced in willow is about 7mm diameter, Figures 6.28a, 6.28b, and 6.28c. Moreover, the agglomerates produced from the combustion of willow particles were brittle while those produced from the combustion of white wood and miscanthus particles were tougher and harder. This is a clear indication that, agglomeration had occurred in the bed. Formation of agglomerates in the bed was attributed to the reactions between the alkali metals from the biomass fuels and the silica from the bed materials, sand as earlier explained. The elemental compositions of both the inner core and the outer surface of the lumps were examined using the Energy Dispersive X-Ray Spectroscopy, EDX. These observable features in the samples are a clear indication that, agglomeration occurred in the bed during the combustion experiments on the selected biomass fuels. Unlike willow, traces of agglomerates were observed and consistent with both white wood and miscanthus at 750 ^{0}C but became obvious at 802 ^{0}C. Scanning electron microscopy (SEM) images of the agglomerates produced from the combustion of the selected biomass fuels (wood, miscanthus) at 750 ^{0}C are shown in Figure 6.29A and 6.29B while SEM of agglomerates produced from willow particles is shown in Figure 6.30C.

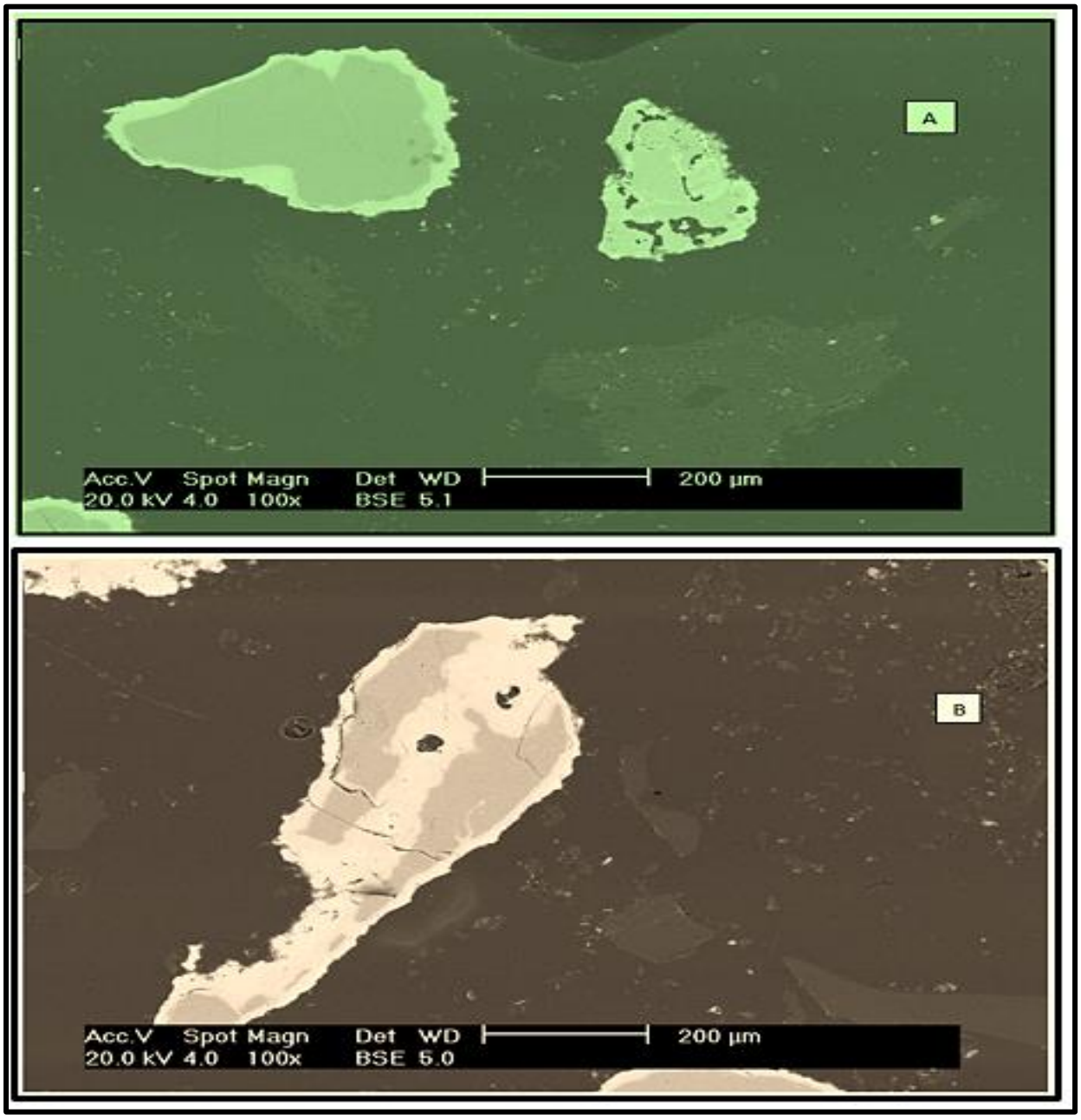

Figure 6-29: (A) SEM image of agglomerates from the combustion of <1mm wood particles at 750 ^{0}C (B) SEM image of agglomerates from the combustion of <1mm miscanthus particles at 750 ^{0}C.

Letters A-Q on the figures represents nomenclature for easy identification and discussions of the images. There are two noticeable sections on image A based on its brightness. The overall

dark area in Figures 6.29 A, 6.29B, and 6.30C is made up of the mixture of coal and resin used for the preparation of the specimen for SEM analyses while the brighter sections contained the molten < 1mm wood, miscanthus, and willow particles respectively at 750 ^{0}C. SEM images of the samples are shown in Figures 6.29 to 6.37.

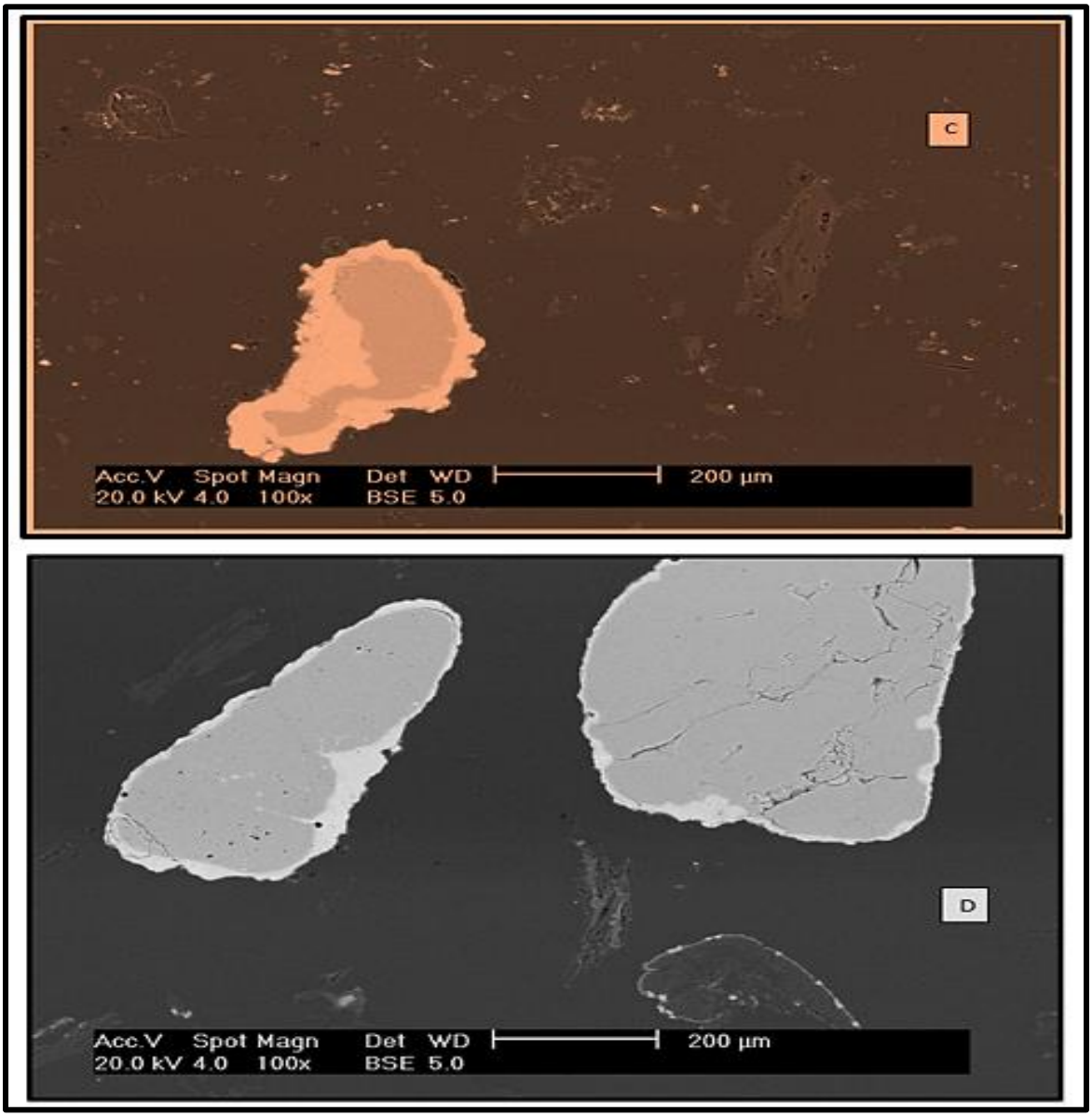

Figure 6-30 (C) SEM image of agglomerates from the combustion of <1mm willow particles at 750 ^{0}C

(D) SEM image of agglomerates from the combustion of <1mm miscanthus particles at 802 ^{0}C

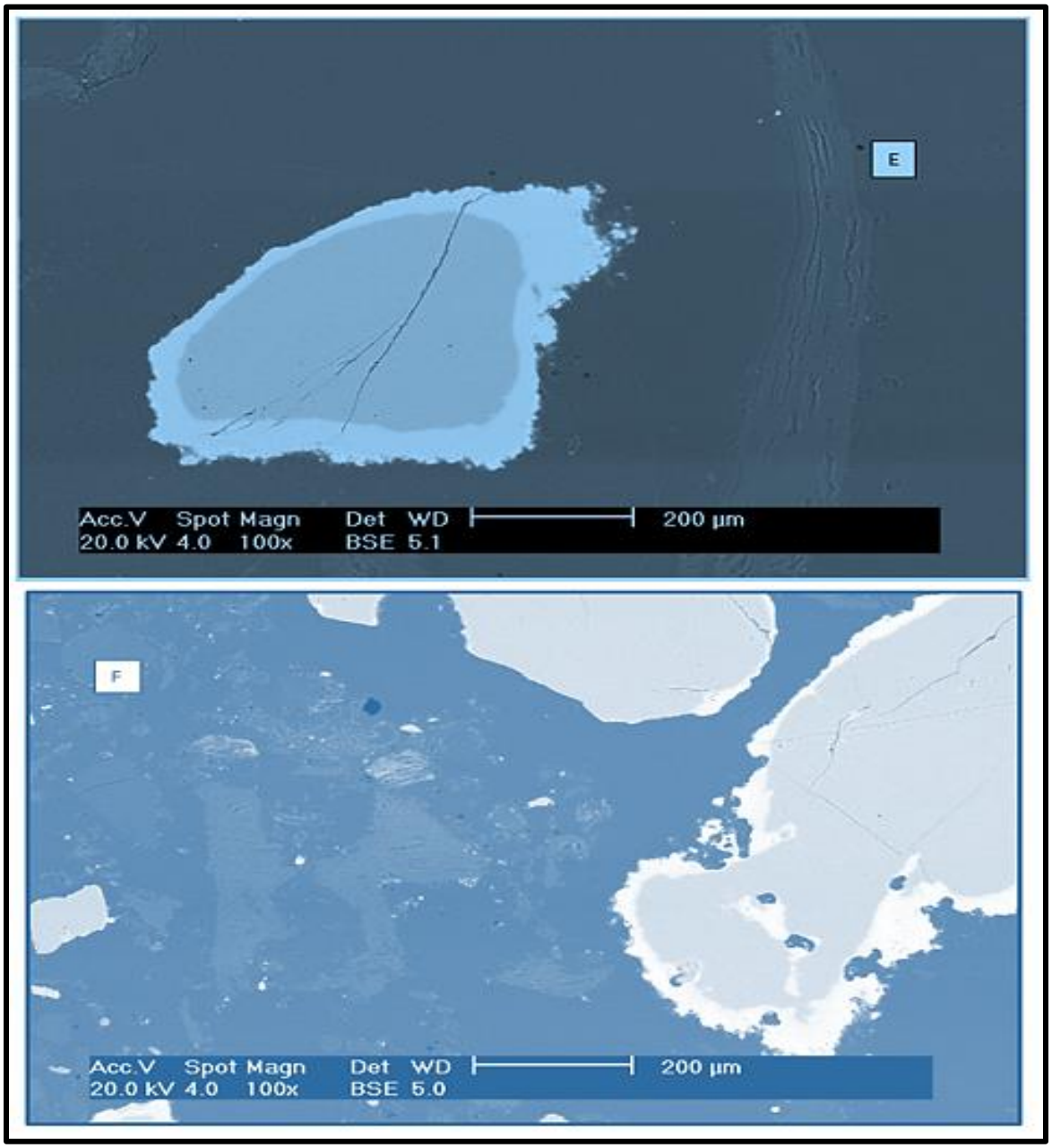

Figure 6-31(E) SEM image of agglomerates from the combustion of <1mm white wood particles at 802 ^{0}C
(F) SEM image of agglomerates from the combustion of <1mm willow particles at 802 ^{0}C

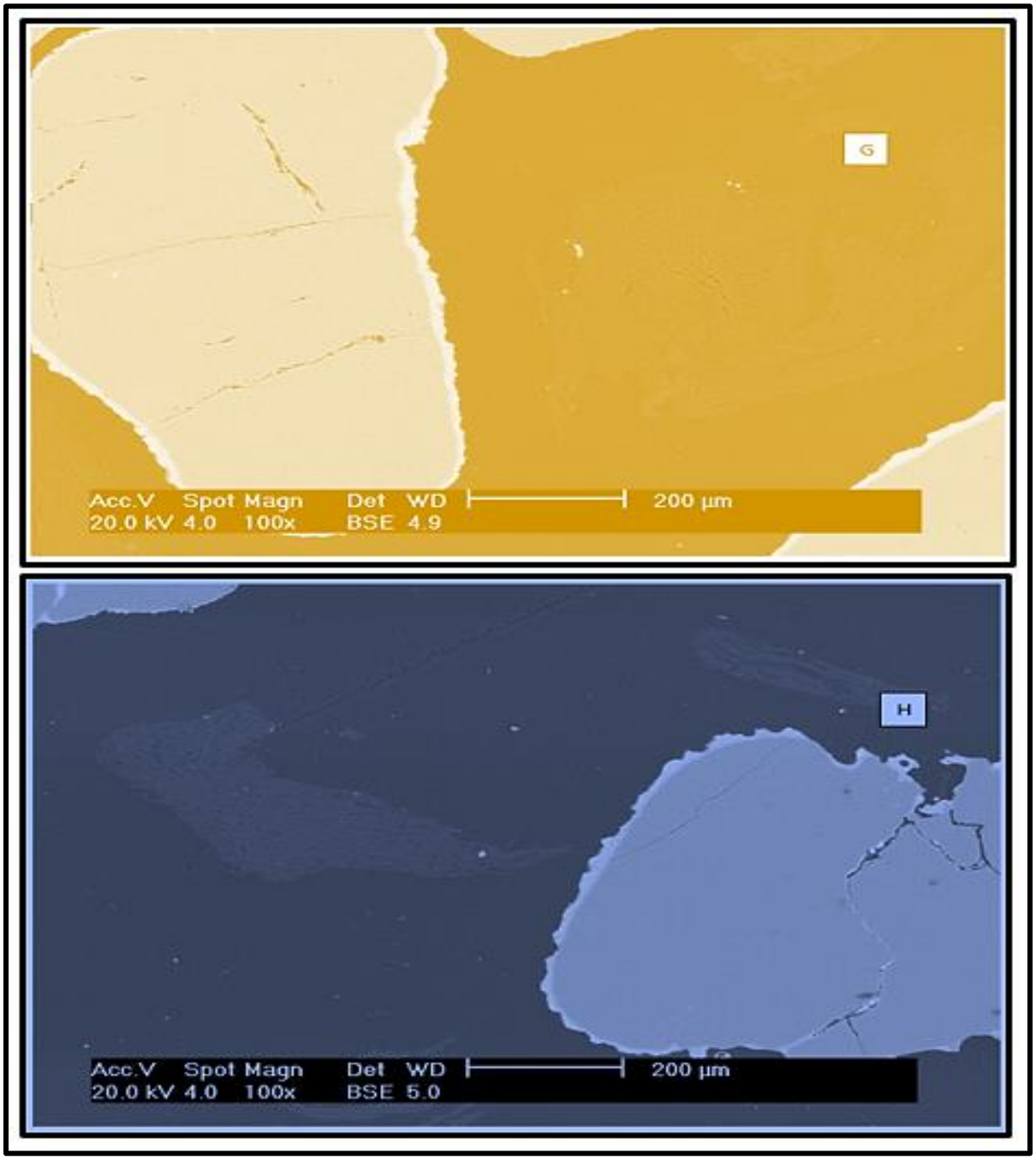

Figure 6-32 (G) SEM image of agglomerates from the combustion of <1mm mixture of wood + miscanthus particles at 802 ^{0}C, (H) SEM image of agglomerates from the combustion of the mixture of willow + wood particles at 802 ^{0}C

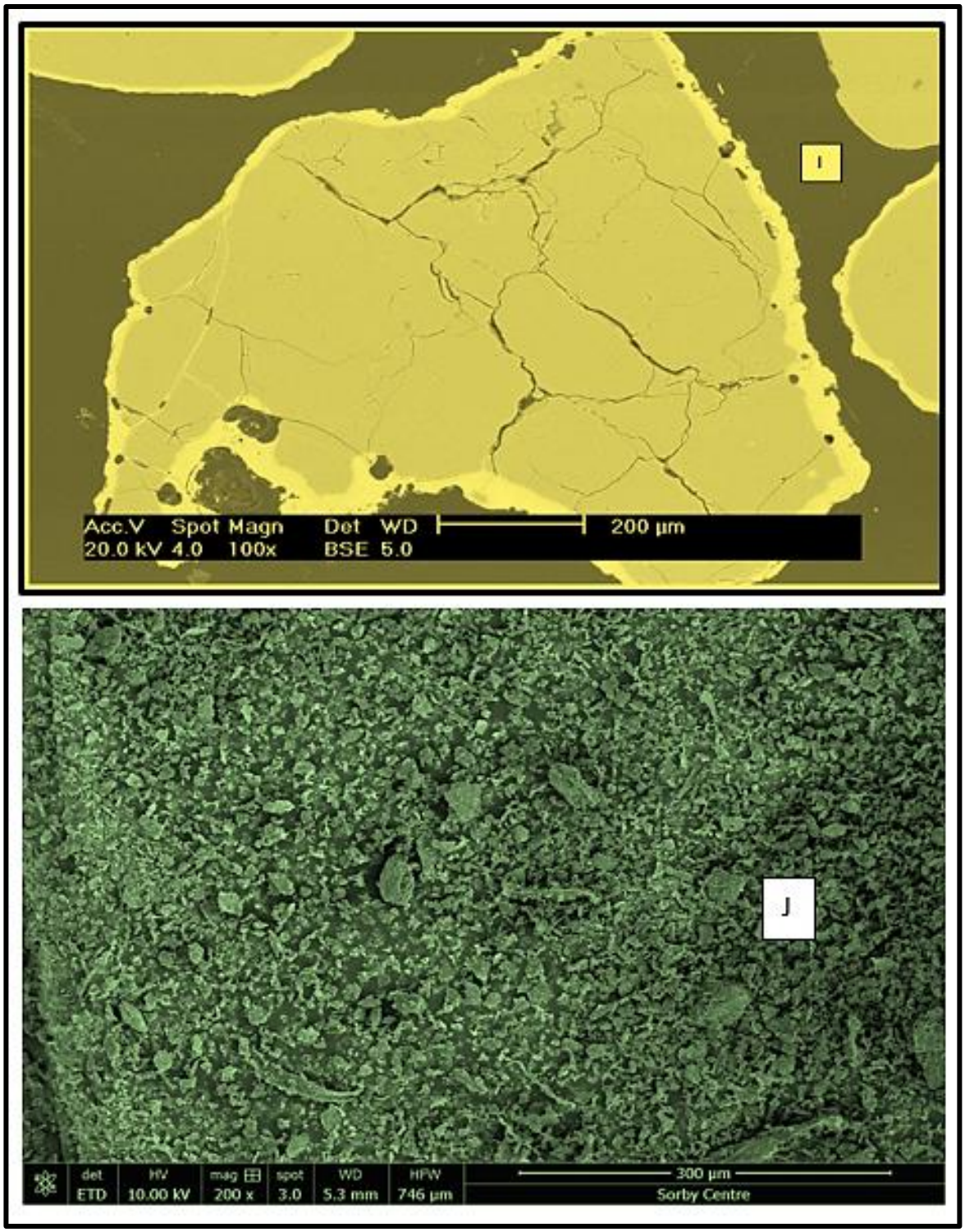

Figure 6-33 (I) SEM image of agglomerates from the combustion of the mixture of miscanthus + willow particles at 802 ^{0}C, (J) Powder image of the mixture of Kaolin + wood particles at 802 ^{0}C.

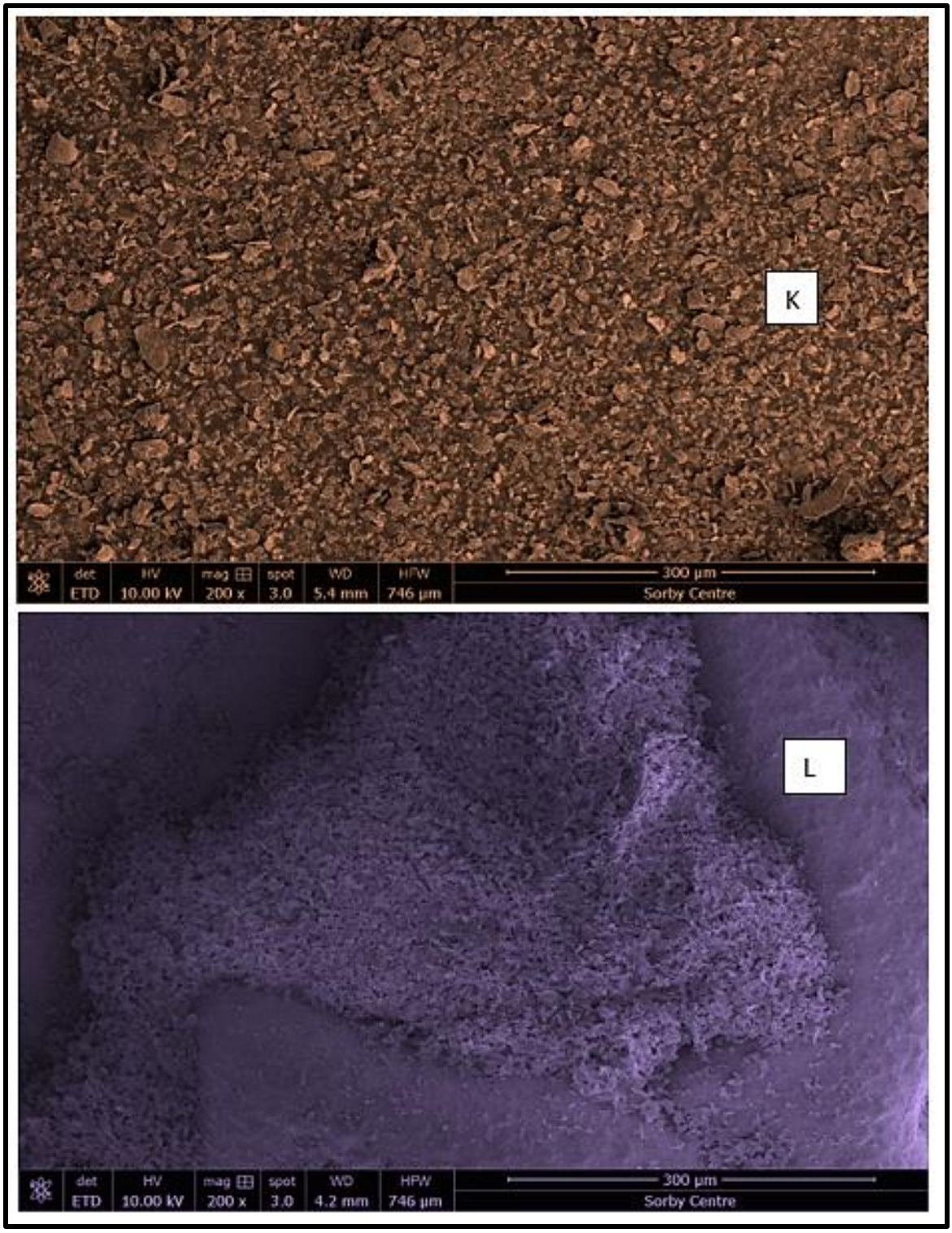

Figure 6-34 (K) Powder image of the mixture of Kaolin + wood particles at 802 ^{0}C (L) Powder image of the mixture of Kaolin + willow particles at 802 ^{0}C

Figures 6.33 J and 6.34K are powder images of the mixtures of wood particles and kaolin at 802^{0}C while Figures 6.34 L, 6.35 M, 6.35N, & 6.36 O are the powder images of the blends of mixture of Kaolin + willow, miscanthus, wood, and willow particles respectively with kaolin at 802 ^{0}C. It has very weak electron conductivity hence; it was subjected to powder imaging. No molten of the substances was observed in the particles after the combustion process. This buttressed the simulation results with Factsage software on binary phase diagrams whereby, it was forecasted that, with the addition of kaolin to the bed materials, agglomeration would occur at elevated temperature of 1200 ^{0}C in a potassium K, dominated biomass fuels.

Moreover, as predicted with the Factsage software that, in a sodium Na, dominated biomass fuels, agglomeration would occur at a high temperature of 1300 ^{0}C and not at 802 ^{0}C. Liang and Wang, 2013 in their research concluded that, addition of additives to biomass fuels act as anti-sintering agent that reduces melting or formation of low melting temperature alkali-silicate compounds.

The threadlike feature in figure 6.34L comprised of willow particles while the surrounding fine particles that exhibits continuous phase, composed mostly of the mixture of kaolin and silica sand. Addition of kaolin influenced the combustion of the willow particles in the mixture. Many high melting temperatures alkali-alumina-silicate were produced in the bed during the combustion processes. The potassium-alumina-silicate produced has higher melting temperature. Production of the high melting temperature of these Potassium-alumina-silicates, can improve on the ash sintering and subsequently, agglomeration characteristics of the selected biomass fuels (white wood, willow, and miscanthus).

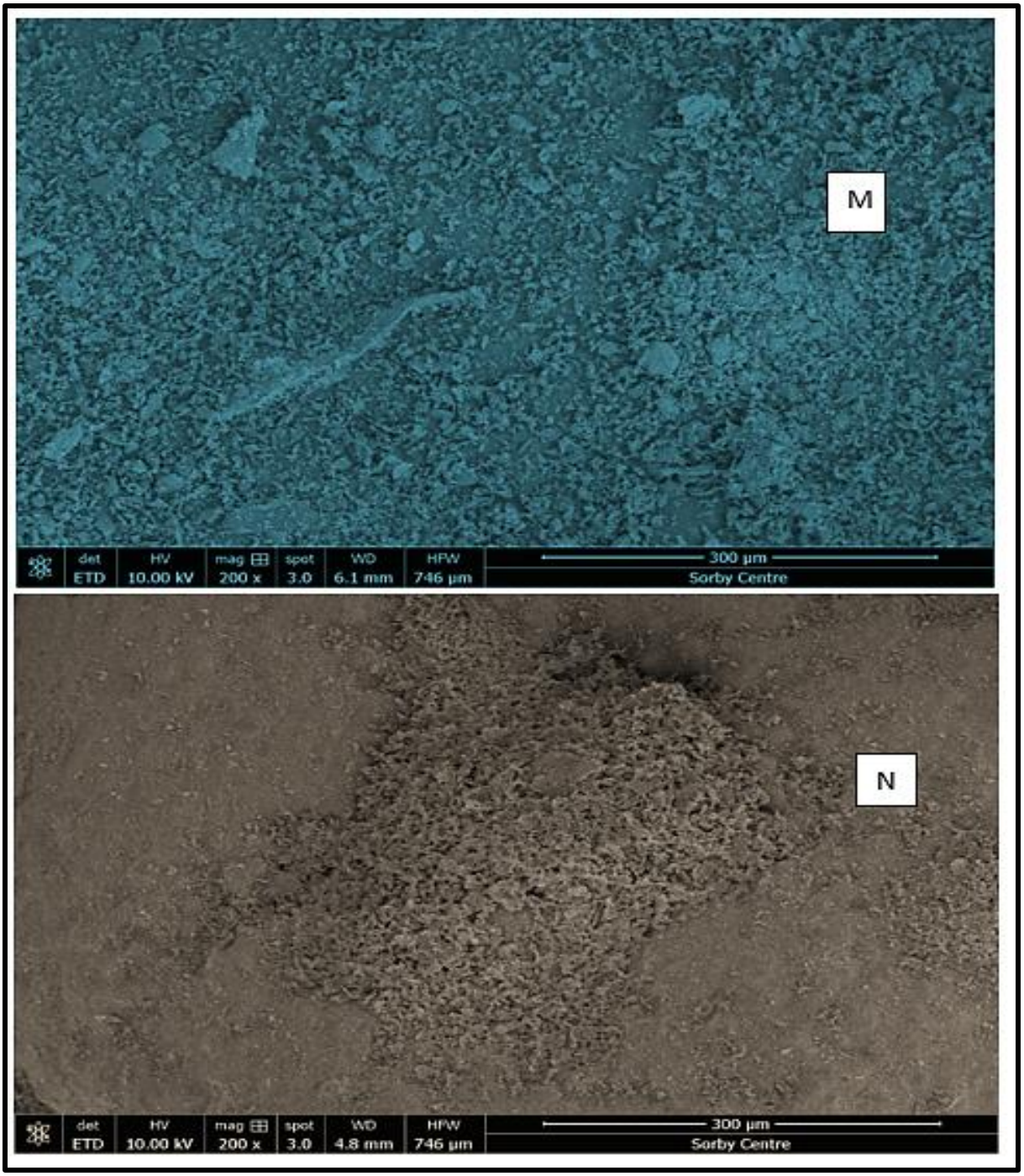

Figure 6-35 (M) Powder image of the mixture of Kaolin + <1mm wood particles before combustion. (N) Powder image of the mixture of Kaolin + <1mm willow particles before combustion.

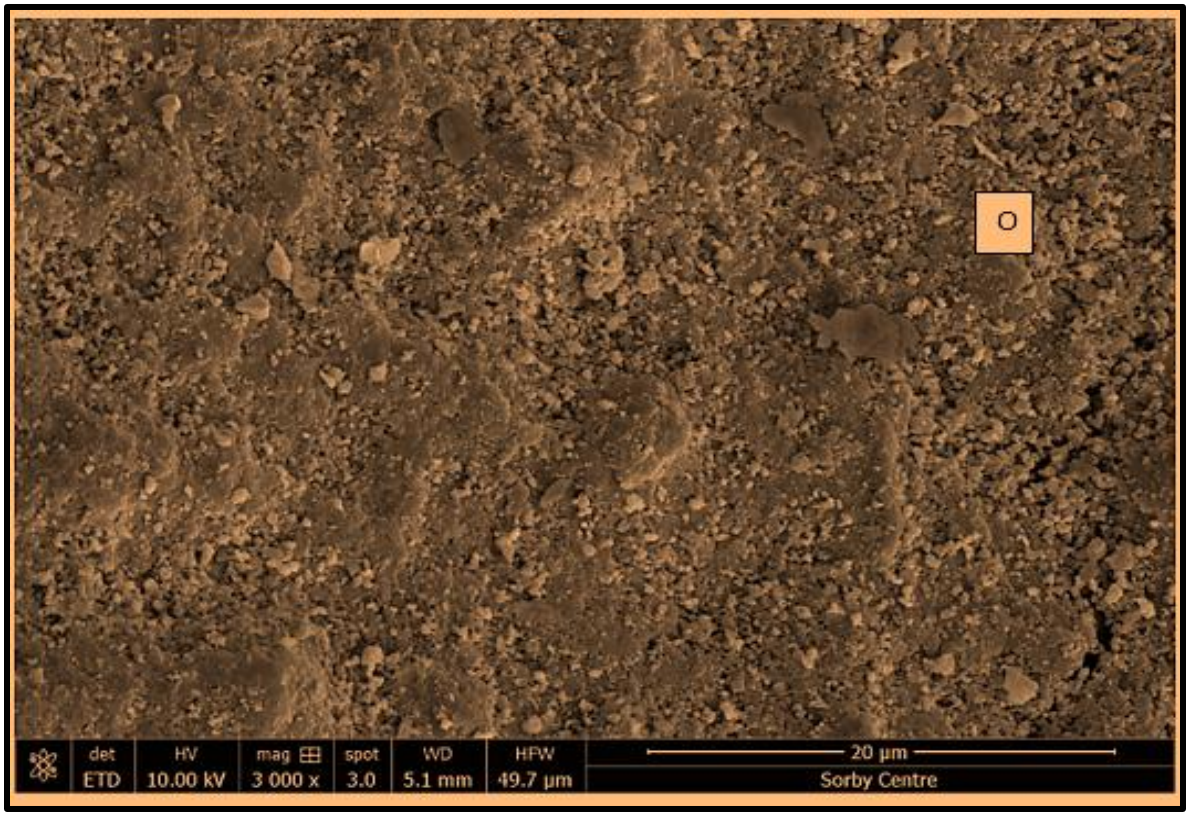

Figure 6-36 (O) Powder image of the mixture of Kaolin + <1mm miscanthus particles before combustion.

Figures 6.35M, N, and 6.36 O are the powder images of the mixtures of Kaolin + <1mm wood particles, Kaolin + <1mm willow particles, and Kaolin + <1mm miscanthus particles respectively before combustion.

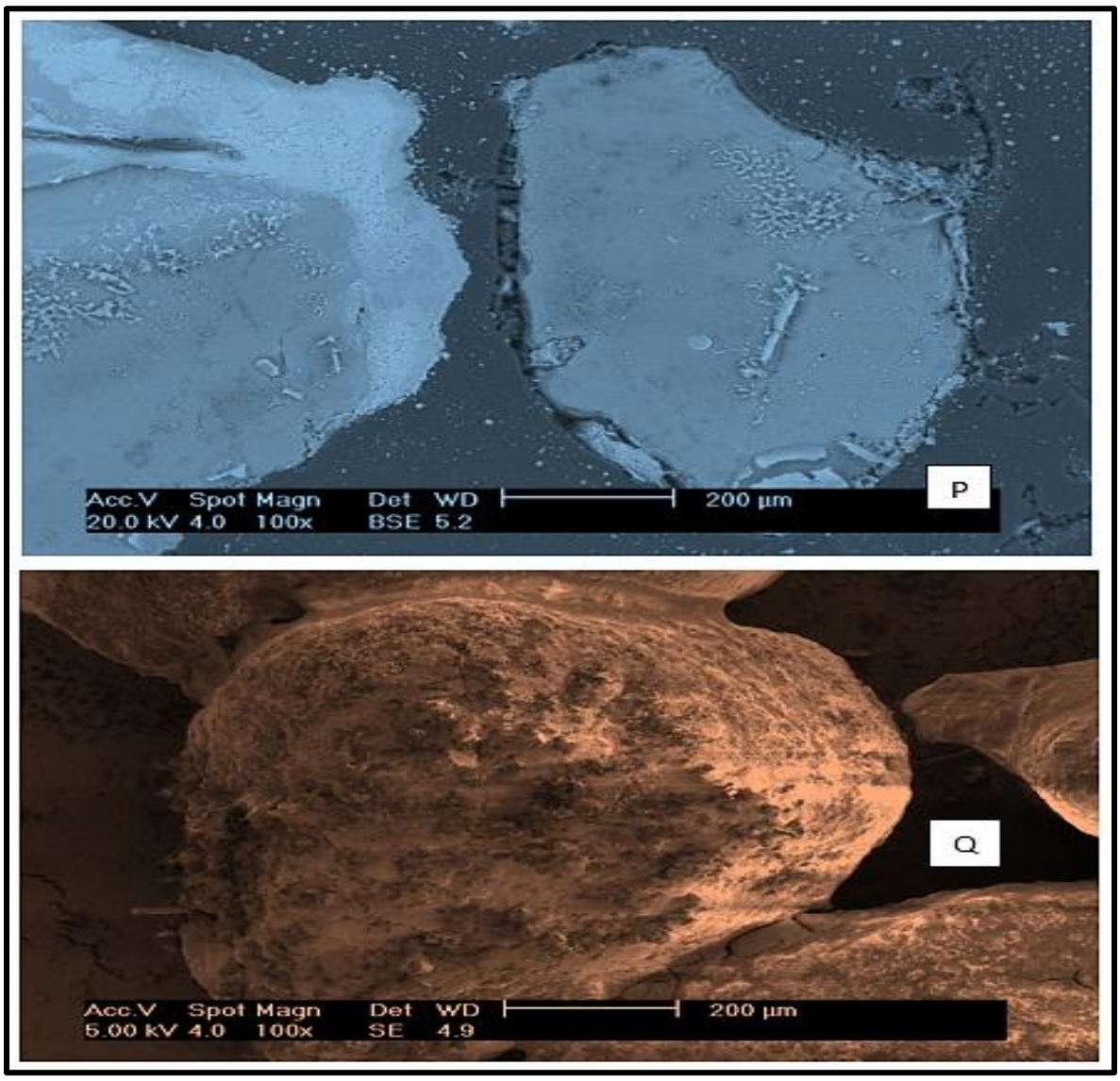

Figure 6-37: (P) SEM image of agglomerates from the combustion of Sand particles + KOH at 350 ^{0}C, (Q) SEM image of agglomerates from the combustion of Sand particles + KOH at 502 ^{0}C.

The two brighter features, Figure 6.37 P are the lumps formed in the bed during the combustion of the mixture of potassium hydroxide, KOH and silica sand at 350^{0}C while the darker areas surrounding the lumps is mostly comprised of carbon and oxygen from resin. The massive block like structure in figure 6.37 Q is the hard, tough, and strong agglomerates formed in the bed during the combustion of potassium hydroxide, KOH and silica sand at 502 ^{0}C. Formation of this

structure was because of the reaction between the potassium K and the silica from sand (bed materials). The reaction produced a low melting temperature, eutectic mixture in the form of alkali-silicate (potassium silicate) that melts speedily at a low temperature of 502 ^{0}C lower than the melting point of silica.

Generally, the results showed that, agglomerates were formed because of a great adhesion between the molten fuel particles in form of alkali – silicate (potassium-silicate or sodium silicate) and the bed particles.

The alkali – silicate (potassium silicate or sodium silicate) has a lower melting point than the parent materials (alkali and silica) therefore, melts considerably and quickly on the surface of the bed materials with the inner core comprise of mostly the bed materials while the outer layer possesses characteristics related to fuel ash.

6.12 Energy Dispersive X-Ray Spectroscopy (EDX) Analyses of the Samples (willow, miscanthus, and white wood) after combustion.

The main technique adopted for these analyses, is the EDX Spot analysis of the selected areas on the electron images. The machine focussed on different spots called the spectra, each spectrum was analysed and the elemental composition at that spot established. Carbon, C and oxygen, O was mostly present in all the images plotted. These elements were believed to have emanated from the adhesive (resin) applied to bind the samples together firmly. Details of both the SEM images and the EDX comprehensive data are contained in appendix A.

SEM and SEM-EDX images of the mixture of KOH with silica sand melted at 350 ^{0}C are shown in Figure 6.38 while the summary of the elemental compositions of each spectrum are contained in Table 6.1. Comprehensive/detailed SEM and the EDX data are contained in appendix A1, Figures 9.1 to 9.5

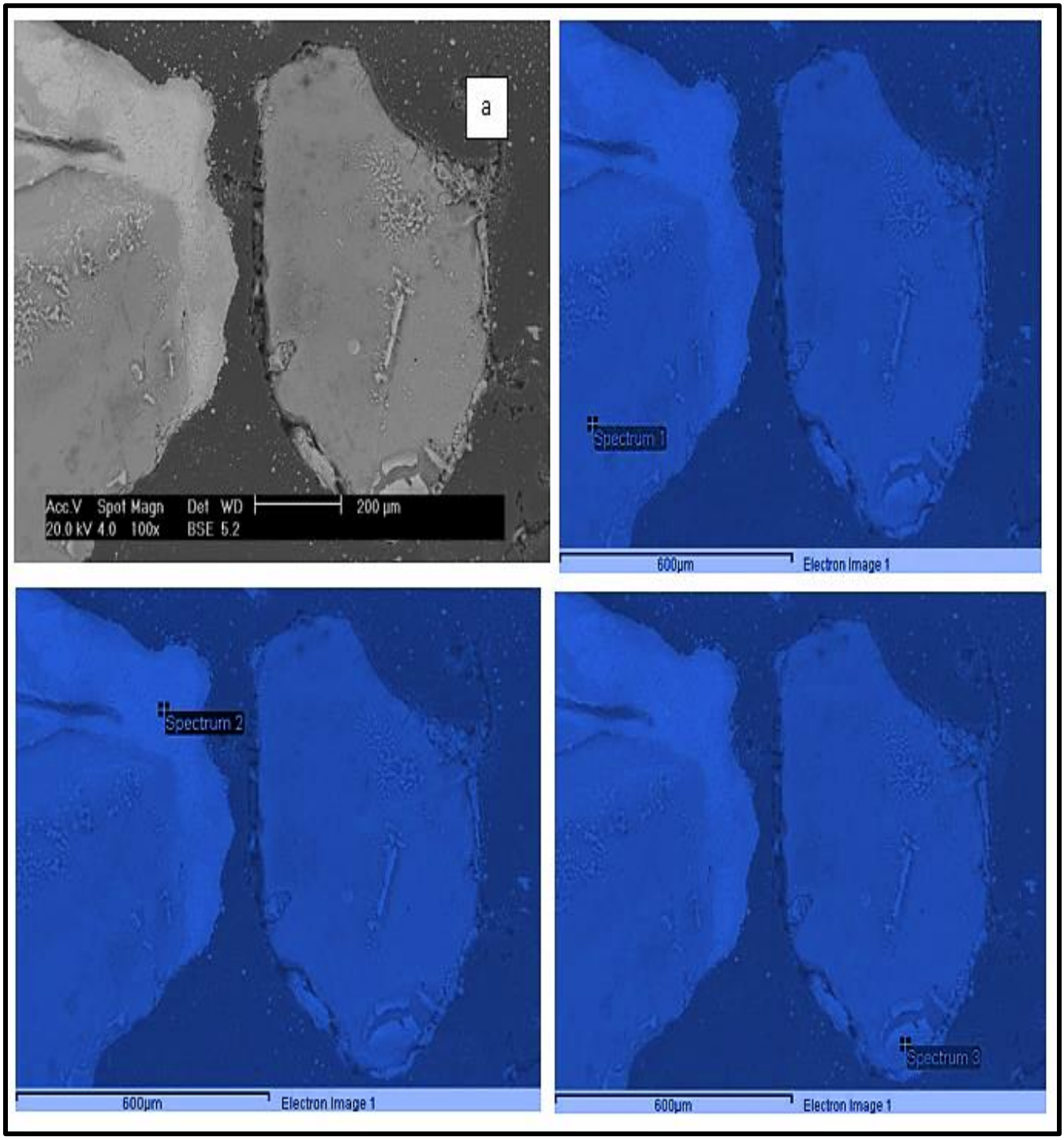

Figure 6-38 SEM images of the mixture of KOH with silica sand melted at 350 ^{0}C and SEM-EDX images of the selected areas (spectra 1, 2, 3) in panel a.

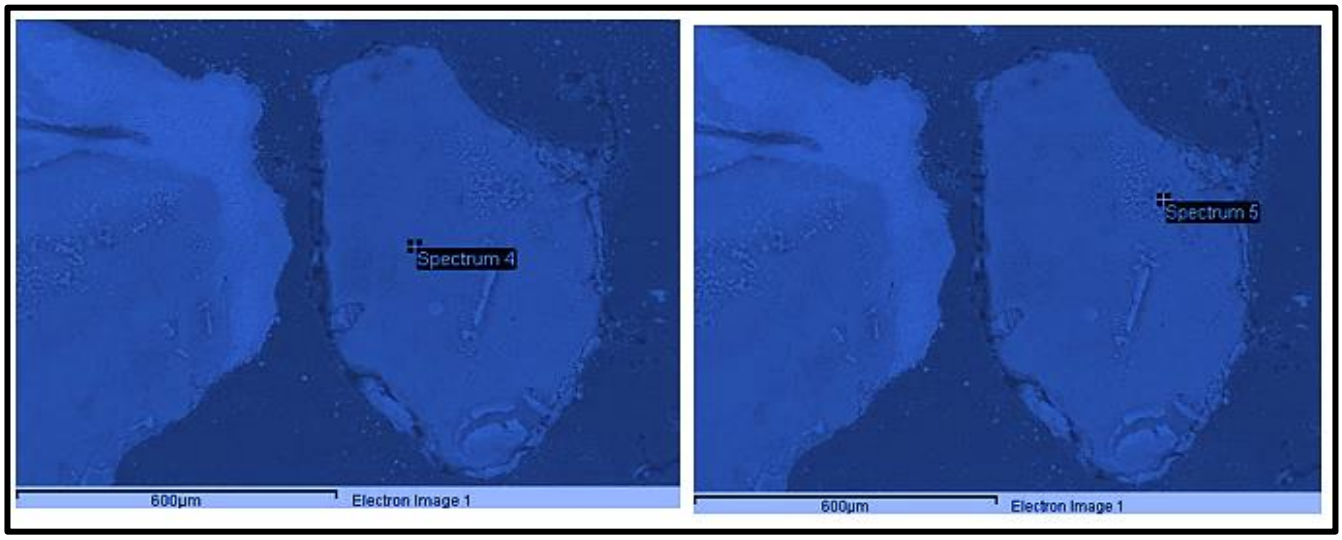

Figure 6-39: (a) SEM image of the mixture of KOH with silica sand melted at 350 ^{0}C and SEM-EDX images of the selected areas (spectra 4 and 5) in panel a.

The two light grey portions in Figure 6.38 panel a, comprised of the molten fraction of the KOH and silica sand in the reality tests conducted at 350 ^{0} C. Spectrum 1 of figure 6.38 is mostly dominated by silicon Si (78.26 wt %) and potassium K-Feldspar (1.80 wt %). Spectrum 2 contained mostly potassium K-Feldspar (41.07 wt %), Si (12.40 wt %), and Fe (0.61 wt %) as a trace element. Concentration of K in this region is higher than that in spectrum 1. In addition to Si, K, and Fe in spectrum 2, spectrum 3 contained Calcium, Ca (0.88 wt %) although in a negligible amount. Spectra 4, and 5, Figure 6.39 were mostly dominated by silicon Si (50.90 wt %), (72.87 wt %), and (52.41 wt %) respectively. Concisely, Si and K generally dominated the sample. Si and K completely dominated agglomerates emanated from the reality tests while Ca and Fe were trace elements in the mixture, Table 6.1.

Table 6-1: EDX spot analysis results of KOH + Sand at 350 ^{0}C

Wt %	Spectrum 1	2	3	4	5
Si	78	12	51	73	52
K	2	41	14	4	20
Ca	0	0	1	0	0
Fe	0	1	1	0	0

Mixture of willow with white wood particles melted at 802 ^{0}C

SEM and SEM-EDX images of the mixture of willow with white wood melted at 802 ^{0}C is as shown in Figure 6.40. The EDX machine spotted three spectra 1, 2, and 3. Elemental composition of each spectrum are depicted in Table 6.2 while overall EDX comprehensive data are presented in appendix A2, Figures 9.6 to 9.10

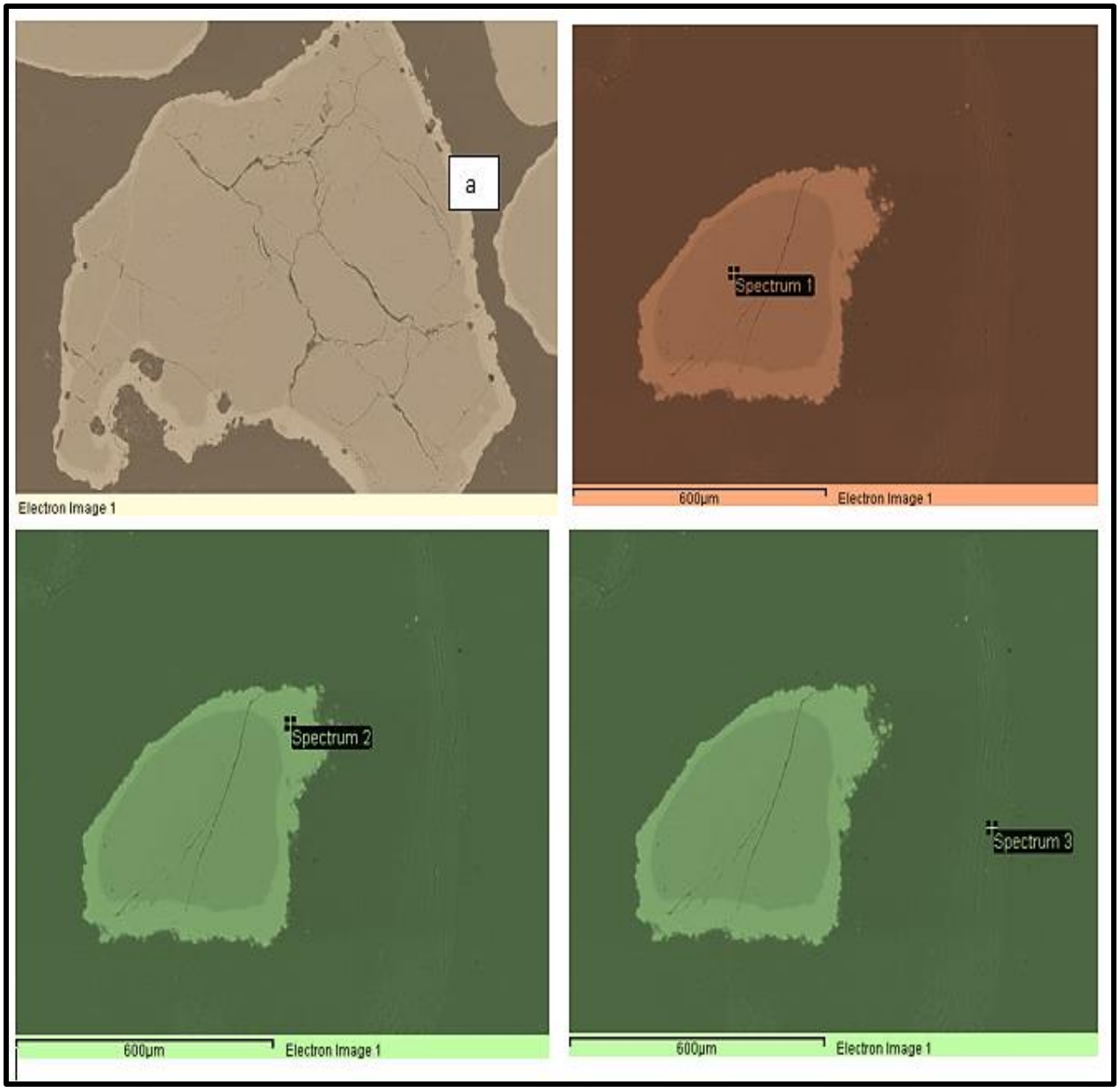

Figure 6-40: SEM image of the mixture of willow with white wood melted at 802 ^{0}C and SEM-EDX images of the selected areas in panel a.

Brighter area of the grey zone of spectrum 1 Figure 6.40 is made up of the melted part of the mixture of willow and wood at 802^0 C. It was dominated by Si (74.31 wt %). It clearly implies that, the region may also comprise of mostly K-silicate. Spectrum 2 contained some additional elements to Si and K; Calcium Ca – Wollastonite (3.35 wt %), Phosphorus P (1.22 wt %), Aluminium Al (3.58 wt %), Iron Fe (4.96 wt %), (12.40 wt %), while the major dominating element was Silicon Si (39.70 wt %). Element mapping, Figure 6.41 of panel a in Figure 6.40 revealed the elemental compositions as K, Si, Al, C, O, Cl, Fe, Mg, Ca, and Na.

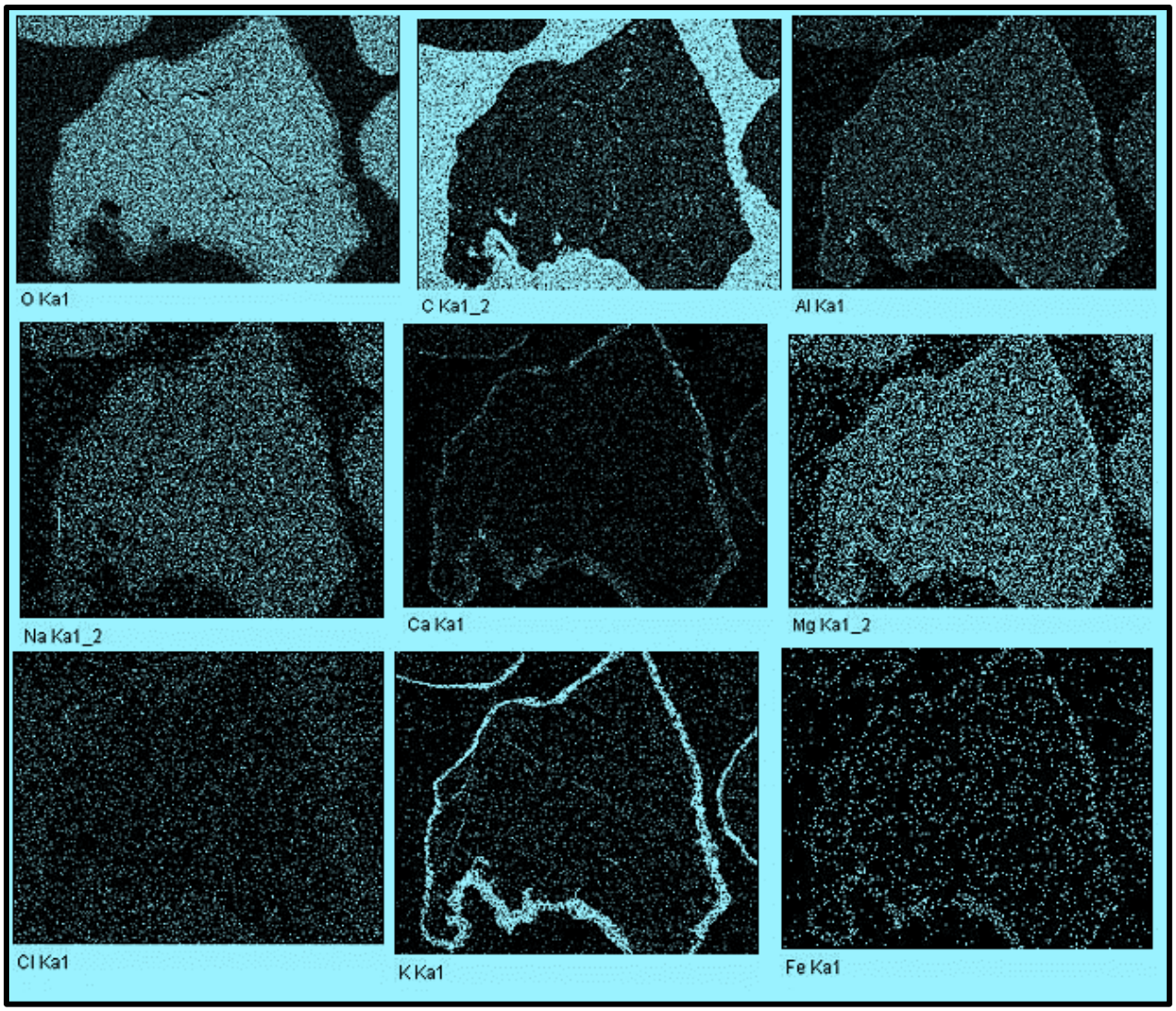

Figure 6-41: Element mapping of panel a in figure 6.40; mixture of willow with white wood melted at 802 ^{0}C

Table 6-2: EDX Spot analysis of blends of willow, white wood, and miscanthus at 802 ^{0}C

Wt %	Wood + Willow					Miscanthus + Wood					Willow + Miscanthus				
	1	2	3	4	5	1	2	3	4	5	1	2	3	4	5
Si	74	40	46	0	0	39	20	0	0	0	67	61	0	0	0
K	0	23	21	0	0	0	12	0	0	0	10	0	0	0	0
Na	0	0	0	0	0	0	0	0	0	0	0	0	0	0	0
Mg	0	4	2	0	0	0	2	0	0	0	1	0	0	0	0
Al	0	4	4	0	0	0	2	0	0	0	0	0	0	0	0
Ca	0	3	3	0	0	0	3	0	0	0	2	0	0	0	0
S	0	0	0	0	0	0	0	0	0	0	0	0	0	0	0
Cl	0	0	0	0	0	0	0	0	0	0	0	0	0	0	0
P	0	1	2	0	0	0	2	0	0	0	0	0	0	0	0
Fe	0	0	3	0	0	0	1	0	0	0	1	0	0	0	0

It is worthwhile to note that, numbers 1,2,3,4 and 5 represents the spectra. The elements present in each spectrum are as shown in Table 6.2 while detailed SEM and EDX data are contained in appendix A.

Figure 6.42 comprised of SEM-EDX images of the mixture of 50% wood and 50% miscanthus particles melted at 802 ^{0}C. Spectrum 1 consisted of mostly Si (38.52 wt %). The light grey region indicated the melted alkali-silicate mixture. Spectrum 2 comprised of mostly Si (19.54 wt %) and other elements like; K-Feldspar (11.45 wt %), Mg (2.23 wt %), Al (2.15 wt %), P (1.74 wt %), Fe (1.28 wt %), Ca (3.16 wt %). Spectrum 3 of the electron image comprised mostly of, carbon C (74.53 wt %) and oxygen O (20.00 wt %) that emanated from the adhesive.

Mixture of wood with miscanthus particles melted at 802 ^{0}C

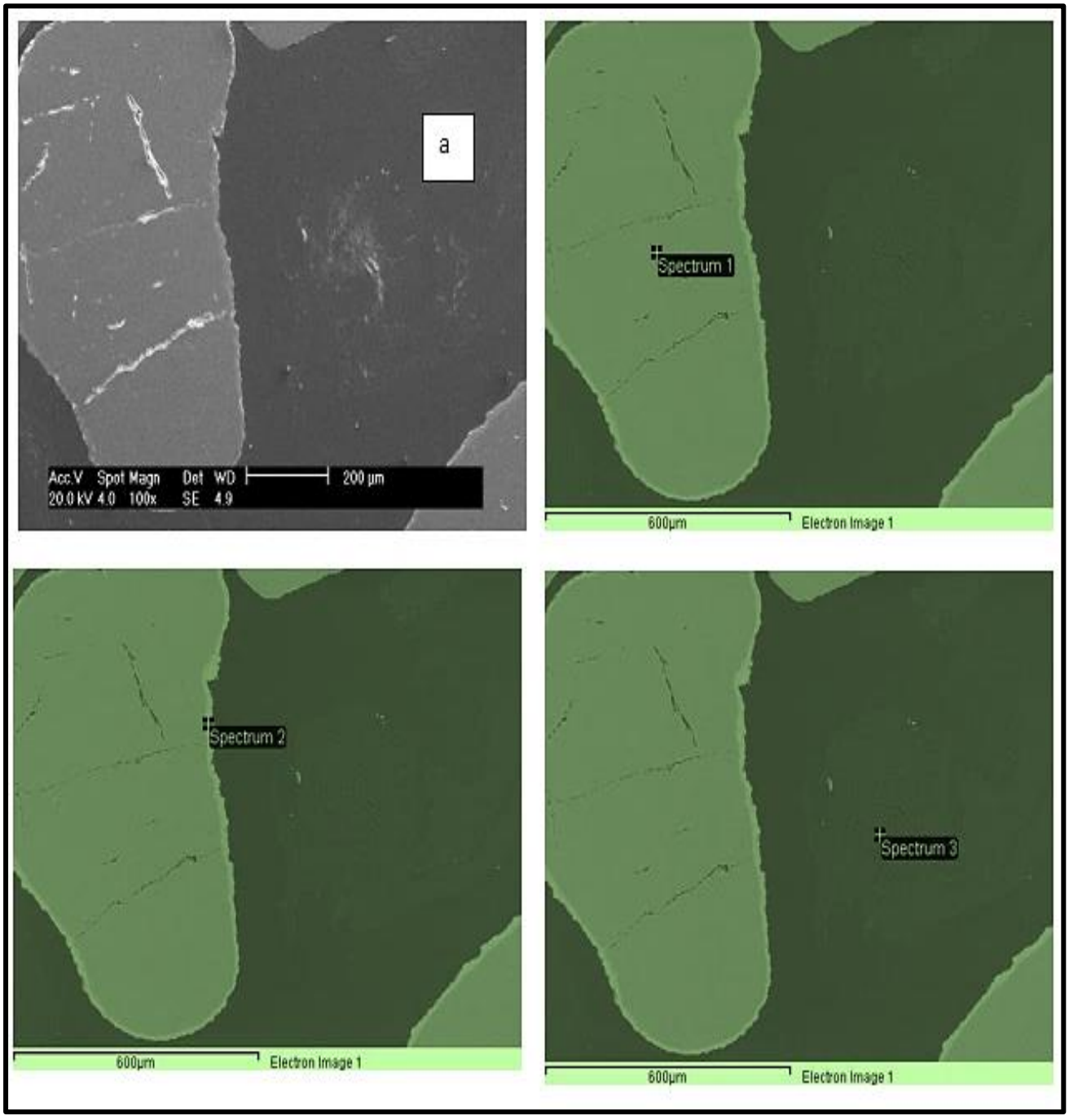

Figure 6-42: SEM image of the mixture of wood with miscanthus melted at 802 ^{0}C and SEM-EDX images of the selected areas in panel a.

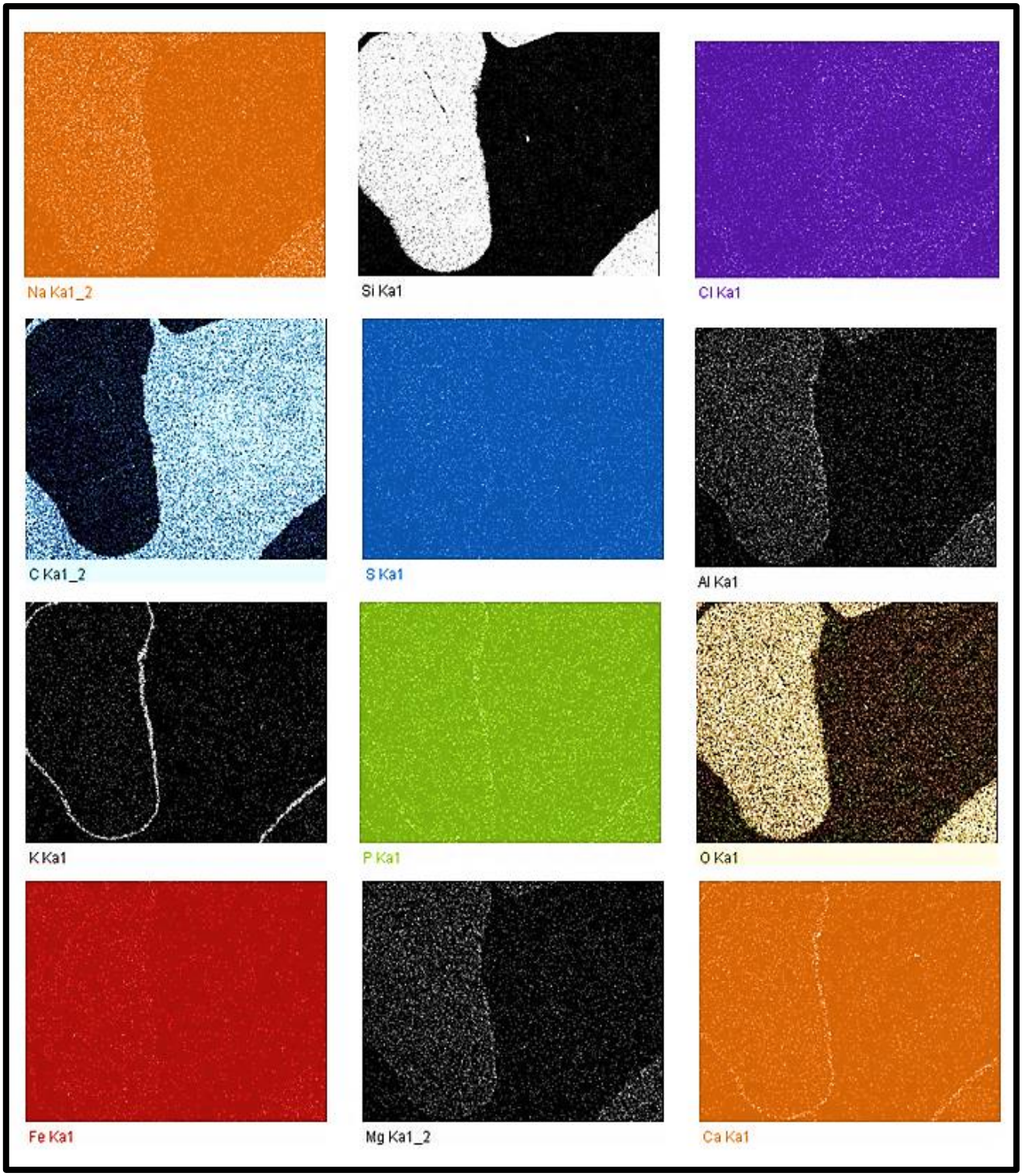

Figure 6-43: Element mapping of panel a in Figure 6.42, mixture of white wood with miscanthus melted at 802 ^{0}C.

The element mapping, Figure 6.43 revealed the overall elemental composition of the mixture of 50% wood particles with 50% miscanthus particles. The following elements were discovered to be contained in the entire image; Na, Si, Cl, C, S, Al, K, P, O, Fe, Mg, and Ca.

Mixture of willow and miscanthus particles melted at 802 ^{0}C

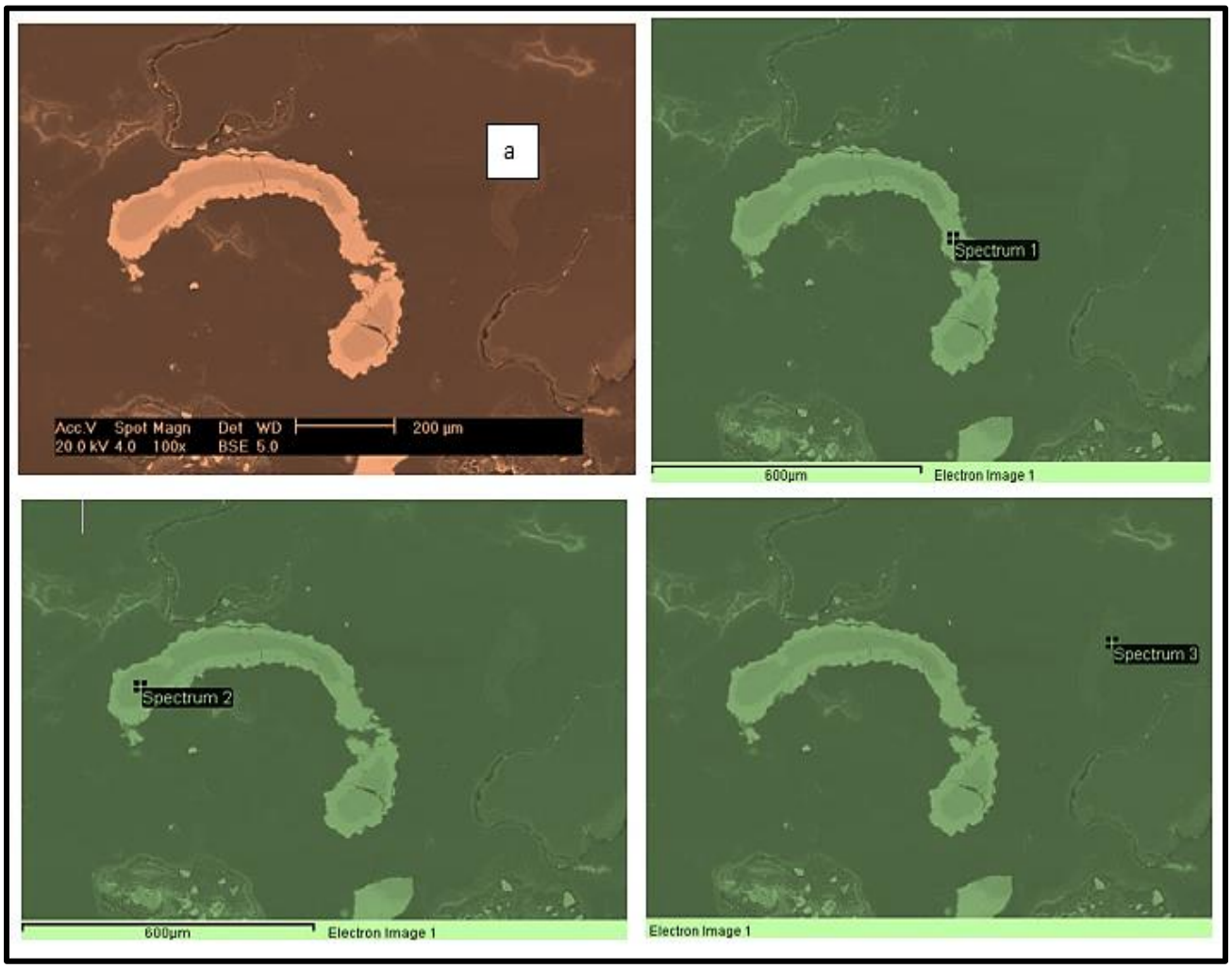

Figure 6-44: SEM image of the mixtures of willow and miscanthus melted at 802 ^{0}C and SEM-EDX images of the selected areas in panel a.

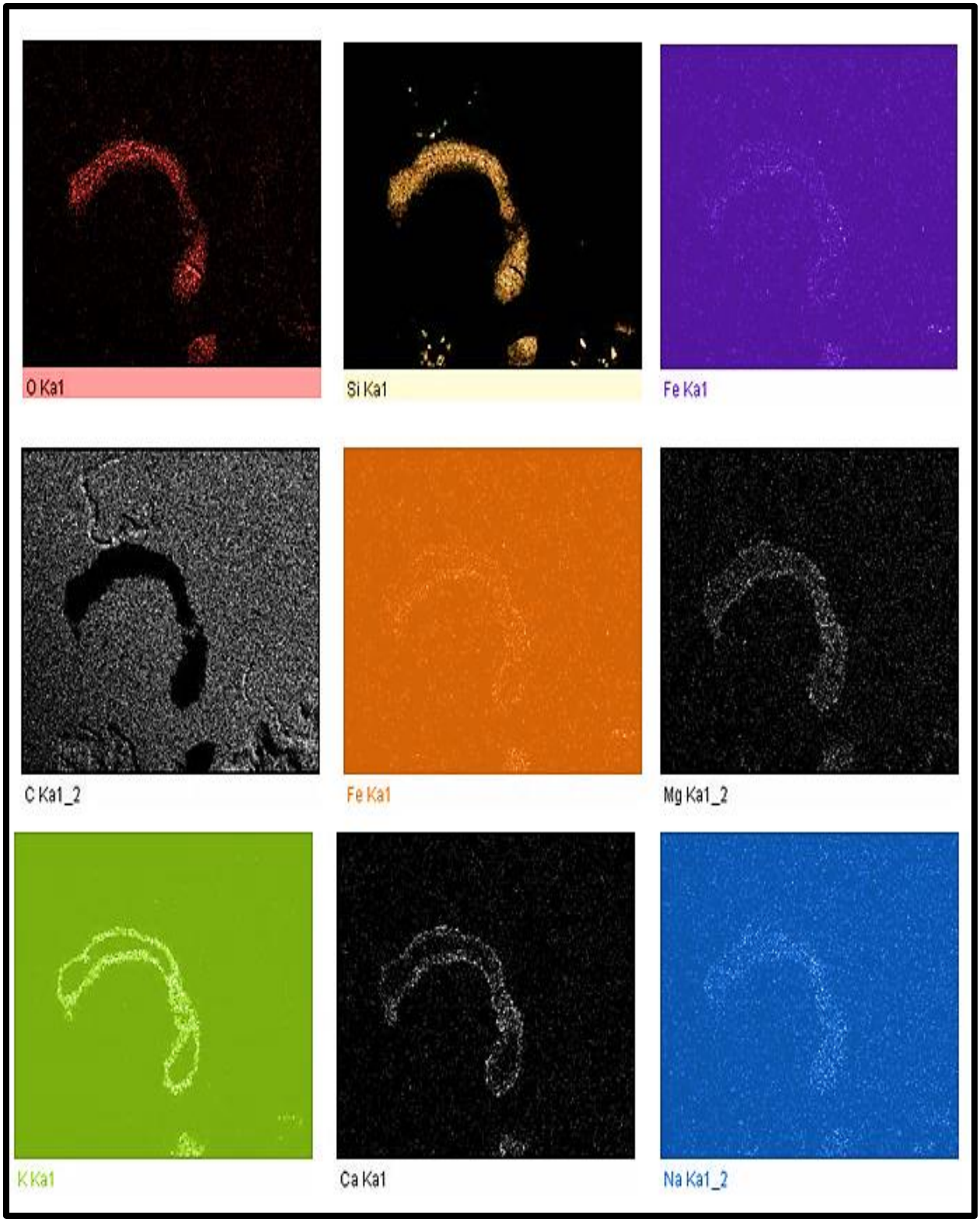

Figure 6-45: Element mapping of panel a in figure 6.44 mixture of willow + miscanthus at 802 ^{0}C.

Figure 6.44 is made up of the SEM-EDX image of the mixtures of 50% willow with 50% miscanthus particles at 802 ^{0}C. Panel a in Figure 6.44 was divided into three spectra. It showed that, spectrum 1 consisted of Si (66.62 wt %), K (9.93 WT %), Ca (2.01 wt %), Mg (1.30 wt %), and traces of Fe and Na. Spectrum 2 contained mostly Si (61.00 wt %) while spectrum 3 is made up of C and O. There is strong correlation between K and Si for the enhancement of low melting temperature K-Silicate build up, hence, formation of agglomerates in the bed. Element mapping Figure 6.45 (willow + miscanthus) contained the following elements; O, Si, Fe, C, Mg, K, Ca, and Na. Comprehensive EDX and SEM are contained in appendix A, Figures 9.34 to 6.36

Wood particles melted at 802 ^{0}C

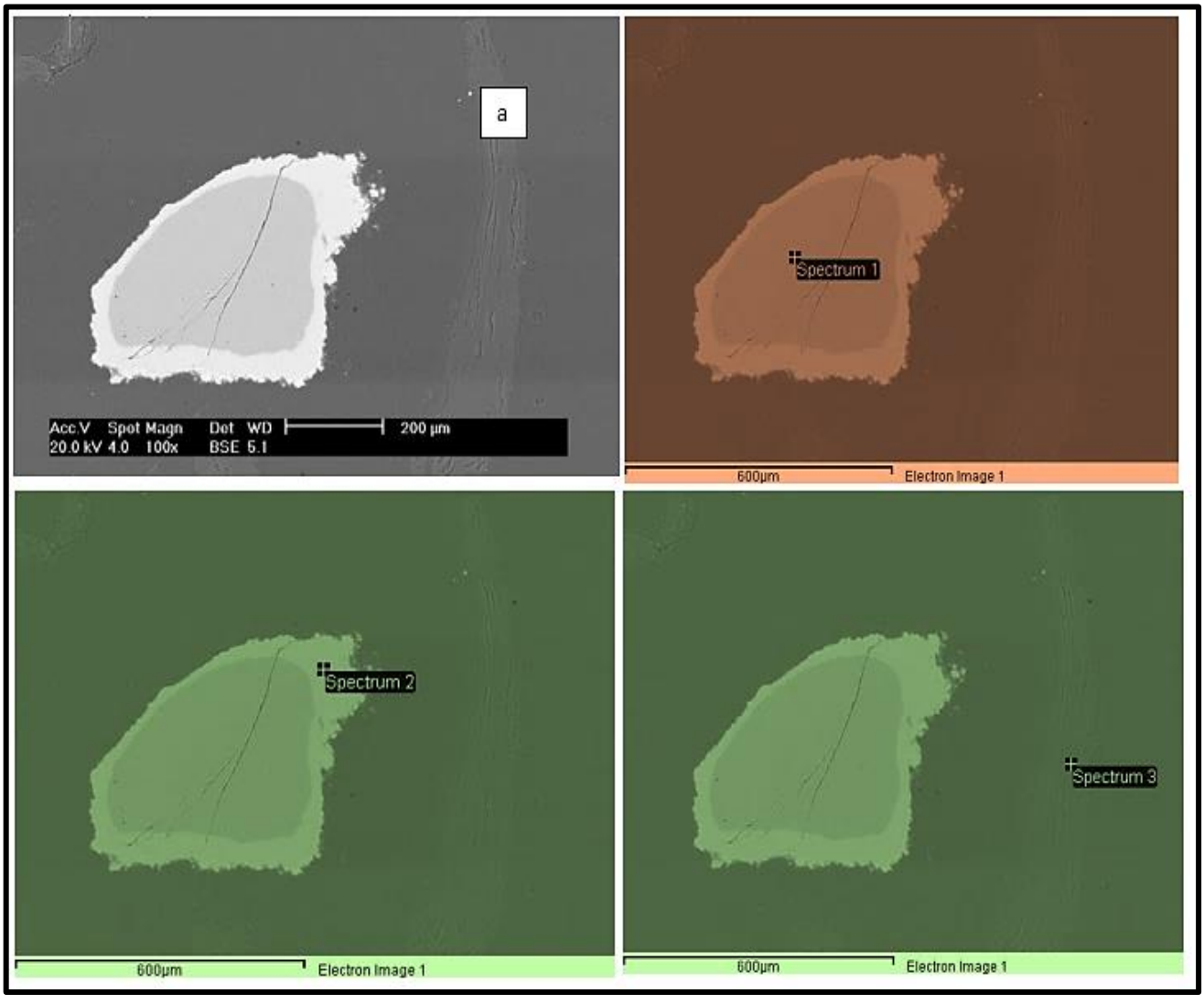

Figure 6-46: SEM image of wood melted at 802 ^{0}C and SEM-EDX images of the selected areas in panel a.

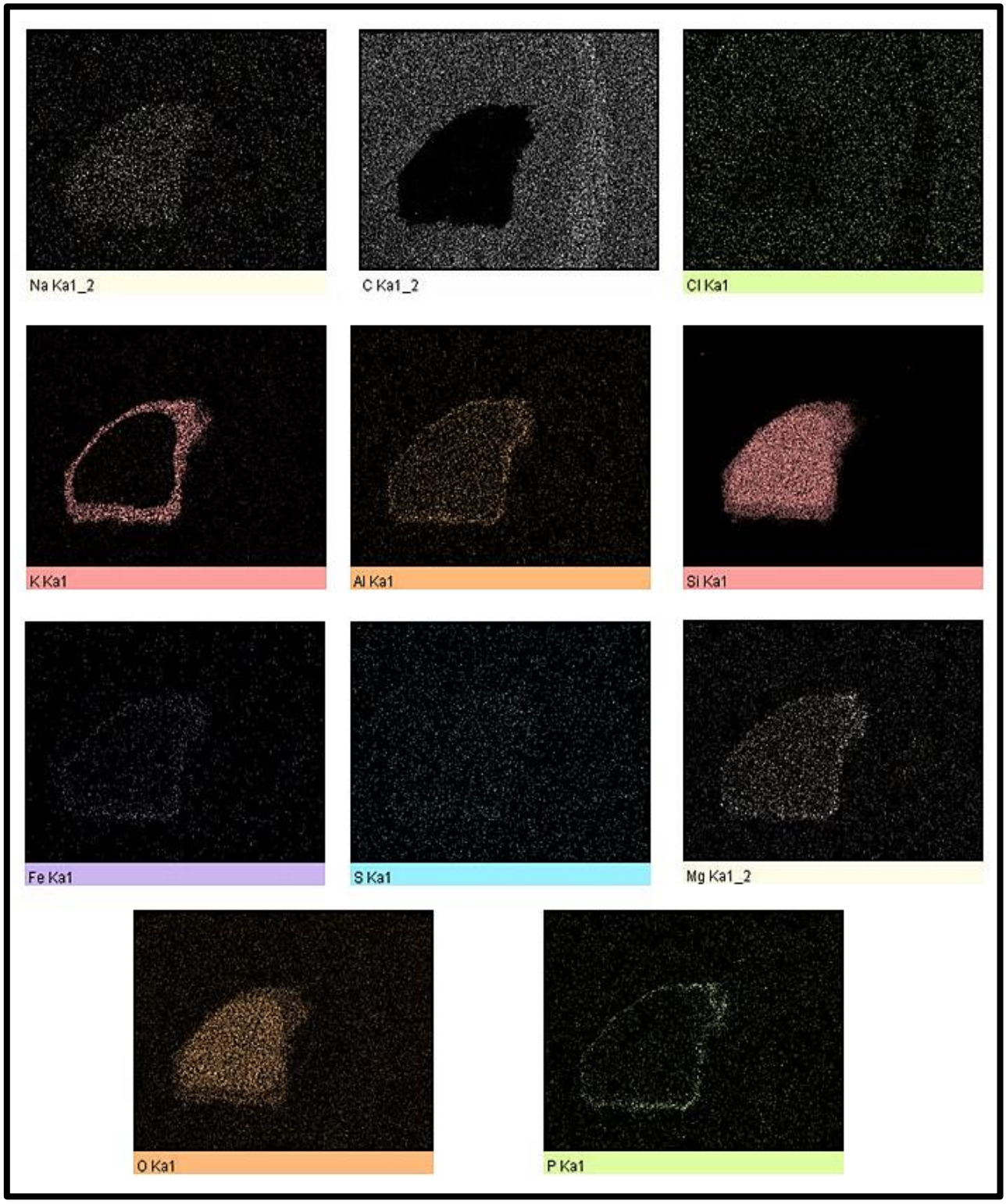

Figure 6-47: Element mapping of panel a in figure 6.46, wood @ 802 ^{0}C

Light grey area, spectrum 1, Figure 6.46 contained fused alkali-silicate in the form of K-silicate as revealed by the EDX and the element mapping, Figure 6.47. Si (79.45 wt %) - in addition to C and O from the adhesive, potentially dominates the region. Spectrum 2 was specifically dominated by Si (55.66 wt %) and K-Feldspar (22.83 wt %). Other elements making up the region are Ca - Wollastonite (3.04 wt %), Mg (1.19 wt %), and Fe (38.52 wt %). Tendency of formation of K-Silicate is high hence, production of the fused sample. Spectrum 3 is made up of C and O with infinitesimal amount of chlorine Cl (0.46 wt %) and K (0.20 wt %). Details are shown in Appendix A4, Figures 9.16 to 9.20

Wood particles melted at 750 ^{0}C

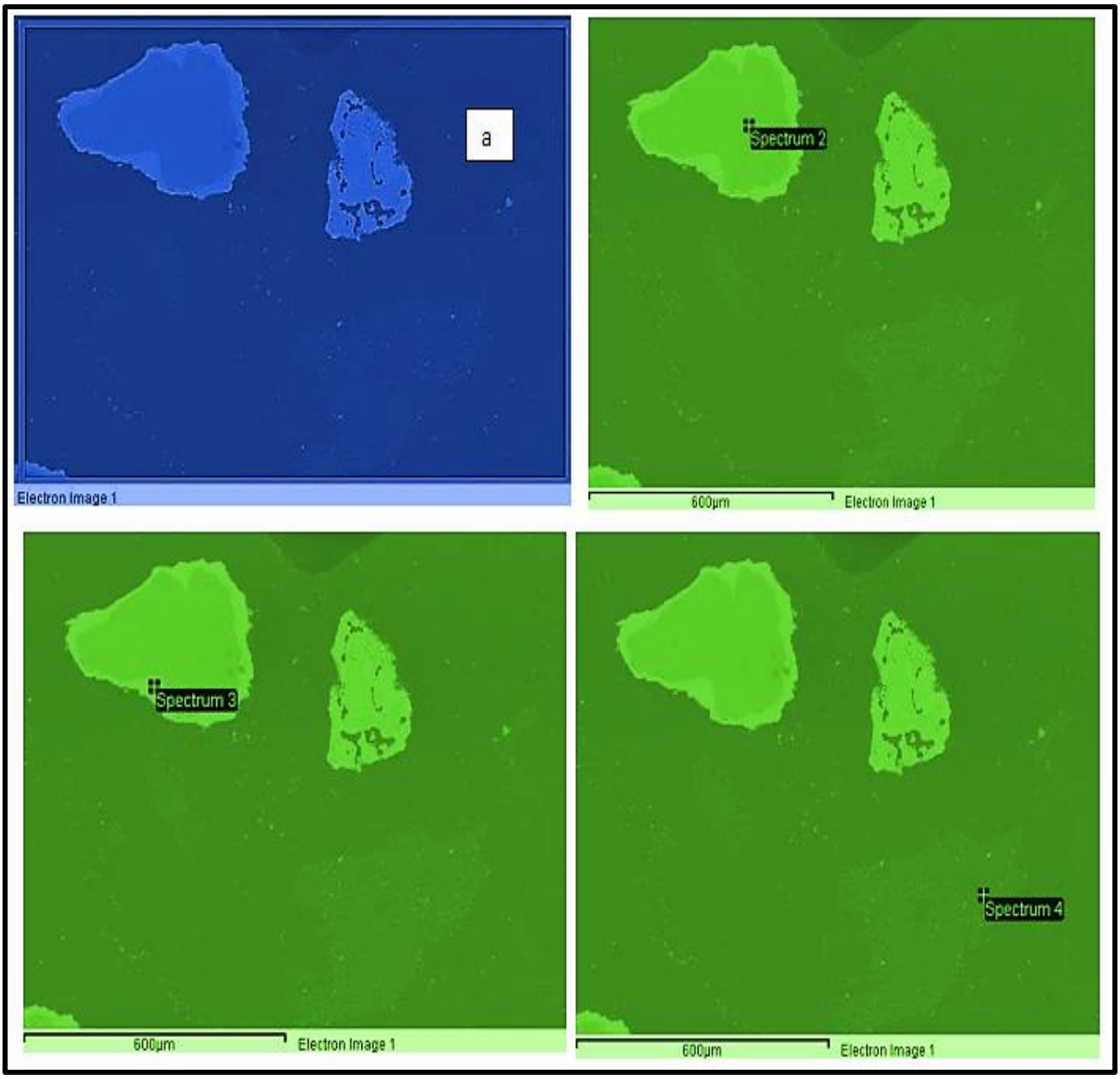

Figure 6-48: SEM image of wood melted at 750 ^{0}C and SEM-EDX images of the selected areas in panel a.

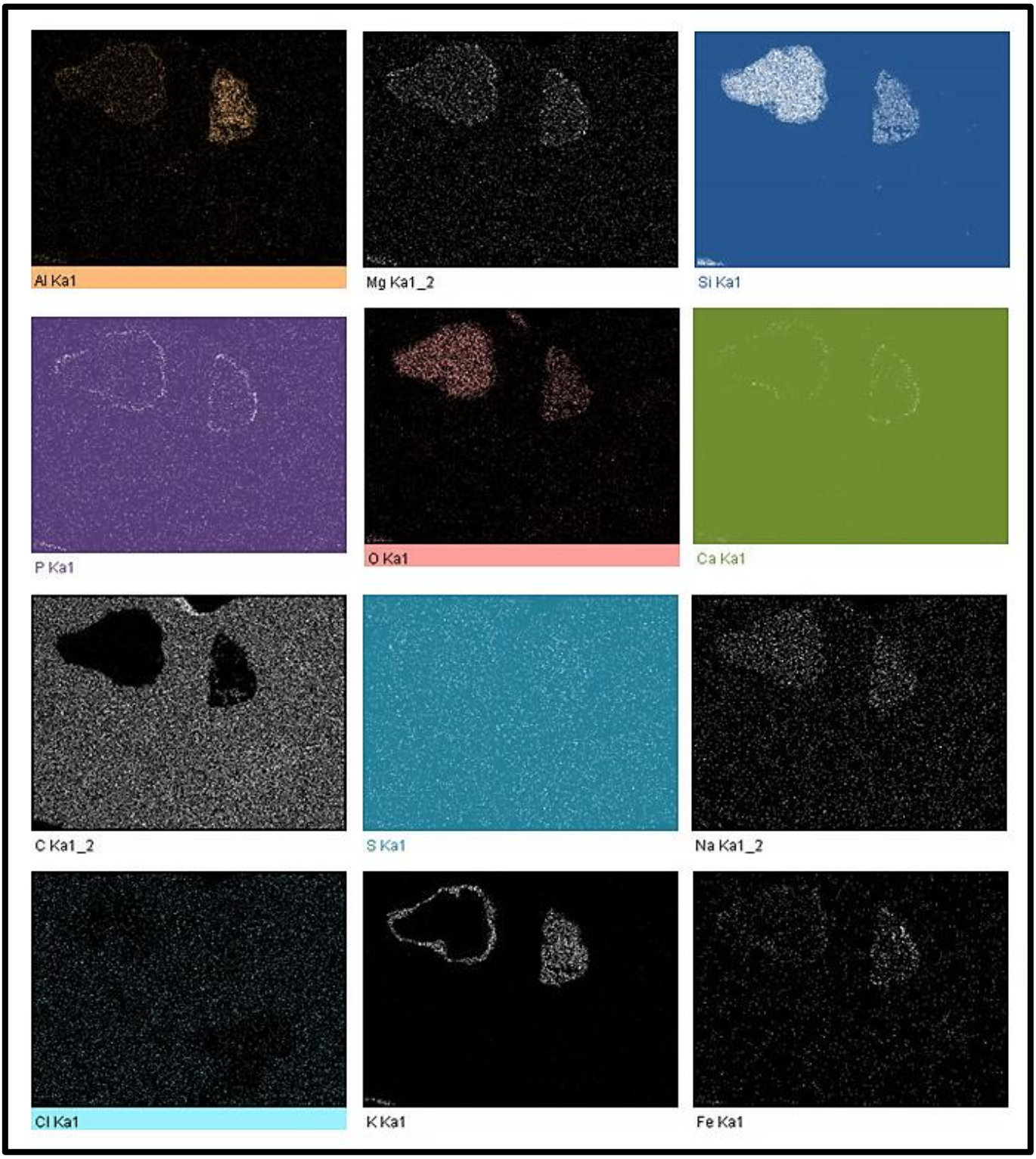

Figure 6-49: Element mapping of panel a in figure 6.48 wood at 750 ^{0}C

Figure 6.49 contained the element mapping of white wood melted at 750 ^{0}C. It consisted of Al, Mg, Si, P, O, Ca, C, S, Na, K, Cl, and Fe as shown in the images. Spectrum 2, Figure 6.48 was dominated with Si (75.28 wt %) in addition to C and O. The indication is that, a melt that is highly rich in silica had been formed in that region meanwhile, the periphery of the brighter grey area (spectrum 3) is very rich in potassium K-Feldspar (22.79 wt %), and silicon Si (41.48 wt %). It also contained calcium Ca Wollastonite (3.12 wt %), Mg (2.77 wt %), P (1.06 wt %), and Fe (5.10 wt %). This showed a good correlation between K, Na, Ca, and Si. A close examination of the grey portion, Figure 6.48 confirmed that, the interior of the agglomerates consisted majorly the silica (bed materials) while the periphery or the outer layer contained mostly the fuel ash. The tendency of K/Na-silicate formation is also very high. However, spectrum 4 is made - up of the adhesive zone with O and C dominating the area. Complete SEM and EDX data are shown in Appendix A5, Figures 9.21 to 9.25

Miscanthus particles melted at 750 ^{0}C

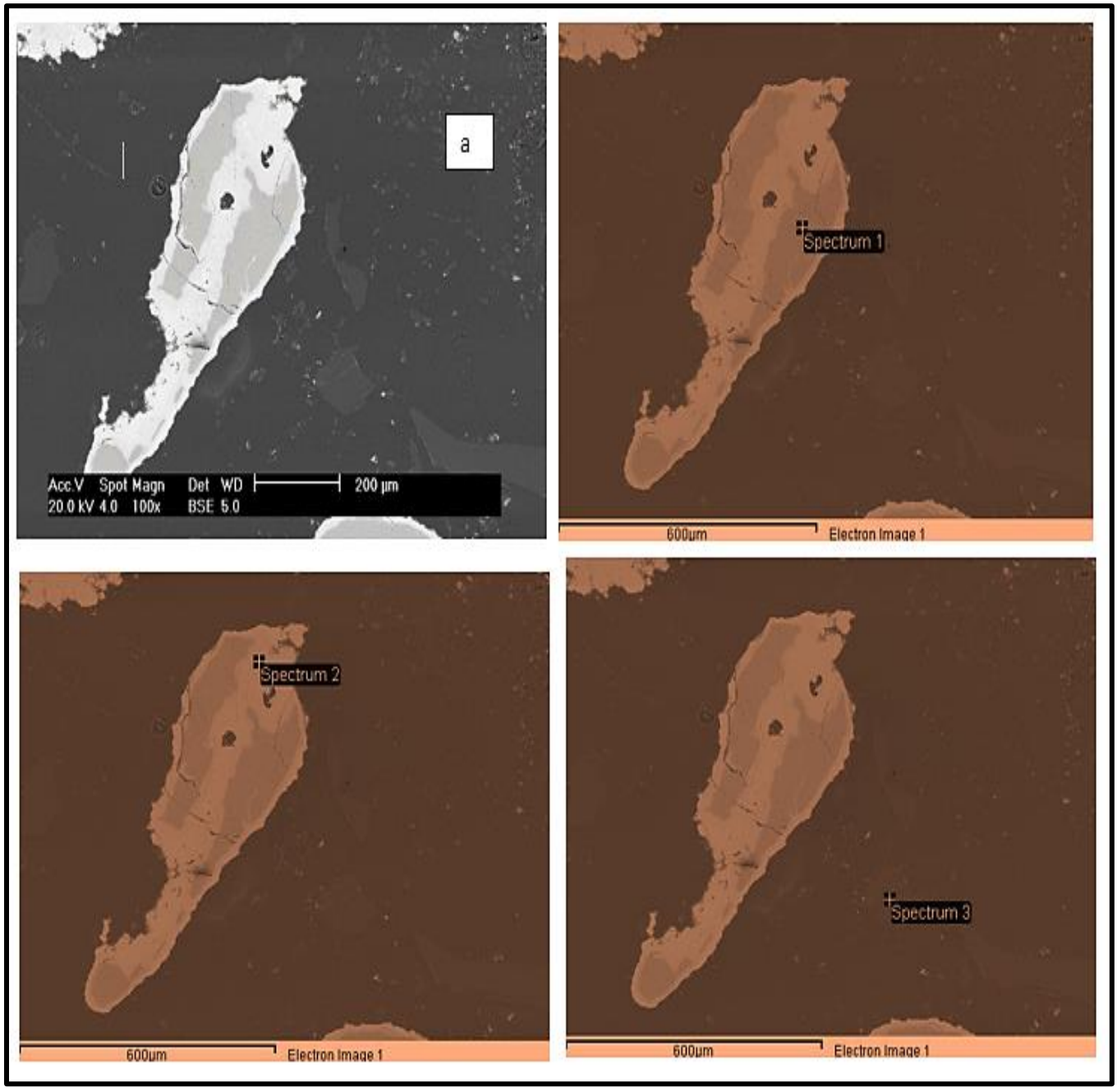

Figure 6-50 SEM image of miscanthus melted at 750 ^{0}C and SEM-EDX images of the selected areas in panel a.

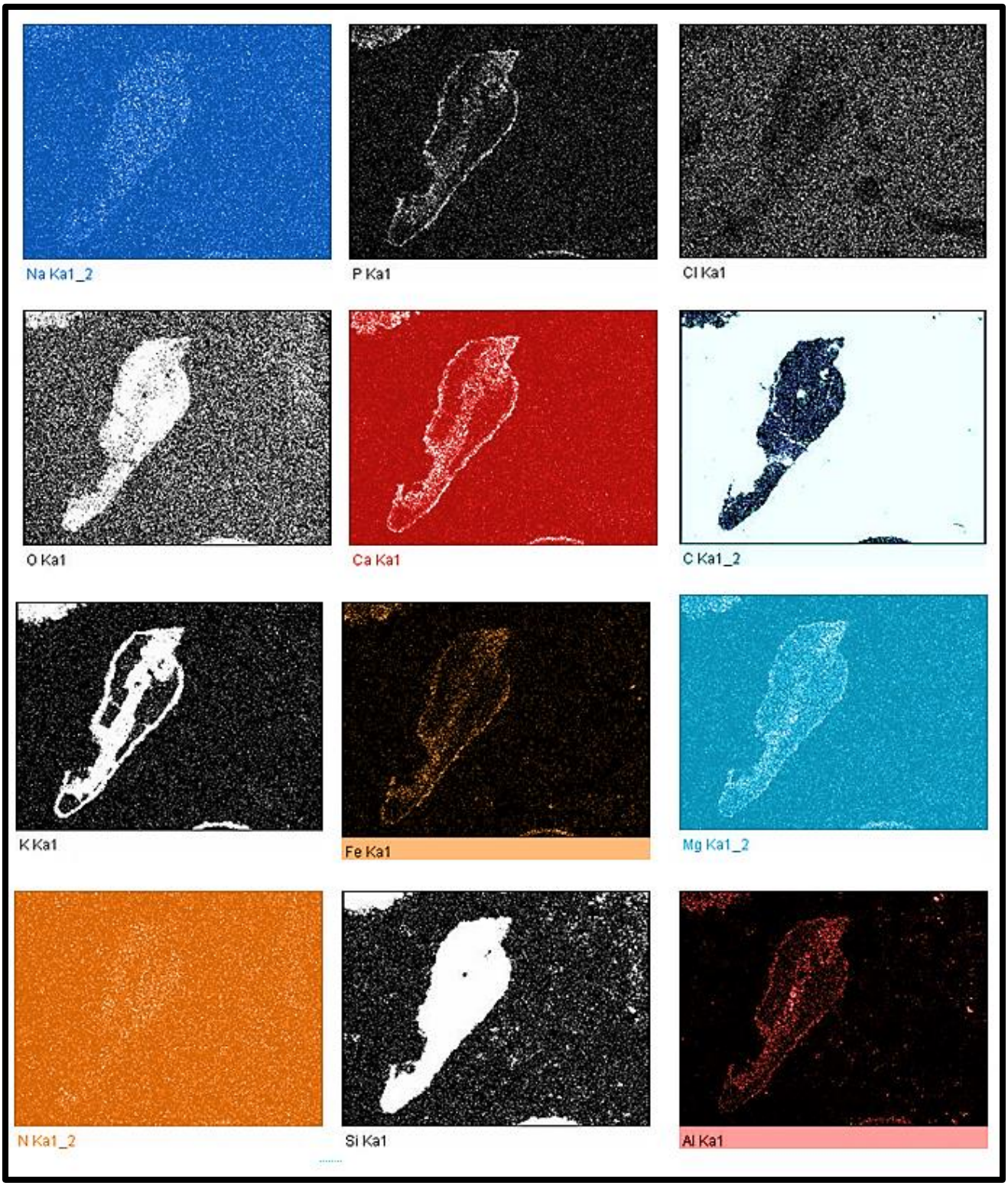

Figure 6-51: Element mapping of panel a in figure 6.50 miscanthus at 750 ^{0}C.

Darker section of the grey zone of Spectrum 1 of Figure 6.50 has Si (88.97 wt %) as the major element. The lighter area of the grey zone has Si (48.76 wt %), Mg (1.78 wt %), Al (5.23 wt %), P (4.60 wt %), K (23.72 wt %), Ca (8.95 wt %), and Fe (1.74 wt %). Concentration of Si, K, and Ca is very high in the region. The tendency of formation of K-Ca-silicate is also very high. Spectrum 3 contained exclusively C and O with little Si (1.59 wt %). These are also depicted in the element mapping, Figure 6.51 while comprehensive EDX and SEM data are contained in Appendix A6, Figures 9.26 to 9.30. Elemental composition, EDX of the samples are shown in Table 6.3

Table 6-3: EDX Spot analysis of willow, white wood, and miscanthus at 750 ^{0}C

Wt %	Willow					Wood					Miscanthus				
	1	2	3	4	5	1	2	3	4	5	1	2	3	4	5
Si	85	58	0	0	0	75	41	1	0	0	89	49	0	0	0
K	0	23	0	0	0	0	23	0	0	0	0	24	0	0	0
Mg	0	2	0	0	0	0	3	0	0	0	0	2	0	0	0
Al	0	0	0	0	0	0	4	1	0	0	0	5	0	0	0
Ca	0	4	0	0	0	0	3	0	0	0	0	9	0	0	0
S	0	0	1	0	0	0	0	0	0	0	0	0	2	0	0
P	0	0	0	0	0	0	1	0	0	0	0	0	0	0	0
Fe	0	1	0	0	0	0	5	0	0	0	0	2	0	0	0

Willow particles melted at 750 ^{0}C

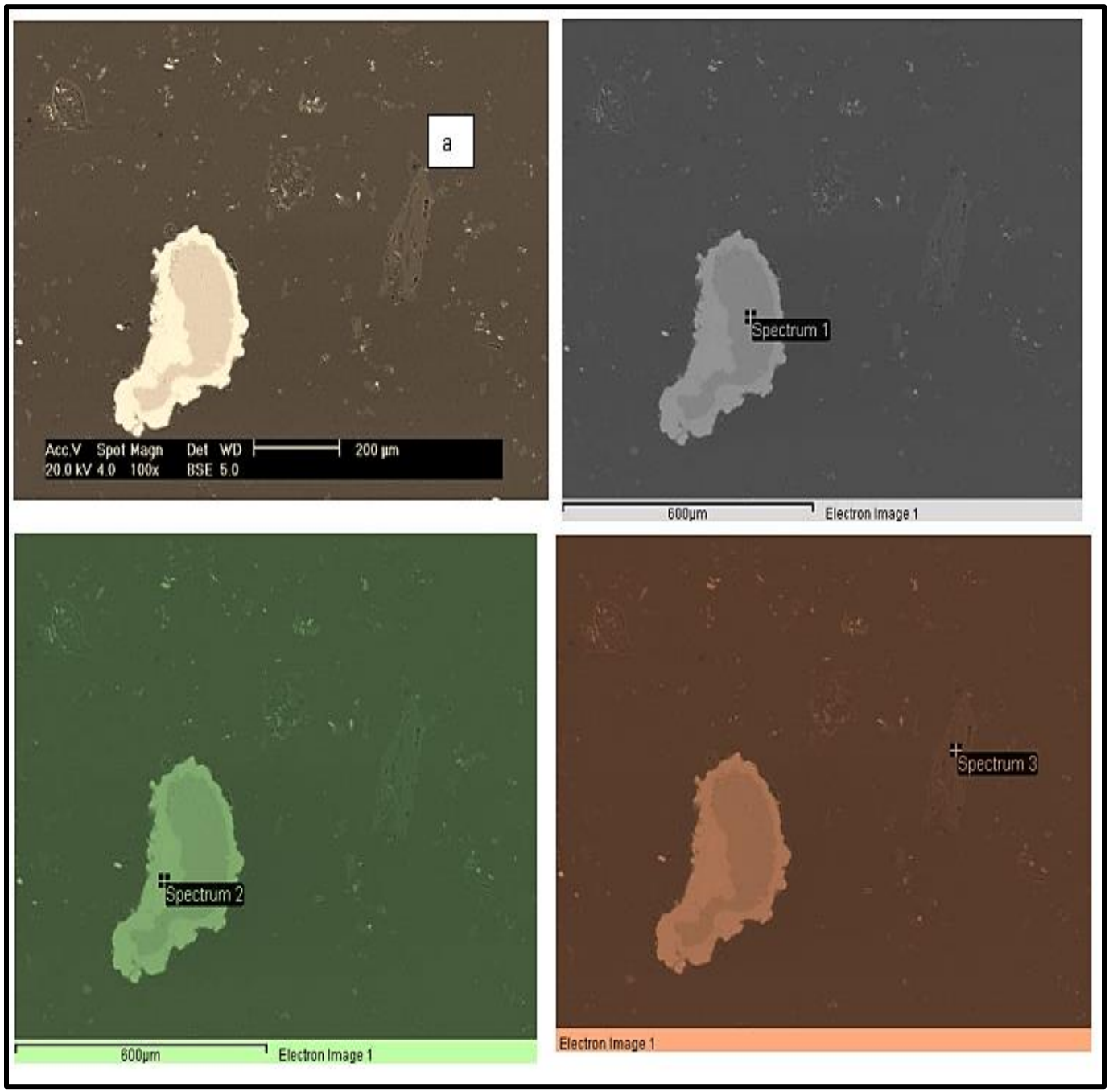

Figure 6-52: SEM image of willow melted at 750 ^{0}C and SEM-EDX images of the selected areas in panel a.

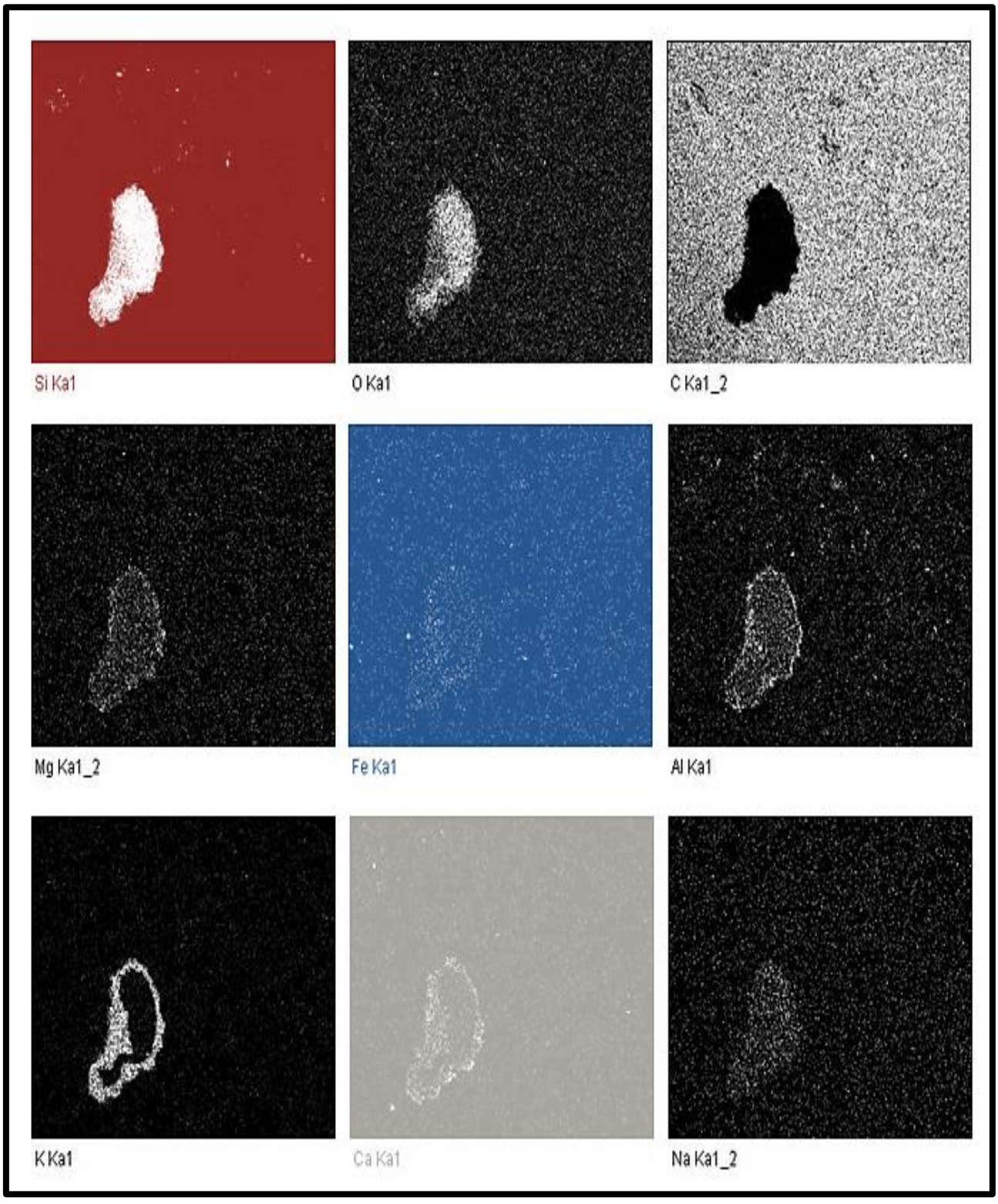

Figure 6-53: Element mapping of panel a in figure 6.48 willow melted at 750 ^{0}C

Inner core of the grey section of Figure 6.52 is predominantly covered with Si (84.81 wt %) thereby affirming that, the region is mostly made up of the bed materials while the outer layer spectrum 2, potassium K in addition to Si. There is likelihood of the presence of biomass fuel ash in large quantity in the region. Spectrum 3 comprised of the adhesives C and O. Detailed analyses are contained in Appendix A7, Figures 9.31 to 9.33

Willow Particles Melted at 802 ^{0}C

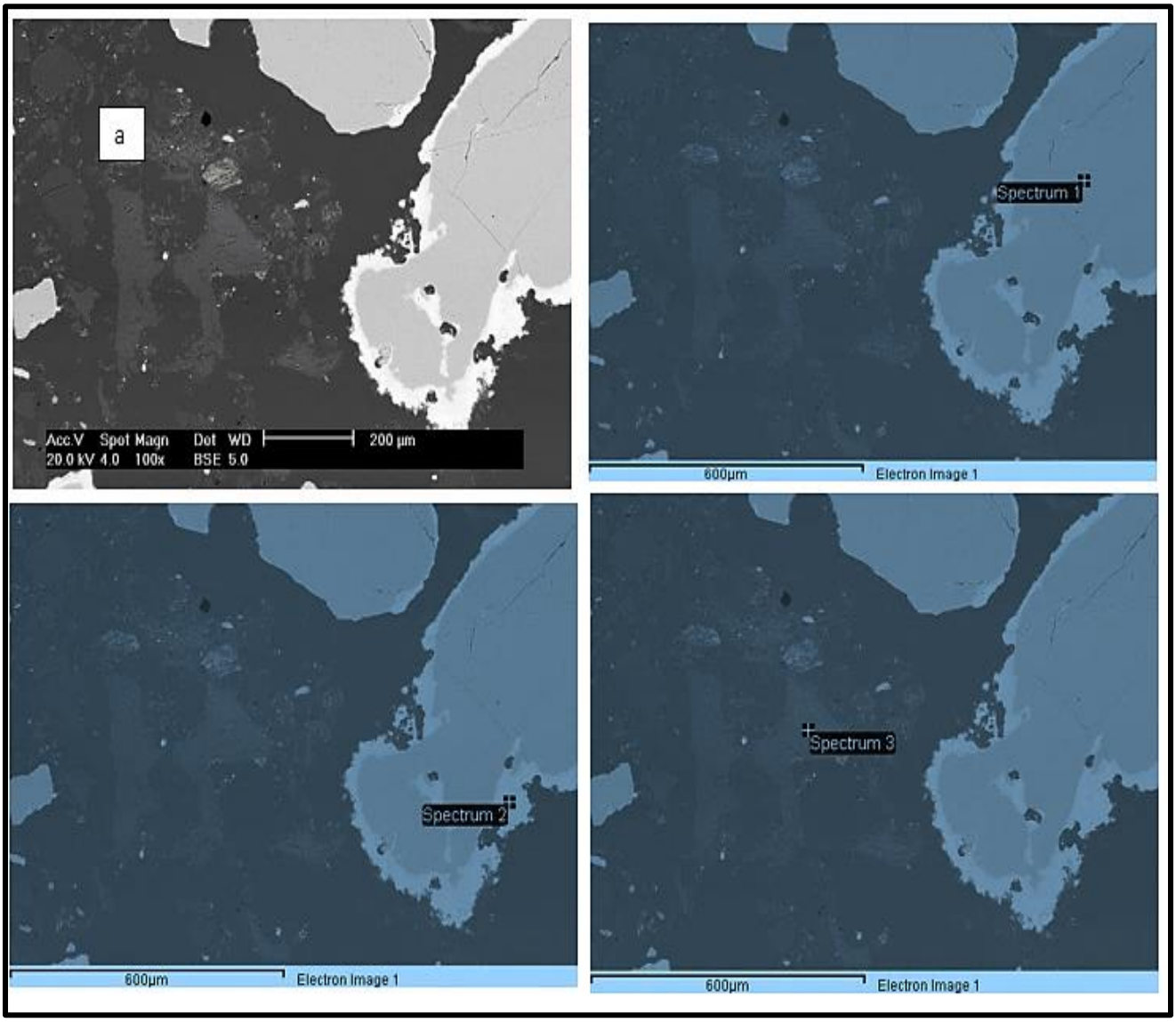

Figure 6-54: SEM image of willow melted at 802 ^{0}C and SEM-EDX images of the selected areas in panel a.

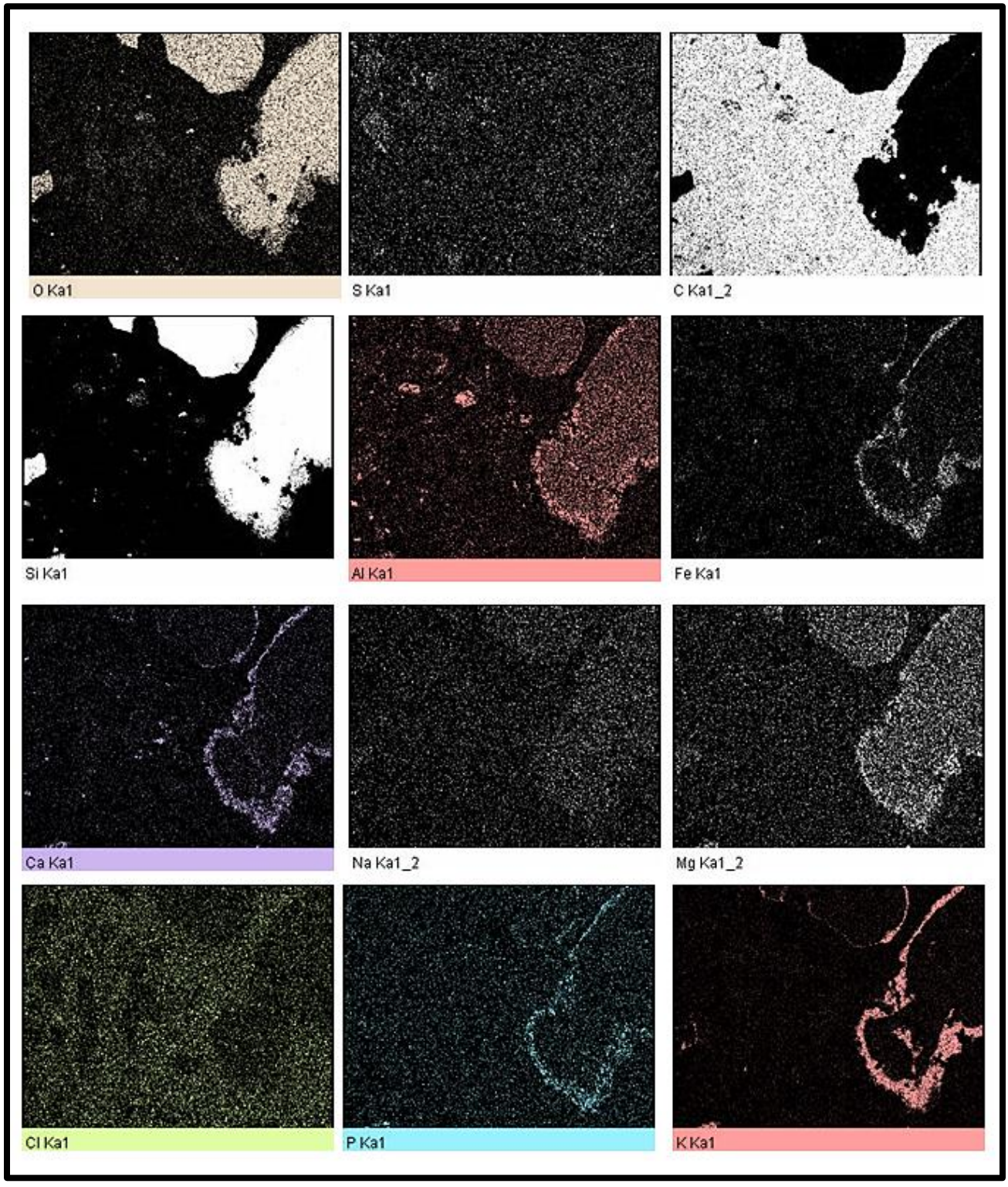

Figure 6-55: Element mapping of panel a in figure 6.54, willow at 802 ^{0}C.

Spectrum 1, Figure 6.54, willow particles melted at 802 ^{0}C is prevalently covered with Si (84.84 wt %). This clearly indicated that, the interior of the grey zone is made - up of Si. Spectrum 2 contained Si (43.95 wt %), K (25.39 wt %), Fe (18.16 wt %), Mg (3.20 wt %), Al (1.33 wt %), Ca (1.07 wt %). Other trace elements are S, P, and Na, Table 6.4. Spectrum 3 contained mostly traces of Na, Mg, Si, S, and Ca in addition to C and O that dominated the region. Element mapping, Figure 6.55 also showed these elements while the overall EDX data are contained in appendix A9, Figures 9.37 to 9.41

Table 6-4: EDX Spot analysis results of willow, white wood, and miscanthus at 802^{0}C

Wt %	Willow					Wood					Miscanthus				
	1	2	3	4	5	1	2	3	4	5	1	2	3	4	5
Si	84	44	0	0	0	79	56	0	0	0	76	42	0	0	0
K	0	25	0	0	0	0	23	0	0	0	0	16	0	0	0
Na	0	0	0	0	0	0	0	0	0	0	0	0	0	0	0
Mg	0	3	0	0	0	0	1	0	0	0	0	3	0	0	0
Al	0	1	0	0	0	0	0	0	0	0	0	2	0	0	0
Ca	0	1	0	0	0	0	3	0	0	0	0	3	2	0	0
S	0	0	0	0	0	0	0	0	0	0	0	0	0	0	0
Cl	0	0	0	0	0	0	0	0	0	0	0	0	0	0	0
P	0	0	0	0	0	0	0	0	0	0	0	0	0	0	0
Fe	0	18	0	0	0	0	0	0	1	0	0	4	0	0	0

Miscanthus particles melted at 802 ^{0}C

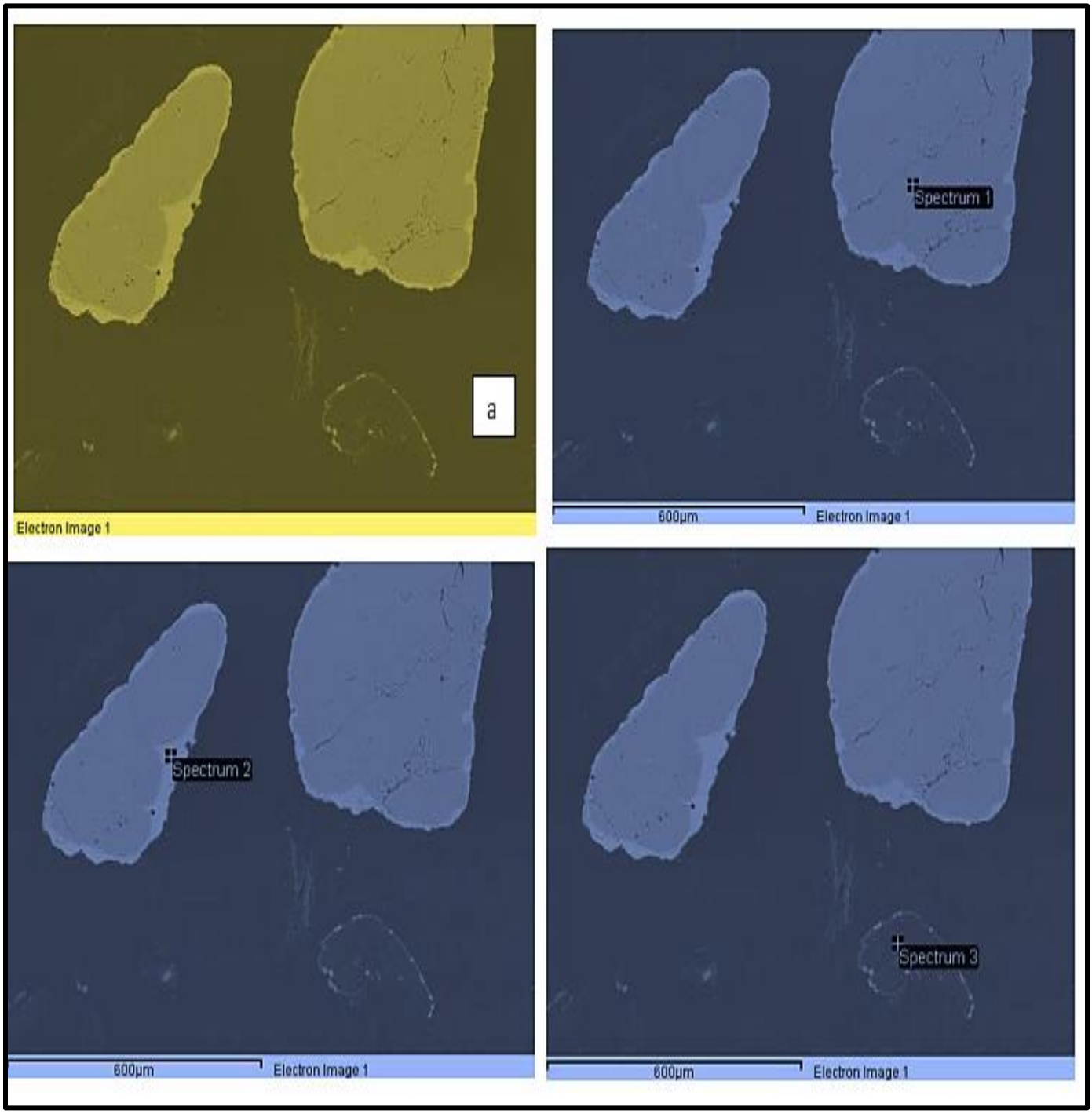

Figure 6-56: SEM image of miscanthus melted at 802 ^{0}C and SEM-EDX images of the selected areas in panel a.

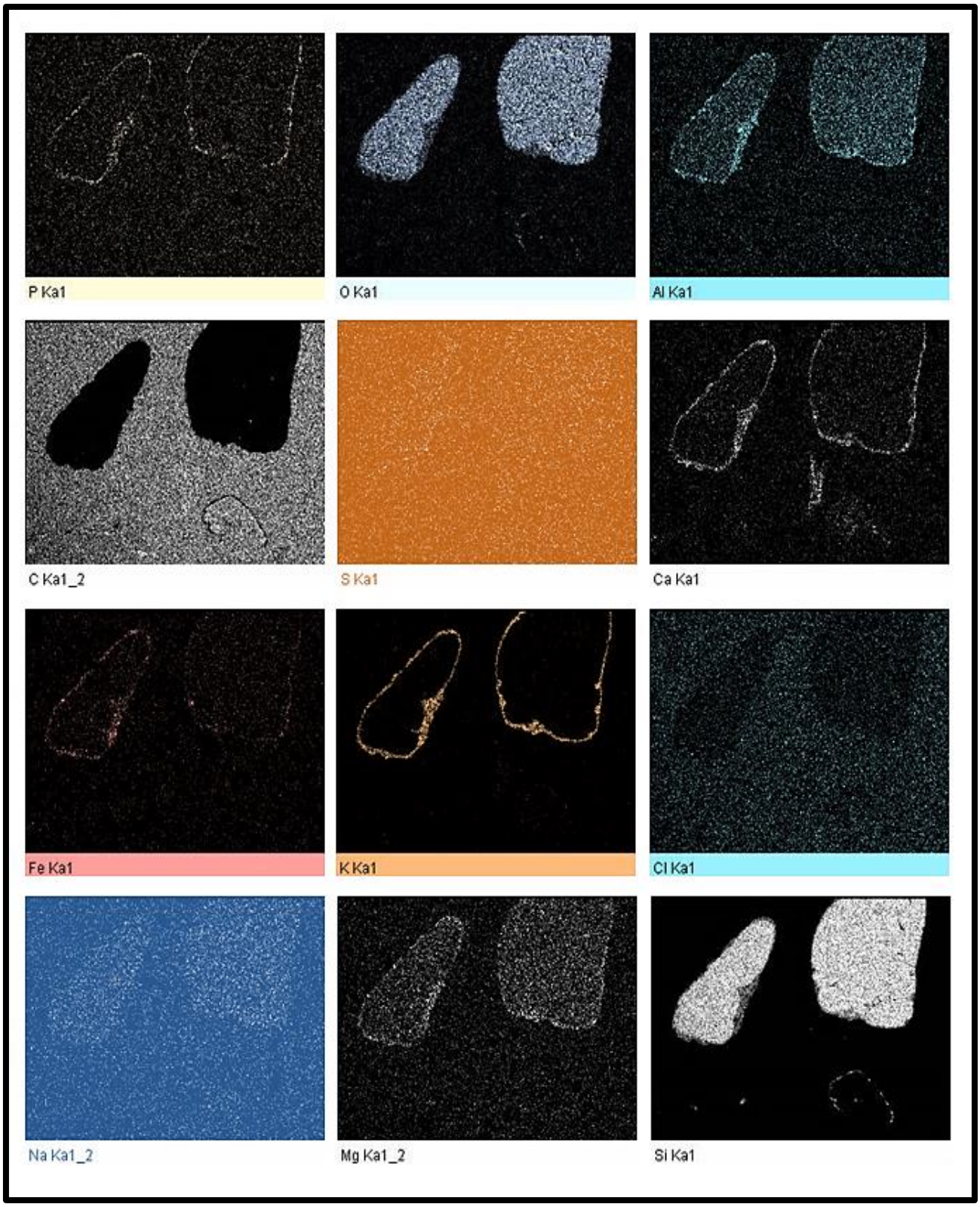

Figure 6-57: Element mapping of panel a in figure 6.52, miscanthus at 802 ^{0}C.

Inner part of the grey portion in Figure 6.56, spectrum 1, is predominantly covered with Si (75.84 wt %) while the lighter part of spectrum 2 (periphery) contained the following elements Mg (2.63 wt %), Al (1.70 wt %), Si (42.30 wt %), P (0.65 wt %), K -Feldspar (15.62 wt %), Ca-Wollastonite (3.21 wt %) and Fe (4.10 wt %). The region represents the melted miscanthus particles. High concentration of Si in the region can induce tendency for the formation of low melting temperature K-Ca-silicate. Spectrum 3 contained C, O, Ca and traces of Cl and K. Detailed data are contained in Appendix A10, Figures 9.42 to 9.46.

In the overall, agglomeration behaviours of white wood, miscanthus, and willow were studied and ascertained in this research. SEM and EDX clearly indicated that, agglomeration occurred during the combustion of the selected problematic biomass fuels. Increase in the size of the particles from <1mm before combustion to between 6mm to 8mm diameter after combustion is another clarification of agglomeration in the bed. Research showed that, melting of the biomass fuels took place because of the formation of eutectic mixture in the bed. Eutectic mixture was formed from the reactions between alkali metals in the biomass fuels and the silica in the bed materials (sand) in the form of a low melting temperature alkali-silicate, precisely potassium-silicate (K/Na-silicate). The low melting eutectic mixture melts abruptly below the temperature of the parent materials (alkali metals and silica). Additive was added in a blending ratio of 10% of the bed materials. This agreed with Wang [187] where the same ratio was used in their research. However, it may be flexible depending on the combustion technology adopted.

6.13 Summary

Series of experiments conducted in this research overwhelmingly revealed that, agglomeration is a major problem combating the combustion of biomass fuels and biomass fuels blend with bed materials. It constitutes a real threat to the generation of alternative energy from the combustion of these energy-producing fuels. This is because of the consequences that usually follow the combustion complications which include; defluidization of the bed if the combustion

bed is a fluidized bed, the loss of the whole contents and intents, reduced production competitiveness and quality assurance in a fixed bed.

A different approach to solving agglomeration occurrence during the combustion of the selected problematic biomass fuels (miscanthus, willow, and white wood) have been adopted in this present research. The use of Gooch ceramic crucible as the combustion chamber, Factsage software application to predict the eutectic points and temperatures on both the binary and the ternary phase diagrams, series of the combustion experiments conducted on the biomass fuels. The reality tests carried out on the mixture of potassium hydroxide, KOH with the quartz sand, and finally, the post combustion analyses (SEM and EDX) carried out on the samples retrieved at 700 ^{0} C, 750 ^{0} C, and 802 ^{0} C during the combustion processes of the biomass fuels were adequately analysed.

It is worthwhile to note that, biomass fuels have numerous similar characteristics therefore, they possessed almost the same average sintering temperature of 760 ^{0} C as earlier discussed in chapter 2. This fact corroborated the experimental results emanated from this present study whereby, agglomeration occurred at 750 ^{0}C and 802 ^{0}C in the laboratory-scale fixed bed. The agglomerates produced at 802 ^{0}C appeared massive and tougher when compared with agglomerates produced at 750 ^{0}C. The agglomerates produced from <1mm diameter white wood and miscanthus particles seemed harder than those from the <1mm willow particles at the same temperature and other operating conditions. This had been discussed earlier.

Consequently, agglomerates were produced in the combustion bed because of the thermo-chemical reactions that occurred between the alkali metals (mostly potassium, K and Sodium, Na) the silica from the quartz sand.

Generally, in all the simulation results obtained from the ternary phase diagrams, temperature at which agglomeration was predicted to occur is higher than predicted on the binary phase diagrams. This may have been attributed to the fact that, the eutectic mixtures produced in the ternary phase diagrams were generated from the reaction of three components; kaolin, alkali, and silica while in the binary phase diagram, the eutectic mixtures were generated from two components; alkali and kaolin. Moreover, the eutectic mixture produced in the ternary phase diagram was in the form of alkali – aluminium – silicate while in the binary phase diagrams, it

was in the form of alkali-silicate. Consequently, the melting temperature of the eutectic mixture produced in the ternary phase diagram is higher than that in the binary phase diagrams. Therefore, agglomerates would be produced at these elevated temperatures as forecasted with the Factsage software on both the binary and the ternary phase diagrams.

7 Conclusions and Recommendations for Future Works

7.1 Introduction

Fossil fuels (coal, crude oil, and natural gas) are vigorously debasing and depleting from its reserve therefore, no longer dependable as a reliable energy source. Moreover, the emissions (combustion products) emanating from its combustion processes are sources of heavy pollution to the environment. The poised for researchers to perpetually scout or rummage for a friendlier and renewable alternative energy source is highly applauded, hence the adoption of a fixed bed combustion technology for the combustion of biomass fuels and agglomeration tests. However, series of problems are encountered during the combustion of biomass fuels in the combustion beds among which are; agglomeration, erosion, fouling, and slagging to mention a few. The scope of this research is limited to '' the reduction of agglomeration in a laboratory - scale fixed bed using a Gooch crucible as the combustion chamber while adding kaolin as additive''. This chapter discusses the overall discoveries during the research work (PhD) in its entire totality, with a view to recommending other areas not adequately covered as proposed future works.

7.2 General Research Conclusions

Findings from this research are also applicable to other combustion beds especially the fluidized beds. A unique approach was adopted at solving the agglomeration problems. Introduction of a Gooch ceramic crucible as the combustion chamber was to ensure that, higher temperature distribution is achieved within the chamber. This is a significant contribution to knowledge in this research work. Maximum temperature attained with the conventional ceramic crucible was 445 ^{0} C while 802 ^{0}C was achieved with the Gooch ceramic crucible. This temperature, 802 ^{0}C was able to melt the biomass fuels particles during the combustion processes. Simultaneous and critical comparison of the combustion experiments, simulation results (Factsage software applications), and the reality tests conducted by heating KOH + silica sand formed the main technique and approach in this research.

In this research, it was established that, formation of a low melting temperature alkali-silicate in the form of potassium, K –silicates or sodium, Na – silicates were the bed rock upon which agglomeration in the combustion beds depended. The low melting temperature alkali-silicate (eutectic compound) has a lower melting temperature than the parent materials therefore, melts quickly in the bed during combustion.

Post combustion analyses, SEM revealed that, elongation in the sizes of the biomass particles from < 1mm before combustion to 6mm or 10mm after combustion, was a clear indication and confirmation of occurrence of agglomeration in the bed. EDX confirmed the elemental compositions of the agglomerates. The inner core contained silicon, Si while the outer layer contained mostly potassium, K emanated from the fuel ashes. Details of the comprehensive SEM and EDX data are contained in appendices A of this thesis.

Addition of additive, kaolin facilitated chemical reaction in the bed that produced a higher melting temperature (eutectic compound) in the form of alkali-alumina-silicates. This has a higher melting temperature than the parent materials therefore, would melt at elevated temperatures, 1200 ^{0}C if the dominant alkali is potassium, K and at 1700 ^{0}C if the dominant alkali is sodium, Na. Therefore, kaolin is a dependable and reliable additive to reduce agglomeration during the combustion of biomass fuels in combustion beds (fixed and fluidized beds).

The reality experiments conducted also buttressed the formation of agglomerates via alkali-silicates formation in the bed. Potassium hydroxide KOH was heated with silica sand. At 350 ^{0}C, lumps of particles in form of agglomerates were produced. At 502 ^{0}C, stronger and harder agglomerates were produced. This is also a confirmation of alkali-silicate existence in agglomeration chemistry. Brittle and weak agglomerates were produced when 10% kaolin was added to the mixture of KOH and silica sand.

As a limitation, the experiment could not be performed beyond the agglomeration tests. The maximum temperature achieved in the bed 802 ^{0}C, could not confirm agglomeration at higher temperatures when additive was added. This has been added to the future works to continue this research. Details of the discoveries are as epitomized underneath;

7.3 Prediction of Eutectic points on Phase Diagrams

The intention of this sub-section was to investigate and affirm the temperature at which fusion of biomass fuel particles and bed materials occurred in the bed during combustion with additive, kaolin added. Moreover, this led to the determination of the safe working temperature of the combustion equipment (SWT) which was recommended to be below the eutectic temperature, when additive (kaolin) was added. Conclusions were drawn as follows;

- With the addition of additive (kaolin) to the bed contents, in Potassium, K dominated biomass fuels, agglomeration was predicted to occur in the bed at the temperature of 1200 ^{0}C and pressure of one bar on binary phase diagrams. Only two components (kaolin and potassium oxide) were considered simultaneously.
- Eutectic temperature in Sodium, Na dominated biomass fuel was at a higher temperature of 1700 ^{0}C at the same operating conditions.
- With the addition of additive (kaolin) to the bed materials, initial agglomeration was forecasted to occur in the bed at the temperature of 1550 ^{0}C and pressure of one bar on ternary phase diagrams where three components were considered simultaneously.
- Variation in the value of the compositions of the components (kaolin and potassium oxide respectively) $Al_2Si_2O_5(OH)_4$ and K_2O was discovered not have any significant influence on the eutectic temperatures on both the binary and the ternary phase diagrams. Percentage of the components was in either mole or grams as earlier showcased.
- Pressure has a significant influence on the formation of agglomerates in a laboratory-scale fixed bed during the combustion of biomass fuels. This was confirmed with the results obtained from Factsage software applications on the determination of eutectic temperatures on binary and ternary phase diagrams. The higher the pressure in the bed, the lower is the risk of agglomeration in the beds during the combustion processes of the biomass fuels.

7.4 Reality test on the selected biomass fuels

The motive behind this sub-division was to investigate experimentally and ascertain the mechanisms of the reactions between alkali metals and silica. Potassium hydroxide was pre-mixed with silica sand and the mixture was heated in a Gooch crucible (combustion chamber). Findings from these tests are as discussed below:

- Agglomeration was found to occur in the combustion bed at a very low temperature of 350 ^{0}C. The potassium hydroxide melts abruptly at 350 ^{0}C thereby creating muggy and moist particles that adhere stickily to the silica sand. This corroborated the affirmation that, agglomerates are produced because of the intimate reactions between the alkali metal (Potassium K) from the Potassium hydroxide and the silica (SiO_2) from the sand, to form a low temperature alkali-silicate that melts quickly.
- A eutectic compound was formed (Potassium silicate, $K_2Si_2O_3$). It has a lower melting temperature than the parent materials (KOH and SiO_2) and therefore melts quickly at a lower temperature of 350 ^{0}C thereby producing a massive and huge lump of blocks called agglomerates in the bed. Harder and stronger agglomerates were formed when the temperature was increased to 502^0 C.
- Addition of additive in this case, only reduces the magnitude and hardness of the agglomerates produced in the bed even at the same operating conditions. Brittle agglomerates were produced.

7.5 Post Combustion Analyses on the Bed Samples

The idea of this sub-section was to further establish agglomeration tendencies in the selected biomass fuels (willow, white wood, and miscanthus). Samples were retrieved at different temperatures, 700 ^{0}C, 750 ^{0}C, and 802 ^{0}C. The samples were later subjected to both the SEM and the EDX.

Scanning Electron Microscopy (SEM) analyses conducted explicitly revealed the morphological structures of all the samples considered. The SEM revealed the structures, shape, and sizes of the agglomerates produced during the combustion processes while the EDX showed the

elements contained in the agglomerates (elemental composition). All the combustion experiments conducted on the selected biomass fuels (white wood, miscanthus, and willow) produced agglomerates except for when additive (kaolin) was added to the mixture. Therefore, it can be concluded that, biomass fuels have the potentials and tendencies to produce agglomerates during their combustion processes. Moreover, there was elongation in the size of the biomass particles from <1mm to 10mm diameter during the combustion involving wood and miscanthus while combustion involving willow particles produced elongated particles from <1mm to about 6mm diameter. Comparing the samples before and after combustion, there was a huge increase in the size and shapes of the samples after combustion in the bed. This served as confirmation that, agglomeration had occurred in the bed.

Energy Dispersive X-Ray Spectroscopy (EDX) exclusively affirmed the elemental compositions making up the samples. Spot analyses, element mapping, and spectra analyses showed that, the samples were massively dominated by the alkali metals particularly, Potassium K and Sodium, Na. Presence of some trace elements was observed, while the percentage of some trace elements in the samples is negligible. EDX analyses showed the element making up the samples. In all the samples examined, the common and the dominated elements are the alkali, potassium, K, sodium, Na, and the alkali earth metals, magnesium, Mg, calcium, Ca. In addition, silicon, Si was present in large quantity in all the samples. Other trace elements are phosphorous, P, iron, Fe, S, and Cl. Depending on the spotted area; concentration of each element varies per spot. Concentration of individual elements in the samples was further clarified with the mappings of SEM images. Meanwhile, EDX could not be carried out on some samples because they have very poor electron conductivity hence, only powder imaging was conducted on them.

Impact of Additive on the control of agglomeration during the combustion of selected biomass fuels was fully established. Kaolin was pre-mixed with the bed contents to examine the agglomeration tendencies and behaviours in the experiments conducted. Agglomeration was predicted to occur in the bed at elevated temperature of 1200 ^{0}C if the biomass fuel is dominated with potassium, K while agglomeration would occur in the combustion bed at 1700 ^{0}C if the biomass fuel were dominated with sodium, Na.

Formation of thermal NO_X and Probable damage to the combustion equipment may be completely avoided thereby, reducing the cost of emergency breakdown maintenance.

7.6 Closing Assertion

Agglomerates are usually produced during the combustion of the problematic biomass fuels at temperatures slightly above the average sintering temperatures of typical biomass fuels (700 ^{0}C to 760 ^{0}C). Addition of additives (mostly kaolin) to bed contents could increase agglomeration time and cause agglomeration to occur at elevated temperatures between 1200 ^{0}C to 1700 ^{0}C depending on the dominant alkali metals (K or Na) as predicted by the Factsage software applications. In potassium, K dominated biomass fuels, agglomeration will occur in the combustion bed at a temperature of 1200 ^{0}C while in sodium Na, dominated biomass fuels, agglomeration will occur in the bed at a temperature of 1700^{0}C. The presupposition is that, adoption of kaolin as additive during biomass fuels combustion in a laboratory - scale fixed bed with a Gooch crucible as the combustion chamber, could reduce and prevent agglomeration from occurring. With these facts, utilization of the fixed bed technology could be a reliable option for the combustion of biomass fuels for the generation of alternative energy via heat and power or combined heat and power (CHP).

Addition of kaolin (pre-mixed or in the process) as additive during the combustion of biomass fuels in a fixed bed could contribute significantly to a reduction in agglomeration formation thereby, encourage generation of heat and power from organic matters and energy crops in future. Adoption of kaolin is cost effective because, downtime and cost of maintenance of the rig because of unexpected shut down resulting from agglomeration accumulation in the combustion chamber would be averted.

With Gooch crucible as the combustion chamber in a Laboratory-scale, fixed bed combustion of biomass fuels, higher temperature of 802 ^{0}C was achieved compared to 445 ^{0}C that was realized when the conventional ceramic crucible was used. The implication is that, a high thermal resistant Gooch ceramic crucible may be the preferred combustion chamber for this purpose.

7.6.1 Overall Comparative Analyses of the Research Innovations

Literature Survey	Factsage software Applications	Laboratory Experiments	Reality Tests
Agglomeration occurred in the combustion chamber as from 760 ^{0}C to 889 ^{0}C depending on the operating conditions.	With the addition of kaolin to the bed contents, agglomeration was predicted to occur at between 1200 ^{0}C to 1700 ^{0}C on binary phase diagrams, depending on the dominating alkali metals. Under the same operating conditions, agglomeration was predicted to set in at between 1550 ^{0}C to 1700 ^{0}C or higher on ternary phase diagrams. The higher the pressure in the combustion chamber, the higher is the agglomeration temperature and time.	Agglomerates were produced at between 750 ^{0}C to 802 ^{0}C in the Gooch ceramic crucible. With the addition of kaolin, agglomerates were **not** produced at the same operating conditions. With these results, kaolin is confirmed as a reliable additive to control agglomeration in fixed bed combustion of biomass fuels.	Agglomerates were produced at very low temperatures of between 350 ^{0}C to 502 ^{0}C. This occurred when KOH was added to Silica sand and then, heated directly inside the Gooch crucible. This confirms the low melting temperature potentials of K-Silicates.

7.7 Future Work

This sub-section consists of broad overview of the whole thesis with concentration on the newly identified discoveries during the research work. However, since the research has a scope that does not permit immediate application and development of the new findings, the author is recommending these findings as future work that could continue on it. Various suggestions that would enhance further breakthrough in harnessing alternative source of energy mostly from organic matters and energy crops have been provided. The author also applauded the adoption of a fixed bed technology as a reliable combustion technology option for the combustion of biomass fuels or biomass fuel blends because of its cost effectiveness. Among others, the followings are recommended:

7.7.1 Limitations of the cartridge and the burner

The maximum temperature of 802^0C achieved within the combustion chamber, using the cartridges and the burner does not permit verification of the occurrence of agglomeration at elevated temperatures when kaolin was added to the bed mixture. Therefore, further research to include experiment that would verify production of agglomerates at elevated temperatures, as predicted with Factsage software on binary phase diagrams, 1200 ^{0}C and 1700 ^{0}C on the ternary phase diagrams is hereby recommended. This could not be achieved with the present Roxio burner.

7.7.2 Scope of the Factsage software Database

Database of the Factsage software does not include data for the direct blending of K_20 and SiO_2 (potassium oxide and silica respectively) in the database, so that eutectic points for these mixtures can be located on phase diagrams. Presently, this is not included in the present version of Factsage software used for this research, version 6.3. Manufacturers of Factsage software are to be notified. Relevant information on this had been sourced from previous works done by other researchers.

7.7.3 Agglomeration Control via Materials Selection

High alumina-rich sand can greatly reduce agglomeration in the combustor bed during combustion of biomass fuels. This is because, there is every tendency that, formation of alkali-alumina-silicate that has a higher melting point than the alkali and silica would occur. The implication is that, agglomeration will take place at elevated temperatures above the safe working temperatures, 1000 ^{0}C (SWT) of the combustion equipment. It is not advisable to operate the combustion equipment at any temperature higher than the safe working temperature.

7.7.4 Ash Fusion Test

Agglomeration confirmation tests should be extended to include ''ash fusion test'' to further establish agglomeration tendencies in the chambers during combustion. Presently, the facilities to conduct the ash fusion tests experiment are not available at the combustion laboratory of the Mechanical Engineering Department of the University of Sheffield.

7.7.5 Constraints of Laboratory space

Mechanical Engineering Department of the University of Sheffield is to speed up the construction of a modern and well spacious combustion laboratory to avert future rationalization of space and incessant embargo on combustion activities in the laboratory. This is a key factor in research activities because, the consequence is intolerably elongation of student's time limit while awaiting the suspension of such embargo or waiting for other students to complete their experiment before the remaining students could be free to perform their experiments.

7.7.6 High Temperature Resistant Crucible

To guarantee a successful combustion of biomass fuels without any major impediment, high heat resistant Gooch ceramic crucible may be a preferred combustion chamber. This is to

forestall a situation, whereby the combustion chamber would crack and completely break before the completion of the experiments.

This is to ensure that, the integrity of the obtained results is not compromised in any way. One of the ceramic crucible utilized for the conduct of the combustion experiment in this research, got broken because of the intense heat applied on it, Figure 7.1

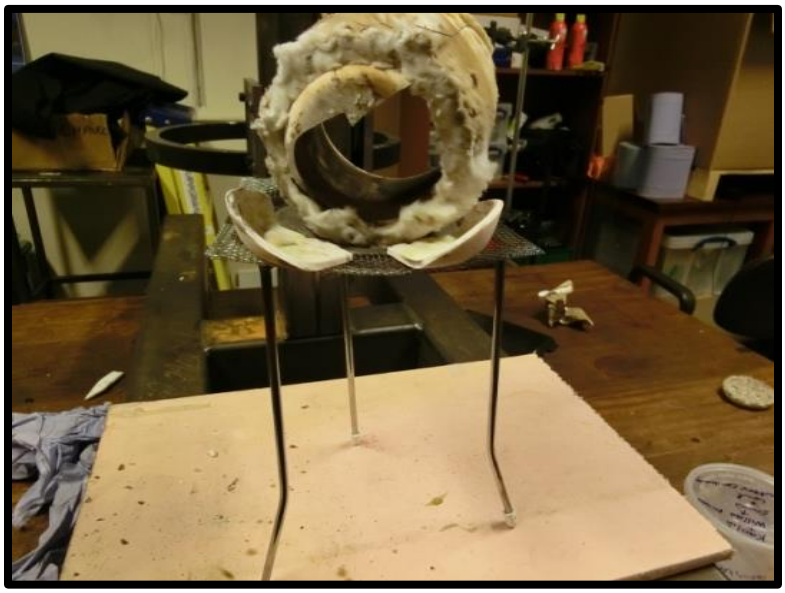

Figure 7-1: Wreckage of the ceramic crucible after the series of combustion experiments.

7.7.7 Proposed Paper Journal Publications

- Establishing Agglomeration Potentials in biomass fuels through Post combustion analyses and Factsage software applications (Chapter 5, 6, 7)
- Comparative analyses of energy crops and organic residues in terms of combustion characterization (1, 2, 3, 4)

- Influence of kaolin (additive) on agglomeration control during the combustion of problematic biomass fuels in a laboratory - scale fixed bed using a Gooch ceramic crucible as the combustion chamber (chapters 2, 5, 6, 7).

7.8 Reports Submitted During the Period of this Research

D.O Akindele, C.W Wilson, M Akram et al., "Six Monthly Reports submitted to Biomass and Fossil Fuels Research Alliance, BF2RA on Reduction of Agglomeration in a 350Kw Fluidized Bed Combustion of Biomass Fuels", 2013.

D.O Akindele, C.W Wilson, M Akram et al., "Annual Reports submitted to Biomass and Fossil Fuels Research Alliance, BF2RA on Reduction of Agglomeration in a 350Kw Fluidized Bed Combustion of Biomass Fuels", 2013.

7.9 Seminar Attended During the Period of the Research

D.O Akindele, C.W Wilson, M Akram et al., "Stakeholders Seminar on BF2RA Research Projects E. ON Technology Centre, Ratcliffe on Soar", 26th March 2013.

8 References

1. van Eyk, P.J., A. Kosminski, and P.J. Ashman, *Control of Agglomeration and Defluidization during Fluidized-Bed Combustion of South Australian Low-Rank Coals.* Energy & Fuels, 2012. **26**(1): p. 118-129.
2. Demirbas, A., *Potential applications of renewable energy sources, biomass combustion problems in boiler power systems and combustion related environmental issues.* Progress in energy and combustion science, 2005. **31**(2): p. 171-192.
3. Jenkins, B., L. Baxter, and T. Miles, *Combustion properties of biomass.* Fuel processing technology, 1998. **54**(1): p. 17-46.
4. Demirbas, A., *Combustion characteristics of different biomass fuels.* Progress in energy and combustion science, 2004. **30**(2): p. 219-230.
5. Chirone, R., F. Miccio, and F. Scala, *Mechanism and prediction of bed agglomeration during fluidized bed combustion of a biomass fuel: effect of the reactor scale.* Chemical engineering journal, 2006. **123**(3): p. 71-80.
6. Demirbas, A., D. Gullu, A. Caglar, and F. Akdeniz, *Estimation of calorific values of fuels from lignocellulosics.* Energy Sources, 1997. **19**(8): p. 765-770.
7. Lin, W., K. Dam-Johansen, and F. Frandsen, *Agglomeration in bio-fuel fired fluidized bed combustors.* Chemical engineering journal, 2003. **96**(1): p. 171-185.
8. Gingrich, N. and L. Heaton, *Structure of alkali metals in the liquid state.* The Journal of Chemical Physics, 1961. **34**(3): p. 873-878.
9. Clark Jr, S.P., *Effect of pressure on the melting points of eight alkali halides.* The Journal of Chemical Physics, 1959. **31**(6): p. 1526-1531.
10. Brus, E., M. Öhman, and A. Nordin, *Mechanisms of bed agglomeration during fluidized-bed combustion of biomass fuels.* Energy & Fuels, 2005. **19**(3): p. 825-832.
11. Skrifvars, B.-J., M. Hupa, A. Moilanen, and R. Lundqvist, *Characterization of biomass ashes*, in *Applications of Advanced technology to ash-related problems in boilers*. 1996, Springer. p. 383-398.
12. Hein, K. and J. Bemtgen, *EU clean coal technology—co-combustion of coal and biomass.* Fuel processing technology, 1998. **54**(1): p. 159-169.
13. Formisani, B., G. De Cristofaro, and R. Girimonte, *A fundamental approach to the phenomenology of fluidization of size segregating binary mixtures of solids.* Chemical Engineering Science, 2001. **56**(1): p. 109-119.
14. Howard, J., *Fluidized Beds. Combustion and Applications.* Applied Science Publishers, Ripple Road, Barking, Essex, England, 1983., 1983.
15. Yu, C., J. Qin, H. Nie, M. Fang, and Z. Luo, *Experimental research on agglomeration in straw-fired fluidized beds.* Applied energy, 2011. **88**(12): p. 4534-4543.
16. Haworth, I.D.C. and S.R. Turns, *FUNDAMENTALS OF COMBUSTION Spring 2008 ANGEL: https://cms. psu. edu–ME 530.* 2008.
17. Liu, Z., B. Fei, Z. Jiang, and X. Liu, *Combustion characteristics of bamboo-biochars.* Bioresour Technol, 2014. **167**: p. 94-9.
18. Troschinetz, A.M. and J.R. Mihelcic, *Sustainable recycling of municipal solid waste in developing countries.* Waste Management, 2009. **29**(2): p. 915-923.
19. Haugan, M.P., *Energy conservation and the principle of equivalence.* Annals of Physics, 1979. **118**(1): p. 156-186.
20. Hilgevoord, J., *The uncertainty principle for energy and time.* American Journal of Physics, 1996. **64**(12): p. 1451-1456.

21. Koppejan, J. and S. Van Loo, *The handbook of biomass combustion and co-firing*. 2012: Routledge.
22. Visser, H.J.M., J. Kiel, and H. Veringa, *The influence of fuel composition on agglomeration behaviour in fluidised-bed combustion*. 2004: Energy research Centre of the Netherlands ECN Delft.
23. Aho, M. and E. Ferrer, *Importance of coal ash composition in protecting the boiler against chlorine deposition during combustion of chlorine-rich biomass.* Fuel, 2005. **84**(2): p. 201-212.
24. Dayton, D.C., D. Belle-Oudry, and A. Nordin, *Effect of coal minerals on chlorine and alkali metals released during biomass/coal cofiring.* Energy & Fuels, 1999. **13**(6): p. 1203-1211.
25. Grubb, M., C. Vrolijk, and D. Brack, *The Kyoto Protocol. A guide and assessment.* 1999.
26. Gokcol, C., B. Dursun, B. Alboyaci, and E. Sunan, *Importance of biomass energy as alternative to other sources in Turkey.* Energy policy, 2009. **37**(2): p. 424-431.
27. Demirbas, A., *Importance of biomass energy sources for Turkey.* Energy policy, 2008. **36**(2): p. 834-842.
28. Demirbas, A., *The importance of biomass.* Energy Sources, 2004. **26**(4): p. 361-366.
29. Berndes, G., M. Hoogwijk, and R. van den Broek, *The contribution of biomass in the future global energy supply: a review of 17 studies.* Biomass and Bioenergy, 2003. **25**(1): p. 1-28.
30. Upreti, B.R., *Conflict over biomass energy development in the United Kingdom: some observations and lessons from England and Wales.* Energy policy, 2004. **32**(6): p. 785-800.
31. Cannell, M.G., *Carbon sequestration and biomass energy offset: theoretical, potential and achievable capacities globally, in Europe and the UK.* Biomass and Bioenergy, 2003. **24**(2): p. 97-116.
32. Franck, J. and W.E. Loomis, *Photosynthesis in plants.* Soil Science, 1949. **68**(3): p. 275.
33. Norris, L., R. Norris, and M. Calvin, *A survey of the rates and products of short-term photosynthesis in plants of nine phyla.* Journal of experimental botany, 1955. **6**(1): p. 64-74.
34. Franklin, H.M., *The interaction of New Zealand native plants with nitrogen in Canterbury's agricultural landscapes*. 2014, Lincoln University.
35. Escaño, C.R. and S.P. Tababa, *Fruit production and the management of slopelands in the Philippines*. 1998: Food & Fertilizer Technology Center.
36. Hu, J.-L. and S.-C. Wang, *Total-factor energy efficiency of regions in China.* Energy policy, 2006. **34**(17): p. 3206-3217.
37. Thollander, P. and M. Ottosson, *An energy efficient Swedish pulp and paper industry–exploring barriers to and driving forces for cost-effective energy efficiency investments.* Energy Efficiency, 2008. **1**(1): p. 21-34.
38. Wang, W., Y. Yung, A. Lacis, T.a. Mo, and J. Hansen, *Greenhouse effects due to man-made perturbations of trace gases.* Science, 1976. **194**(4266): p. 685-690.
39. Xuejie, G., Z. Zongci, D. Yihui, H. Ronghui, and F. Giorgi, *Climate change due to greenhouse effects in China as simulated by a regional climate model.* Advances in Atmospheric Sciences, 2001. **18**(6): p. 1224-1230.
40. Parikh, J. and V. Shukla, *Urbanization, energy use and greenhouse effects in economic development: Results from a cross-national study of developing countries.* Global Environmental Change, 1995. **5**(2): p. 87-103.
41. Bruggink, G. and E. Heuvelink, *Influence of light on the growth of young tomato, cucumber and sweet pepper plants in the greenhouse: effects on relative growth rate, net assimilation rate and leaf area ratio.* Scientia Horticulturae, 1987. **31**(3-4): p. 161-174.
42. Baxter, L., *Biomass-coal co-combustion: opportunity for affordable renewable energy.* Fuel, 2005. **84**(10): p. 1295-1302.

43. Bushnell, D.J., C. Haluzok, and A. Dadkhah-Nikoo, *Biomass Fuel Characterization: Testing and Evaluating the Combustion Characteristics of Selected Biomass Fuels: Final Report May 1, 1988-July, 1989*. 1990, USDOE Bonneville Power Administration, Portland, OR (USA); Oregon State Univ., Corvallis, OR (USA). Dept. of Mechanical Engineering.
44. Bergman, T.L., F.P. Incropera, D.P. DeWitt, and A.S. Lavine, *Fundamentals of heat and mass transfer*. 2011: John Wiley & Sons.
45. Martin, H., *Heat and mass transfer between impinging gas jets and solid surfaces.* Advances in heat transfer, 1977. **13**: p. 1-60.
46. Glasgow, L.A., *Heat Transfer by Conduction.* Transport Phenomena: An Introduction to Advanced Topics: p. 83-100.
47. Eckert, E.R.G. and R.M. Drake Jr, *Analysis of heat and mass transfer.* 1987.
48. Paul, A. and T. DebRoy, *Free surface flow and heat transfer in conduction mode laser welding.* Metallurgical Transactions B, 1988. **19**(6): p. 851-858.
49. Arpaci, V.S., *Conduction heat transfer.* 1966.
50. Myers, G.E., *Analytical methods in conduction heat transfer.* 1971.
51. Holman, J., *Heat transfer, Eighth SI Metric Edition*. 2001, McGraw-Hill Inc.
52. Holman, J., *Heat transfer, 1986.* Mc Gran–Hill Book Company, Soythern Methodist University, 1986.
53. Natarajan, E., A. Nordin, and A. Rao, *Overview of combustion and gasification of rice husk in fluidized bed reactors.* Biomass and Bioenergy, 1998. **14**(5): p. 533-546.
54. Gel'perin, N., V. Ainshtein, and V. Kvasha, *Principles of Fluidization Technique.* Khimiya, Moscow, 1967.
55. Werther, J., *Fluidized-Bed Reactors*. 1992: Wiley Online Library.
56. Yang, W.-C., *Bubbling fluidized beds.* CHEMICAL INDUSTRIES-NEW YORK-MARCEL DEKKER-, 2003: p. 53-112.
57. Kumar, A., K. Eskridge, D.D. Jones, and M.A. Hanna, *Steam–air fluidized bed gasification of distillers grains: effects of steam to biomass ratio, equivalence ratio and gasification temperature.* Bioresource technology, 2009. **100**(6): p. 2062-2068.
58. Wen, C.-Y. and E.S. Lee, *Coal conversion technology.* NASA STI/Recon Technical Report A, 1979. **79**: p. 53776.
59. Kunii, D. and O. Levenspiel, *Fluidization engineering*. 2013: Elsevier.
60. Basu, P. and L. Cheng, *An analysis of loop seal operations in a circulating fluidized bed.* Chemical Engineering Research and Design, 2000. **78**(7): p. 991-998.
61. Daizo, K. and O. Levenspiel, *Fluidization engineering.* 1991.
62. Carless, J.R. and A. Sheak, *Changes in the particle size distribution during tableting of sulphathiazole powder.* J Pharm Pharmacol, 1976. **28**(1): p. 17-22.
63. Warnecke, R., *Gasification of biomass: comparison of fixed bed and fluidized bed gasifier.* Biomass and Bioenergy, 2000. **18**(6): p. 489-497.
64. Sousa, F.W., A.G. Oliveira, J.P. Ribeiro, M.F. Rosa, D. Keukeleire, and R.F. Nascimento, *Green coconut shells applied as adsorbent for removal of toxic metal ions using fixed-bed column technology.* Journal of environmental management, 2010. **91**(8): p. 1634-1640.
65. Zijerveld, R.C., F. Johnsson, A. Marzocchella, J.C. Schouten, and C.M. van den Bleek, *Fluidization regimes and transitions from fixed bed to dilute transport flow.* Powder Technology, 1998. **95**(3): p. 185-204.
66. Falk, G., F. Herrmann, and G.B. Schmid, *Energy forms or energy carriers.* American Journal of Physics, 1983. **51**(12): p. 1074-1077.

67. Llorente, M.F., R.E. Cuadrado, J.M. Laplaza, and J.C. García, *Combustion in bubbling fluidised bed with bed material of limestone to reduce the biomass ash agglomeration and sintering.* Fuel, 2006. **85**(14): p. 2081-2092.
68. Kaper, W.H. and M.J. Goedhart, *'Forms of Energy', an intermediary language on the road to thermodynamics? Part I.* International Journal of Science Education, 2002. **24**(1): p. 81-95.
69. McAuliffe, C. and D. Merrick, *Coal combustion and conversion technology.* 1984.
70. Jin, Y., J. Zhu, Z. Wang, and Z. Yu, *Fluidization engineering principles.* Beijing, Tsinghua Univ. Pub, 2001.
71. Miles, T.R., T. Miles Jr, L. Baxter, R. Bryers, B. Jenkins, and L. Oden, *Alkali deposits found in biomass power plants: A preliminary investigation of their extent and nature. Volume 1*. 1995, National Renewable Energy Lab., Golden, CO (United States); Miles (Thomas R.), Portland, OR (United States); Sandia National Labs., Livermore, CA (United States); Foster Wheeler Development Corp., Livingston, NJ (United States); California Univ., Davis, CA (United States); Bureau of Mines, Albany, OR (United States). Albany Research Center.
72. Miles, T.R., L.L. Baxter, R.W. Bryers, B.M. Jenkins, and L.L. Oden, *Boiler deposits from firing biomass fuels.* Biomass and Bioenergy, 1996. **10**(2): p. 125-138.
73. Fahmi, R., A. Bridgwater, L. Darvell, J. Jones, N. Yates, S. Thain, and I. Donnison, *The effect of alkali metals on combustion and pyrolysis of Lolium and Festuca grasses, switchgrass and willow.* Fuel, 2007. **86**(10): p. 1560-1569.
74. Ravindranath, N., H. Somashekar, M. Nagaraja, P. Sudha, G. Sangeetha, S. Bhattacharya, and P.A. Salam, *Assessment of sustainable non-plantation biomass resources potential for energy in India.* Biomass and Bioenergy, 2005. **29**(3): p. 178-190.
75. Srirangan, K., L. Akawi, M. Moo-Young, and C.P. Chou, *Towards sustainable production of clean energy carriers from biomass resources.* Applied energy, 2012. **100**: p. 172-186.
76. Long, H., X. Li, H. Wang, and J. Jia, *Biomass resources and their bioenergy potential estimation: a review.* Renewable and Sustainable Energy Reviews, 2013. **26**: p. 344-352.
77. Lewandowski, I., J.M. Scurlock, E. Lindvall, and M. Christou, *The development and current status of perennial rhizomatous grasses as energy crops in the US and Europe.* Biomass and Bioenergy, 2003. **25**(4): p. 335-361.
78. Mullen, C.A. and A.A. Boateng, *Chemical composition of bio-oils produced by fast pyrolysis of two energy crops.* Energy Fuels, 2008. **22**(3): p. 2104-2109.
79. McKendry, P., *Energy production from biomass (part 1): overview of biomass.* Bioresource technology, 2002. **83**(1): p. 37-46.
80. Zhang, J. and K.R. Smith, *Household air pollution from coal and biomass fuels in China: measurements, health impacts, and interventions.* Environmental Health Perspectives, 2007: p. 848-855.
81. Werkelin, J., B.-J. Skrifvars, M. Zevenhoven, B. Holmbom, and M. Hupa, *Chemical forms of ash-forming elements in woody biomass fuels.* Fuel, 2010. **89**(2): p. 481-493.
82. McKendry, P., *Energy production from biomass (part 2): conversion technologies.* Bioresource technology, 2002. **83**(1): p. 47-54.
83. Demirbaş, A., *Biomass resource facilities and biomass conversion processing for fuels and chemicals.* Energy conversion and management, 2001. **42**(11): p. 1357-1378.
84. Sami, M., K. Annamalai, and M. Wooldridge, *Co-firing of coal and biomass fuel blends.* Progress in energy and combustion science, 2001. **27**(2): p. 171-214.
85. Ji, X., Y. Deng, and P. Wang, *Characters of atmosphere pressure, pure oxygen fixed bed gasification of seven kinds coal.* Clean Coal Tech, 2004. **25**(4): p. 50-52.

86. Collot, A.-G., Y. Zhuo, D. Dugwell, and R. Kandiyoti, *Co-pyrolysis and co-gasification of coal and biomass in bench-scale fixed-bed and fluidised bed reactors.* Fuel, 1999. **78**(6): p. 667-679.
87. Saxena, S., *Devolatilization and combustion characteristics of coal particles.* Progress in Energy and Combustion Science, 1990. **16**(1): p. 55-94.
88. Khadse, A., M. Qayyumi, S. Mahajani, and P. Aghalayam, *Underground coal gasification: A new clean coal utilization technique for India.* Energy, 2007. **32**(11): p. 2061-2071.
89. Park, D.K., S.D. Kim, S.H. Lee, and J.G. Lee, *Co-pyrolysis characteristics of sawdust and coal blend in TGA and a fixed bed reactor.* Bioresource technology, 2010. **101**(15): p. 6151-6156.
90. Mishra, S., P. Senapati, and D. Panda, *Rheological behavior of coal-water slurry.* Energy Sources, 2002. **24**(2): p. 159-167.
91. Dhooge, P.M., D.E. Stilwell, and S.M. Park, *Electrochemical studies of coal slurry oxidation mechanisms.* Journal of the Electrochemical Society, 1982. **129**(8): p. 1719-1724.
92. Papachristodoulou, G. and O. Trass, *Coal slurry fuel technology.* The Canadian Journal of Chemical Engineering, 1987. **65**(2): p. 177-201.
93. Logos, C. and Q. Nguyen, *Effect of particle size on the flow properties of a South Australian coal-water slurry.* Powder Technology, 1996. **88**(1): p. 55-58.
94. Roh, N.-S., D.-H. Shin, D.-C. Kim, and J.-D. Kim, *Rheological behaviour of coal-water mixtures. 1. Effects of coal type, loading and particle size.* Fuel, 1995. **74**(8): p. 1220-1225.
95. Norinaga, K., H. Kumagai, J.-i. Hayashi, and T. Chiba, *Classification of water sorbed in coal on the basis of congelation characteristics.* Energy & Fuels, 1998. **12**(3): p. 574-579.
96. Vassilev, S.V. and C.G. Vassileva, *A new approach for the classification of coal fly ashes based on their origin, composition, properties, and behaviour.* Fuel, 2007. **86**(10): p. 1490-1512.
97. Laskowski, J.S., *Coal preparation.* Developments in mineral processing, 2001. **14**: p. 1-8.
98. Yarzab, R.F., P.H. Given, W. Spackman, and A. Davis, *Dependence of coal liquefaction behaviour on coal characteristics. 4. Cluster analyses for characteristics of 104 coals.* Fuel, 1980. **59**(2): p. 81-92.
99. Gale, W.F. and T.C. Totemeier, *Smithells metals reference book*. 2003: Butterworth-Heinemann.
100. Smoot, L.D. and P.J. Smith, *Coal combustion and gasification*. 2013: Springer Science & Business Media.
101. Pratt, D.T., L. Smoot, and D. Pratt, *Pulverized-coal combustion and gasification*. 1979: Springer.
102. Galbreath, K.C. and C.J. Zygarlicke, *Mercury speciation in coal combustion and gasification flue gases.* Environmental science & technology, 1996. **30**(8): p. 2421-2426.
103. Clarke, L.B., *The fate of trace elements during coal combustion and gasification: an overview.* Fuel, 1993. **72**(6): p. 731-736.
104. Radulovic, P.T., M.U. Ghani, and L.D. Smoot, *An improved model for fixed bed coal combustion and gasification.* Fuel, 1995. **74**(4): p. 582-594.
105. Kiga, T., S. Takano, N. Kimura, K. Omata, M. Okawa, T. Mori, and M. Kato, *Characteristics of pulverized-coal combustion in the system of oxygen/recycled flue gas combustion.* Energy Conversion and Management, 1997. **38**: p. S129-S134.
106. Arias, B., C. Pevida, F. Rubiera, and J. Pis, *Effect of biomass blending on coal ignition and burnout during oxy-fuel combustion.* Fuel, 2008. **87**(12): p. 2753-2759.
107. Akgun, F. and R. Essenhigh, *Self-ignition characteristics of coal stockpiles: theoretical prediction from a two-dimensional unsteady-state model.* Fuel, 2001. **80**(3): p. 409-415.
108. Chin, O.C. and K.M. Siddiqui, *Characteristics of some biomass briquettes prepared under modest die pressures.* Biomass and Bioenergy, 2000. **18**(3): p. 223-228.
109. Ndiema, C., P. Manga, and C. Ruttoh, *Influence of die pressure on relaxation characteristics of briquetted biomass.* Energy Conversion and Management, 2002. **43**(16): p. 2157-2161.

110. Singh, R., *Equilibrium moisture content of biomass briquettes.* Biomass and Bioenergy, 2004. **26**(3): p. 251-253.
111. Oladeji, J., *Fuel characterization of briquettes produced from corncob and rice husk resides.* The Pacific Journal of Science and Technology, 2010. **11**(1): p. 101-106.
112. Roy, M.M. and K.W. Corscadden, *An experimental study of combustion and emissions of biomass briquettes in a domestic wood stove.* Applied energy, 2012. **99**: p. 206-212.
113. Demirbaş, A., *Relationships between lignin contents and heating values of biomass.* Energy conversion and management, 2001. **42**(2): p. 183-188.
114. Demirbaş, A., *Calculation of higher heating values of biomass fuels.* Fuel, 1997. **76**(5): p. 431-434.
115. Erol, M., H. Haykiri-Acma, and S. Küçükbayrak, *Calorific value estimation of biomass from their proximate analyses data.* Renewable energy, 2010. **35**(1): p. 170-173.
116. Yin, C.-Y., *Prediction of higher heating values of biomass from proximate and ultimate analyses.* Fuel, 2011. **90**(3): p. 1128-1132.
117. Friedl, A., E. Padouvas, H. Rotter, and K. Varmuza, *Prediction of heating values of biomass fuel from elemental composition.* Analytica Chimica Acta, 2005. **544**(1): p. 191-198.
118. Raveendran, K., A. Ganesh, and K.C. Khilar, *Influence of mineral matter on biomass pyrolysis characteristics.* Fuel, 1995. **74**(12): p. 1812-1822.
119. Uddin, M.A., H. Tsuda, S. Wu, and E. Sasaoka, *Catalytic decomposition of biomass tars with iron oxide catalysts.* Fuel, 2008. **87**(4): p. 451-459.
120. Kirubakaran, V., V. Sivaramakrishnan, R. Nalini, T. Sekar, M. Premalatha, and P. Subramanian, *A review on gasification of biomass.* Renewable and Sustainable Energy Reviews, 2009. **13**(1): p. 179-186.
121. Demirbas, A., *Relationships between heating value and lignin, moisture, ash and extractive contents of biomass fuels.* Energy exploration & exploitation, 2002. **20**(1): p. 105-111.
122. Sheng, C. and J. Azevedo, *Estimating the higher heating value of biomass fuels from basic analysis data.* Biomass and Bioenergy, 2005. **28**(5): p. 499-507.
123. Senneca, O., P. Salatino, and S. Masi, *The influence of char surface oxidation on thermal annealing and loss of combustion reactivity.* Proceedings of the Combustion Institute, 2005. **30**(2): p. 2223-2230.
124. Senneca, O., R. Chirone, and P. Salatino, *Oxidative pyrolysis of solid fuels.* Journal of analytical and applied pyrolysis, 2004. **71**(2): p. 959-970.
125. Öhman, M., A. Nordin, B.-J. Skrifvars, R. Backman, and M. Hupa, *Bed agglomeration characteristics during fluidized bed combustion of biomass fuels.* Energy & Fuels, 2000. **14**(1): p. 169-178.
126. Jinapong, N., M. Suphantharika, and P. Jamnong, *Production of instant soymilk powders by ultrafiltration, spray drying and fluidized bed agglomeration.* Journal of Food Engineering, 2008. **84**(2): p. 194-205.
127. Natarajan, E., M. Öhman, M. Gabra, A. Nordin, T. Liliedahl, and A. Rao, *Experimental determination of bed agglomeration tendencies of some common agricultural residues in fluidized bed combustion and gasification.* Biomass and Bioenergy, 1998. **15**(2): p. 163-169.
128. Pérez-Lombard, L., J. Ortiz, and C. Pout, *A review on buildings energy consumption information.* Energy and buildings, 2008. **40**(3): p. 394-398.
129. Nutalapati, D., R. Gupta, B. Moghtaderi, and T. Wall, *Assessing slagging and fouling during biomass combustion: A thermodynamic approach allowing for alkali/ash reactions.* Fuel processing technology, 2007. **88**(11): p. 1044-1052.

130. Obernberger, I., F. Biedermann, W. Widmann, and R. Riedl, *Concentrations of inorganic elements in biomass fuels and recovery in the different ash fractions.* Biomass and Bioenergy, 1997. **12**(3): p. 211-224.
131. Lin, C.-L., M.-Y. Wey, and C.-Y. Lu, *Prediction of defluidization time of alkali composition at various operating conditions during incineration.* Powder Technology, 2006. **161**(2): p. 150-157.
132. Bale, C., E. Bélisle, P. Chartrand, S. Decterov, G. Eriksson, K. Hack, I.-H. Jung, Y.-B. Kang, J. Melançon, and A. Pelton, *FactSage thermochemical software and databases—recent developments.* Calphad, 2009. **33**(2): p. 295-311.
133. Naik, S., V.V. Goud, P.K. Rout, K. Jacobson, and A.K. Dalai, *Characterization of Canadian biomass for alternative renewable biofuel.* Renewable energy, 2010. **35**(8): p. 1624-1631.
134. Lundholm, K., A. Nordin, M. Öhman, and D. Boström, *Reduced bed agglomeration by co-combustion biomass with peat fuels in a fluidized bed.* Energy & Fuels, 2005. **19**(6): p. 2273-2278.
135. Mettanant, V., P. Basu, and J. Butler, *Agglomeration of biomass fired fluidized bed gasifier and combustor.* The Canadian Journal of Chemical Engineering, 2009. **87**(5): p. 656-684.
136. Paisley, M.A., *Biomass gasification system and method*. 2004, Google Patents.
137. Timofeeva, E.V., A.N. Gavrilov, J.M. McCloskey, Y.V. Tolmachev, S. Sprunt, L.M. Lopatina, and J.V. Selinger, *Thermal conductivity and particle agglomeration in alumina nanofluids: experiment and theory.* Physical Review E, 2007. **76**(6): p. 061203.
138. Skrifvars, B.-J., M. Öhman, A. Nordin, and M. Hupa, *Predicting bed agglomeration tendencies for biomass fuels fired in FBC boilers: a comparison of three different prediction methods.* Energy & Fuels, 1999. **13**(2): p. 359-363.
139. Marchal, P., R. David, J. Klein, and J. Villermaux, *Crystallization and precipitation engineering—I. An efficient method for solving population balance in crystallization with agglomeration.* Chemical Engineering Science, 1988. **43**(1): p. 59-67.
140. van Eyk, P.J., A. Kosminski, and P.J. Ashman, *Control of agglomeration and defluidization during fluidized-bed combustion of south Australian low-rank coals.* Energy & Fuels, 2011. **26**(1): p. 118-129.
141. Armesto, L., A. Bahillo, K. Veijonen, A. Cabanillas, and J. Otero, *Combustion behaviour of rice husk in a bubbling fluidised bed.* Biomass and Bioenergy, 2002. **23**(3): p. 171-179.
142. Dunne, D. and J. Agnew, *Thermal upgrading of low-grade, low-rank South Australia coal.* Energy Sources, 1992. **14**(2): p. 169-181.
143. Mullinger, P., *Overcoming Barriers to the Utilisation of South Australian Low Rank Coals.* Chemeca 2010: Engineering at the Edge; 26-29 September 2010, Hilton Adelaide, South Australia, 2010: p. 389.
144. Manzoori, A.R. and P.K. Agarwal, *The fate of organically bound inorganic elements and sodium chloride during fluidized bed combustion of high sodium, high sulphur low rank coals.* Fuel, 1992. **71**(5): p. 513-522.
145. Bartels, M., W. Lin, J. Nijenhuis, F. Kapteijn, and J.R. van Ommen, *Agglomeration in fluidized beds at high temperatures: Mechanisms, detection and prevention.* Progress in energy and combustion science, 2008. **34**(5): p. 633-666.
146. McCullough, D.P., P.J. van Eyk, P.J. Ashman, and P.J. Mullinger, *Investigation of agglomeration and defluidization during spouted-bed gasification of high-sodium, high-sulfur South Australian lignite.* Energy & Fuels, 2011. **25**(7): p. 2772-2781.
147. Müller, M., K.-J. Wolf, A. Smeda, and K. Hilpert, *Release of K, Cl, and S species during co-combustion of coal and straw.* Energy & Fuels, 2006. **20**(4): p. 1444-1449.

148. Vuthaluru, H.B. and D.-k. Zhang, *Effect of Ca-and Mg-bearing minerals on particle agglomeration defluidisation during fluidised-bed combustion of a South Australian lignite.* Fuel processing technology, 2001. **69**(1): p. 13-27.
149. Manzoori, A.R. and P.K. Agarwal, *Agglomeration and defluidization under simulated circulating fluidized-bed combustion conditions.* Fuel, 1994. **73**(4): p. 563-568.
150. Andreae, M.O. and P. Merlet, *Emission of trace gases and aerosols from biomass burning.* Global biogeochemical cycles, 2001. **15**(4): p. 955-966.
151. Nussbaumer, T., *Combustion and co-combustion of biomass: fundamentals, technologies, and primary measures for emission reduction.* Energy & Fuels, 2003. **17**(6): p. 1510-1521.
152. Spliethoff, H. and K. Hein, *Effect of co-combustion of biomass on emissions in pulverized fuel furnaces.* Fuel processing technology, 1998. **54**(1): p. 189-205.
153. Permchart, W. and V.I. Kouprianov, *Emission performance and combustion efficiency of a conical fluidized-bed combustor firing various biomass fuels.* Bioresource technology, 2004. **92**(1): p. 83-91.
154. Lv, P., Z. Xiong, J. Chang, C. Wu, Y. Chen, and J. Zhu, *An experimental study on biomass air–steam gasification in a fluidized bed.* Bioresource technology, 2004. **95**(1): p. 95-101.
155. Narvaez, I., A. Orio, M.P. Aznar, and J. Corella, *Biomass gasification with air in an atmospheric bubbling fluidized bed. Effect of six operational variables on the quality of the produced raw gas.* Industrial & Engineering Chemistry Research, 1996. **35**(7): p. 2110-2120.
156. Hughes, R.W., D.Y. Lu, E.J. Anthony, and A. Macchi, *Design, process simulation and construction of an atmospheric dual fluidized bed combustion system for in situ CO 2 capture using high-temperature sorbents.* Fuel processing technology, 2005. **86**(14): p. 1523-1531.
157. Miller, J.A. and P. Glarborg, *Modeling the thermal De-NOx process: Closing in on a final solution.* International Journal of Chemical Kinetics, 1999. **31**(11): p. 757-765.
158. Mahmoudi, S., J. Baeyens, and J.P. Seville, *NOx formation and selective non-catalytic reduction (SNCR) in a fluidized bed combustor of biomass.* Biomass and Bioenergy, 2010. **34**(9): p. 1393-1409.
159. Joshi, N.D. and F.E. Moreno, *Staged low NOx premix gas turbine combustor*. 1990, Google Patents.
160. Kicherer, A., H. Spliethoff, H. Maier, and K. Hein, *The effect of different reburning fuels on NOx-reduction.* Fuel, 1994. **73**(9): p. 1443-1446.
161. Llorente, M.F. and J.C. García, *Comparing methods for predicting the sintering of biomass ash in combustion.* Fuel, 2005. **84**(14): p. 1893-1900.
162. Steenari, B.-M., A. Lundberg, H. Pettersson, M. Wilewska-Bien, and D. Andersson, *Investigation of ash sintering during combustion of agricultural residues and the effect of additives.* Energy & Fuels, 2009. **23**(11): p. 5655-5662.
163. Parikh, J., S. Channiwala, and G. Ghosal, *A correlation for calculating HHV from proximate analysis of solid fuels.* Fuel, 2005. **84**(5): p. 487-494.
164. Scala, F. and R. Chirone, *An SEM/EDX study of bed agglomerates formed during fluidized bed combustion of three biomass fuels.* Biomass and Bioenergy, 2008. **32**(3): p. 252-266.
165. Scala, F. and R. Chirone, *Fluidized bed combustion of alternative solid fuels.* Experimental Thermal and Fluid Science, 2004. **28**(7): p. 691-699.
166. Lin, C.-L. and M.-Y. Wey, *The effect of mineral compositions of waste and operating conditions on particle agglomeration/defluidization during incineration.* Fuel, 2004. **83**(17): p. 2335-2343.
167. Grimm, A., N. Skoglund, D. Boström, C. Boman, and M. Öhman, *Influence of phosphorus on alkali distribution during combustion of logging residues and wheat straw in a bench-scale fluidized bed.* Energy & Fuels, 2012. **26**(5): p. 3012-3023.

168. Öhman, M. and A. Nordin, *A new method for quantification of fluidized bed agglomeration tendencies: a sensitivity analysis.* Energy & Fuels, 1998. **12**(1): p. 90-94.
169. Pronobis, M., *Evaluation of the influence of biomass co-combustion on boiler furnace slagging by means of fusibility correlations.* Biomass and Bioenergy, 2005. **28**(4): p. 375-383.
170. Bryers, R.W., *Fireside slagging, fouling, and high-temperature corrosion of heat-transfer surface due to impurities in steam-raising fuels.* Progress in Energy and Combustion Science, 1996. **22**(1): p. 29-120.
171. Masiá, A.T., B. Buhre, R. Gupta, and T. Wall, *Characterising ash of biomass and waste.* Fuel processing technology, 2007. **88**(11): p. 1071-1081.
172. Stelte, W., J.K. Holm, A.R. Sanadi, S. Barsberg, J. Ahrenfeldt, and U.B. Henriksen, *A study of bonding and failure mechanisms in fuel pellets from different biomass resources.* Biomass and Bioenergy, 2011. **35**(2): p. 910-918.
173. Duku, M.H., S. Gu, and E.B. Hagan, *A comprehensive review of biomass resources and biofuels potential in Ghana.* Renewable and Sustainable Energy Reviews, 2011. **15**(1): p. 404-415.
174. Tinaut, F.V., A. Melgar, J.F. Perez, and A. Horrillo, *Effect of biomass particle size and air superficial velocity on the gasification process in a downdraft fixed bed gasifier. An experimental and modelling study.* Fuel processing technology, 2008. **89**(11): p. 1076-1089.
175. Liu, H., Y. Feng, S. Wu, and D. Liu, *The role of ash particles in the bed agglomeration during the fluidized bed combustion of rice straw.* Bioresource technology, 2009. **100**(24): p. 6505-6513.
176. Nicolis, G. and I. Prigogine, *Self-organization in nonequilibrium systems*. Vol. 191977. 1977: Wiley, New York.
177. Gardiner, W.C., *Rates and mechanisms of chemical reactions.* 1969.
178. Dunning Jr, T.H., L.B. Harding, R.A. Bair, R.A. Eades, and R.L. Shepard, *Theoretical studies of the energetics and mechanisms of chemical reactions: abstraction reactions.* The Journal of Physical Chemistry, 1986. **90**(3): p. 344-356.
179. Espenson, J.H., *Chemical kinetics and reaction mechanisms*. 1981: McGraw-Hill.
180. Minyaev, R., *GRADIENT LINES ON THE MULTIDIMENSIONAL POTENTIAL-ENERGY SURFACES AND MECHANISMS OF CHEMICAL-REACTIONS.* USPEKHI KHIMII, 1994. **63**(11): p. 939-961.
181. Steenari, B.-M. and O. Lindqvist, *High-temperature reactions of straw ash and the anti-sintering additives kaolin and dolomite.* Biomass and Bioenergy, 1998. **14**(1): p. 67-76.
182. Bahng, M.-K., C. Mukarakate, D.J. Robichaud, and M.R. Nimlos, *Current technologies for analysis of biomass thermochemical processing: a review.* Analytica Chimica Acta, 2009. **651**(2): p. 117-138.
183. Raask, E., *Tube erosion by ash impaction.* Wear, 1969. **13**(4): p. 301-315.
184. Schure, M.R., M.N. Myers, K.D. Caldwell, C. Byron, K.P. Chan, and J.C. Giddings, *Separation of coal fly ash using continuous steric field-flow fractionation.* Environmental science & technology, 1985. **19**(8): p. 686-689.
185. Burtscher, H., U. Baltensperger, N. Bukowiecki, P. Cohn, C. Hüglin, M. Mohr, U. Matter, S. Nyeki, V. Schmatloch, and N. Streit, *Separation of volatile and non-volatile aerosol fractions by thermodesorption: instrumental development and applications.* Journal of Aerosol Science, 2001. **32**(4): p. 427-442.
186. Clément, B. and R. Zeyen. *The Phebus fission product and source term international programmes*. in *International Conference New Energy for New Europe, Bled, Slovenia*. 2005.
187. Piotrowska, P., A. Grimm, N. Skoglund, C. Boman, M. Öhman, M. Zevenhoven, D. Boström, and M. Hupa, *Fluidized-bed combustion of mixtures of rapeseed cake and bark: The resulting bed agglomeration characteristics.* Energy & Fuels, 2012. **26**(4): p. 2028-2037.

188. Huang, Y., D. McIlveen-Wright, S. Rezvani, Y. Wang, N. Hewitt, and B. Williams, *Biomass co-firing in a pressurized fluidized bed combustion (PFBC) combined cycle power plant: a techno-environmental assessment based on computational simulations.* Fuel processing technology, 2006. **87**(10): p. 927-934.
189. Baker, H. and H. Okamoto, *Alloy phase diagrams.* ASM International, ASM Handbook., 1992. **3**: p. 501.
190. Boström, D., N. Skoglund, A. Grimm, C. Boman, M. Ohman, M. Broström, and R. Backman, *Ash transformation chemistry during combustion of biomass.* Energy & Fuels, 2011. **26**(1): p. 85-93.
191. De Boer, F.R., W. Mattens, R. Boom, A. Miedema, and A. Niessen, *Cohesion in metals.* 1988.
192. Zhanmin, C., S. Xiaoyan, and Q. Zhiyu, *Thermodynamic Modeling Software FactSage and Its Application [J].* Chinese Journal of Rare Metals, 2008. **2**: p. 021.
193. Hanxu, L., N. Yoshihiko, D. Zhongbing, and M. ZHANG, *Application of the FactSage to predict the ash melting behavior in reducing conditions.* Chinese Journal of Chemical Engineering, 2006. **14**(6): p. 784-789.
194. Gheribi, A., C. Audet, S. Le Digabel, E. Bélisle, C. Bale, and A. Pelton, *Calculating optimal conditions for alloy and process design using thermodynamic and property databases, the FactSage software and the Mesh Adaptive Direct Search algorithm.* Calphad, 2012. **36**: p. 135-143.
195. Petzow, G. and G. Effenberg, *Ternary alloys. A comprehensive compendium of evaluated constitutional data and phase diagrams. Vol. 4.* 1991.
196. Nayeb-Hashemi, A., *Phase diagrams of binary magnesium alloys.* ASM International, Metals Park, Ohio 44073, USA, 1988. 370, 1988.
197. Grimm, A., M. Öhman, T.s. Lindberg, A. Fredriksson, and D. Boström, *Bed agglomeration characteristics in fluidized-bed combustion of biomass fuels using olivine as bed material.* Energy & Fuels, 2012. **26**(7): p. 4550-4559.
198. Luyben, W.L., *Process modeling, simulation and control for chemical engineers*. 1989: McGraw-Hill Higher Education.
199. Thoma, J. and B.O. Bouamama, *Modelling and simulation in thermal and chemical engineering: A bond graph approach*. 2013: Springer Science & Business Media.
200. Iwata, K., M. Onosato, K. Teramoto, and S. Osaki, *A modelling and simulation architecture for virtual manufacturing systems.* CIRP Annals-Manufacturing Technology, 1995. **44**(1): p. 399-402.
201. Oh, M. and C.C. Pantelides, *A modelling and simulation language for combined lumped and distributed parameter systems.* Computers & Chemical Engineering, 1996. **20**(6): p. 611-633.
202. Öhman, M. and A. Nordin, *The role of kaolin in prevention of bed agglomeration during fluidized bed combustion of biomass fuels.* Energy & Fuels, 2000. **14**(3): p. 618-624.
203. Öhman, M., L. Pommer, and A. Nordin, *Bed agglomeration characteristics and mechanisms during gasification and combustion of biomass fuels.* Energy & Fuels, 2005. **19**(4): p. 1742-1748.
204. Boman, C., A. Nordin, D. Boström, and M. Öhman, *Characterization of inorganic particulate matter from residential combustion of pelletized biomass fuels.* Energy & Fuels, 2004. **18**(2): p. 338-348.
205. Öhman, M., D. Boström, A. Nordin, and H. Hedman, *Effect of kaolin and limestone addition on slag formation during combustion of wood fuels.* Energy & Fuels, 2004. **18**(5): p. 1370-1376.
206. Wang, L., J.E. Hustad, Ø. Skreiberg, G. Skjevrak, and M. Grønli, *A critical review on additives to reduce ash related operation problems in biomass combustion applications.* Energy Procedia, 2012. **20**: p. 20-29.
207. Vamvuka, D., D. Zografos, and G. Alevizos, *Control methods for mitigating biomass ash-related problems in fluidized beds.* Bioresource technology, 2008. **99**(9): p. 3534-3544.

208. Fitzpatrick, E., K. Bartle, M.L. Kubacki, J. Jones, M. Pourkashanian, A. Ross, A. Williams, and K. Kubica, *The mechanism of the formation of soot and other pollutants during the co-firing of coal and pine wood in a fixed bed combustor.* Fuel, 2009. **88**(12): p. 2409-2417.
209. Dai, J., S. Sokhansanj, J.R. Grace, X. Bi, C.J. Lim, and S. Melin, *Overview and some issues related to co-firing biomass and coal.* The Canadian Journal of Chemical Engineering, 2008. **86**(3): p. 367-386.
210. Tsai, M.-Y., K.-T. Wu, C.-C. Huang, and H.-T. Lee, *Co-firing of paper mill sludge and coal in an industrial circulating fluidized bed boiler.* Waste Management, 2002. **22**(4): p. 439-442.
211. Wang, C., F. Wang, Q. Yang, and R. Liang, *Thermogravimetric studies of the behavior of wheat straw with added coal during combustion.* Biomass and Bioenergy, 2009. **33**(1): p. 50-56.
212. Vuthaluru, H., *Thermal behaviour of coal/biomass blends during co-pyrolysis.* Fuel processing technology, 2004. **85**(2): p. 141-155.
213. Simoneit, B.R., *Biomass burning—a review of organic tracers for smoke from incomplete combustion.* Applied Geochemistry, 2002. **17**(3): p. 129-162.
214. Wei, X., U. Schnell, and K.R. Hein, *Behaviour of gaseous chlorine and alkali metals during biomass thermal utilisation.* Fuel, 2005. **84**(7): p. 841-848.
215. Minkova, V., M. Razvigorova, M. Goranova, L. Ljutzkanov, and G. Angelova, *Effect of water vapour on the pyrolysis of solid fuels: 1. Effect of water vapour during the pyrolysis of solid fuels on the yield and composition of the liquid products.* Fuel, 1991. **70**(6): p. 713-719.
216. Azargohar, R., S. Nanda, J.A. Kozinski, A.K. Dalai, and R. Sutarto, *Effects of temperature on the physicochemical characteristics of fast pyrolysis bio-chars derived from Canadian waste biomass.* Fuel, 2014. **125**: p. 90-100.
217. Saastamoinen, J. and J.-R. Richard, *Simultaneous drying and pyrolysis of solid fuel particles.* Combustion and Flame, 1996. **106**(3): p. 288-300.
218. Brodowski, S., W. Amelung, L. Haumaier, C. Abetz, and W. Zech, *Morphological and chemical properties of black carbon in physical soil fractions as revealed by scanning electron microscopy and energy-dispersive X-ray spectroscopy.* Geoderma, 2005. **128**(1): p. 116-129.
219. d'Alfonso, A., B. Freitag, D. Klenov, and L. Allen, *Atomic-resolution chemical mapping using energy-dispersive x-ray spectroscopy.* Physical Review B, 2010. **81**(10): p. 100101.
220. Eggins, S., L. Kinsley, and J. Shelley, *Deposition and element fractionation processes during atmospheric pressure laser sampling for analysis by ICP-MS.* Applied Surface Science, 1998. **127**: p. 278-286.
221. Baxter, L.L., T.R. Miles, B.M. Jenkins, T. Milne, D. Dayton, R.W. Bryers, and L.L. Oden, *The behavior of inorganic material in biomass-fired power boilers: field and laboratory experiences.* Fuel processing technology, 1998. **54**(1): p. 47-78.
222. Hentschel, K., *Mapping the spectrum.* Astrophysics and Space Science, 2003. **284**(3): p. 1111-1112.
223. Merkus, H.G., *Particle size measurements: fundamentals, practice, quality*. Vol. 17. 2009: Springer Science & Business Media.
224. Iinuma, Y., E. Brüggemann, T. Gnauk, K. Müller, M. Andreae, G. Helas, R. Parmar, and H. Herrmann, *Source characterization of biomass burning particles: The combustion of selected European conifers, African hardwood, savanna grass, and German and Indonesian peat.* Journal of Geophysical Research: Atmospheres, 2007. **112**(D8).
225. Viana, H., D. Vega-Nieva, L.O. Torres, J. Lousada, and J. Aranha, *Fuel characterization and biomass combustion properties of selected native woody shrub species from central Portugal and NW Spain.* Fuel, 2012. **102**: p. 737-745.

226. Obernberger, I. and G. Thek, *Physical characterisation and chemical composition of densified biomass fuels with regard to their combustion behaviour.* Biomass and Bioenergy, 2004. **27**(6): p. 653-669.
227. Mendelssohn, I.A. and M.T. Postek, *Elemental analysis of deposits on the roots of Spartina alterniflora Loisel.* American Journal of Botany, 1982: p. 904-912.
228. Mani, S., L.G. Tabil, and S. Sokhansanj, *Effects of compressive force, particle size and moisture content on mechanical properties of biomass pellets from grasses.* Biomass and Bioenergy, 2006. **30**(7): p. 648-654.
229. Lu, H., E. Ip, J. Scott, P. Foster, M. Vickers, and L.L. Baxter, *Effects of particle shape and size on devolatilization of biomass particle.* Fuel, 2010. **89**(5): p. 1156-1168.
230. Zhang, Y., B. Jin, and W. Zhong, *Experimental investigation on mixing and segregation behavior of biomass particle in fluidized bed.* Chemical Engineering and Processing: Process Intensification, 2009. **48**(3): p. 745-754.
231. Phanphanich, M. and S. Mani, *Impact of torrefaction on the grindability and fuel characteristics of forest biomass.* Bioresource technology, 2011. **102**(2): p. 1246-1253.
232. Riano, D., E. Chuvieco, S. Condés, J. González-Matesanz, and S.L. Ustin, *Generation of crown bulk density for Pinus sylvestris L. from lidar.* Remote Sensing of Environment, 2004. **92**(3): p. 345-352.
233. Kaliyan, N., R.V. Morey, M.D. White, and D.G. Tiffany. *A tub-grinding/roll-press compaction system to increase biomass bulk density: preliminary study*. in *2009 Reno, Nevada, June 21-June 24, 2009*. 2009: American Society of Agricultural and Biological Engineers.
234. Miller, B.B., D.R. Dugwell, and R. Kandiyoti, *Partitioning of trace elements during the combustion of coal and biomass in a suspension-firing reactor.* Fuel, 2002. **81**(2): p. 159-171.
235. Varol, M., A. Atimtay, B. Bay, and H. Olgun, *Investigation of co-combustion characteristics of low quality lignite coals and biomass with thermogravimetric analysis.* Thermochimica Acta, 2010. **510**(1): p. 195-201.
236. Tillman, D.A., *Biomass cofiring: the technology, the experience, the combustion consequences.* Biomass and Bioenergy, 2000. **19**(6): p. 365-384.
237. Pérez-Ramírez, J. and S. Abelló, *Thermal decomposition of hydrotalcite-like compounds studied by a novel tapered element oscillating microbalance (TEOM): Comparison with TGA and DTA.* Thermochimica Acta, 2006. **444**(1): p. 75-82.
238. Fahmi, R., A.V. Bridgwater, I. Donnison, N. Yates, and J. Jones, *The effect of lignin and inorganic species in biomass on pyrolysis oil yields, quality and stability.* Fuel, 2008. **87**(7): p. 1230-1240.
239. Parikh, J., S. Channiwala, and G. Ghosal, *Product distribution from woody biomass in a bench-scale pyrolyzer.* Gas, 2003. **4**(7): p. 8.
240. Bale, C., P. Chartrand, S. Degterov, G. Eriksson, K. Hack, R.B. Mahfoud, J. Melançon, A. Pelton, and S. Petersen, *FactSage thermochemical software and databases.* Calphad, 2002. **26**(2): p. 189-228.
241. Kubaschewski, O., *Iron—Binary phase diagrams*. 2013: Springer Science & Business Media.
242. Porter, D.A., K.E. Easterling, and M. Sherif, *Phase Transformations in Metals and Alloys, (Revised Reprint)*. 2009: CRC press.
243. Wang, D., H. Tan, and Y. Li, *Multiple maxima of GFA in three adjacent eutectics in Zr–Cu–Al alloy system–A metallographic way to pinpoint the best glass forming alloys.* Acta Materialia, 2005. **53**(10): p. 2969-2979.
244. Yi, S., E. Park, J. Ok, W. Kim, and D. Kim, *(Icosahedral phase+ α-Mg) two phase microstructures in the Mg–Zn–Y ternary system.* Materials Science and Engineering: A, 2001. **300**(1): p. 312-315.

245. Lin, C.-L., T.-H. Peng, and W.-J. Wang, *Effect of particle size distribution on agglomeration/defluidization during fluidized bed combustion.* Powder Technology, 2011. **207**(1): p. 290-295.
246. Yaverbaum, L., *Fluidized bed combustion of coal and waste materials.* 1977.
247. Wang, L., G. Skjevrak, J.E. Hustad, and Ø. Skreiberg, *Investigation of biomass ash sintering characteristics and the effect of additives.* Energy & Fuels, 2013. **28**(1): p. 208-218.

9 Appendix

Appendix A: Comprehensive data of the SEM and EDX examinations of the samples (Agglomerates)

Appendix A1: Comprehensive data of the SEM and EDX examinations of the mixture of KOH + silica sand samples at 350 ^{0}C.

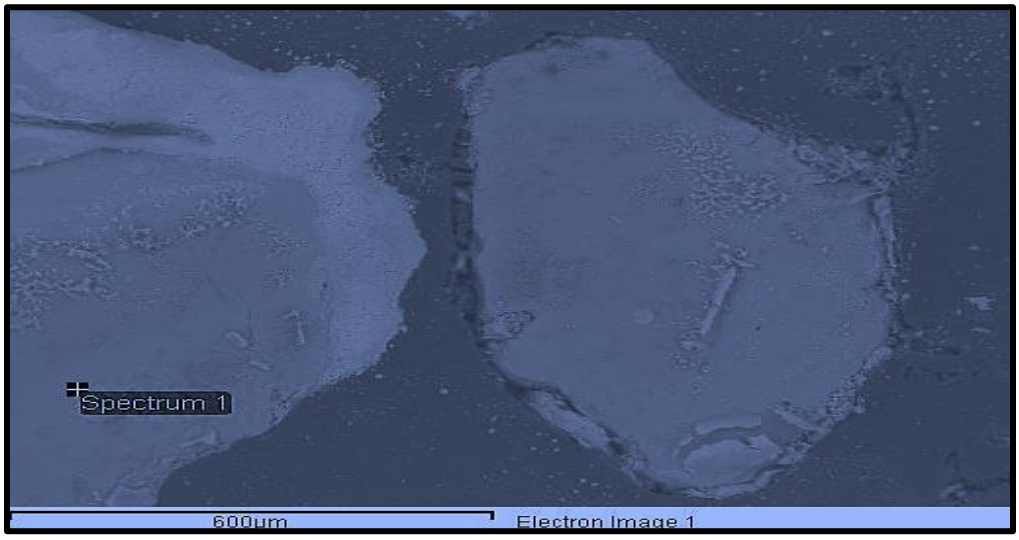

Figure 9-1 EDX spot analysis of the mixture of KOH + Silica Sand sample at 350 ^{0}C (spectrum 1)

Spectrum processing:
No peaks omitted
Processing option: All elements analysed
Number of iterations = 5
C CaCO3 1-Jun-1999 12:00 AM
O SiO2 1-Jun-1999 12:00 AM
Si SiO2 1-Jun-1999 12:00 AM
K MAD-10 Feldspar 1-Jun-1999 12:00 AM

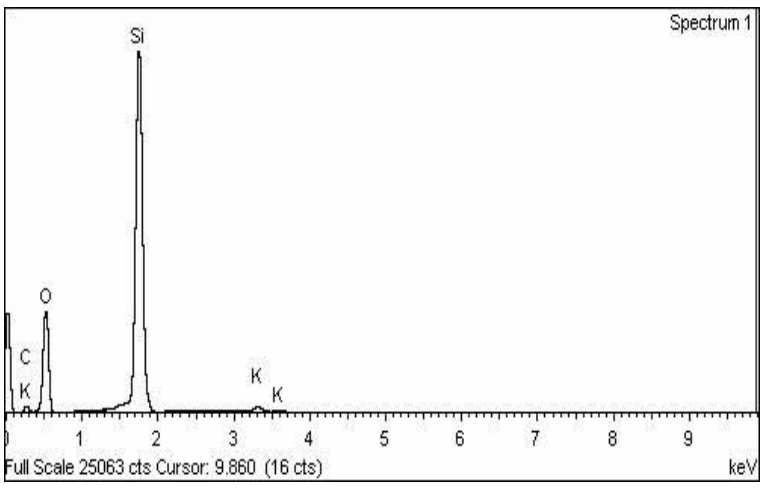

Element	Weight%	Atomic%
C K	22.23	16.84
O K	100.88	57.38
Si K	78.26	25.36
K	1.80	0.42
Totals	203.17	

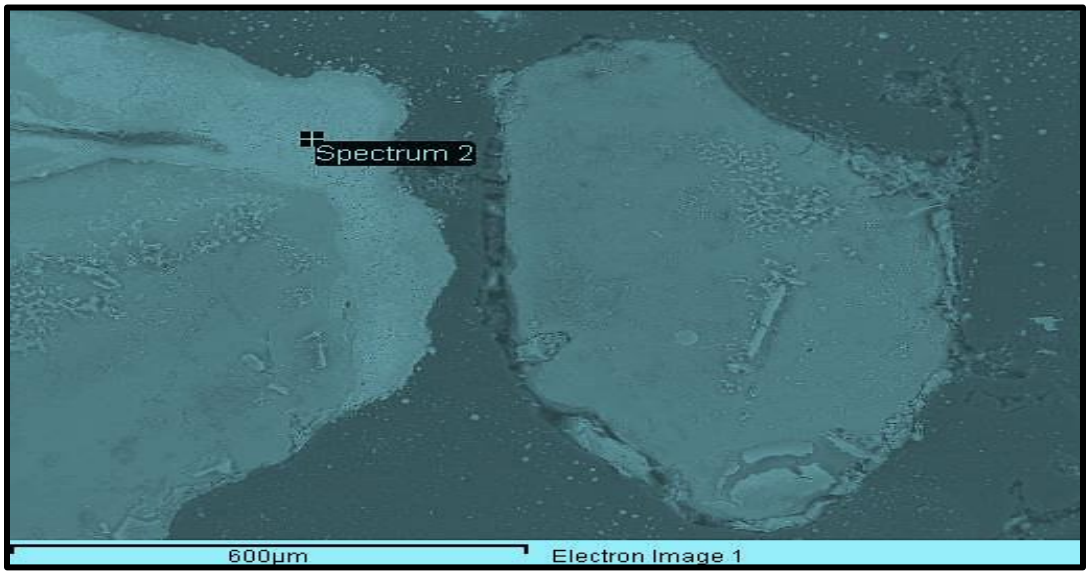

Figure 9-2 EDX spot analysis of the mixture of KOH + Silica Sand sample at 350 ^{0}C (spectrum 2)

Spectrum processing:
No peaks omitted
Processing option: All elements analysed
Number of iterations = 3
Standard:
C CaCO3 1-Jun-1999 12:00 AM
O SiO2 1-Jun-1999 12:00 AM
Si SiO2 1-Jun-1999 12:00 AM
K MAD-10 Feldspar 1-Jun-1999 12:00 AM
Fe Fe 1-Jun-1999 12:00 AM

Element	Weight%	Atomic%
C K	5.12	17.90
O K	7.19	18.88
Si K	12.46	18.64
K K	41.07	44.13
Fe K	0.61	0.46
Totals	66.44	

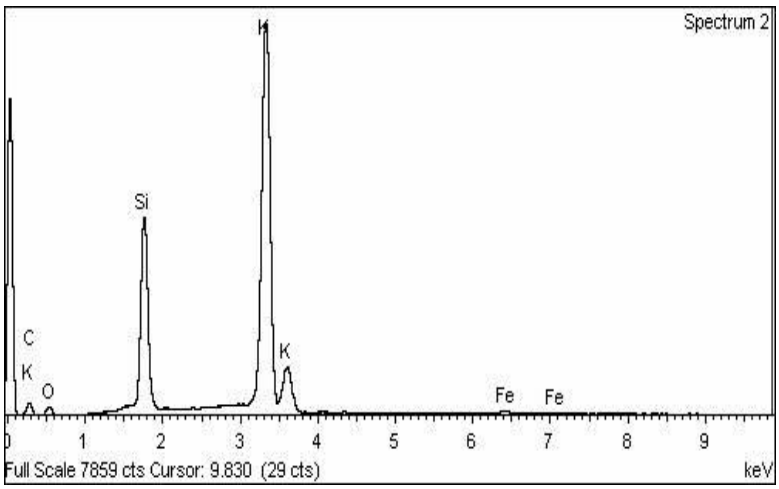

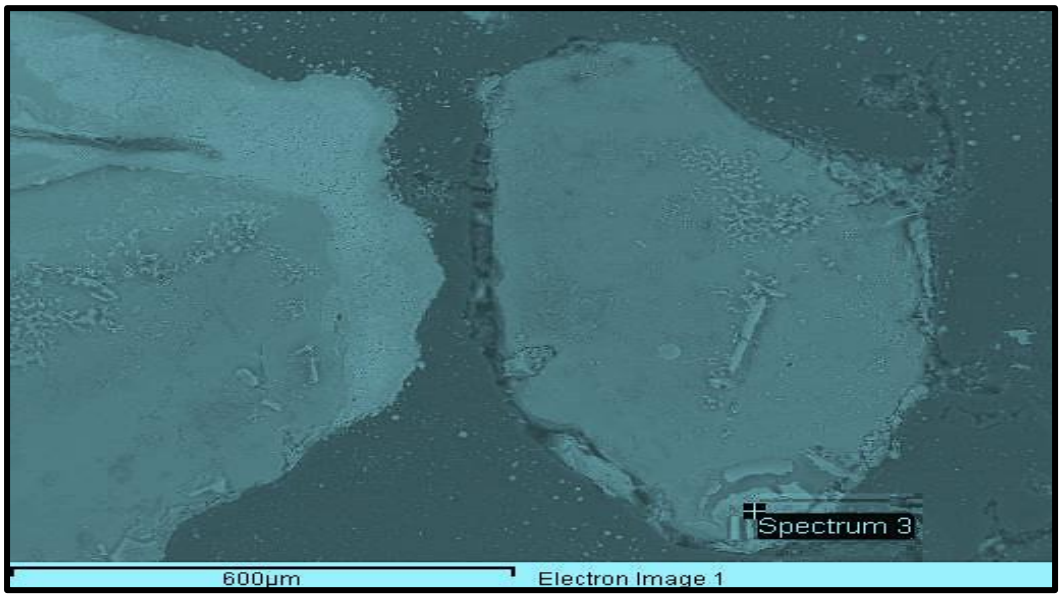

Figure 9-3 EDX spot analysis of the mixture of KOH + Silica Sand sample at 350 ^{0}C (spectrum 3)

Spectrum processing:
No peaks omitted
Processing option: All elements analysed
Number of iterations = 6
C CaCO3 1-Jun-1999 12:00 AM
O SiO2 1-Jun-1999 12:00 AM
Si SiO2 1-Jun-1999 12:00 AM
K MAD-10 Feldspar 1-Jun-1999 12:00 AM
Ca Wollastonite 1-Jun-1999 12:00 AM
Fe Fe 1-Jun-1999 12:00 AM

Element	Weight%	Atomic%
C K	66.60	45.41
O K	71.52	36.61
Si K	50.90	14.84
K K	13.74	2.88
Ca K	0.88	0.18
Fe K	0.62	0.09
Totals	204.26	

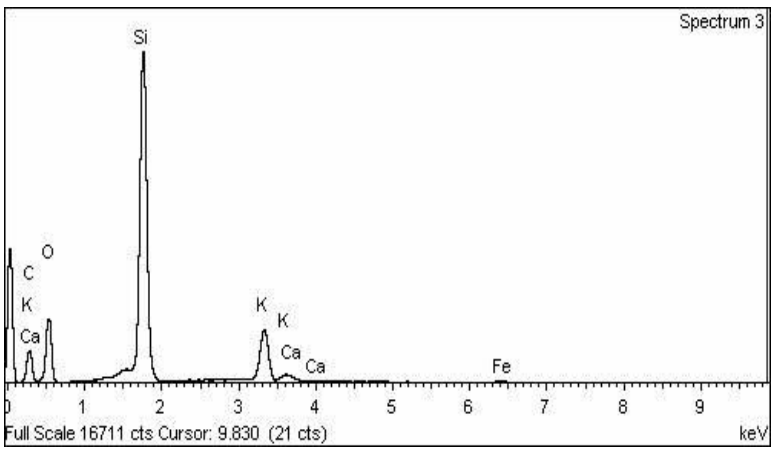

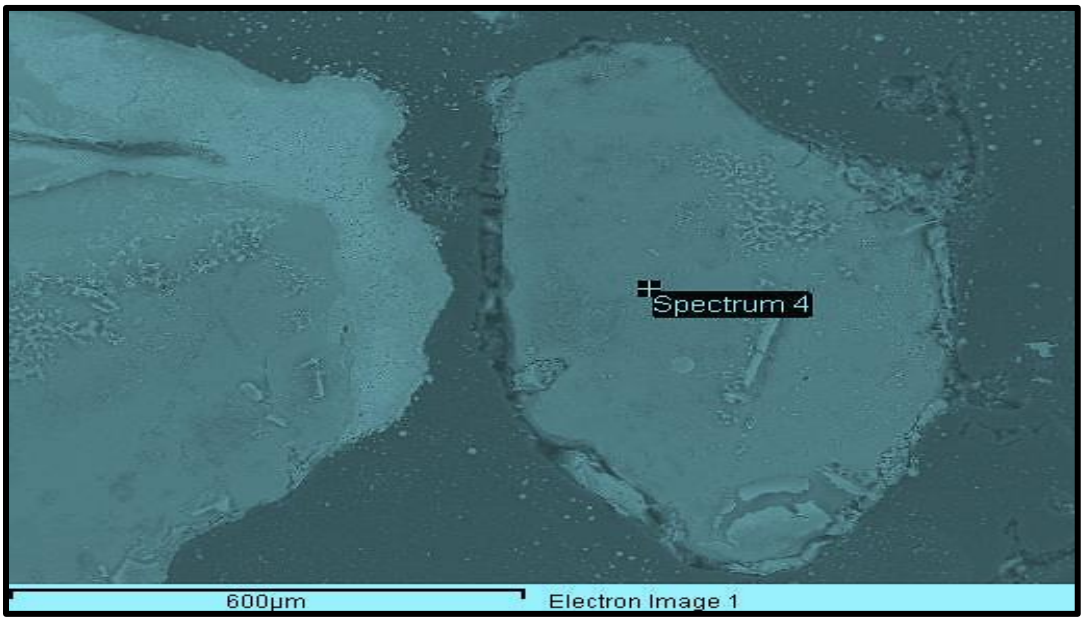

Figure 9-4 EDX spot analysis of the mixture of KOH + Silica Sand sample at 350 ^{0}C (spectrum 4)

Spectrum processing:
No peaks omitted

Processing option: All elements analysed
Number of iterations = 5

Standard:
C CaCO3 1-Jun-1999 12:00 AM
O SiO2 1-Jun-1999 12:00 AM
Si SiO2 1-Jun-1999 12:00 AM
K MAD-10 Feldspar 1-Jun-1999 12:00 AM

Element	Weight%	Atomic%
C K	86.58	50.18
O K	71.38	31.06
Si K	72.87	18.06
K K	3.92	0.70
Totals	234.75	

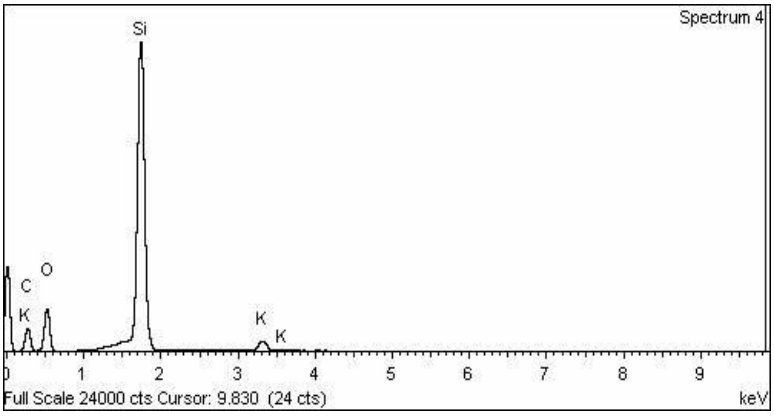

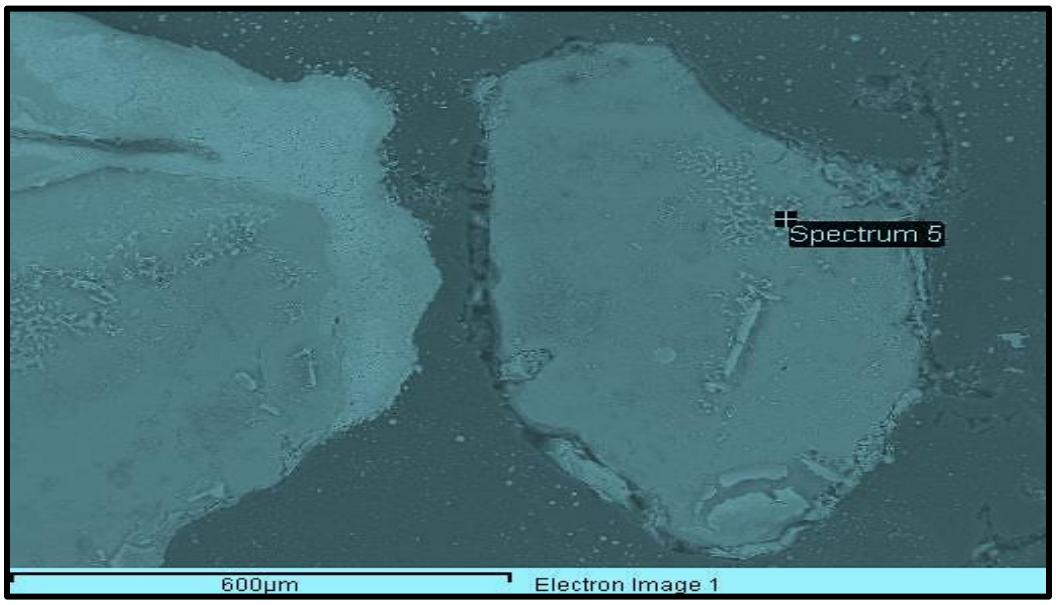

Figure 9-5 EDX spot analysis of the mixture of KOH + Silica Sand sample at 350 ^{0}C (spectrum 5)

Spectrum processing:
No peaks omitted

Processing option: All elements analysed
Number of iterations = 6

Standard:
C CaCO3 1-Jun-1999 12:00 AM
O SiO2 1-Jun-1999 12:00 AM
Si SiO2 1-Jun-1999 12:00 AM
K MAD-10 Feldspar 1-Jun-1999 12:00 AM

Element	Weight%	Atomic%
C K	115.73	51.58
O K	106.52	35.65
Si K	52.41	9.99
K K	20.32	2.78
Totals	294.97	

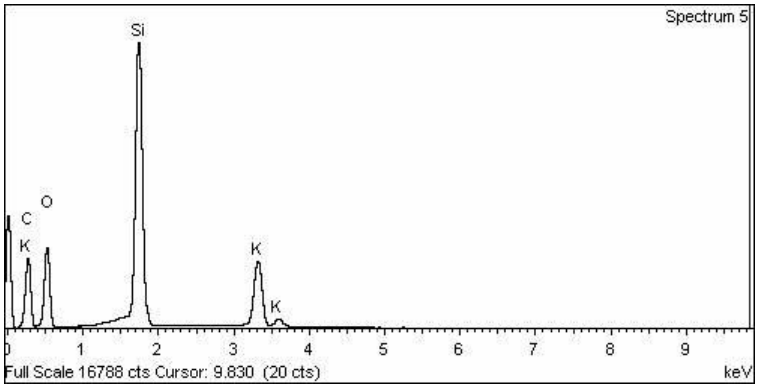

Appendix A2: Comprehensive data of the SEM and EDX examinations of the mixture of willow + wood samples at 802 ^{0}C

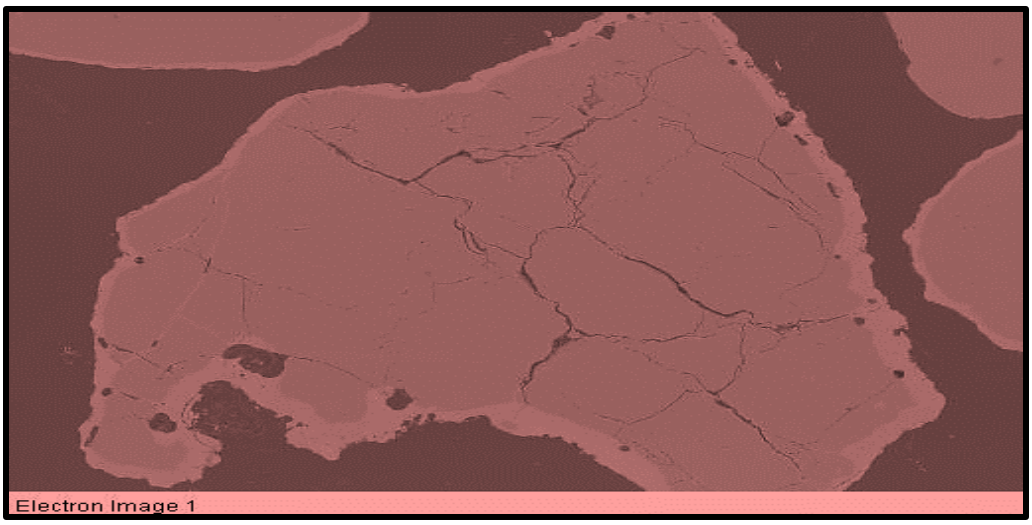

Figure 9-6 SEM image of the mixture of Willow + Wood sample @ 802 ^{0}C

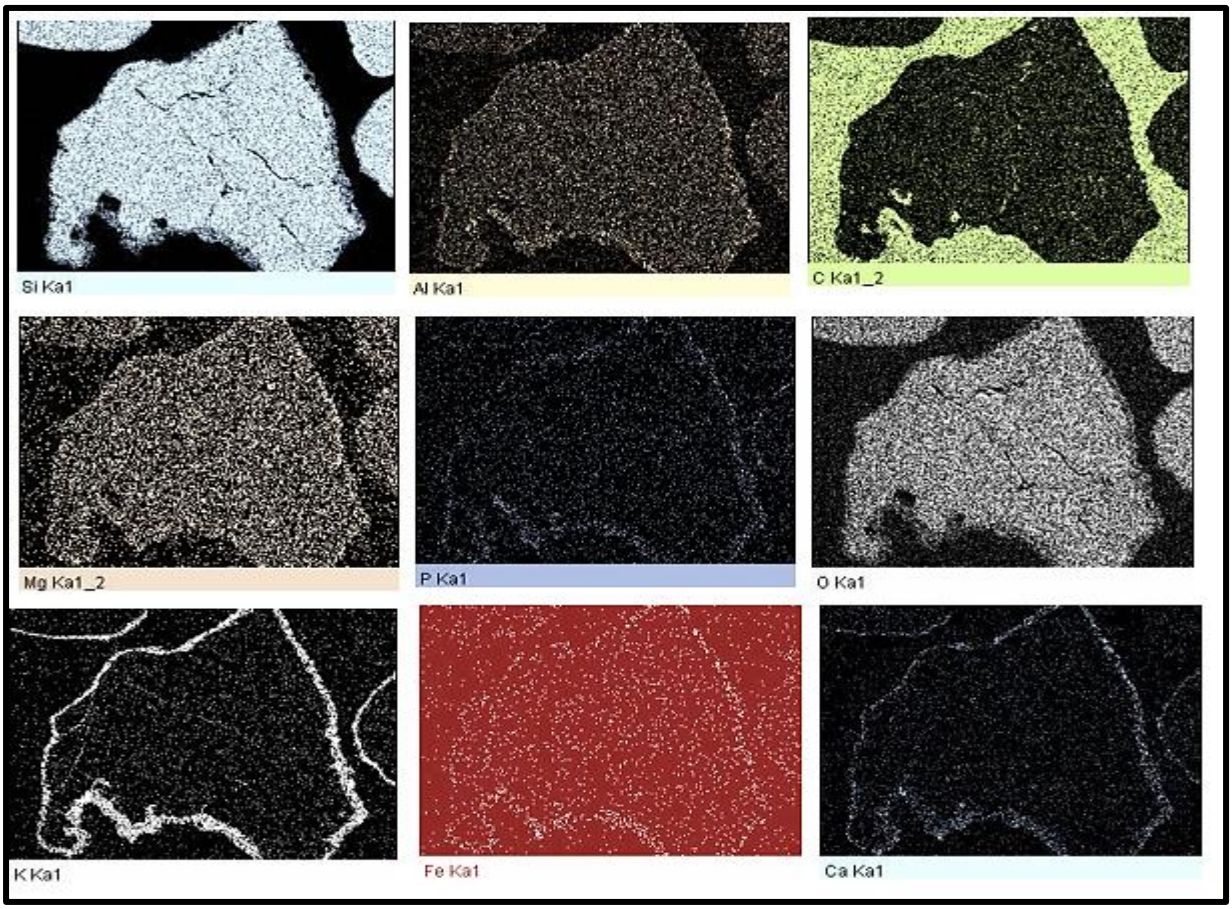

Figure 9-7 Element mapping of the electron image of the mixture of Willow + Wood sample @ 802 ^{0}C

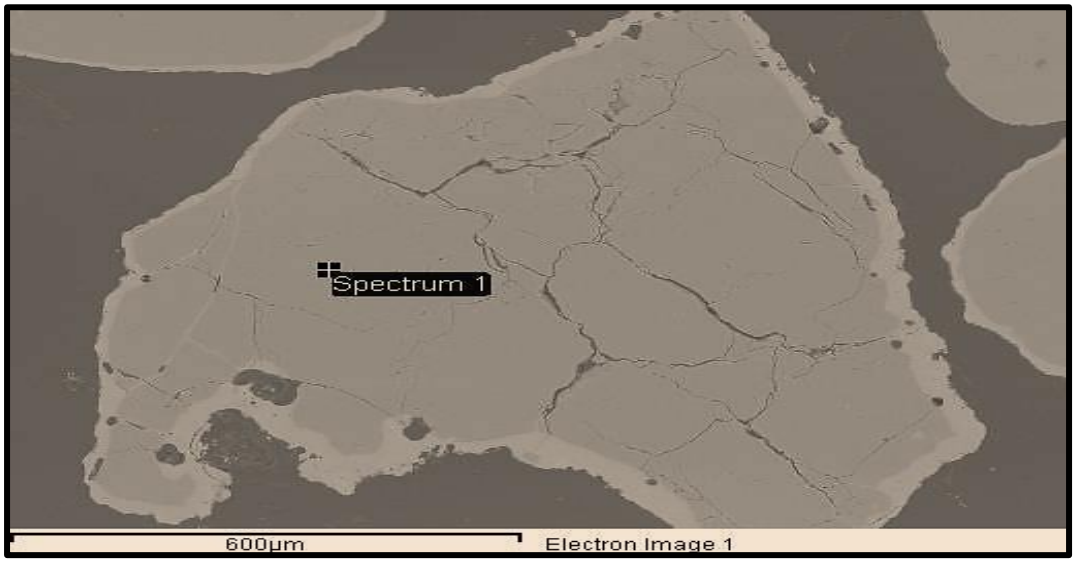

Figure 9-8 EDX Spot Analysis of the mixture of willow + wood sample @ 802 ^{0}C (spectrum 1)

Spectrum processing:
No peaks omitted
Processing option: All elements analysed
Number of iterations = 7
Standard:
C CaCO3 1-Jun-1999 12:00 AM
O SiO2 1-Jun-1999 12:00 AM
Si SiO2 1-Jun-1999 12:00 AM

Element	Weight%	Atomic%
C K	103.87	42.21
O K	147.12	44.88
Si K	74.31	12.91
Totals	325.30	

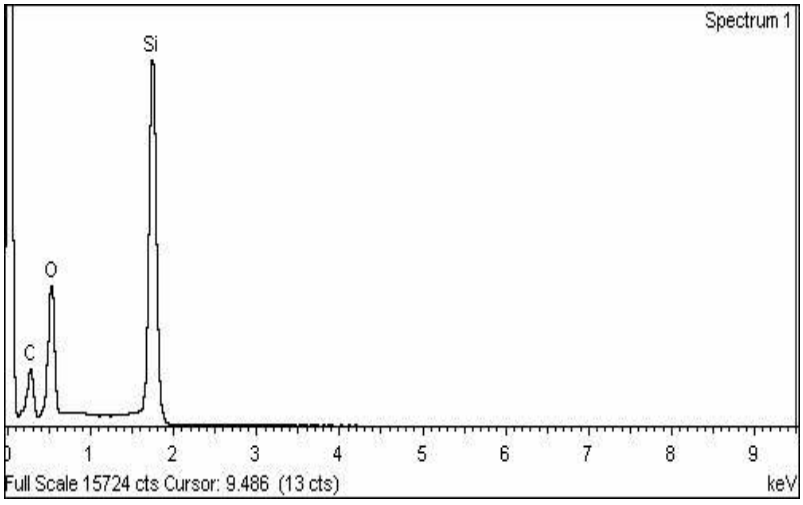

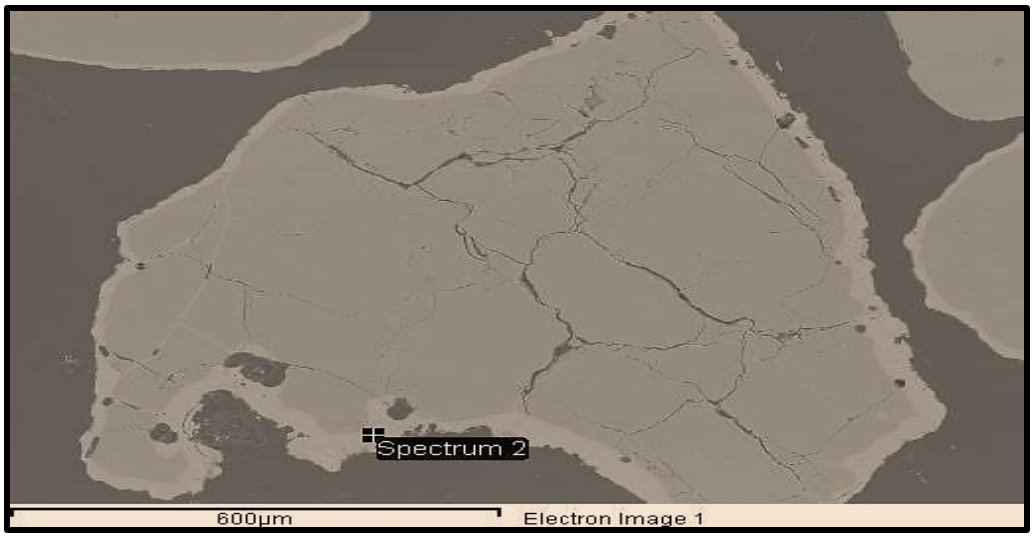

Figure 9-9 EDX Spot Analysis of the mixture of Willow + Wood sample @ 802 0 C (spectrum 2)

Number of iterations = 5
Mg MgO 1-Jun-1999 12:00 AM
Al Al2O3 1-Jun-1999 12:00 AM
Si SiO2 1-Jun-1999 12:00 AM
P GaP 1-Jun-1999 12:00 AM
K MAD-10 Feldspar 1-Jun-1999 12:00 AM
Ca Wollastonite 1-Jun-1999 12:00 AM
Fe Fe 1-Jun-1999 12:00 AM

Element	Weight%	Atomic%
C K	46.45	32.77
O K	86.86	46.00
Mg K	3.71	1.29
Al K	3.58	1.12
Si K	39.70	11.98
P K	1.22	0.33
K K	23.30	5.05
Ca K	3.35	0.71
Fe K	4.96	0.75
Totals	213.13	

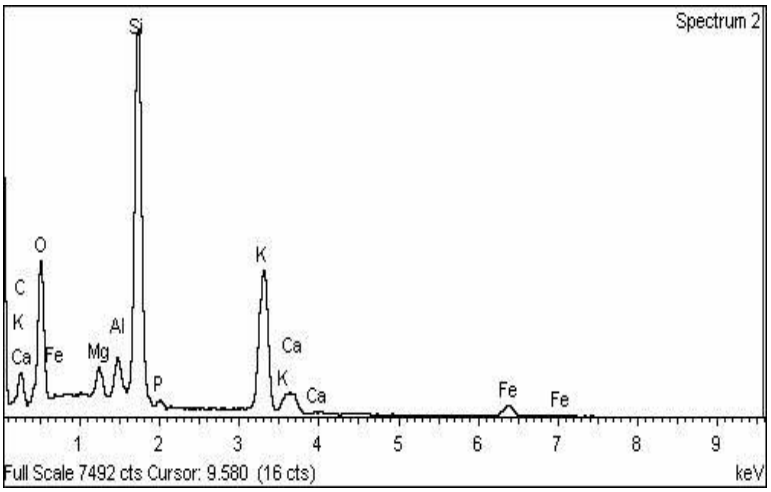

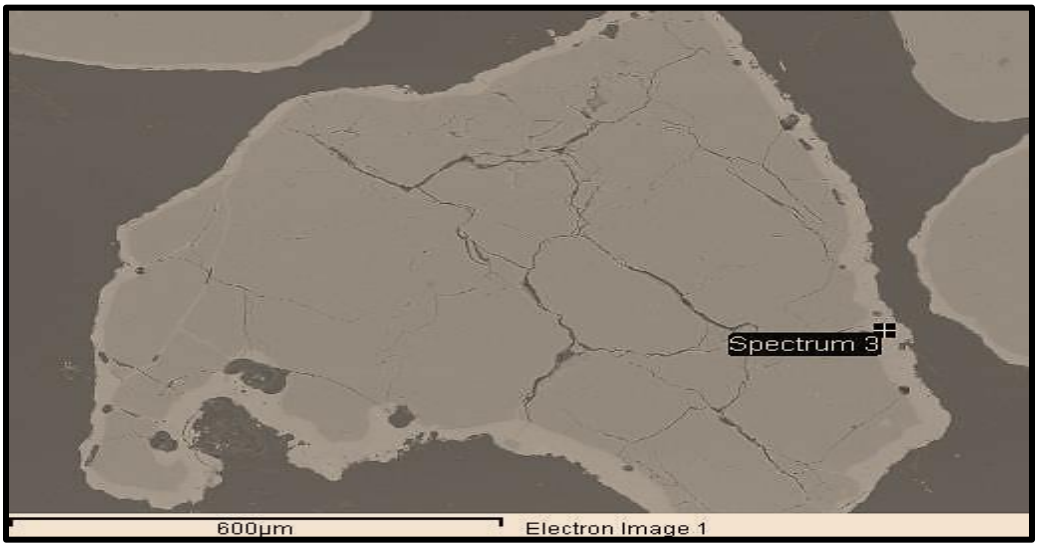

Figure 9-10 EDX Spot Analysis of the mixture of Willow + Wood sample @ 802 0 C (spectrum 3)

Peak possibly omitted : 8.090 keV
C CaCO3 1-Jun-1999 12:00 AM
O SiO2 1-Jun-1999 12:00 AM
Mg MgO 1-Jun-1999 12:00 AM
Al Al2O3 1-Jun-1999 12:00 AM
Si SiO2 1-Jun-1999 12:00 AM
P GaP 1-Jun-1999 12:00 AM
K MAD-10 Feldspar 1-Jun-1999 12:00 AM
Ca Wollastonite 1-Jun-1999 12:00 AM
Fe Fe 1-Jun-1999 12:00 AM

Element	Weight%	Atomic%
C K	108.98	48.10
O K	115.14	38.15
Mg K	1.80	0.39
Al K	4.10	0.81
Si K	46.28	8.74
P K	1.46	0.25
K K	21.44	2.91
Ca K	3.12	0.41
Fe K	2.61	0.25
Totals	304.92	

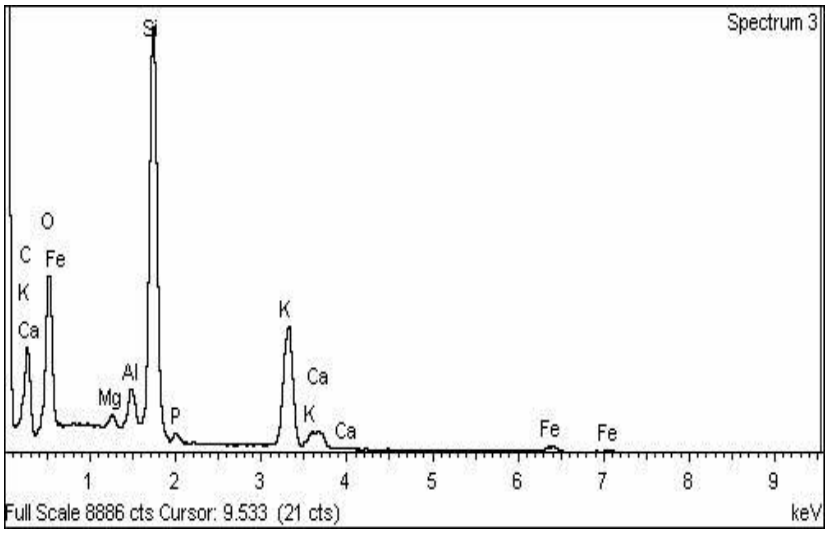

Appendix A3: Comprehensive data of the SEM and EDX examinations of the mixture of wood + miscanthus samples at 802 ^{0}C

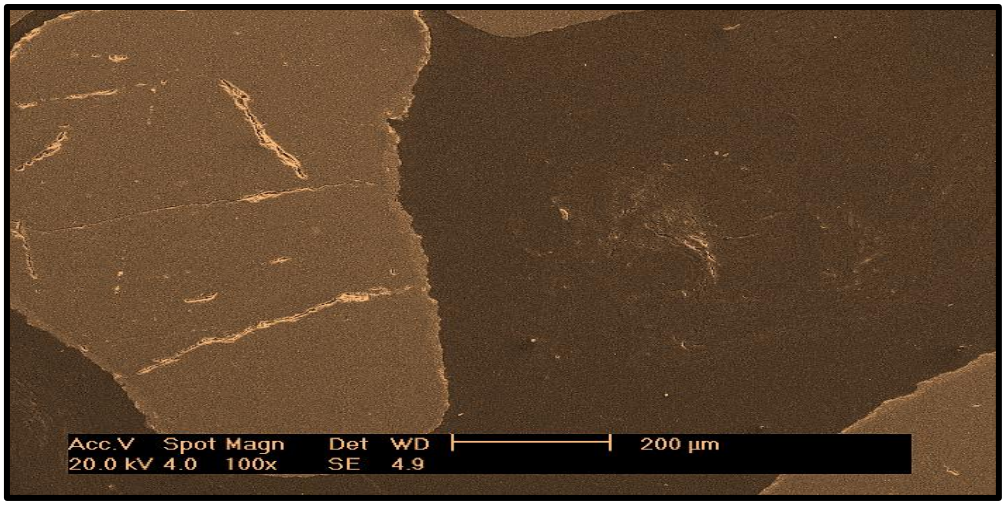

Figure 9-11 SEM image of the mixture of wood + miscanthus sample at 802 0C

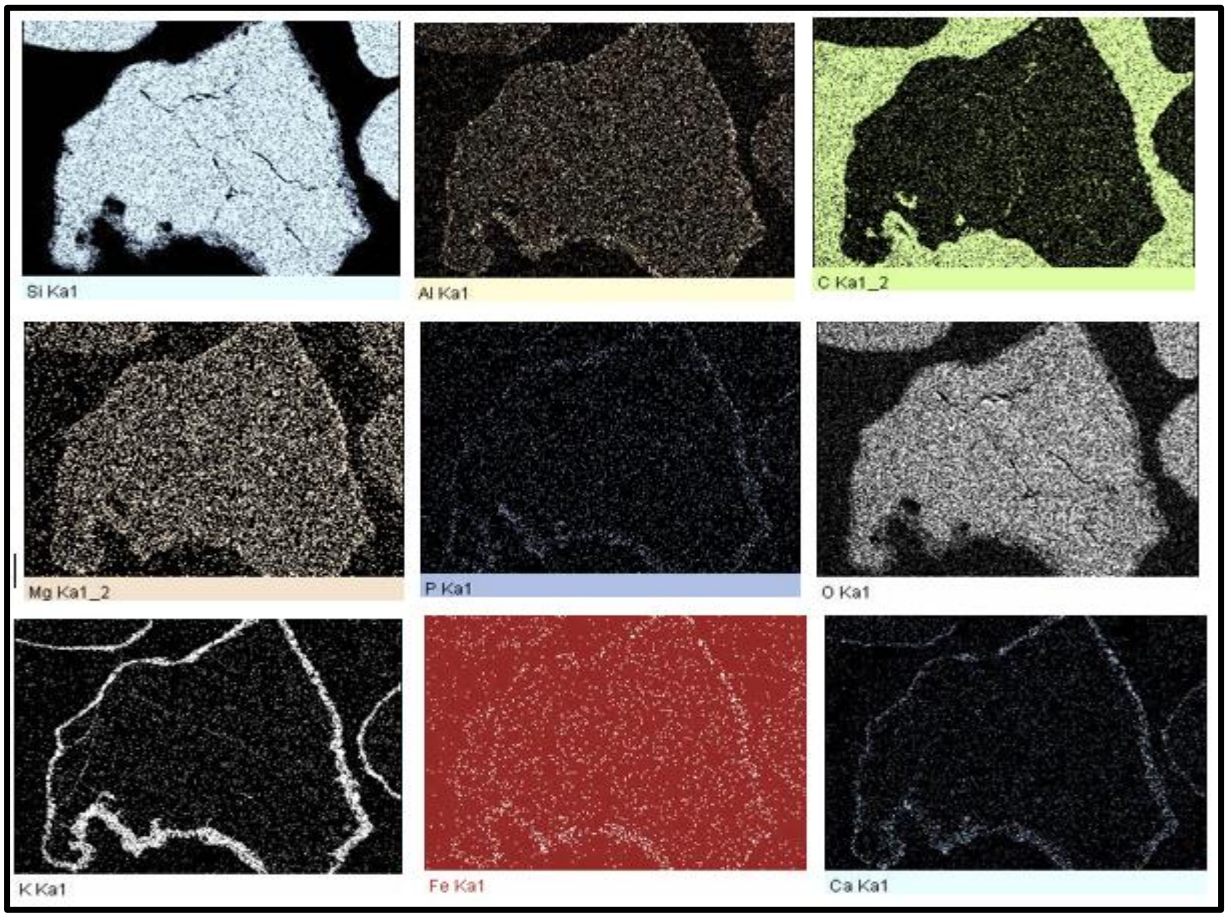

Figure 9-12 Element mapping of the mixture of Wood + Miscanthus sample @ 802 ^{0}C

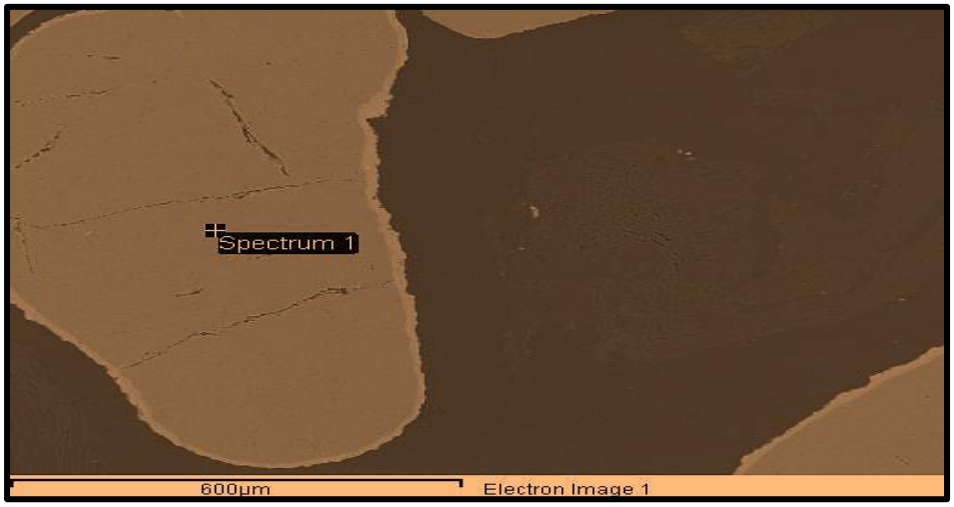

Figure 9-13 EDX Spot analysis of Wood + Miscanthus sample @ 802 ^{0}C (spectrum 1)

Spectrum processing:
No peaks omitted

Processing option: All elements analysed
Number of iterations = 6

Standard:
C CaCO3 1-Jun-1999 12:00 AM
O SiO2 1-Jun-1999 12:00 AM
Si SiO2 1-Jun-1999 12:00 AM

Element	Weight%	Atomic%
C K	69.97	46.57
O K	84.98	42.46
Si K	38.52	10.96
Totals	193.48	

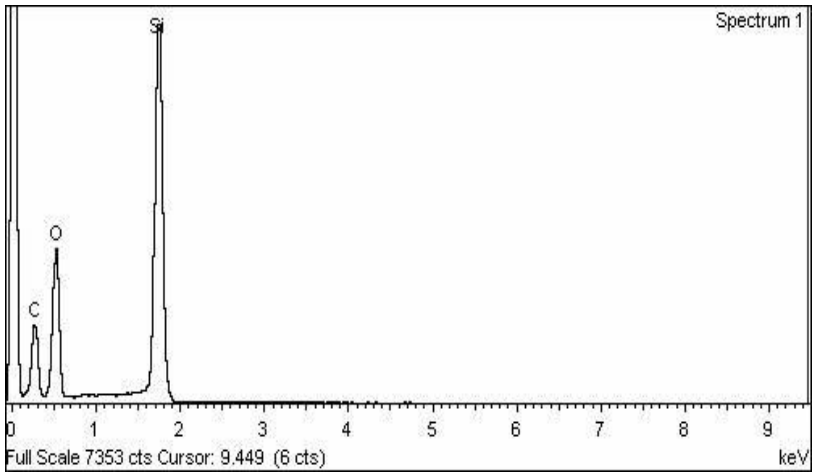

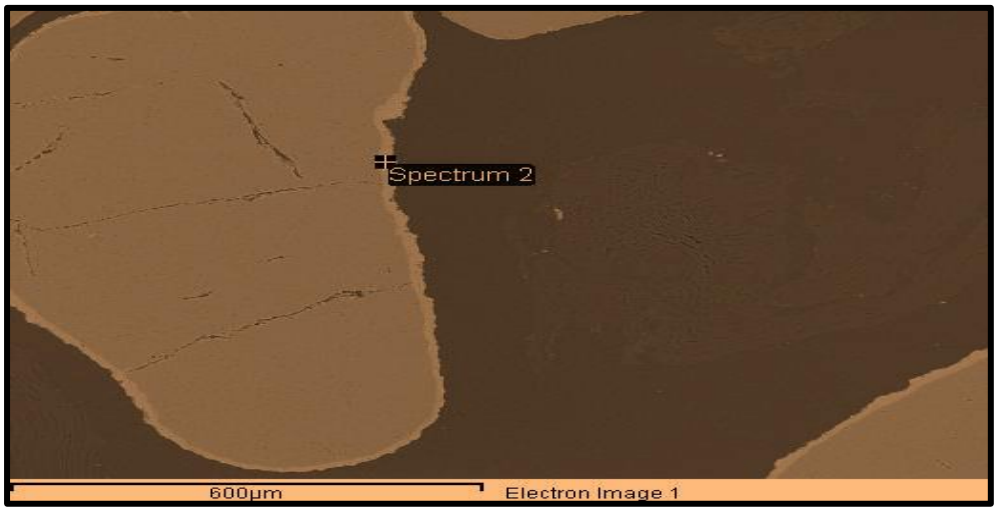

Figure 9-14 EDX Spot analysis of Wood + Miscanthus sample @ 802 ^{0}C (spectrum 2)

Spectrum processing :
Processing option : All elements analysed
Number of iterations = 6
C CaCO3 1-Jun-1999 12:00 AM
O SiO2 1-Jun-1999 12:00 AM
Mg MgO 1-Jun-1999 12:00 AM
Al Al2O3 1-Jun-1999 12:00 AM
Si SiO2 1-Jun-1999 12:00 AM
P GaP 1-Jun-1999 12:00 AM
K MAD-10 Feldspar 1-Jun-1999 12:00 AM
Ca Wollastonite 1-Jun-1999 12:00 AM
Fe Fe 1-Jun-1999 12:00 AM

Element	Weight%	Atomic%
C K	77.75	56.03
O K	60.19	32.57
Mg K	2.23	0.79
Al K	2.15	0.69
Si K	19.54	6.02
P K	1.74	0.49
K K	11.45	2.53
Ca K	3.16	0.68
Fe K	1.28	0.20
Totals	179.48	

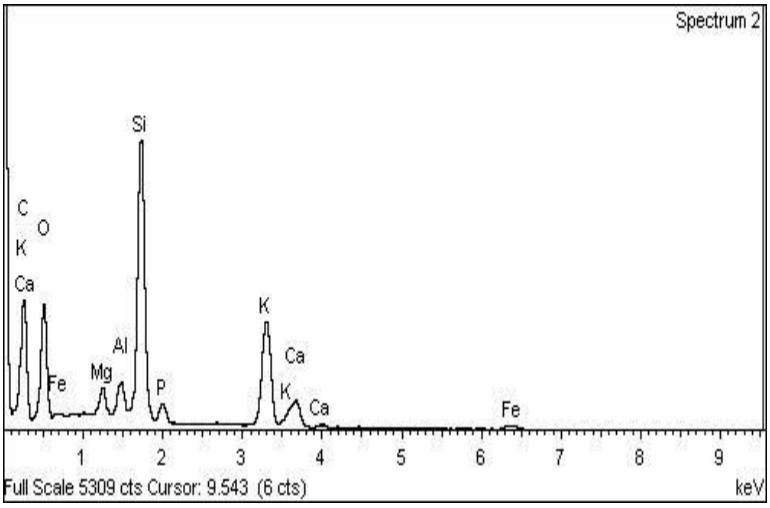

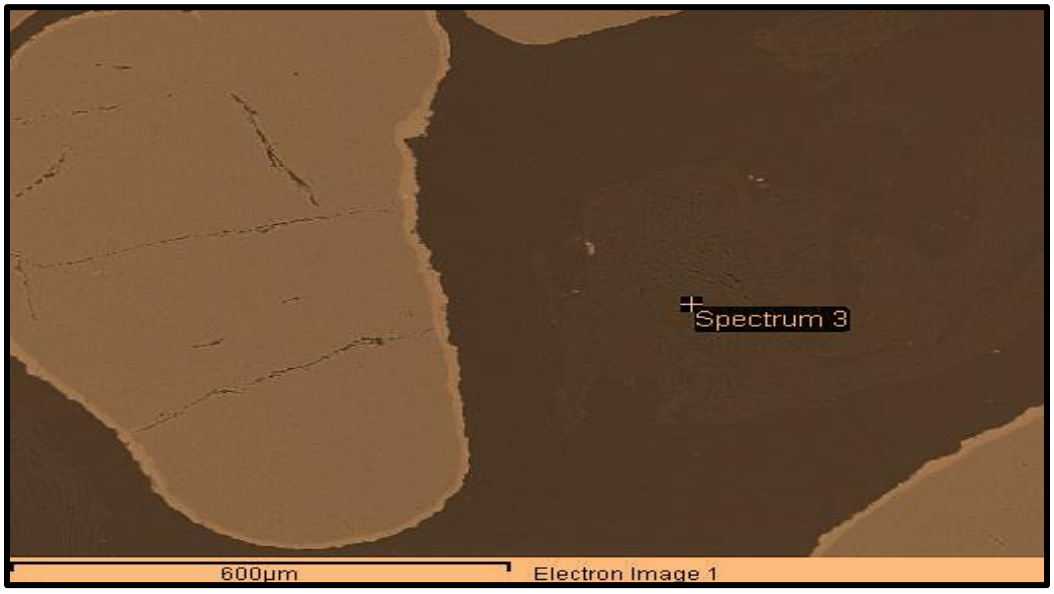

Figure 9-15 EDX Spot analysis of Wood + Miscanthus sample @ 802 ^{0}C (spectrum 3)

Spectrum processing:
Peak possibly omitted: 3.331 keV

Processing option: All elements analysed
Number of iterations = 4

Standard:
C CaCO3 1-Jun-1999 12:00 AM
O SiO2 1-Jun-1999 12:00 AM

Element	Weight%	Atomic%
C K	74.53	83.23
O K	20.00	16.77
Totals	94.53	

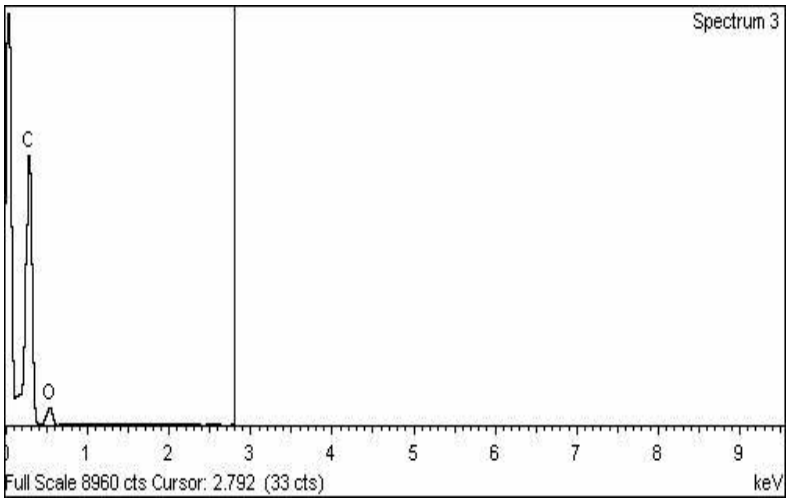

Appendix A4: Comprehensive data of SEM and EDX examinations of wood sample at 802 ^{0}C

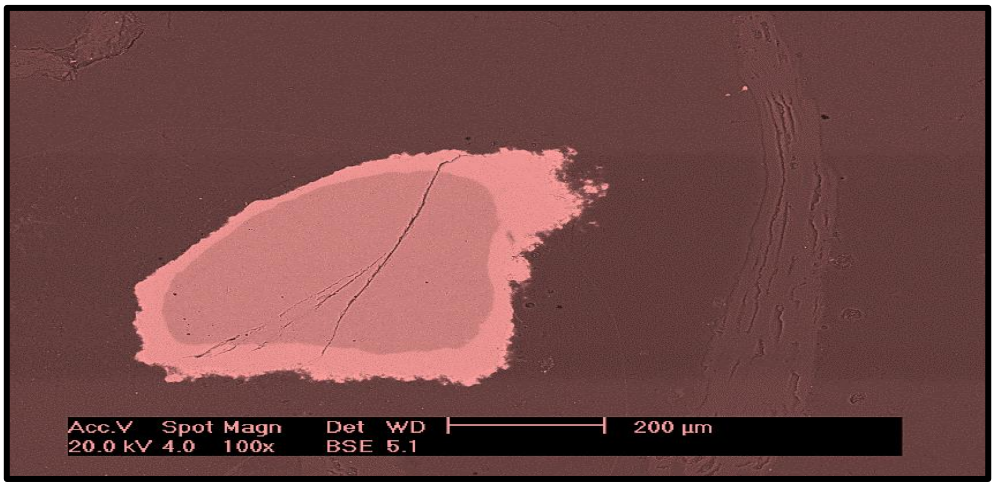

Figure 9-16 SEM image of wood sample @ 802 ^{0}C

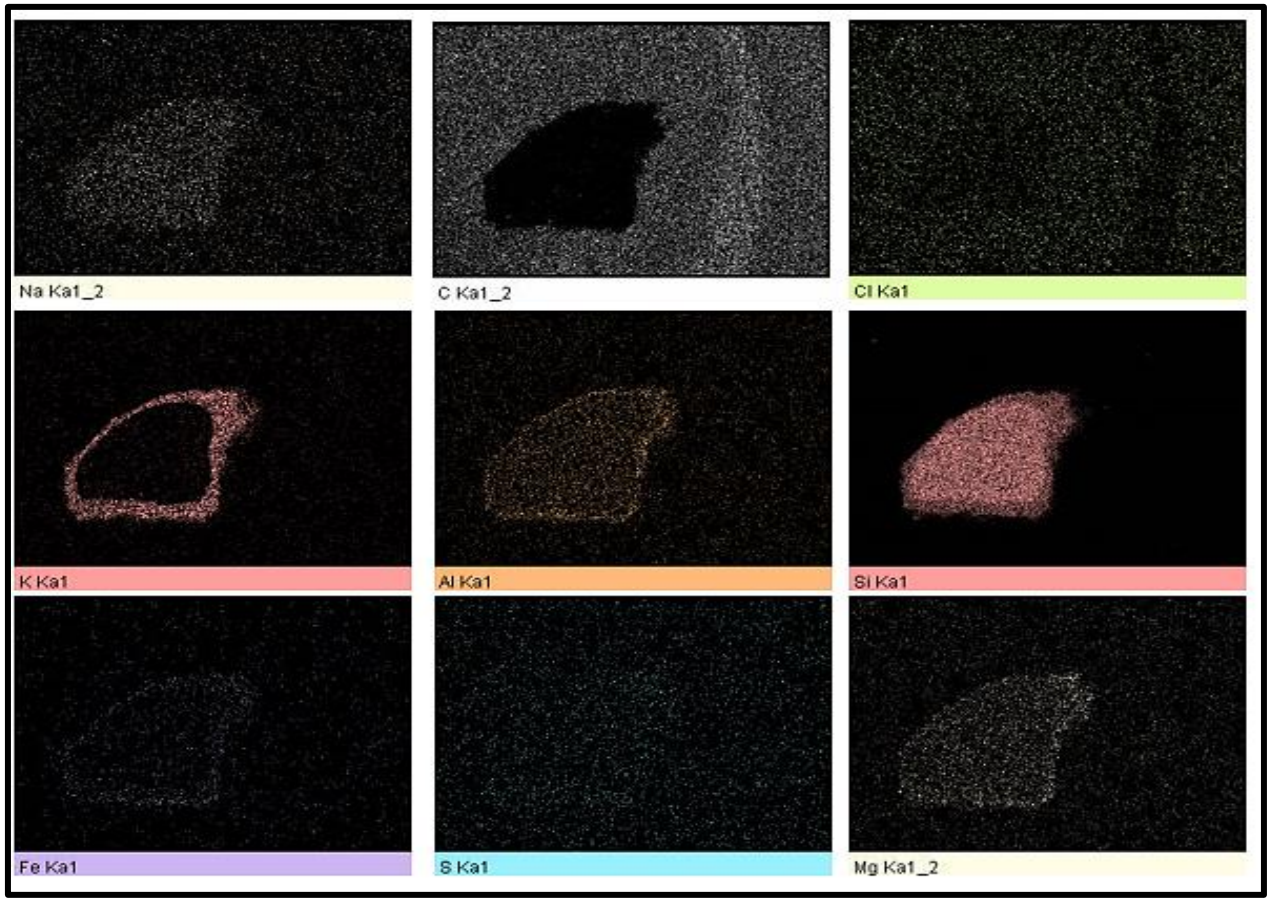

Figure 9-17 Element mapping of wood sample @ 802 ^{0}C

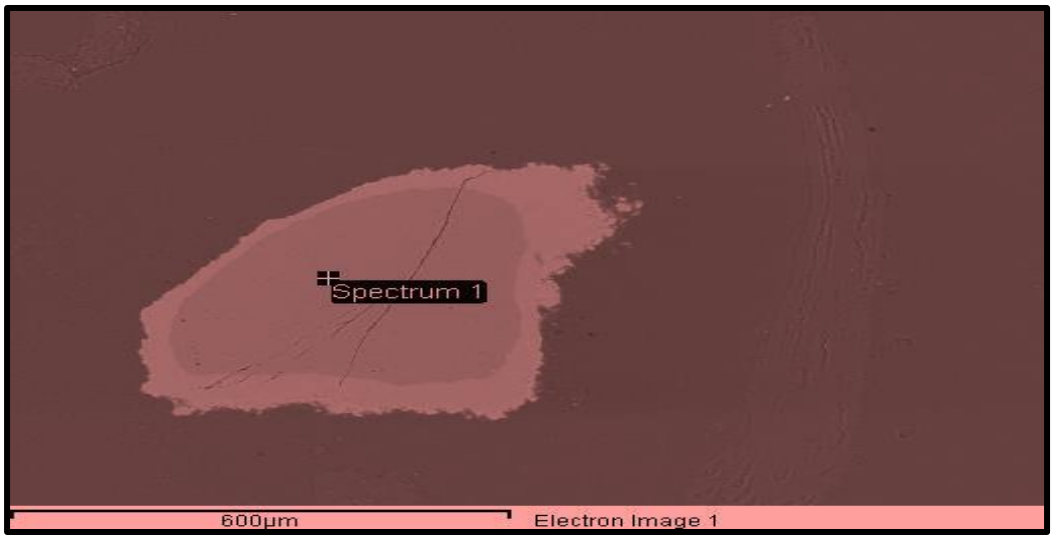

Figure 9-18 EDX Spot analysis of wood sample @ 802 ^{0}C (spectrum 1)

Spectrum processing:
No peaks omitted

Processing option: All elements analysed
Number of iterations = 7

Standard:
C CaCO3 1-Jun-1999 12:00 AM
O SiO2 1-Jun-1999 12:00 AM
Si SiO2 1-Jun-1999 12:00 AM

Element	Weight%	Atomic%
C K	138.71	46.73
O K	165.37	41.83
Si K	79.42	11.44
Totals	383.50	

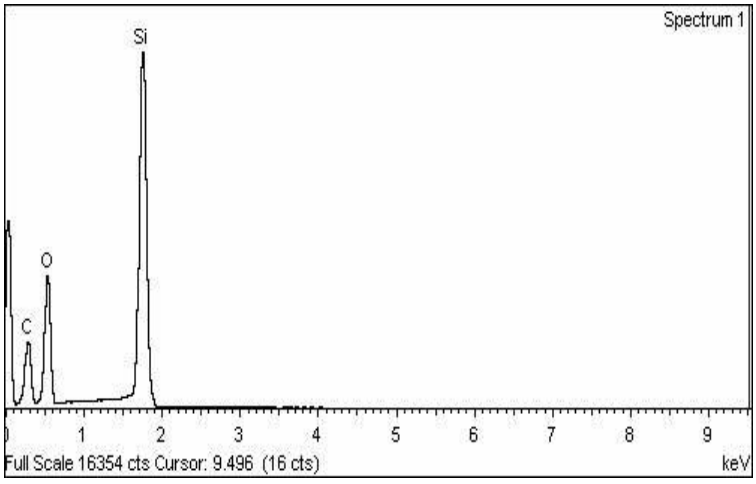

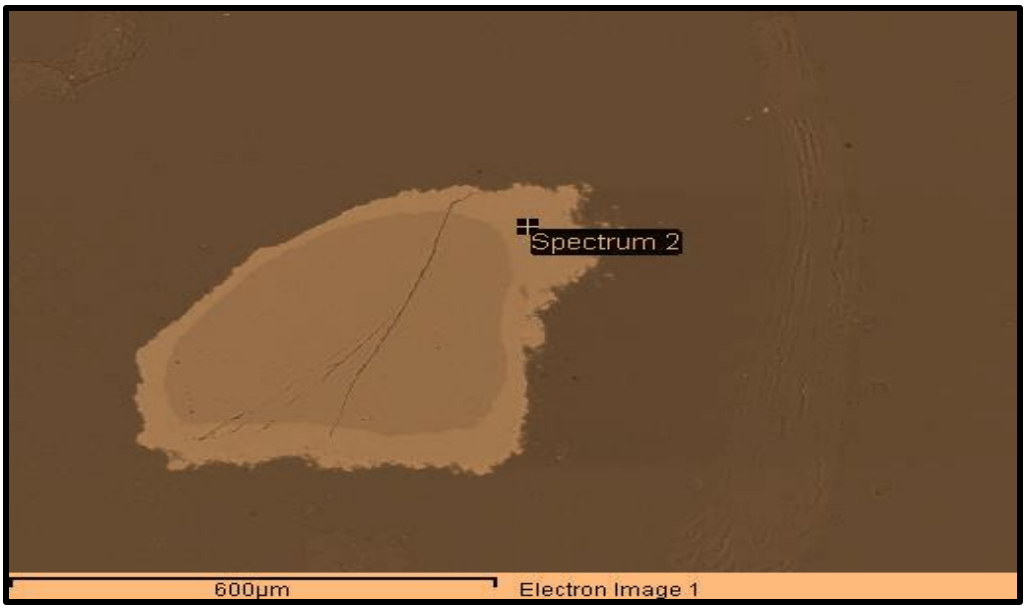

Figure 9-19 EDX Spot analysis of Wood sample @ 802 ^{0}C (spectrum 2)

Spectrum processing :
No peaks omitted
Processing option : All elements analysed
Number of iterations = 6
Standard :
C CaCO3 1-Jun-1999 12:00 AM
O SiO2 1-Jun-1999 12:00 AM
Mg MgO 1-Jun-1999 12:00 AM
Si SiO2 1-Jun-1999 12:00 AM
K MAD-10 Feldspar 1-Jun-1999 12:00 AM
Ca Wollastonite 1-Jun-1999 12:00 AM
Fe Fe 1-Jun-1999 12:00 AM

Element	Weight%	Atomic%
C K	195.90	58.32
O K	143.14	31.99
Mg K	1.19	0.17
Si K	55.66	7.09
K K	22.83	2.09
Ca K	3.04	0.27
Fe K	1.15	0.07
Totals	422.91	

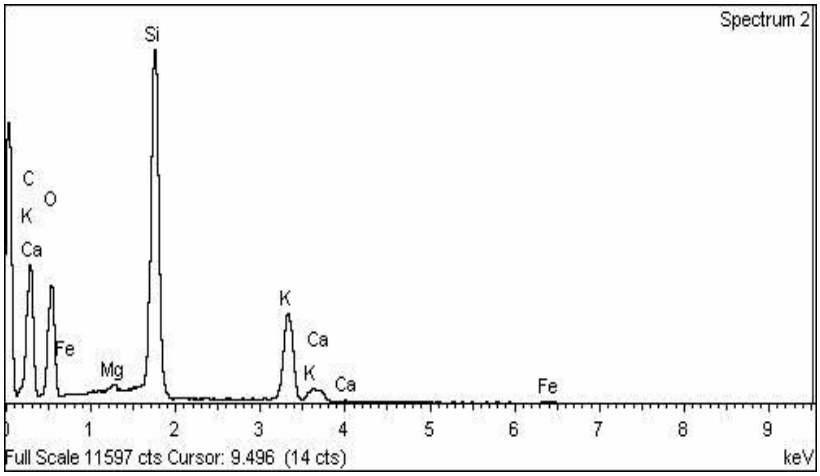

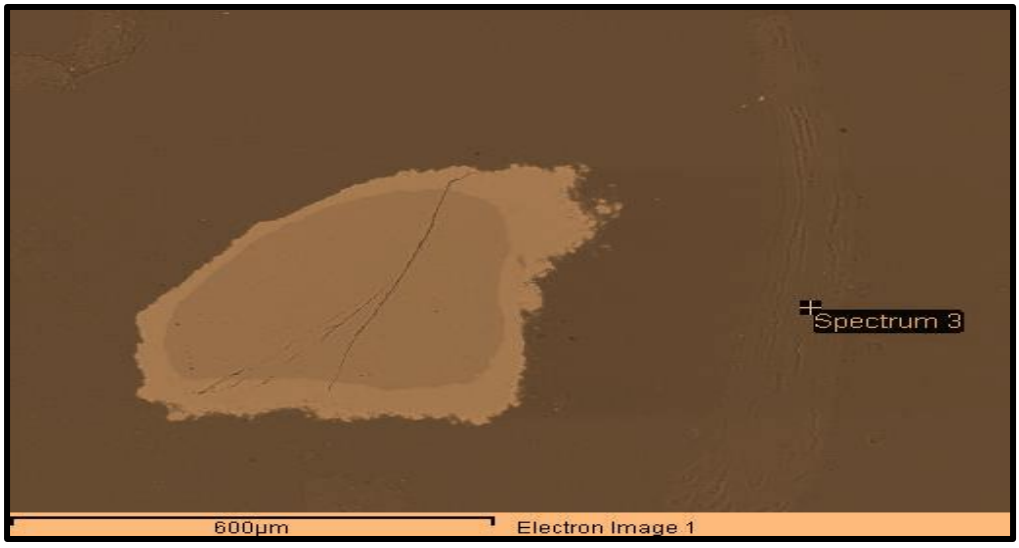

Figure 9-20 EDX Spot analysis of Wood sample @ 802 ^{0}C (spectrum 3)

Spectrum processing:
No peaks omitted

Processing option: All elements analysed
Number of iterations = 4

Standard:
C CaCO3 1-Jun-1999 12:00 AM
O SiO2 1-Jun-1999 12:00 AM
Cl KCl 1-Jun-1999 12:00 AM
K MAD-10 Feldspar 1-Jun-1999 12:00 AM

Element	Weight%	Atomic%
C K	116.99	82.40
O K	33.01	17.45
Cl K	0.46	0.11
K K	0.20	0.04
Totals	150.65	

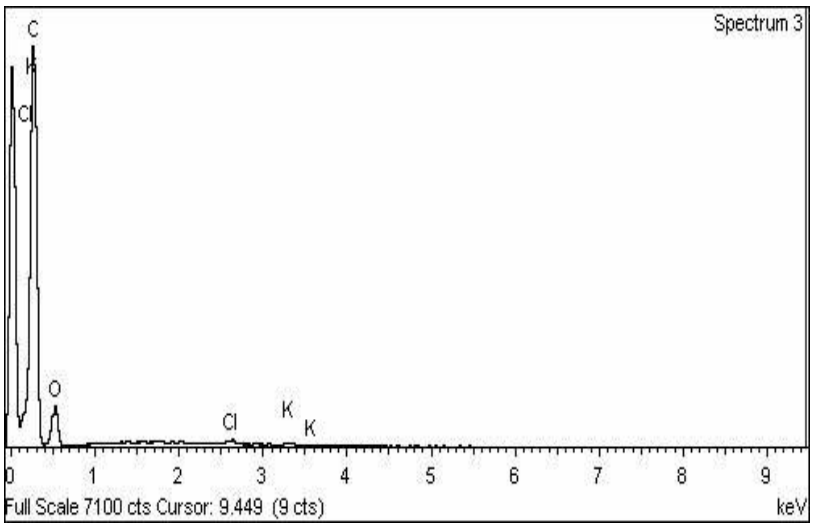

Appendix A5: Comprehensive data of the SEM and EDX examinations of wood sample at 750 ^{0}C

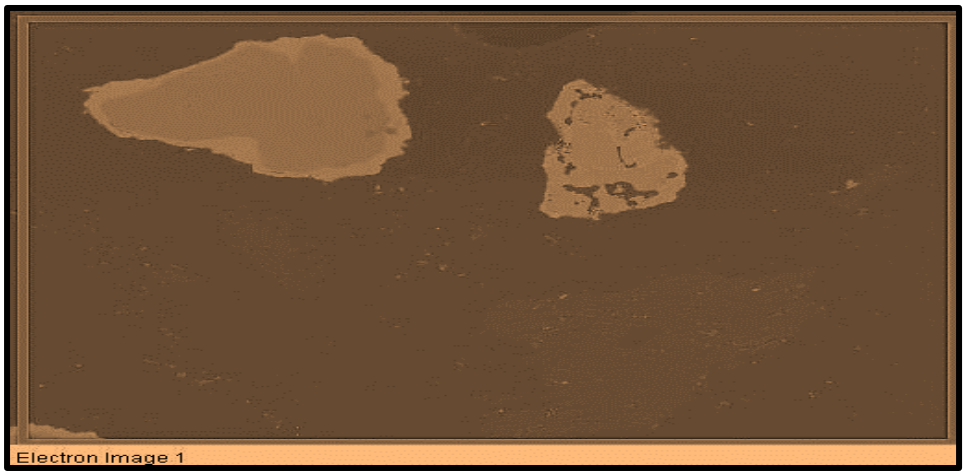

Figure 9-21 SEM image/mapping of wood sample at 750 ^{0}C

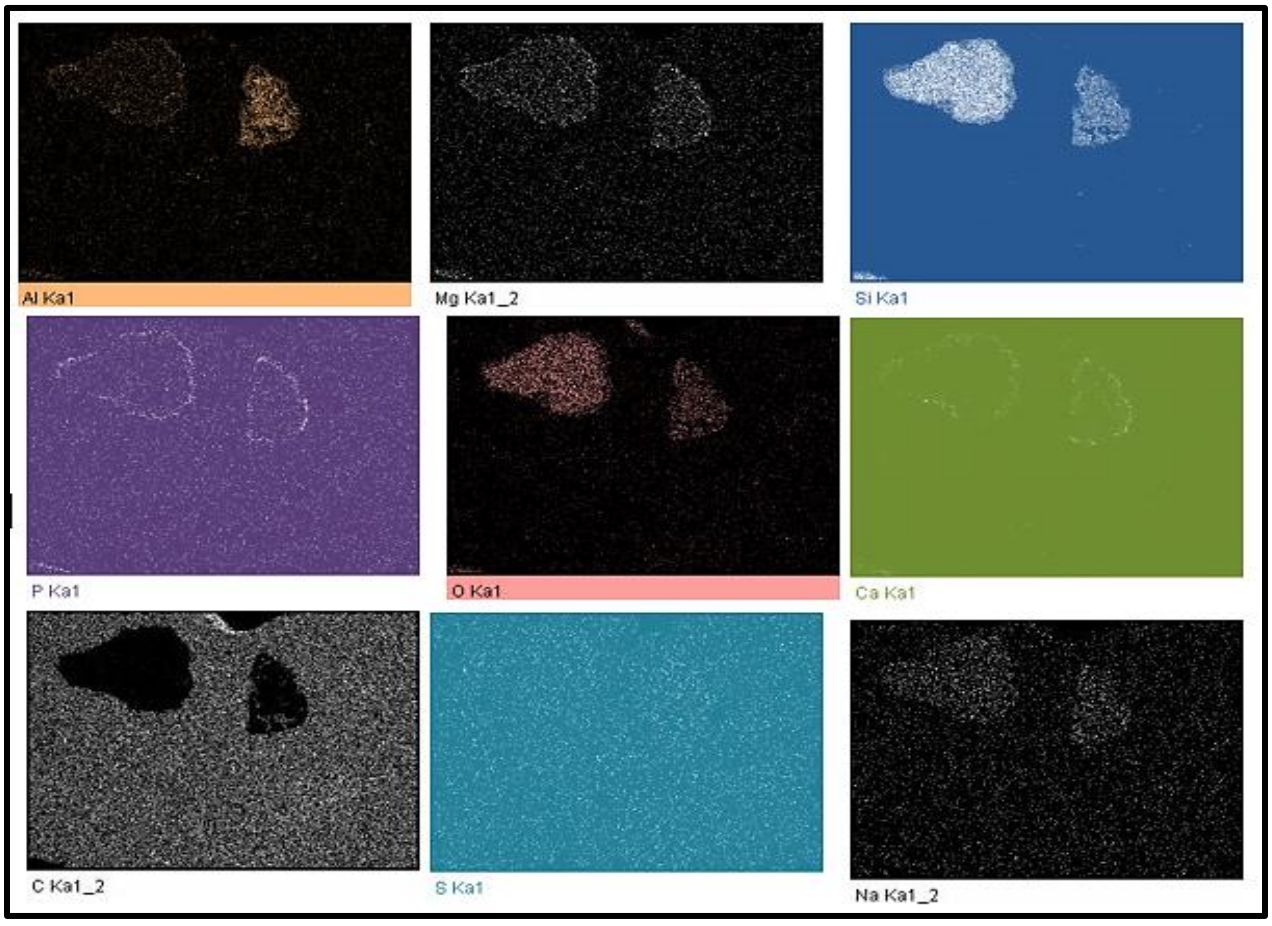

Figure 9-22 Element mapping of wood sample at 750 ^{0}C

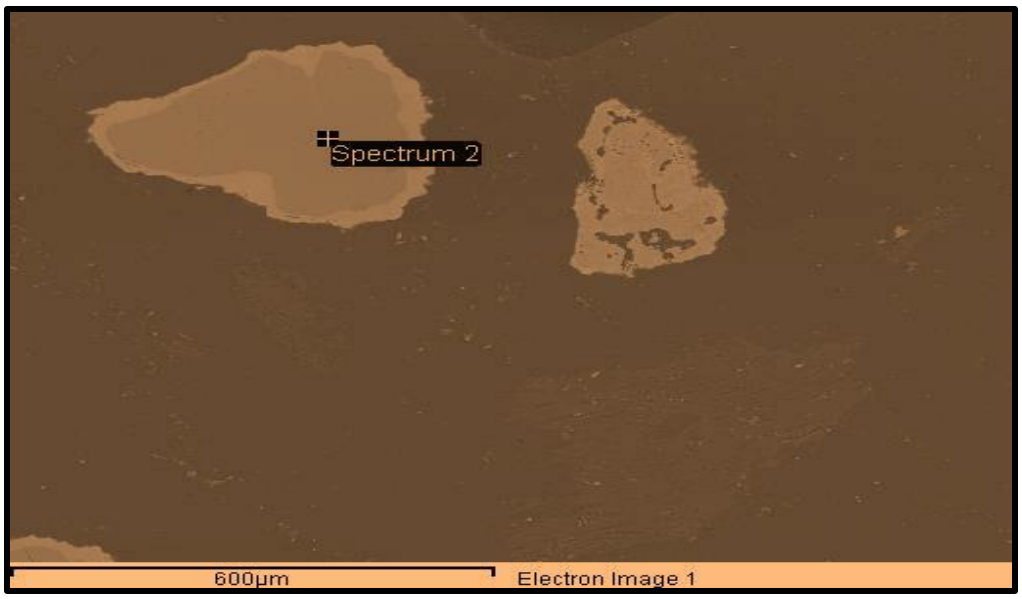

Figure 9-23 EDX Spot analysis of Wood sample at 750 ^{0}C (spectrum 2)

Spectrum processing:
No peaks omitted

Processing option: All elements analysed
Number of iterations = 7
Standard:
C CaCO3 1-Jun-1999 12:00 AM
O SiO2 1-Jun-1999 12:00 AM
Si SiO2 1-Jun-1999 12:00 AM

Element	Weight%	Atomic%
C K	141.68	47.89
O K	162.50	41.23
Si K	75.28	10.88
Totals	379.46	

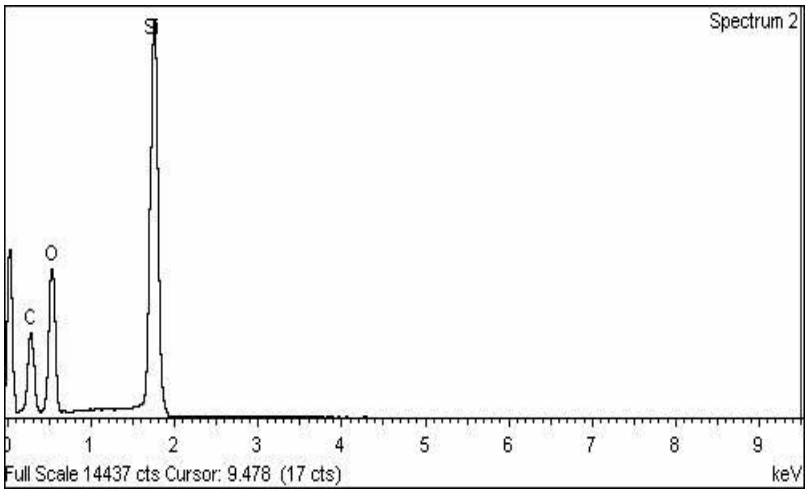

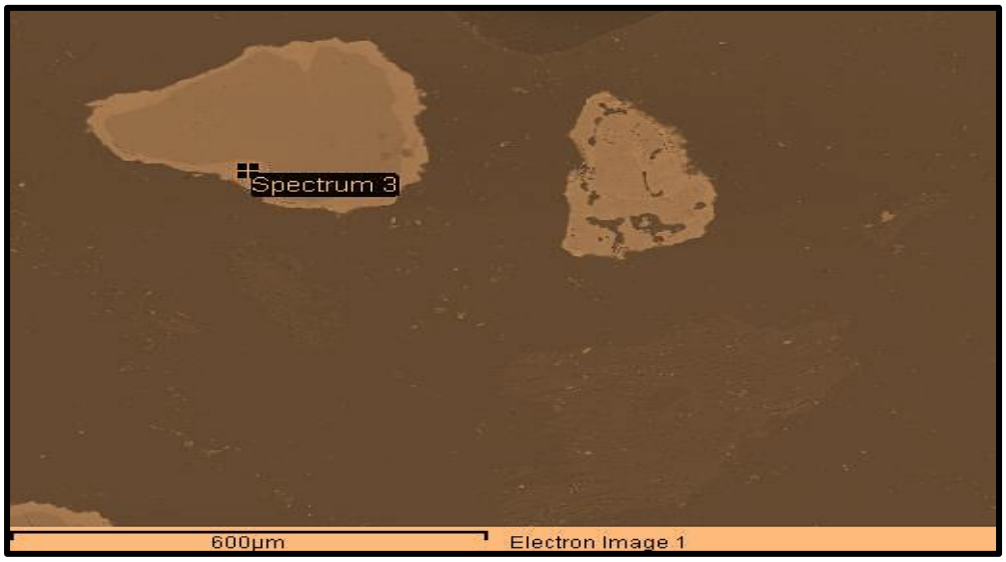

Figure 9-24 EDX Spot analysis of Wood sample @ 750 ^{0}C (spectrum 3)

Spectrum processing:
Processing option : All elements analysed
Number of iterations = 6
C CaCO3 1-Jun-1999 12:00 AM
O SiO2 1-Jun-1999 12:00 AM
Mg MgO 1-Jun-1999 12:00 AM
Al Al2O3 1-Jun-1999 12:00 AM
Si SiO2 1-Jun-1999 12:00 AM
P GaP 1-Jun-1999 12:00 AM
K MAD -10 Feldspar 1-Jun-1999 12:00 AM
Ca Wollastonite 1-Jun-1999 12:00 AM
Fe Fe 1-Jun-1999 12:00 AM

Element	Weight%	Atomic%
C K	138.27	55.44
O K	107.71	32.42
Mg K	2.77	0.55
Al K	3.91	0.70
Si K	41.48	7.11
P K	1.06	0.16
K K	22.79	2.81
Ca K	3.12	0.37
Fe K	5.10	0.44
Totals	326.20	

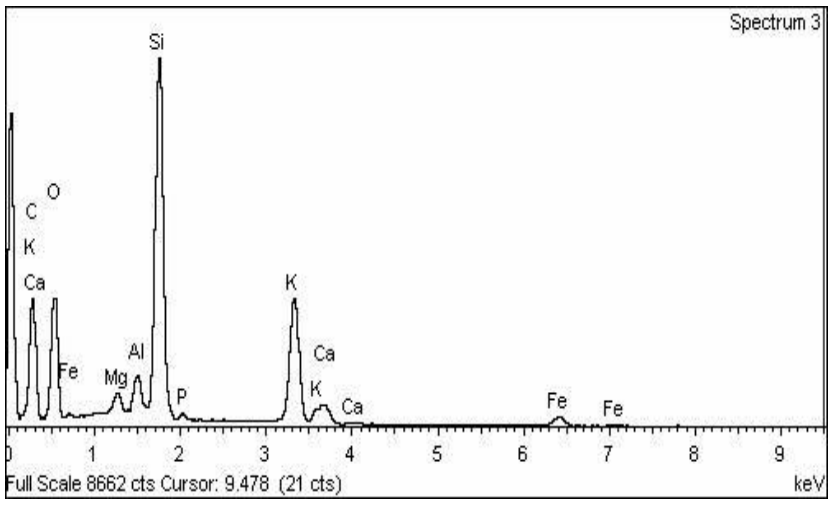

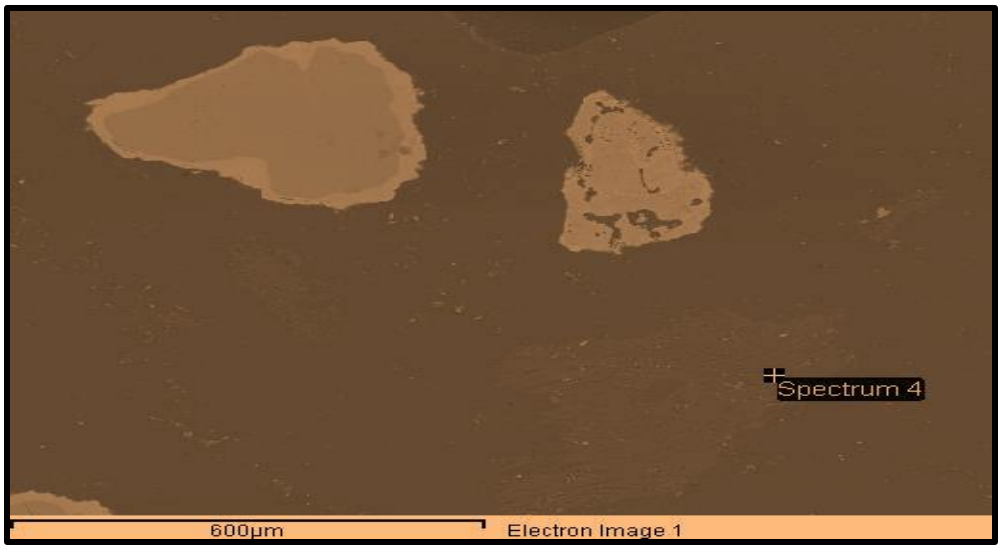

Figure 9-25 EDX Spot analysis of Wood sample at 750 ^{0}C (spectrum 4)

Spectrum processing:
Peaks possibly omitted: 3.325, 3.685 keV

Processing option: All elements analysed
Number of iterations = 4

Standard:
C CaCO3 1-Jun-1999 12:00 AM
O SiO2 1-Jun-1999 12:00 AM
Al Al2O3 1-Jun-1999 12:00 AM
Si SiO2 1-Jun-1999 12:00 AM

Element	Weight%	Atomic%
C K	115.88	73.08
O K	55.62	26.33
Al K	1.03	0.29
Si K	1.12	0.30
Totals	173.65	

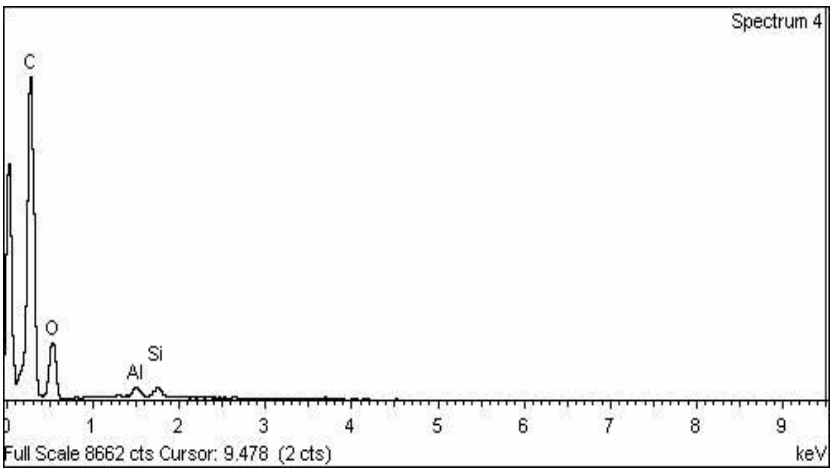

Appendix A6: Comprehensive data of the SEM and EDX examinations miscanthus sample at 750 ^{0}C

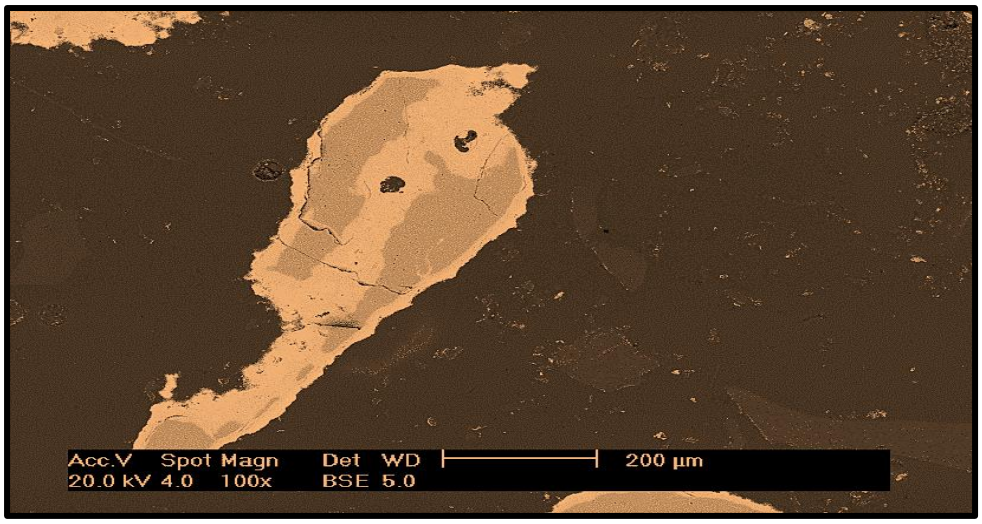

Figure 9-26 SEM image of miscanthus sample at 750 ^{0}C

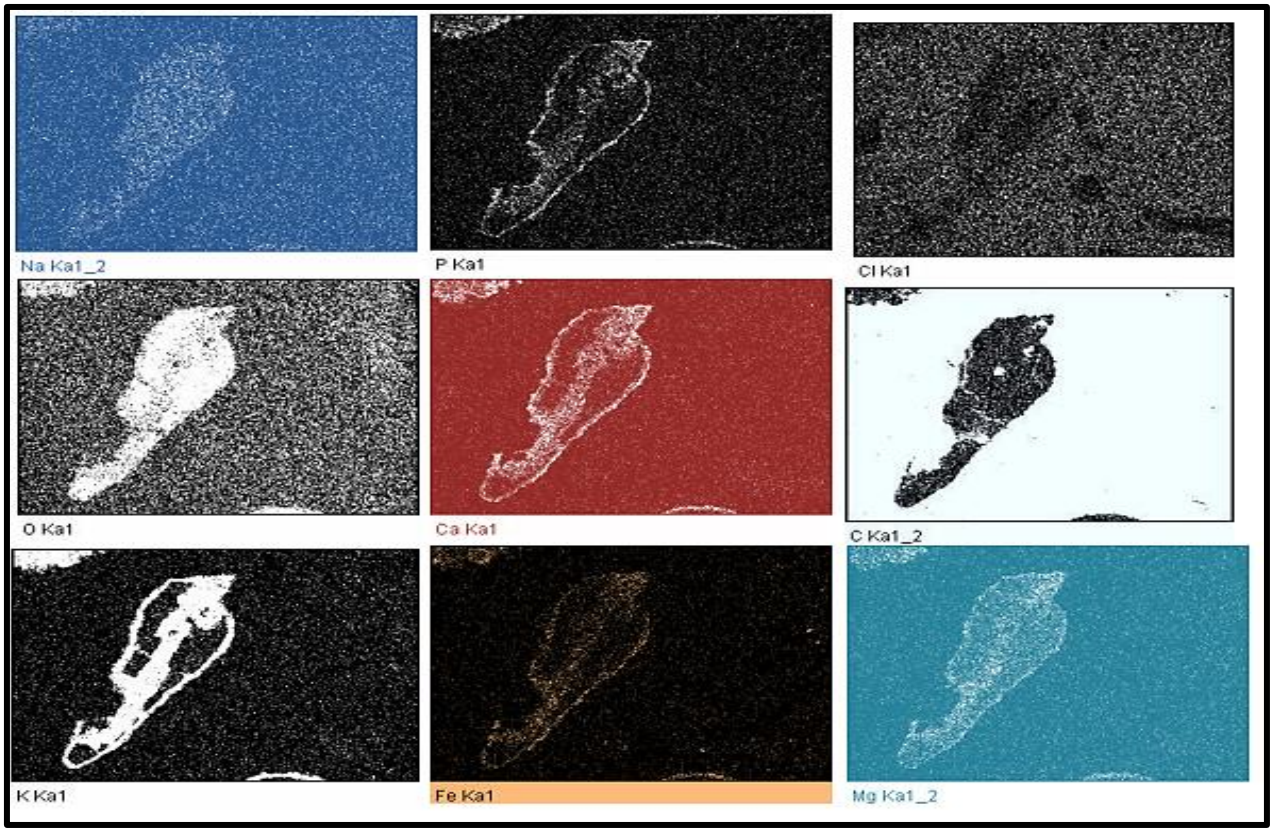

Figure 9-27 Element mapping of miscanthus sample at 750 ^{0}C

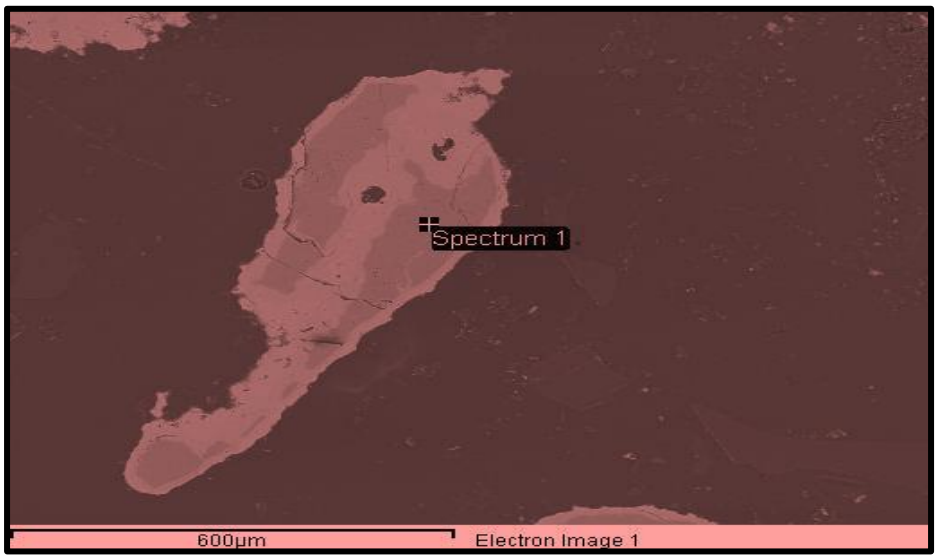

Figure 9-28 EDX Spot analysis of Miscanthus sample at 750 ^{0}C (spectrum 1)

Spectrum processing:
No peaks omitted

Processing option: All elements analysed
Number of iterations = 7

Standard:
C CaCO3 1-Jun-1999 12:00 AM
O SiO2 1-Jun-1999 12:00 AM
Si SiO2 1-Jun-1999 12:00 AM

Element	Weight%	Atomic%
C K	168.60	48.27
O K	190.00	40.84
Si K	88.97	10.89
Totals	447.58	

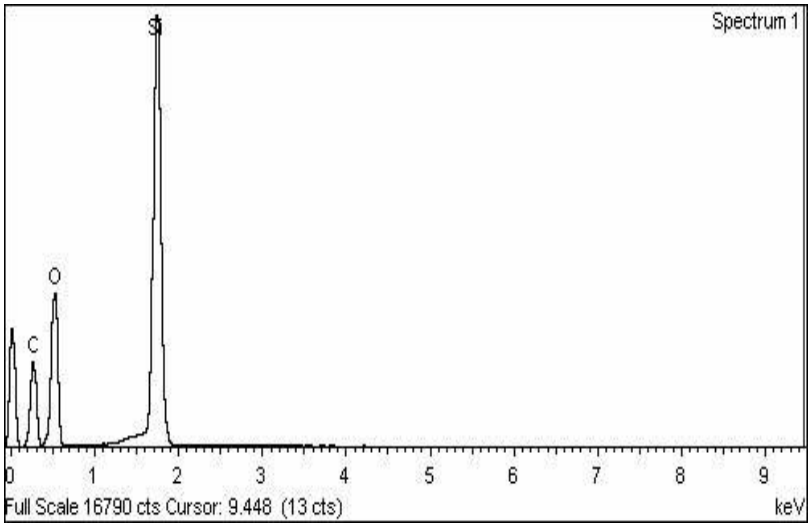

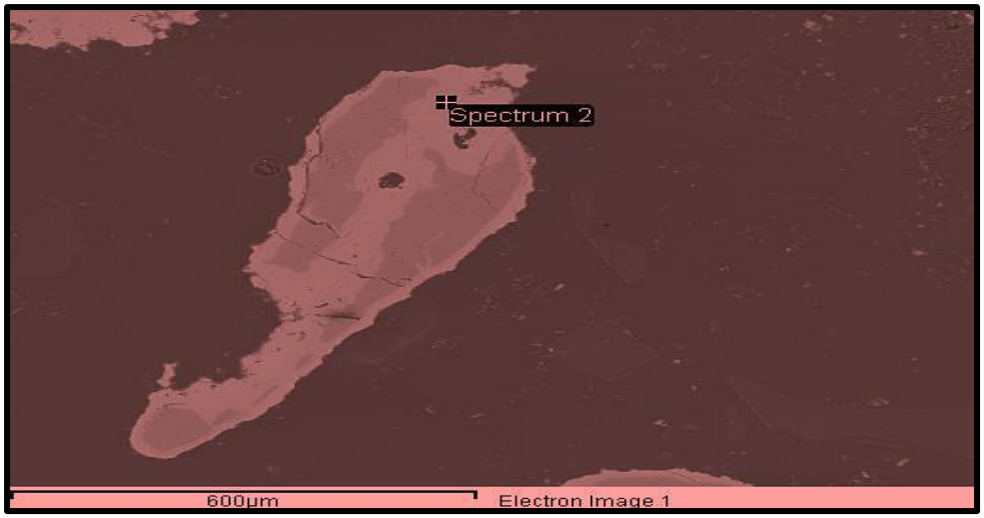

Figure 9-29 EDX Spot analysis of Miscanthus sample at 750 ^{0}C (spectrum 2)

Processing option: All elements analysed
C CaCO3 1-Jun-1999 12:00 AM
O SiO2 1-Jun-1999 12:00 AM
Na Albite 1-Jun-1999 12:00 AM
Mg MgO 1-Jun-1999 12:00 AM
Al Al2O3 1-Jun-1999 12:00 AM
Si SiO2 1-Jun-1999 12:00 AM
P GaP 1-Jun-1999 12:00 AM
K MAD-10 Feldspar 1-Jun-1999 12:00 AM
Ca Wollastonite 1-Jun-1999 12:00 AM

Element	Weight%	Atomic%
C K	127.88	50.50
O K	118.63	35.17
Na K	0.21	0.04
Mg K	1.78	0.35
Al K	5.23	0.92
Si K	48.76	8.23
P K	4.60	0.70
K K	23.72	2.88
Ca K	8.95	1.06
Fe K	1.74	0.15
Totals	341.51	

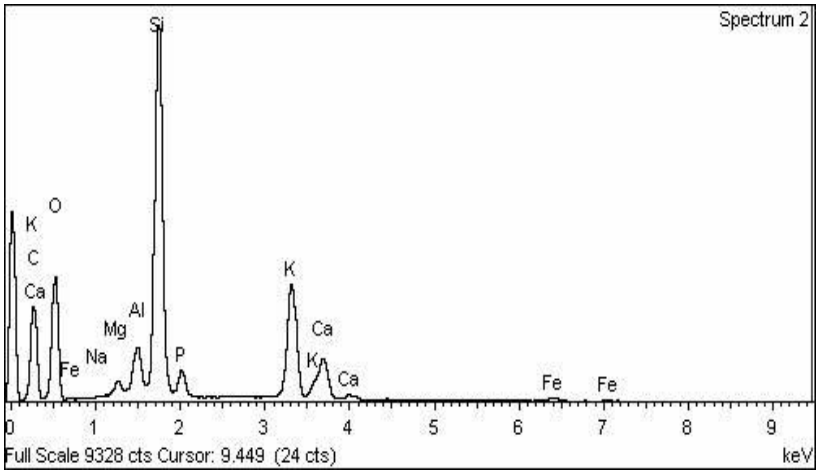

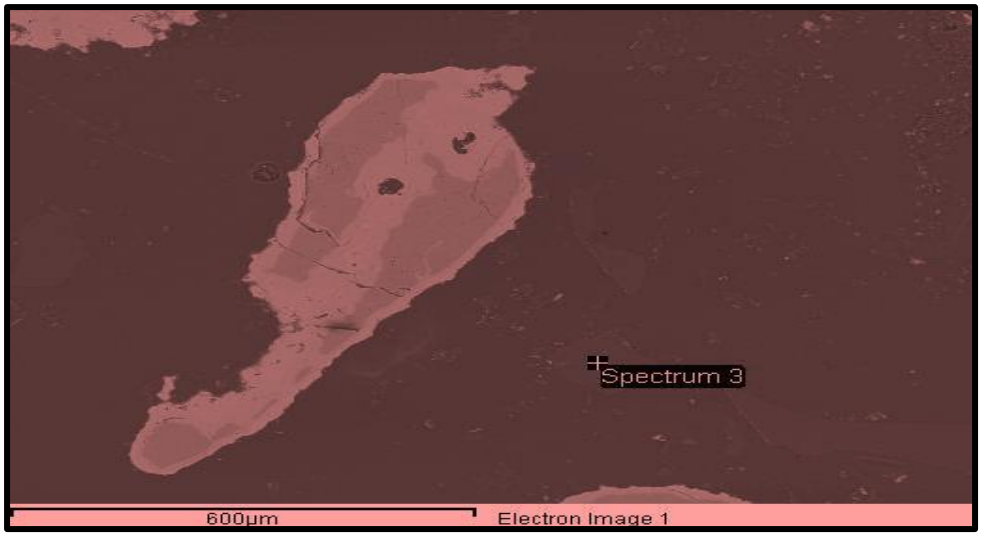

Figure 9-30 EDX Spot analysis of Miscanthus sample at 750 ^{0}C (spectrum 3)

Spectrum processing:
Peaks possibly omitted: 1.515, 3.721 keV

Processing option: All elements analysed
Number of iterations = 5

Standard:
C CaCO3 1-Jun-1999 12:00 AM
O SiO2 1-Jun-1999 12:00 AM
S FeS2 1-Jun-1999 12:00 AM

Element	Weight%	Atomic%
C K	178.44	81.36
O K	53.65	18.37
S K	1.59	0.27
Totals	233.68	

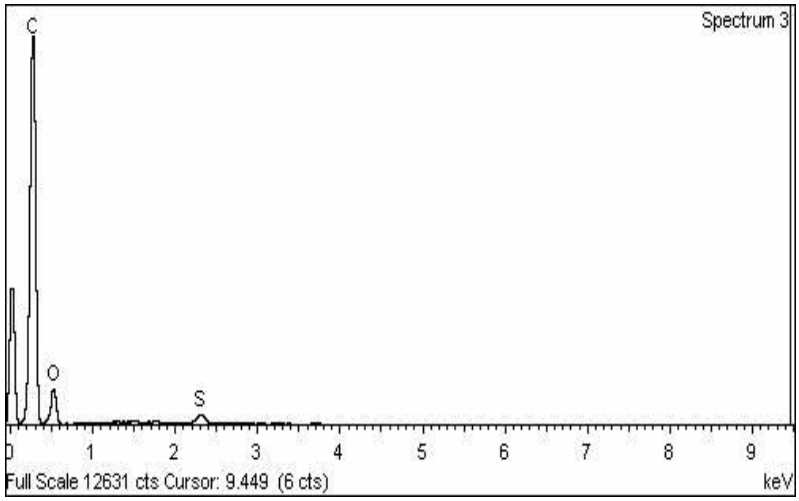

Appendix A7: Comprehensive data of the SEM and EDX examinations willow sample at 750 ^{0}C.

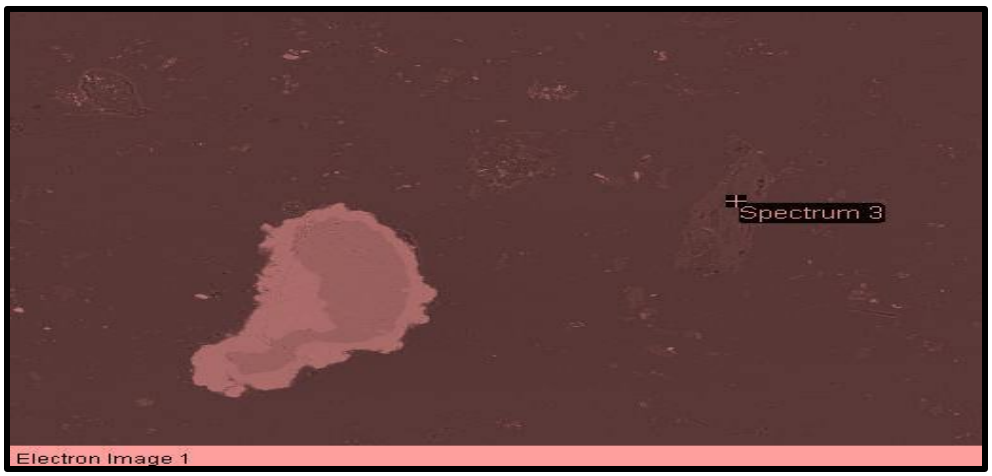

Figure 9-31 SEM image of willow sample at 750 ^{0}C Celsius

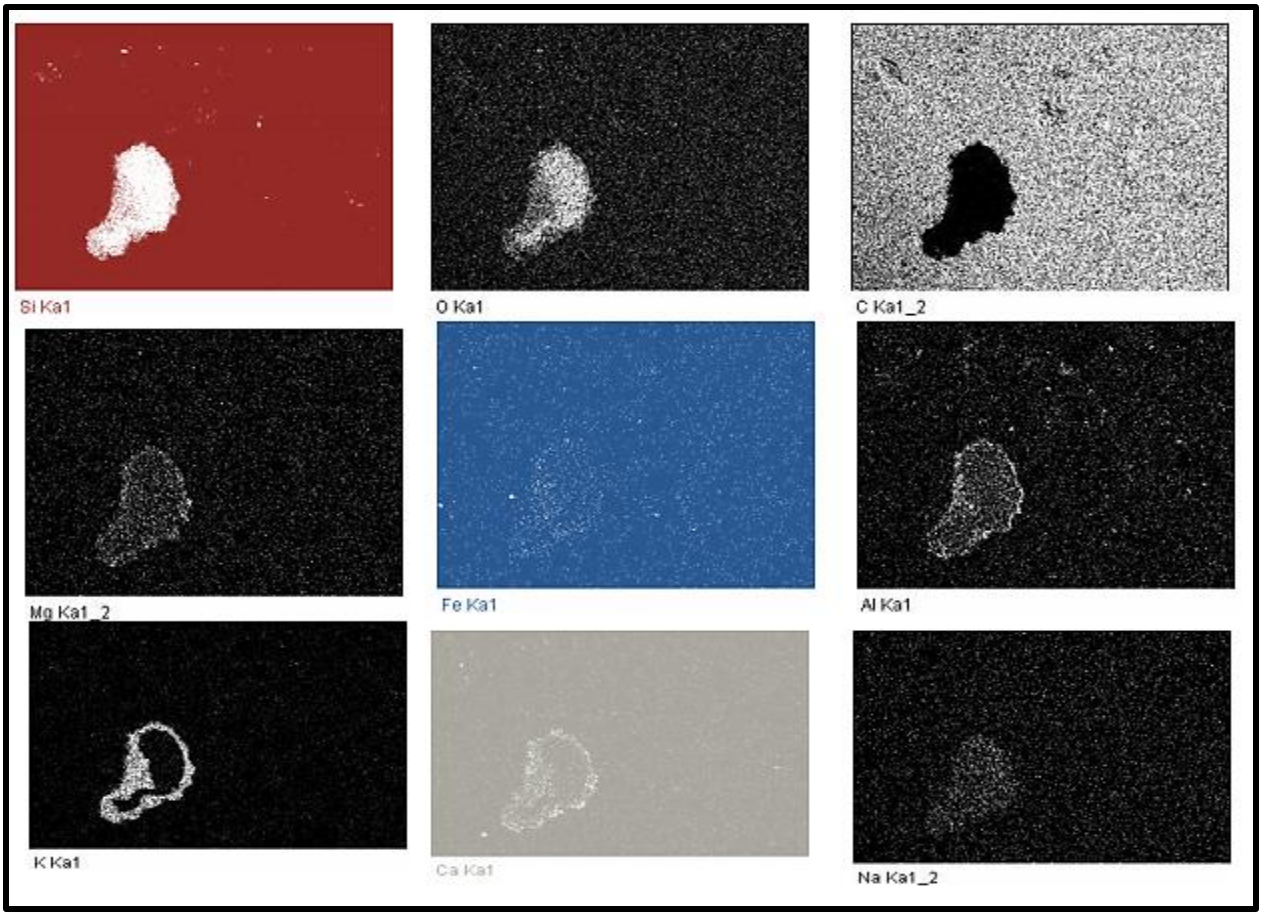

Figure 9-32 Element mapping of willow sample at 750 ^{0}C Celsius

Figure 9-33 EDX Spot analysis of willow sample at 750 ^{0}C (spectrum 1)

Spectrum processing:
No peaks omitted

Processing option: All elements analysed
Number of iterations = 7

Standard:
C CaCO3 1-Jun-1999 12:00 AM
O SiO2 1-Jun-1999 12:00 AM
Si SiO2 1-Jun-1999 12:00 AM

Element	Weight%	Atomic%
C K	108.89	40.19
O K	167.58	46.43
Si K	84.81	13.39
Totals	361.28	

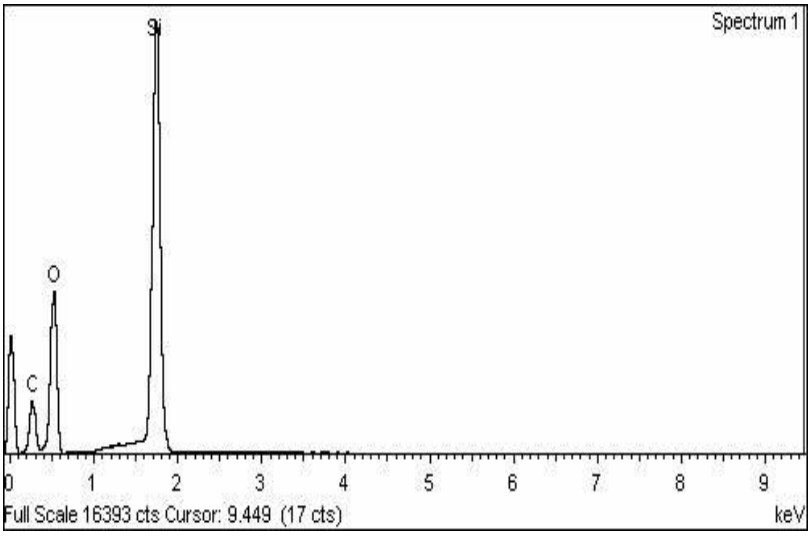

Appendix A8: Comprehensive data of the SEM and EDX examinations of the mixture of willow + miscanthus samples at 802 ^{0}C

Figure 9-34 SEM image of the mixture of willow + miscanthus sample at 802 ^{0}C

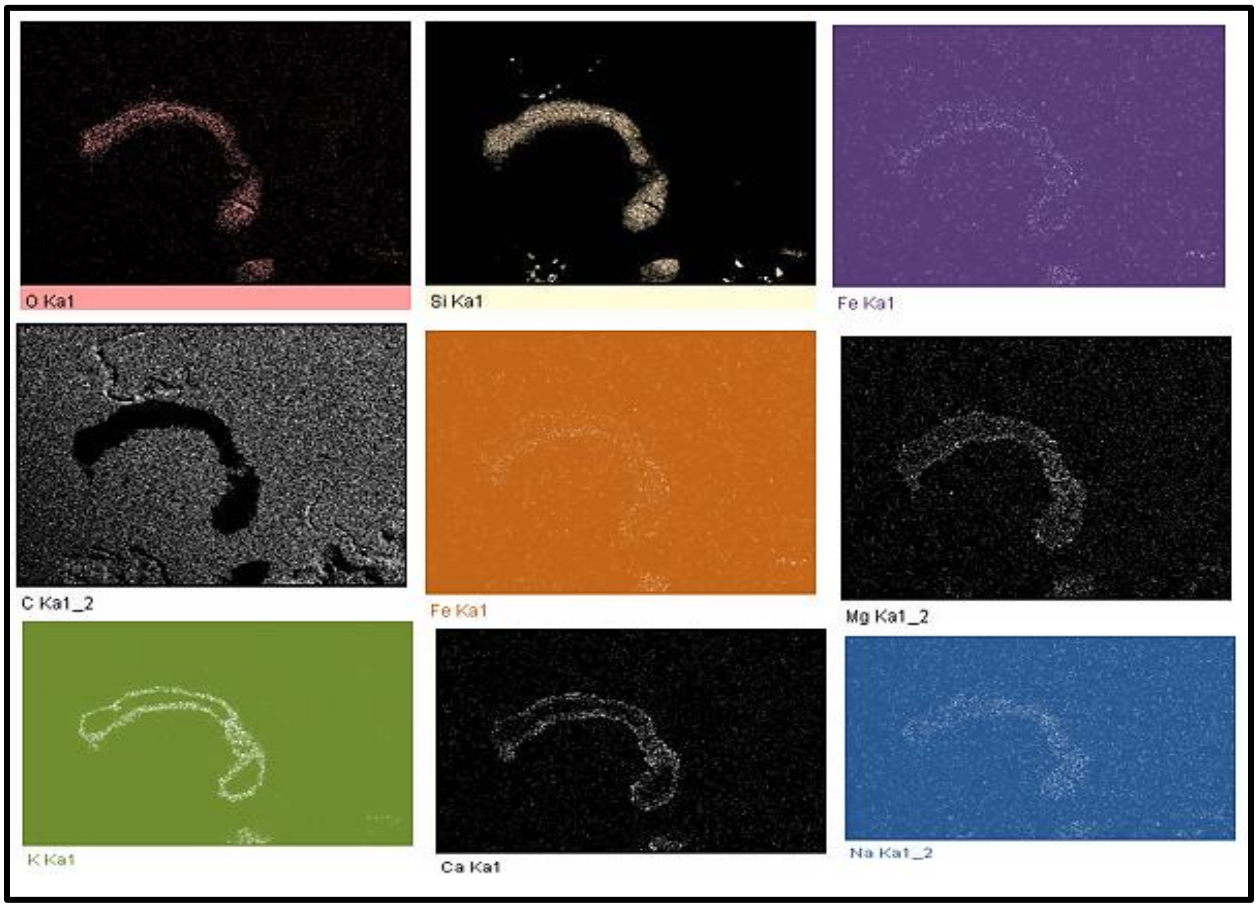

Figure 9-35 Element mapping of the mixture of willow + miscanthus sample at 802 ^{0}C

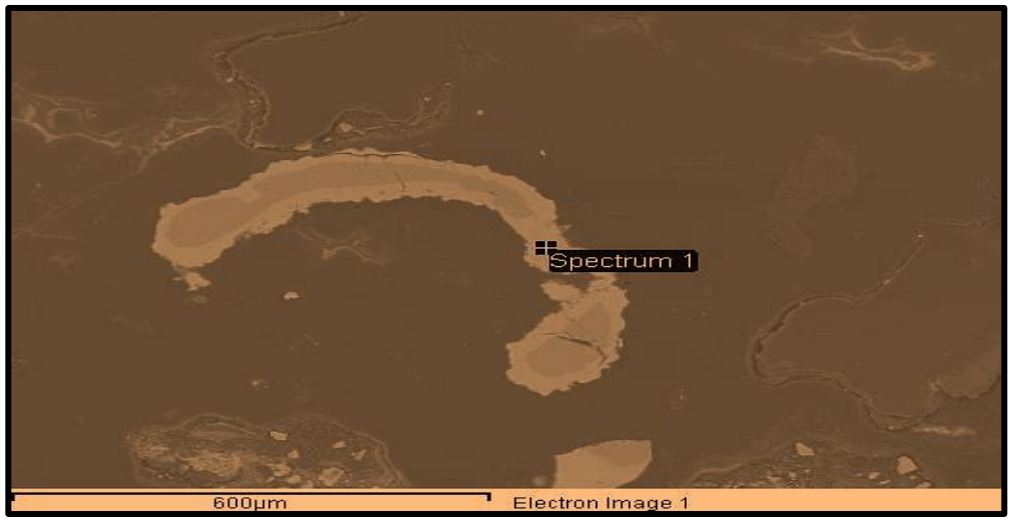

Figure 9-36 EDX Spot analysis of the mixture of willow + miscanthus sample at 802 ^{0}C (spectrum 1)

Processing option: All elements analysed
Number of iterations = 6

C CaCO3 1-Jun-1999 12:00 AM
O SiO2 1-Jun-1999 12:00 AM
Na Albite 1-Jun-1999 12:00 AM
Mg MgO 1-Jun-1999 12:00 AM
Si SiO2 1-Jun-1999 12:00 AM
K MAD-10 Feldspar 1-Jun-1999 12:00 AM
Ca Wollastonite 1-Jun-1999 12:00 AM
Fe Fe 1-Jun-1999 12:00 AM

Element	Weight%	Atomic%
C K	66.54	37.07
O K	106.51	44.54
Na K	0.09	0.03
Mg K	1.30	0.36
Si K	66.62	15.87
K K	9.93	1.70
Ca K	2.01	0.34
Fe K	0.83	0.10
Totals	253.84	

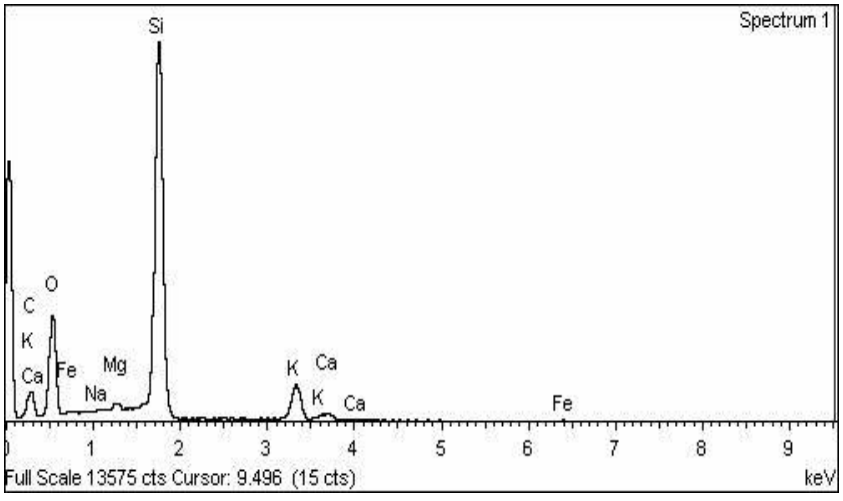

Appendix A9: Comprehensive data of the SEM and EDX examinations of the willow sample at 802 ^{0}C

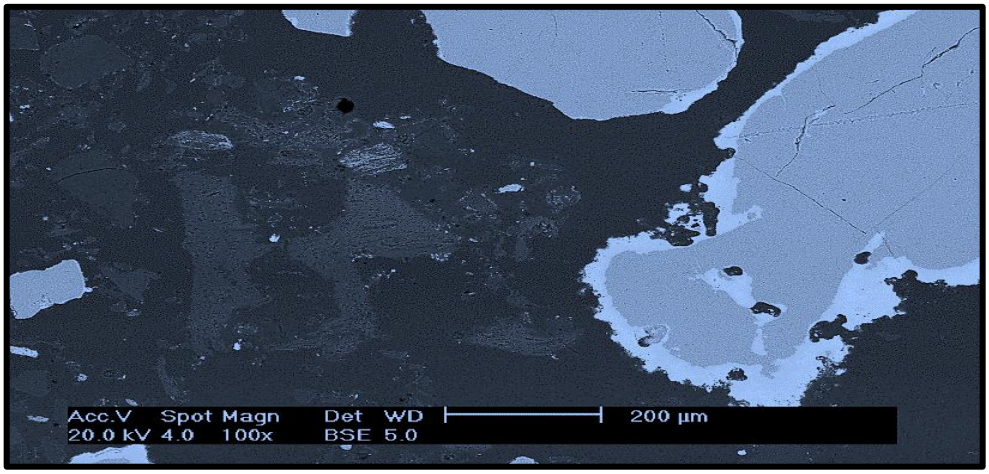

Figure 9-37 SEM image of willow sample at 802 ^{0}C

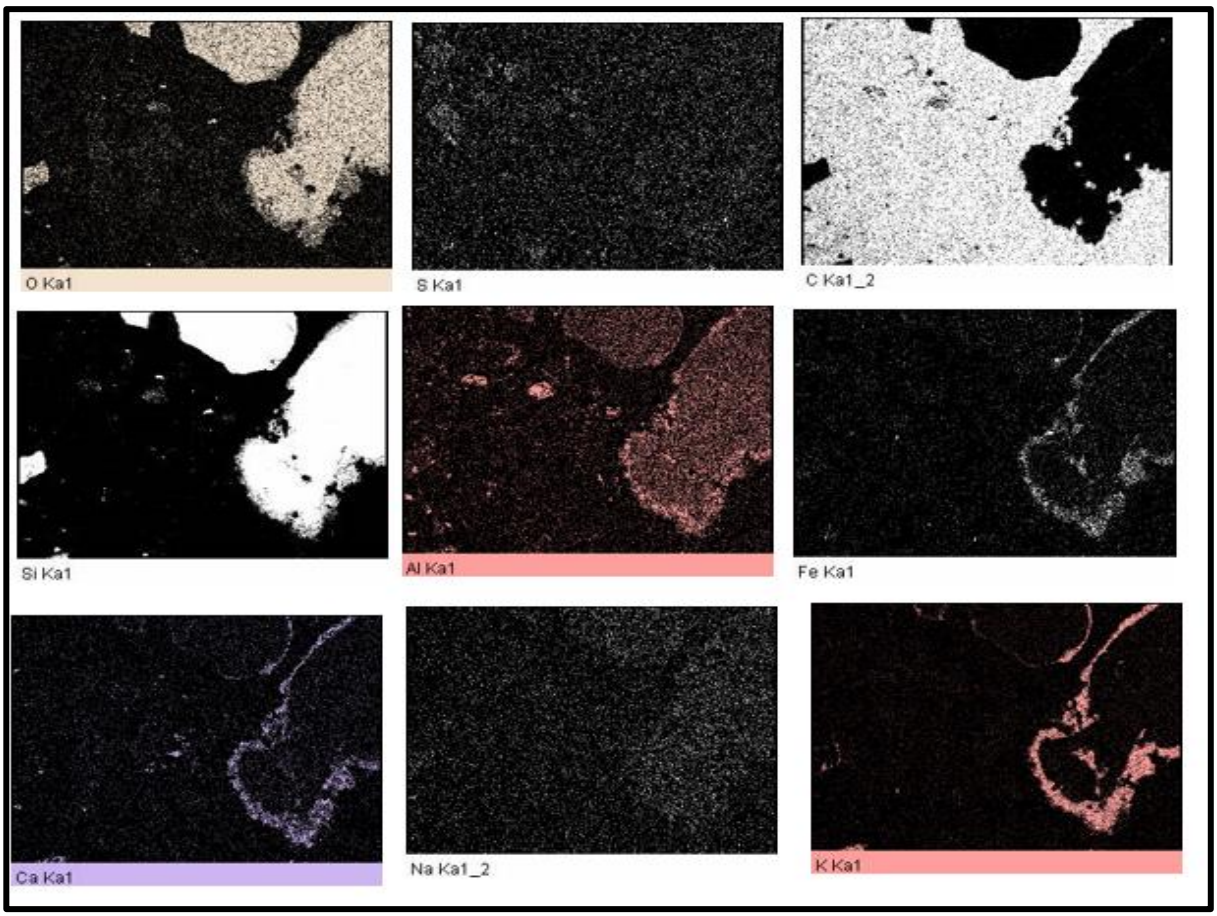

Figure 9-38 Element mapping of willow sample at 802 ^{0}C

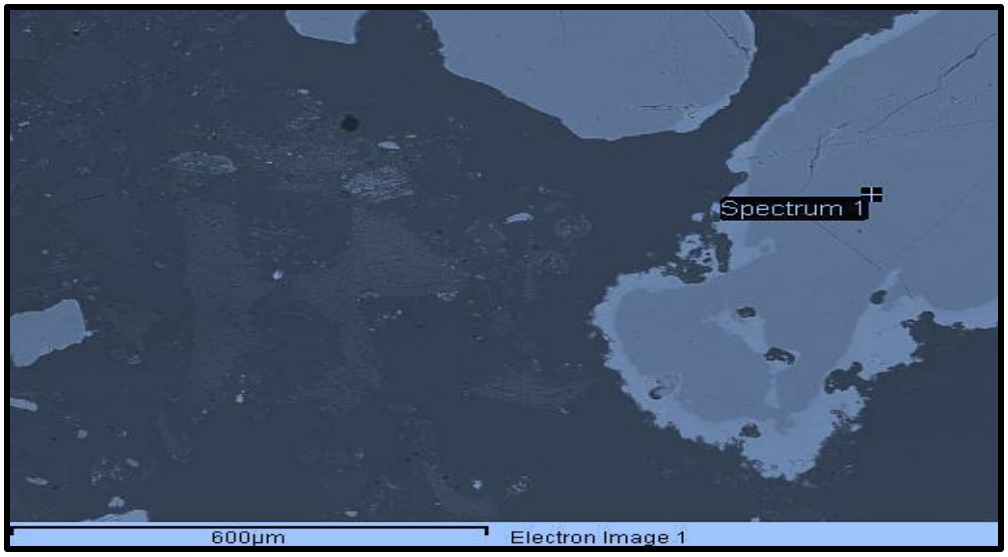

Figure 9-39 EDX Spot analysis of willow sample at 802 ^{0}C (spectrum 1)

Spectrum processing:
Peak possibly omitted: 10.605 keV
Processing option: All elements analysed
Number of iterations = 6

Standard:
C CaCO3 1-Jun-1999 12:00 AM
O SiO2 1-Jun-1999 12:00 AM
Si SiO2 1-Jun-1999 12:00 AM

Element	Weight%	Atomic%
C K	68.39	32.40
O K	141.76	50.41
Si K	84.84	17.19
Totals	294.99	

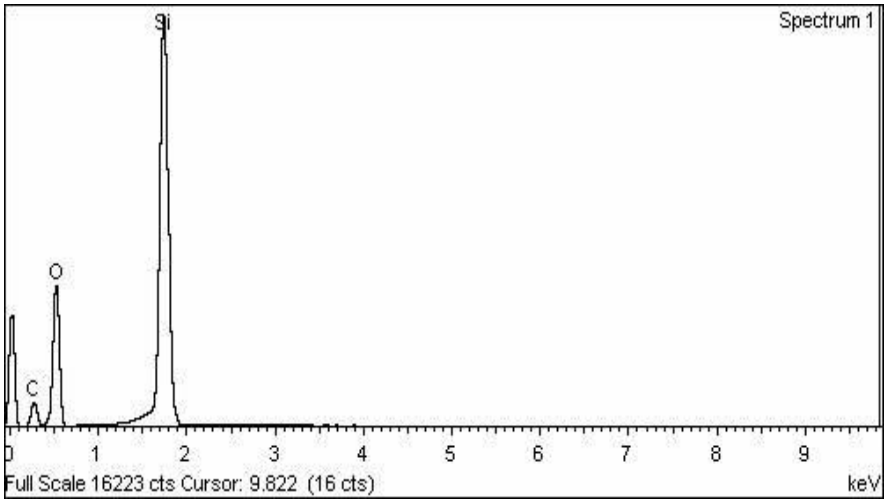

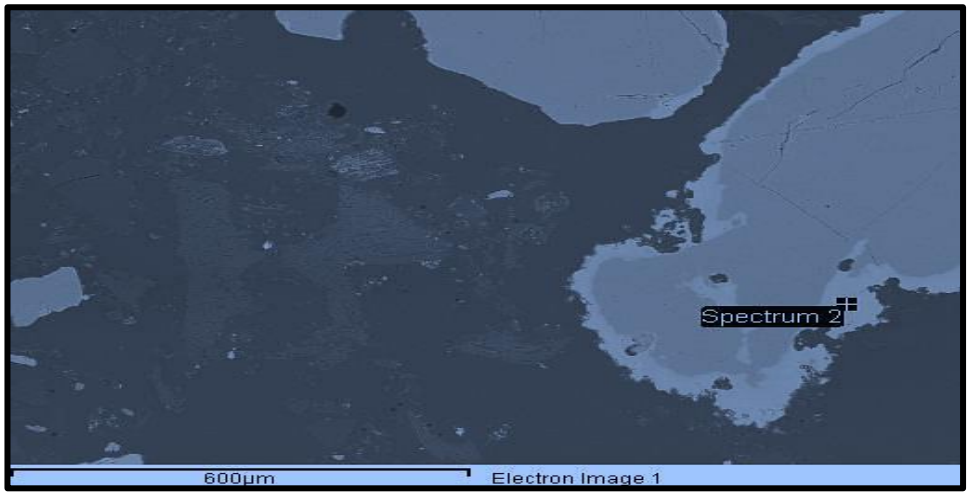

Figure 9-40 EDX Spot analysis of willow sample at 802 ^{0}C (spectrum 2)

C CaCO3 1-Jun-1999 12:00 AM
O SiO2 1-Jun-1999 12:00 AM
Na Albite 1-Jun-1999 12:00 AM
Mg MgO 1-Jun-1999 12:00 AM
Al Al2O3 1-Jun-1999 12:00 AM
Si SiO2 1-Jun-1999 12:00 AM
P GaP 1-Jun-1999 12:00 AM
S FeS2 1-Jun-1999 12:00 AM
K MAD-10 Feldspar 1-Jun-1999 12:00 AM
Ca Wollastonite 1-Jun-1999 12:00 AM
Fe Fe 1-Jun-1999 12:00 AM

Element	Weight%	Atomic%
C K	67.14	38.06
O K	101.17	43.05
Na K	0.26	0.08
Mg K	3.20	0.90
Al K	1.33	0.34
Si K	43.95	10.65
P K	0.38	0.08
S K	0.15	0.03
K K	25.39	4.42
Ca K	1.07	0.18
Fe K	18.16	2.21
Totals	262.19	

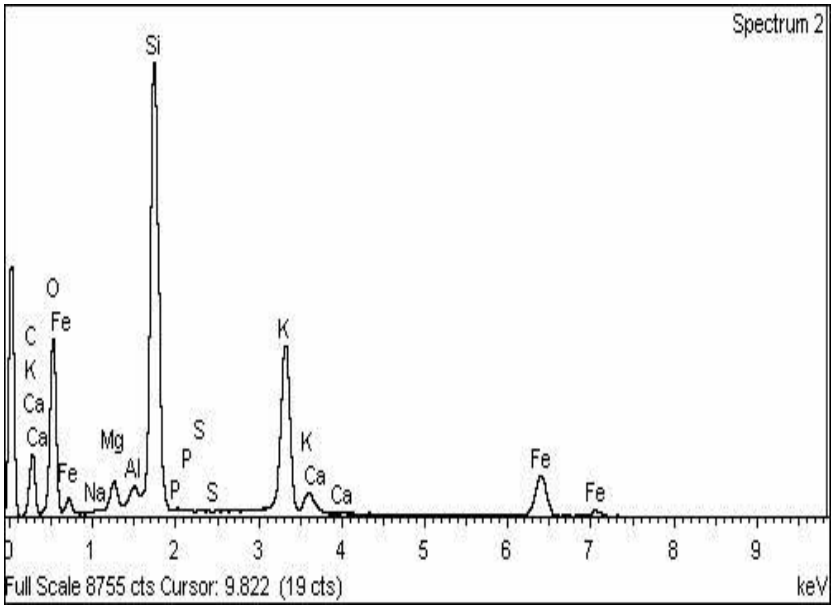

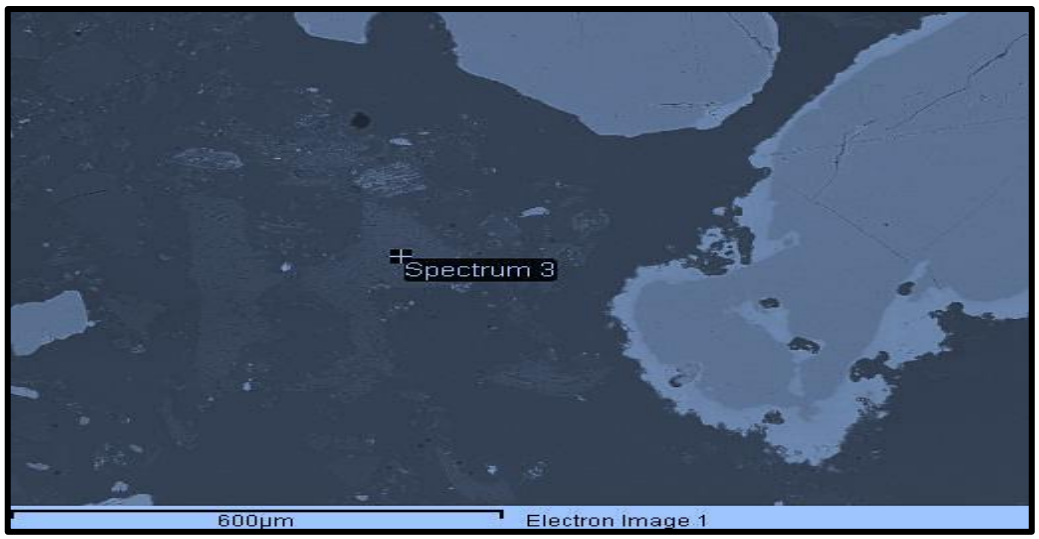

Figure 9-41 EDX Spot analysis of willow sample at 802 ^{0}C (spectrum 3)

Spectrum processing:
No peaks omitted
Processing option: All elements analysed
Number of iterations = 4
Standard:
C CaCO3 1-Jun-1999 12:00 AM
O SiO2 1-Jun-1999 12:00 AM
Na Albite 1-Jun-1999 12:00 AM
Mg MgO 1-Jun-1999 12:00 AM
Si SiO2 1-Jun-1999 12:00 AM
S FeS2 1-Jun-1999 12:00 AM
Ca Wollastonite 1-Jun-1999 12:00 AM

Element	Weight%	Atomic%
C K	166.84	82.83
O K	45.28	16.88
Na K	0.22	0.06
Mg K	0.10	0.03
Si K	0.58	0.12
S K	0.14	0.03
Ca K	0.40	0.06
Totals	213.56	

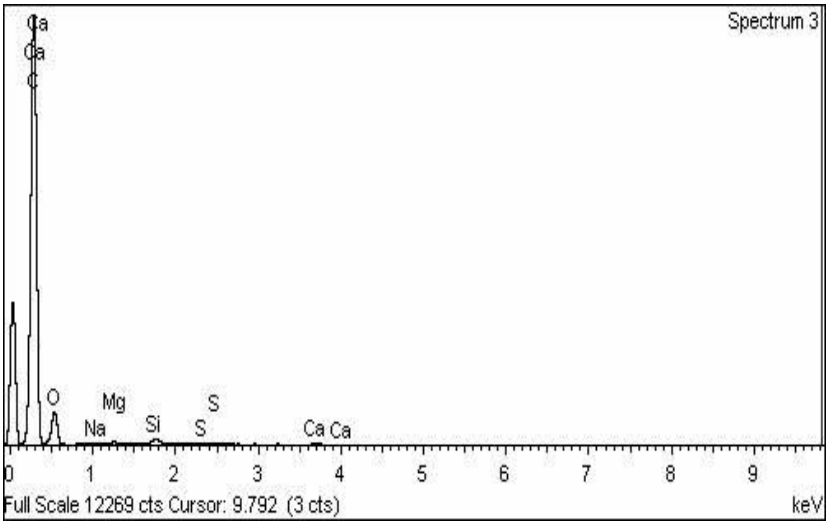

Appendix A10: Comprehensive data of the SEM and EDX examinations of miscanthus sample at 802 ^{0}C

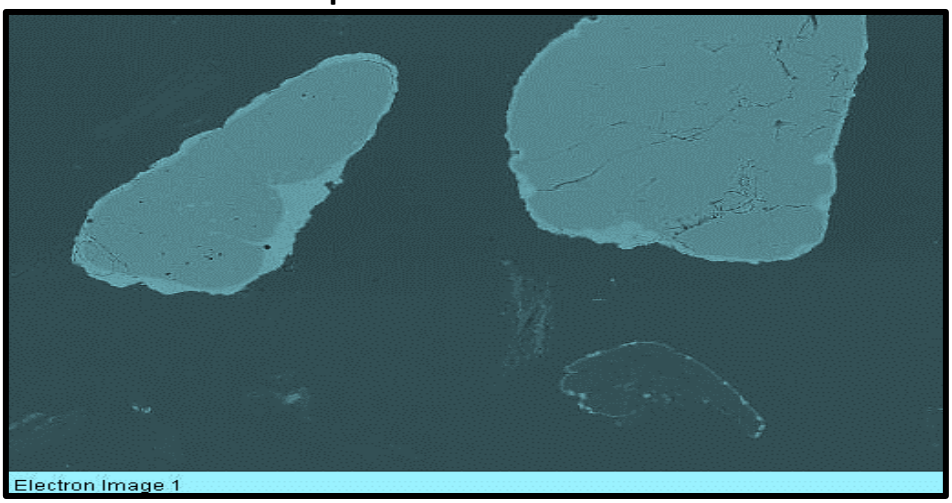

Figure 9-42SEM image of miscanthus sample at 802 ^{0}C

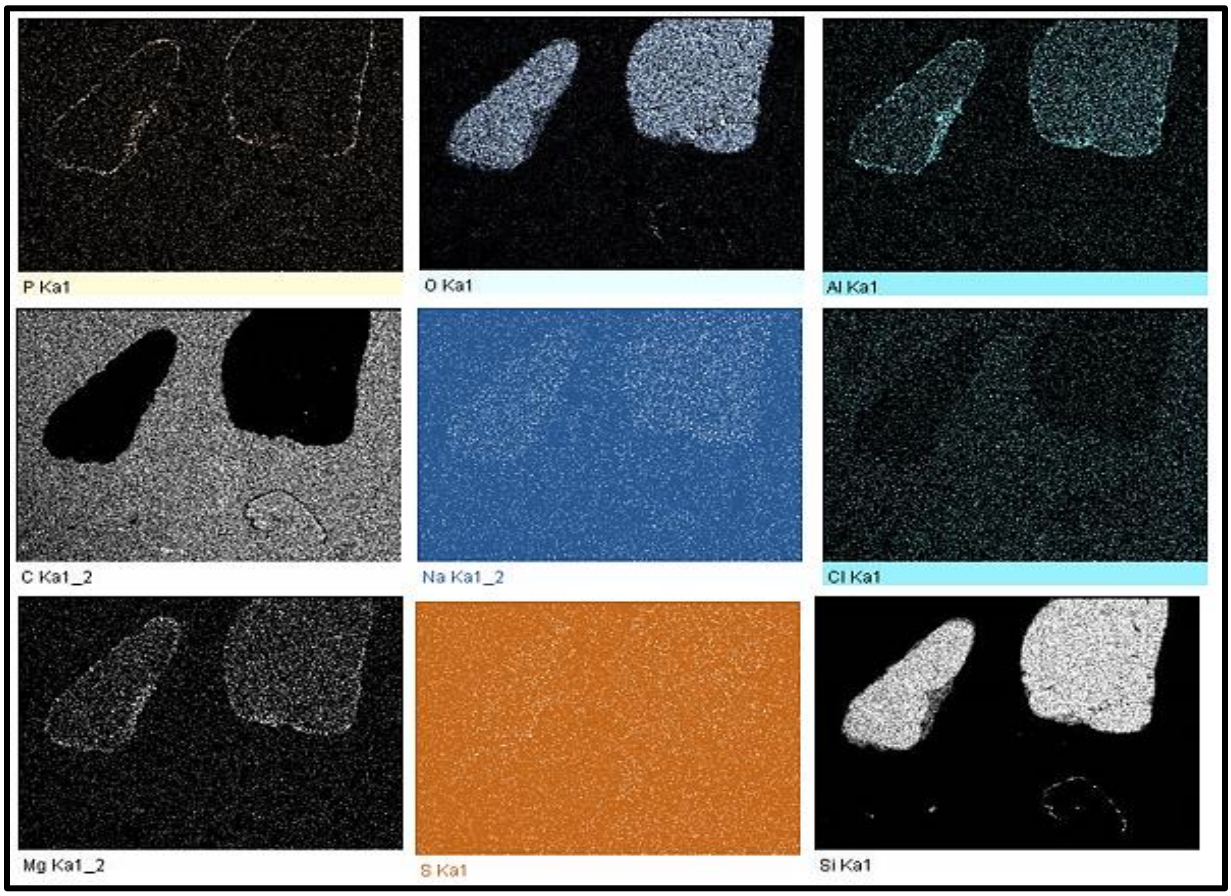

Figure 9-43 Element mapping of miscanthus sample at 802 ^{0}C

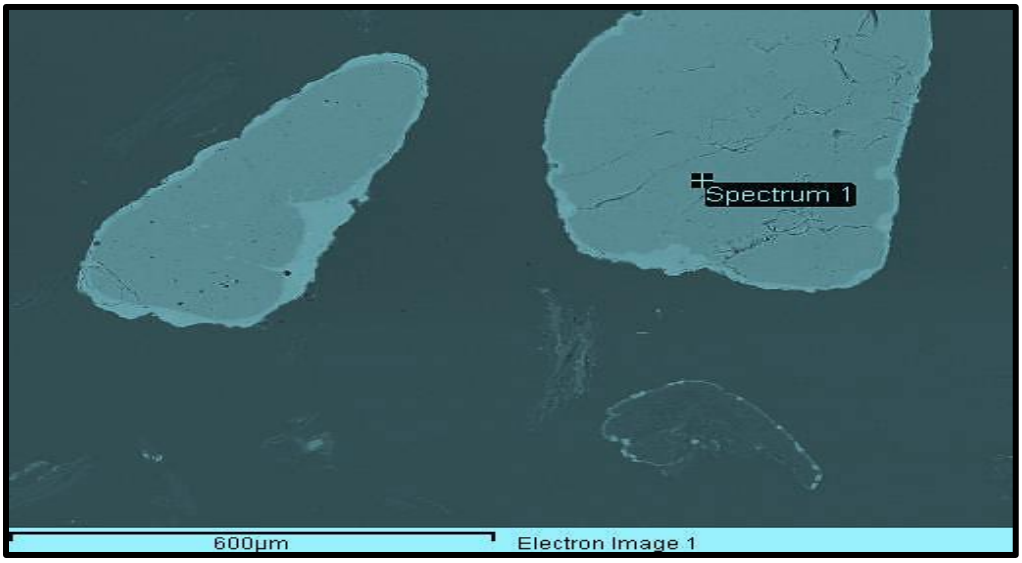

Figure 9-44 EDX Spot analysis of miscanthus sample at 802 ^{0}C (spectrum 1)

Spectrum processing:
No peaks omitted

Processing option: All elements analysed
Number of iterations = 6

Standard:
C CaCO3 1-Jun-1999 12:00 AM
O SiO2 1-Jun-1999 12:00 AM
Si SiO2 1-Jun-1999 12:00 AM

Element	Weight%	Atomic%
C K	54.51	29.93
O K	126.81	52.27
Si K	75.84	17.81
Totals	257.15	

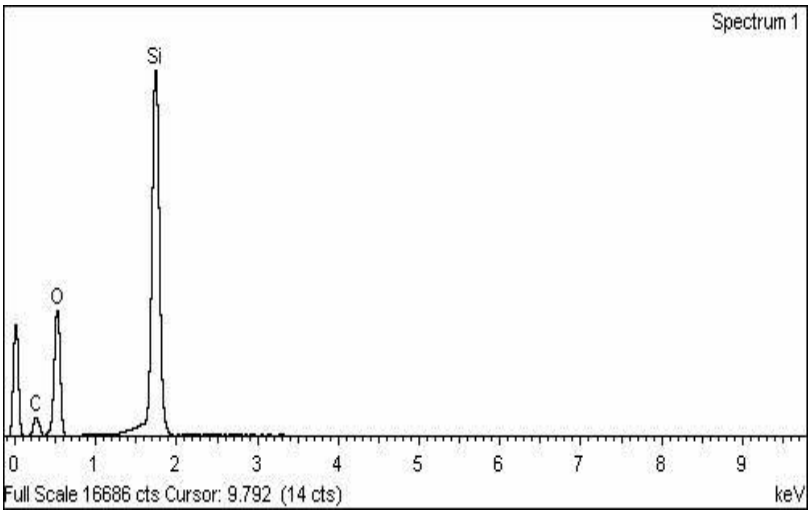

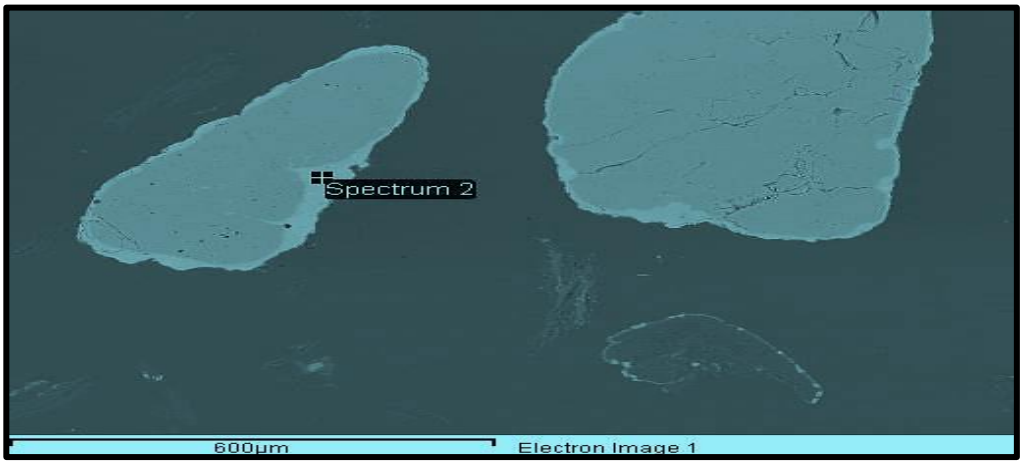

Figure 9-45 EDX Spot analysis of miscanthus sample at 802 ^{0}C (spectrum 2)

Processing option : All elements analysed
Number of iterations = 6
C CaCO3 1-Jun-1999 12:00 AM
O SiO2 1-Jun-1999 12:00 AM
Na Albite 1-Jun-1999 12:00 AM
Mg MgO 1-Jun-1999 12:00 AM
Al Al2O3 1-Jun-1999 12:00 AM
Si SiO2 1-Jun-1999 12:00 AM
P GaP 1-Jun-1999 12:00 AM
K MAD-10 Feldspar 1-Jun-1999 12:00 AM
Ca Wollastonite 1-Jun-1999 12:00 AM
Fe Fe 1-Jun-1999 12:00 AM

Element	Weight%	Atomic%
C K	157.23	57.91
O K	116.05	32.09
Na K	0.22	0.04
Mg K	2.63	0.48
Al K	1.70	0.28
Si K	42.30	6.66
P K	0.65	0.09
K K	15.62	1.77
Ca K	3.21	0.35
Fe K	4.10	0.32
Totals	343.71	

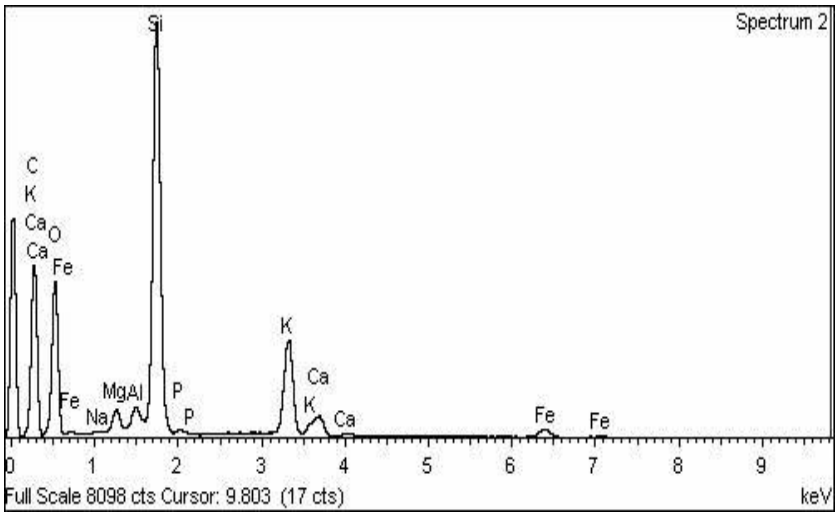

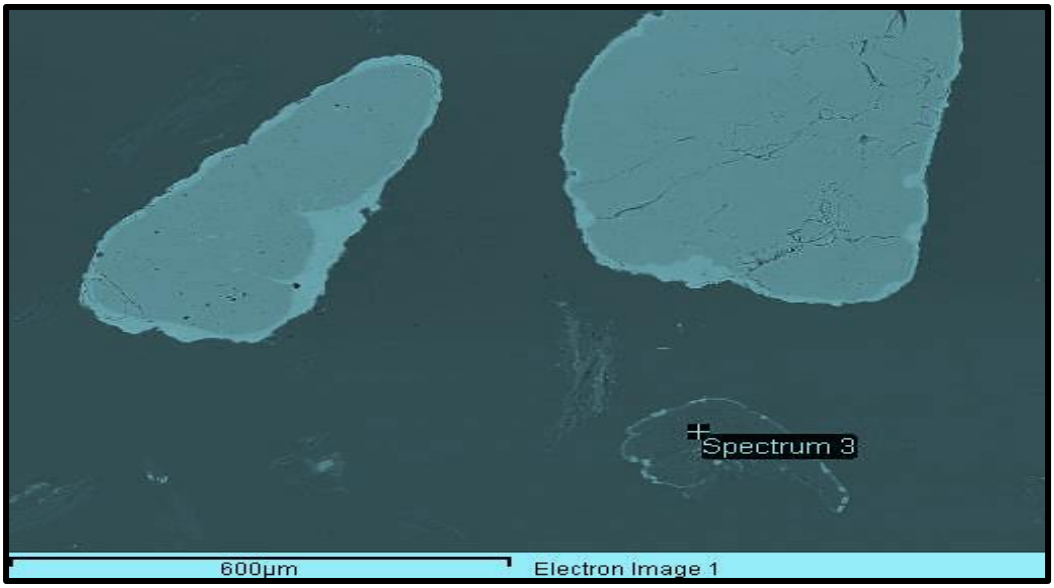

Figure 9-46 EDX Spot analysis of miscanthus sample at 802 ^{0}C (spectrum 3)

Spectrum processing:
No peaks omitted

Processing option: All elements analysed
Number of iterations = 3

Standard:
C CaCO3 1-Jun-1999 12:00 AM
O SiO2 1-Jun-1999 12:00 AM
Cl KCl 1-Jun-1999 12:00 AM
K MAD-10 Feldspar 1-Jun-1999 12:00 AM
Ca Wollastonite 1-Jun-1999 12:00 AM

Element	Weight%	Atomic%
C K	195.28	85.21
O K	43.83	14.36
Cl K	0.83	0.12
K K	0.79	0.11
Ca K	1.59	0.21
Totals	242.31	

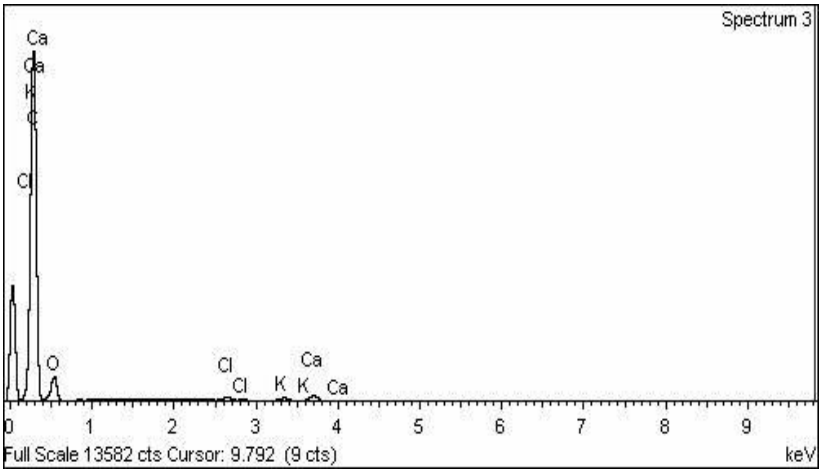

Appendix B: Detailed data of the experimental error analysis

ERROR ANALYSIS

PRE-HEATED SAND + Willow+ coal

(N) Sec	(X) °C	X-Ave	X - XAVG	(X - X-AVG)^2	((X - X-AVG)^2)/N	sqr(((X - X-AVG)^2)/N)
1	56.78	56.78	-340.62	116021.51	12.87	3.59
2	57.03	28.52	-340.37	115851.26	12.85	3.58
3	57.37	19.12	-340.03	115619.93	12.83	3.58
4	57.72	14.43	-339.68	115382.03	12.80	3.58
5	58.07	11.61	-339.33	115144.37	12.77	3.57
6	58.42	9.74	-338.98	114906.97	12.75	3.57
7	58.77	8.40	-338.63	114669.80	12.72	3.57
8	59.11	7.39	-338.29	114439.65	12.69	3.56
9	59.45	6.61	-337.95	114209.73	12.67	3.56
10	59.83	5.98	-337.57	113953.03	12.64	3.56
11	60.18	5.47	-337.22	113716.86	12.61	3.55
12	60.49	5.04	-336.91	113507.88	12.59	3.55
13	60.84	4.68	-336.56	113272.16	12.56	3.54
14	61.19	4.37	-336.21	113036.69	12.54	3.54
15	61.54	4.10	-335.86	112801.47	12.51	3.54
16	61.89	3.87	-335.51	112566.49	12.49	3.53
17	62.23	3.66	-335.17	112338.46	12.46	3.53
18	62.57	3.48	-334.83	112110.66	12.44	3.53
19	62.92	3.31	-334.48	111876.40	12.41	3.52
20	63.26	3.16	-334.14	111649.07	12.38	3.52
21	63.61	3.03	-333.79	111415.30	12.36	3.52
22	63.95	2.91	-333.45	111188.44	12.33	3.51
23	64.29	2.80	-333.11	110961.81	12.31	3.51
24	64.64	2.69	-332.76	110728.75	12.28	3.50
25	65.01	2.60	-332.39	110482.65	12.26	3.50
26	65.39	2.52	-332.01	110230.18	12.23	3.50
27	65.72	2.43	-331.68	110011.16	12.20	3.49
28	66.06	2.36	-331.34	109785.73	12.18	3.49
29	66.4	2.29	-331.00	109560.54	12.15	3.49
30	66.74	2.22	-330.66	109335.57	12.13	3.48
31	67.08	2.16	-330.32	109110.84	12.10	3.48
32	67.41	2.11	-329.99	108892.94	12.08	3.48
33	67.75	2.05	-329.65	108668.66	12.05	3.47
34	68.09	2.00	-329.31	108444.62	12.03	3.47
35	68.43	1.96	-328.97	108220.80	12.00	3.46
36	68.76	1.91	-328.64	108003.79	11.98	3.46

37	69.1	1.87	-328.30	107780.43	11.96	3.46
38	69.44	1.83	-327.96	107557.30	11.93	3.45
39	69.77	1.79	-327.63	107340.96	11.91	3.45
40	70.11	1.75	-327.29	107118.29	11.88	3.45
41	70.45	1.72	-326.95	106895.85	11.86	3.44
42	70.78	1.69	-326.62	106680.17	11.83	3.44
43	71.12	1.65	-326.28	106458.18	11.81	3.44
44	71.46	1.62	-325.94	106236.43	11.78	3.43
45	71.79	1.60	-325.61	106021.42	11.76	3.43
46	72.13	1.57	-325.27	105800.12	11.74	3.43
47	72.46	1.54	-324.94	105585.55	11.71	3.42
48	72.8	1.52	-324.60	105364.71	11.69	3.42
49	73.13	1.49	-324.27	105150.58	11.66	3.42
50	73.46	1.47	-323.94	104936.67	11.64	3.41
51	73.8	1.45	-323.60	104716.51	11.62	3.41
52	74.14	1.43	-323.26	104496.58	11.59	3.40
53	74.44	1.40	-322.96	104302.71	11.57	3.40
54	74.74	1.38	-322.66	104109.02	11.55	3.40
55	75.07	1.36	-322.33	103896.18	11.52	3.39
56	75.41	1.35	-321.99	103677.11	11.50	3.39
57	75.75	1.33	-321.65	103458.27	11.48	3.39
58	76.08	1.31	-321.32	103246.09	11.45	3.38
59	76.41	1.30	-320.99	103034.13	11.43	3.38
60	76.75	1.28	-320.65	102815.97	11.40	3.38
61	77.08	1.26	-320.32	102604.45	11.38	3.37
62	77.41	1.25	-319.99	102393.15	11.36	3.37
63	77.75	1.23	-319.65	102175.68	11.33	3.37
64	78.11	1.22	-319.29	101945.66	11.31	3.36
65	78.48	1.21	-318.92	101709.52	11.28	3.36
66	78.81	1.19	-318.59	101499.14	11.26	3.36
67	79.15	1.18	-318.25	101282.62	11.23	3.35
68	79.48	1.17	-317.92	101072.68	11.21	3.35
69	79.81	1.16	-317.59	100862.96	11.19	3.34
70	80.14	1.14	-317.26	100653.46	11.17	3.34
71	80.46	1.13	-316.94	100450.52	11.14	3.34
72	80.8	1.12	-316.60	100235.12	11.12	3.33
73	81.12	1.11	-316.28	100032.60	11.10	3.33
74	81.45	1.10	-315.95	99823.96	11.07	3.33
75	81.78	1.09	-315.62	99615.54	11.05	3.32
76	82.11	1.08	-315.29	99407.34	11.03	3.32
77	82.44	1.07	-314.96	99199.36	11.00	3.32
78	82.77	1.06	-314.63	98991.60	10.98	3.31

79	83.09	1.05	-314.31	98790.34	10.96	3.31
80	83.41	1.04	-313.99	98589.28	10.94	3.31
81	83.74	1.03	-313.66	98382.16	10.91	3.30
82	84.06	1.03	-313.34	98181.52	10.89	3.30
83	84.39	1.02	-313.01	97974.82	10.87	3.30
84	84.71	1.01	-312.69	97774.60	10.85	3.29
85	85.04	1.00	-312.36	97568.33	10.82	3.29
86	85.36	0.99	-312.04	97368.53	10.80	3.29
87	85.68	0.98	-311.72	97168.92	10.78	3.28
88	86	0.98	-311.40	96969.52	10.76	3.28
89	86.32	0.97	-311.08	96770.33	10.73	3.28
90	86.64	0.96	-310.76	96571.34	10.71	3.27
91	86.97	0.96	-310.43	96366.35	10.69	3.27
92	87.28	0.95	-310.12	96173.98	10.67	3.27
93	87.6	0.94	-309.80	95975.61	10.65	3.26
94	87.92	0.94	-309.48	95777.44	10.62	3.26
95	88.2	0.93	-309.20	95604.21	10.61	3.26
96	88.49	0.92	-308.91	95424.96	10.59	3.25
97	88.8	0.92	-308.60	95233.53	10.56	3.25
98	89.13	0.91	-308.27	95029.96	10.54	3.25
99	89.44	0.90	-307.96	94838.93	10.52	3.24
100	89.75	0.90	-307.65	94648.09	10.50	3.24
101	90.07	0.89	-307.33	94451.30	10.48	3.24
102	90.38	0.89	-307.02	94260.85	10.46	3.23
103	90.73	0.88	-306.67	94046.06	10.43	3.23
104	91.06	0.88	-306.34	93843.77	10.41	3.23
105	91.37	0.87	-306.03	93653.93	10.39	3.22
106	91.69	0.87	-305.71	93458.18	10.37	3.22
107	92.01	0.86	-305.39	93262.63	10.35	3.22
108	92.32	0.85	-305.08	93073.38	10.32	3.21
109	92.63	0.85	-304.77	92884.33	10.30	3.21
110	92.94	0.84	-304.46	92695.47	10.28	3.21
111	93.25	0.84	-304.15	92506.80	10.26	3.20
112	93.56	0.84	-303.84	92318.32	10.24	3.20
113	93.88	0.83	-303.52	92123.97	10.22	3.20
114	94.18	0.83	-303.22	91941.94	10.20	3.19
115	94.49	0.82	-302.91	91754.04	10.18	3.19
116	94.8	0.82	-302.60	91566.34	10.16	3.19
117	95.11	0.81	-302.29	91378.82	10.14	3.18
118	95.42	0.81	-301.98	91191.50	10.12	3.18
119	95.73	0.80	-301.67	91004.37	10.09	3.18
120	96.04	0.80	-301.36	90817.43	10.07	3.17

121	96.34	0.80	-301.06	90636.70	10.05	3.17
122	96.65	0.79	-300.75	90450.14	10.03	3.17
123	96.96	0.79	-300.44	90263.77	10.01	3.16
124	97.26	0.78	-300.14	90083.60	9.99	3.16
125	97.57	0.78	-299.83	89897.61	9.97	3.16
126	97.87	0.78	-299.53	89717.80	9.95	3.15
127	98.17	0.77	-299.23	89538.17	9.93	3.15
128	98.48	0.77	-298.92	89352.75	9.91	3.15
129	98.79	0.77	-298.61	89167.51	9.89	3.14
130	99.09	0.76	-298.31	88988.44	9.87	3.14
131	99.39	0.76	-298.01	88809.54	9.85	3.14
132	99.69	0.76	-297.71	88630.83	9.83	3.14
133	99.99	0.75	-297.41	88452.29	9.81	3.13
134	100.29	0.75	-297.11	88273.94	9.79	3.13
135	100.58	0.75	-296.82	88101.70	9.77	3.13
136	100.88	0.74	-296.52	87923.70	9.75	3.12
137	101.14	0.74	-296.26	87769.57	9.74	3.12
138	101.4	0.73	-296.00	87615.59	9.72	3.12
139	101.69	0.73	-295.71	87443.99	9.70	3.11
140	102.01	0.73	-295.39	87254.84	9.68	3.11
141	102.33	0.73	-295.07	87065.89	9.66	3.11
142	102.62	0.72	-294.78	86894.84	9.64	3.10
143	102.91	0.72	-294.49	86723.95	9.62	3.10
144	103.19	0.72	-294.21	86559.11	9.60	3.10
145	103.48	0.71	-293.92	86388.56	9.58	3.10
146	103.77	0.71	-293.63	86218.17	9.56	3.09
147	104.06	0.71	-293.34	86047.95	9.54	3.09
148	104.32	0.70	-293.08	85895.48	9.53	3.09
149	104.58	0.70	-292.82	85743.14	9.51	3.08
150	104.86	0.70	-292.54	85579.24	9.49	3.08
151	105.14	0.70	-292.26	85415.50	9.47	3.08
152	105.46	0.69	-291.94	85228.56	9.45	3.07
153	105.78	0.69	-291.62	85041.82	9.43	3.07
154	106.06	0.69	-291.34	84878.59	9.42	3.07
155	106.35	0.69	-291.05	84709.70	9.40	3.07
156	106.64	0.68	-290.76	84540.97	9.38	3.06
157	106.93	0.68	-290.47	84372.41	9.36	3.06
158	107.22	0.68	-290.18	84204.03	9.34	3.06
159	107.48	0.68	-289.92	84053.20	9.32	3.05
160	107.73	0.67	-289.67	83908.30	9.31	3.05
161	108.02	0.67	-289.38	83740.38	9.29	3.05
162	108.34	0.67	-289.06	83555.28	9.27	3.04

163	108.66	0.67	-288.74	83370.38	9.25	3.04
164	108.95	0.66	-288.45	83203.00	9.23	3.04
165	109.23	0.66	-288.17	83041.55	9.21	3.04
166	109.52	0.66	-287.88	82874.49	9.19	3.03
167	109.8	0.66	-287.60	82713.36	9.18	3.03
168	110.1	0.66	-287.30	82540.89	9.16	3.03
169	110.38	0.65	-287.02	82380.08	9.14	3.02
170	110.66	0.65	-286.74	82219.43	9.12	3.02
171	110.95	0.65	-286.45	82053.20	9.10	3.02
172	111.23	0.65	-286.17	81892.87	9.08	3.01
173	111.51	0.64	-285.89	81732.69	9.07	3.01
174	111.79	0.64	-285.61	81572.67	9.05	3.01
175	112.07	0.64	-285.33	81412.81	9.03	3.01
176	112.35	0.64	-285.05	81253.10	9.01	3.00
177	112.63	0.64	-284.77	81093.55	9.00	3.00
178	112.91	0.63	-284.49	80934.16	8.98	3.00
179	113.19	0.63	-284.21	80774.93	8.96	2.99
180	113.46	0.63	-283.94	80621.53	8.94	2.99
181	113.74	0.63	-283.66	80462.60	8.93	2.99
182	114.02	0.63	-283.38	80303.83	8.91	2.98
183	114.29	0.62	-283.11	80150.88	8.89	2.98
184	114.57	0.62	-282.83	79992.41	8.87	2.98
185	114.85	0.62	-282.55	79834.11	8.86	2.98
186	115.12	0.62	-282.28	79681.60	8.84	2.97
187	115.39	0.62	-282.01	79529.25	8.82	2.97
188	115.66	0.62	-281.74	79377.03	8.80	2.97
189	115.93	0.61	-281.47	79224.97	8.79	2.96
190	116.2	0.61	-281.20	79073.05	8.77	2.96
191	116.47	0.61	-280.93	78921.27	8.75	2.96
192	116.74	0.61	-280.66	78769.64	8.74	2.96
193	117.01	0.61	-280.39	78618.16	8.72	2.95
194	117.28	0.60	-280.12	78466.82	8.70	2.95
195	117.55	0.60	-279.85	78315.63	8.69	2.95
196	117.81	0.60	-279.59	78170.18	8.67	2.94
197	118.08	0.60	-279.32	78019.27	8.65	2.94
198	118.35	0.60	-279.05	77868.51	8.64	2.94
199	118.61	0.60	-278.79	77723.47	8.62	2.94
200	118.88	0.59	-278.52	77573.00	8.60	2.93
201	119.12	0.59	-278.28	77439.37	8.59	2.93
202	119.38	0.59	-278.02	77294.73	8.57	2.93
203	119.67	0.59	-277.73	77133.56	8.56	2.93
204	119.93	0.59	-277.47	76989.21	8.54	2.92

205	120.19	0.59	-277.21	76845.00	8.52	2.92
206	120.45	0.58	-276.95	76700.92	8.51	2.92
207	120.71	0.58	-276.69	76556.97	8.49	2.91
208	120.98	0.58	-276.42	76407.63	8.48	2.91
209	121.23	0.58	-276.17	76269.48	8.46	2.91
210	121.49	0.58	-275.91	76125.94	8.44	2.91
211	121.74	0.58	-275.66	75988.05	8.43	2.90
212	122	0.58	-275.40	75844.78	8.41	2.90
213	122.24	0.57	-275.16	75712.64	8.40	2.90
214	122.5	0.57	-274.90	75569.63	8.38	2.90
215	122.75	0.57	-274.65	75432.24	8.37	2.89
216	123	0.57	-274.40	75294.98	8.35	2.89
217	123.24	0.57	-274.16	75163.32	8.34	2.89
218	123.48	0.57	-273.92	75031.78	8.32	2.88
219	123.72	0.56	-273.68	74900.36	8.31	2.88
220	123.97	0.56	-273.43	74763.58	8.29	2.88
221	124.22	0.56	-273.18	74626.93	8.28	2.88
222	124.46	0.56	-272.94	74495.86	8.26	2.87
223	124.71	0.56	-272.69	74359.45	8.25	2.87
224	124.94	0.56	-272.46	74234.07	8.23	2.87
225	125.19	0.56	-272.21	74097.90	8.22	2.87
226	125.43	0.56	-271.97	73967.30	8.20	2.86
227	125.67	0.55	-271.73	73836.81	8.19	2.86
228	125.91	0.55	-271.49	73706.44	8.18	2.86
229	126.15	0.55	-271.25	73576.18	8.16	2.86
230	126.39	0.55	-271.01	73446.04	8.15	2.85
231	126.63	0.55	-270.77	73316.01	8.13	2.85
232	126.87	0.55	-270.53	73186.10	8.12	2.85
233	127.11	0.55	-270.29	73056.31	8.10	2.85
234	127.34	0.54	-270.06	72932.03	8.09	2.84
235	127.58	0.54	-269.82	72802.46	8.08	2.84
236	127.82	0.54	-269.58	72673.00	8.06	2.84
237	128.06	0.54	-269.34	72543.66	8.05	2.84
238	128.29	0.54	-269.11	72419.82	8.03	2.83
239	128.53	0.54	-268.87	72290.70	8.02	2.83
240	128.77	0.54	-268.63	72161.70	8.00	2.83
241	129.01	0.54	-268.39	72032.82	7.99	2.83
242	129.25	0.53	-268.15	71904.05	7.98	2.82
243	129.49	0.53	-267.91	71775.39	7.96	2.82
244	129.73	0.53	-267.67	71646.85	7.95	2.82
245	129.98	0.53	-267.42	71513.08	7.93	2.82
246	130.22	0.53	-267.18	71384.78	7.92	2.81

247	130.46	0.53	-266.94	71256.59	7.90	2.81
248	130.7	0.53	-266.70	71128.52	7.89	2.81
249	130.94	0.53	-266.46	71000.56	7.88	2.81
250	131.18	0.52	-266.22	70872.72	7.86	2.80
251	131.42	0.52	-265.98	70744.99	7.85	2.80
252	131.66	0.52	-265.74	70617.38	7.83	2.80
253	131.9	0.52	-265.50	70489.88	7.82	2.80
254	132.14	0.52	-265.26	70362.50	7.81	2.79
255	132.37	0.52	-265.03	70240.53	7.79	2.79
256	132.61	0.52	-264.79	70113.37	7.78	2.79
257	132.86	0.52	-264.54	69981.04	7.76	2.79
258	133.09	0.52	-264.31	69859.41	7.75	2.78
259	133.33	0.51	-264.07	69732.60	7.74	2.78
260	133.56	0.51	-263.84	69611.18	7.72	2.78
261	133.79	0.51	-263.61	69489.86	7.71	2.78
262	134.03	0.51	-263.37	69363.39	7.69	2.77
263	134.27	0.51	-263.13	69237.03	7.68	2.77
264	134.51	0.51	-262.89	69110.78	7.67	2.77
265	134.74	0.51	-262.66	68989.91	7.65	2.77
266	134.98	0.51	-262.42	68863.89	7.64	2.76
267	135.22	0.51	-262.18	68737.99	7.62	2.76
268	135.45	0.51	-261.95	68617.44	7.61	2.76
269	135.69	0.50	-261.71	68491.76	7.60	2.76
270	135.93	0.50	-261.47	68366.20	7.58	2.75
271	136.17	0.50	-261.23	68240.75	7.57	2.75
272	136.4	0.50	-261.00	68120.64	7.56	2.75
273	136.64	0.50	-260.76	67995.41	7.54	2.75
274	136.88	0.50	-260.52	67870.31	7.53	2.74
275	137.11	0.50	-260.29	67750.52	7.52	2.74
276	137.35	0.50	-260.05	67625.64	7.50	2.74
277	137.58	0.50	-259.82	67506.07	7.49	2.74
278	137.82	0.50	-259.58	67381.41	7.47	2.73
279	138.06	0.49	-259.34	67256.87	7.46	2.73
280	138.29	0.49	-259.11	67137.63	7.45	2.73
281	138.53	0.49	-258.87	67013.32	7.43	2.73
282	138.77	0.49	-258.63	66889.12	7.42	2.72
283	139	0.49	-258.40	66770.20	7.41	2.72
284	139.23	0.49	-258.17	66651.39	7.39	2.72
285	139.47	0.49	-257.93	66527.52	7.38	2.72
286	139.7	0.49	-257.70	66408.93	7.37	2.71
287	139.94	0.49	-257.46	66285.29	7.35	2.71
288	140.17	0.49	-257.23	66166.91	7.34	2.71

289	140.41	0.49	-256.99	66043.50	7.33	2.71
290	140.65	0.49	-256.75	65920.20	7.31	2.70
291	140.88	0.48	-256.52	65802.15	7.30	2.70
292	141.12	0.48	-256.28	65679.08	7.29	2.70
293	141.35	0.48	-256.05	65561.24	7.27	2.70
294	141.58	0.48	-255.82	65443.51	7.26	2.69
295	141.82	0.48	-255.58	65320.78	7.25	2.69
296	142.05	0.48	-255.35	65203.27	7.23	2.69
297	142.28	0.48	-255.12	65085.86	7.22	2.69
298	142.51	0.48	-254.89	64968.56	7.21	2.68
299	142.75	0.48	-254.65	64846.27	7.19	2.68
300	142.98	0.48	-254.42	64729.18	7.18	2.68
301	143.21	0.48	-254.19	64612.20	7.17	2.68
302	143.45	0.48	-253.95	64490.25	7.15	2.67
303	143.68	0.47	-253.72	64373.48	7.14	2.67
304	143.91	0.47	-253.49	64256.83	7.13	2.67
305	144.14	0.47	-253.26	64140.27	7.11	2.67
306	144.38	0.47	-253.02	64018.77	7.10	2.66
307	144.61	0.47	-252.79	63902.43	7.09	2.66
308	144.84	0.47	-252.56	63786.20	7.08	2.66
309	145.07	0.47	-252.33	63670.08	7.06	2.66
310	145.3	0.47	-252.10	63554.06	7.05	2.66
311	145.53	0.47	-251.87	63438.14	7.04	2.65
312	145.76	0.47	-251.64	63322.34	7.02	2.65
313	145.98	0.47	-251.42	63211.66	7.01	2.65
314	146.2	0.47	-251.20	63101.09	7.00	2.65
315	146.43	0.46	-250.97	62985.59	6.99	2.64
316	146.65	0.46	-250.75	62875.21	6.97	2.64
317	146.88	0.46	-250.52	62759.92	6.96	2.64
318	147.11	0.46	-250.29	62644.73	6.95	2.64

8877	727.26	0.08	329.86	108808.08	12.07	3.47
8878	727.22	0.08	329.82	108781.69	12.07	3.47
8879	727.17	0.08	329.77	108748.71	12.06	3.47
8880	727.12	0.08	329.72	108715.74	12.06	3.47
8881	727.05	0.08	329.65	108669.58	12.05	3.47
8882	728.07	0.08	330.67	109343.11	12.13	3.48
8883	728.18	0.08	330.78	109415.87	12.14	3.48
8884	728.73	0.08	331.33	109780.03	12.18	3.49
8885	729.01	0.08	331.61	109965.66	12.20	3.49
8886	729.21	0.08	331.81	110098.34	12.21	3.49
8887	729.69	0.08	332.29	110417.11	12.25	3.50
8888	729.62	0.08	332.22	110370.59	12.24	3.50
8889	730.07	0.08	332.67	110669.79	12.28	3.50
8890	730.35	0.08	332.95	110856.17	12.30	3.51
8891	730.77	0.08	333.37	111136.02	12.33	3.51
8892	731.02	0.08	333.62	111302.77	12.35	3.51
8893	731.32	0.08	333.92	111503.03	12.37	3.52
8894	731.61	0.08	334.21	111696.79	12.39	3.52
8895	731.89	0.08	334.49	111884.03	12.41	3.52
8896	732.11	0.08	334.71	112031.25	12.43	3.53
8897	732.69	0.08	335.29	112419.85	12.47	3.53
8898	733.27	0.08	335.87	112809.13	12.51	3.54
8899	733.77	0.08	336.37	113145.25	12.55	3.54
8900	734.27	0.08	336.87	113481.87	12.59	3.55
8901	734.77	0.08	337.37	113818.99	12.63	3.55
8902	735.27	0.08	337.87	114156.61	12.66	3.56
8903	735.77	0.08	338.37	114494.73	12.70	3.56
8904	736.27	0.08	338.87	114833.35	12.74	3.57
8905	736.77	0.08	339.37	115172.47	12.78	3.57
8906	737.27	0.08	339.87	115512.09	12.81	3.58
8907	737.77	0.08	340.37	115852.21	12.85	3.58
8908	738.27	0.08	340.87	116192.83	12.89	3.59
8909	738.77	0.08	341.37	116533.95	12.93	3.60
8910	739.27	0.08	341.87	116875.57	12.96	3.60
8911	739.77	0.08	342.37	117217.70	13.00	3.61
8912	740.27	0.08	342.87	117560.32	13.04	3.61
8913	740.77	0.08	343.37	117903.44	13.08	3.62
8914	741.27	0.08	343.87	118247.06	13.12	3.62
8915	741.77	0.08	344.37	118591.18	13.15	3.63
8916	742.27	0.08	344.87	118935.80	13.19	3.63
8917	742.77	0.08	345.37	119280.92	13.23	3.64
8918	743.27	0.08	345.87	119626.54	13.27	3.64

8919	743.77	0.08	346.37	119972.66	13.31	3.65
8920	744.27	0.08	346.87	120319.28	13.35	3.65
8921	744.77	0.08	347.37	120666.40	13.39	3.66
8922	745.27	0.08	347.87	121014.02	13.42	3.66
8923	745.77	0.08	348.37	121362.14	13.46	3.67
8924	746.27	0.08	348.87	121710.76	13.50	3.67
8925	746.77	0.08	349.37	122059.89	13.54	3.68
8926	747.27	0.08	349.87	122409.51	13.58	3.68
8927	747.77	0.08	350.37	122759.63	13.62	3.69
8928	748.47	0.08	351.07	123250.64	13.67	3.70
8929	749.17	0.08	351.77	123742.62	13.73	3.70
8930	749.87	0.08	352.47	124235.59	13.78	3.71
8931	750.57	0.08	353.17	124729.54	13.84	3.72
8932	751.27	0.08	353.87	125224.47	13.89	3.73
8933	751.97	0.08	354.57	125720.38	13.95	3.73
8934	752.67	0.08	355.27	126217.27	14.00	3.74
8935	753.37	0.08	355.97	126715.14	14.06	3.75
8936	754.07	0.08	356.67	127213.99	14.11	3.76
8937	754.77	0.08	357.37	127713.82	14.17	3.76
8938	755.47	0.08	358.07	128214.63	14.22	3.77
8939	756.17	0.08	358.77	128716.41	14.28	3.78
8940	756.87	0.08	359.47	129219.18	14.33	3.79
8941	757.57	0.08	360.17	129722.93	14.39	3.79
8942	758.27	0.08	360.87	130227.66	14.45	3.80
8943	758.97	0.08	361.57	130733.37	14.50	3.81
8944	759.67	0.08	362.27	131240.06	14.56	3.82
8945	760.37	0.09	362.97	131747.73	14.61	3.82
8946	761.07	0.09	363.67	132256.38	14.67	3.83
8947	761.77	0.09	364.37	132766.01	14.73	3.84
8948	762.47	0.09	365.07	133276.62	14.78	3.84
8949	763.17	0.09	365.77	133788.20	14.84	3.85
8950	763.87	0.09	366.47	134300.77	14.90	3.86
8951	764.57	0.09	367.17	134814.32	14.95	3.87
8952	765.13	0.09	367.73	135225.87	15.00	3.87
8953	765.69	0.09	368.29	135638.04	15.05	3.88
8954	766.25	0.09	368.85	136050.84	15.09	3.88
8955	766.81	0.09	369.41	136464.26	15.14	3.89
8956	767.37	0.09	369.97	136878.32	15.18	3.90
8957	767.93	0.09	370.53	137293.00	15.23	3.90
8958	768.49	0.09	371.09	137708.31	15.28	3.91
8959	769.05	0.09	371.65	138124.24	15.32	3.91
8960	769.61	0.09	372.21	138540.80	15.37	3.92

8961	770.17	0.09	372.77	138957.99	15.41	3.93
8962	770.73	0.09	373.33	139375.81	15.46	3.93
8963	771.29	0.09	373.89	139794.25	15.51	3.94
8964	771.85	0.09	374.45	140213.33	15.55	3.94
8965	772.46	0.09	375.06	140670.53	15.60	3.95
8966	773.07	0.09	375.67	141128.47	15.65	3.96
8967	773.68	0.09	376.28	141587.16	15.71	3.96
8968	774.29	0.09	376.89	142046.60	15.76	3.97
8969	774.9	0.09	377.50	142506.78	15.81	3.98
8970	775.51	0.09	378.11	142967.70	15.86	3.98
8971	776.12	0.09	378.72	143429.37	15.91	3.99
8972	776.73	0.09	379.33	143891.78	15.96	4.00
8973	777.34	0.09	379.94	144354.93	16.01	4.00
8974	777.95	0.09	380.55	144818.83	16.06	4.01
8975	778.56	0.09	381.16	145283.48	16.12	4.01
8976	779.17	0.09	381.77	145748.87	16.17	4.02
8977	779.78	0.09	382.38	146215.00	16.22	4.03
8978	780.39	0.09	382.99	146681.88	16.27	4.03
8979	781	0.09	383.60	147149.50	16.32	4.04
8980	781.61	0.09	384.21	147617.86	16.37	4.05
8981	782.22	0.09	384.82	148086.97	16.43	4.05
8982	782.83	0.09	385.43	148556.82	16.48	4.06
8983	783.44	0.09	386.04	149027.42	16.53	4.07
8984	784.05	0.09	386.65	149498.76	16.58	4.07
8985	784.66	0.09	387.26	149970.85	16.64	4.08
8986	785.27	0.09	387.87	150443.68	16.69	4.09
8987	785.88	0.09	388.48	150917.25	16.74	4.09
8988	786.63	0.09	389.23	151500.54	16.81	4.10
8989	787.38	0.09	389.98	152084.95	16.87	4.11
8990	788.13	0.09	390.73	152670.48	16.94	4.12
8991	788.88	0.09	391.48	153257.14	17.00	4.12
8992	789.63	0.09	392.23	153844.92	17.07	4.13
8993	790.38	0.09	392.98	154433.83	17.13	4.14
8994	791.13	0.09	393.73	155023.86	17.20	4.15
8995	791.88	0.09	394.48	155615.02	17.26	4.15
8996	792.63	0.09	395.23	156207.31	17.33	4.16
8997	793.38	0.09	395.98	156800.71	17.39	4.17
8998	794.13	0.09	396.73	157395.25	17.46	4.18
8999	794.88	0.09	397.48	157990.91	17.53	4.19
9000	795.63	0.09	398.23	158587.69	17.59	4.19
9001	796.38	0.09	398.98	159185.60	17.66	4.20
9002	797.13	0.09	399.73	159784.63	17.72	4.21

9003	797.88	0.09	400.48	160384.79	17.79	4.22
9004	798.63	0.09	401.23	160986.07	17.86	4.23
9005	799.38	0.09	401.98	161588.48	17.92	4.23
9006	800.13	0.09	402.73	162192.02	17.99	4.24
9007	800.88	0.09	403.48	162796.67	18.06	4.25
9008	801.63	0.09	404.23	163402.46	18.13	4.26
9009	802.38	0.09	404.98	164009.37	18.19	4.27
9010	803.13	0.09	405.73	164617.40	18.26	4.27
9011	803.06	0.09	405.66	164560.60	18.25	4.27
9012	802.56	0.09	405.16	164155.19	18.21	4.27
9013	802.11	0.09	404.71	163790.75	18.17	4.26
9014	801.88	0.09	404.48	163604.64	18.15	4.26
9015	800.16	0.09	402.76	162216.18	17.99	4.24
Total	3582555				32780.55	181.05

X	**N**	**X_AVG**
3582555	9015	397.3993

∑(X - X-AVG)^2	295516699.00
(∑(X - X-AVG)^2)/N	32780.55452
SQRT((∑(X - X-AVG)^2)/N)	181.05401

SD = 181.05401